ASSESSING TRANSCRIPTOMIC AND PHYSIOLOGICAL RESPONSES OF ENVIRONMENTAL STRESS IN MUSSELS (*MYTILUS EDULIS*) FROM TWO SITES AND SIZES TO DISCOVER MARKERS CAPABLE OF MONITORING MUSSEL HEALTH

by

Stephanie Anne Hall

Submitted in partial fulfilment of the requirements
for the degree of Doctor of Philosophy

at

Dalhousie University
Halifax, Nova Scotia
July 2022

© Copyright by Stephanie Anne Hall, 2022

Dedicated to my loving family and partner Greg

for all their unconditional support over the years

TABLE OF CONTENTS

List of Tables x

List of Figures xiv

Abstract xvii

List of Abbreviations used xviii

Acknowledgements xxiii

Chapter 1: Introduction 1

1.1 The blue mussel (*Mytilus edulis*) 1

1.1.1 Distribution 1

1.1.2 Morphological and physiological features of blue mussels 1

1.1.3 Reproductive physiology 3

1.2 Mussel aquaculture in Prince Edward Island 4

1.2.1 Mussel aquaculture overview 4

1.2.2 Seed collection 5

1.2.3 Grow-out 5

1.2.4 Industry challenges for mussel aquaculture 5

1.3 Natural and climate change induced fluctuations in environmental conditions 6

1.3.1 Temperature 7

1.3.2 Salinity 8

1.3.3 Dissolved oxygen 9

1.3.4 Ocean chemistry/acidity 11

1.3.5 Nutrient cycling and phytoplankton 12

1.4 Stress response in the blue mussels 13

1.4.1 Behavioural responses 13
1.4.2 Cellular stress response mechanisms 14
1.4.3 Immune system 20
1.4.4 Anaerobiosis 22
1.4.5 Catabolism of energy reserves 26
1.4.6 Metabolic decline and energy conservation 27
1.4.7 Shell repair and dissolution 28
1.5 Differences in response to environmental stress between mussel sizes and locations 29
1.5.1 Inter-individual variability in phenotypes in a single population 29
1.5.2 Population/site differences 30
1.5.3 Age/size related differences 31
1.6 Monitoring stress in mussels 32
1.6.1 Heart rate 32
1.6.2 Neutral red assay 33
1.6.3 Omics tools for monitoring stress 33
1.7 **Project** 34
1.7.1 Rationale and objectives 34
Chapter 2: Evaluating blue mussels (*Mytilus edulis*) responses to acute hypoxia using transcriptomics and heart rate 36
2.1 Introduction 36
2.2 Materials and methods 38
2.2.1 Mussel sites and sizes 38
2.2.2 Hypoxia trial 39
2.2.3 Heart rate monitoring 40

2.2.4 Statistical analysis of heart rate monitoring 40
2.2.5 Sample preservation, RNA extraction and sequencing 41
2.2.6 *De novo* transcriptome assembly 41
2.2.7 Differential expression analysis 42
2.2.8 Annotation and functional analysis 43
2.3 Results 44
2.3.1 Heart rate monitoring 44
2.3.2 Transcriptome assembly and annotation 44
2.3.3 Differential expression analysis 45
2.3.4 Functional analysis 49
2.4 Discussion 69
2.4.1 Heart rate monitoring 69
2.4.2 Transcript expression associated with metabolism and anaerobiosis: 70
2.4.3 Transcript expression associated with metabolic rate depression 72
2.4.4 Energy conservation mechanisms 74
2.4.5 Stress response: 75
2.4.6 Immune Response: 77
2.4.7 Antioxidant: 77
2.4.8 Differences in transcriptomic response in different size mussels 78
2.4.8.1 Reproductive response 79
2.4.8.2 Growth Response: 79
2.4.8.3 Metabolism: 81
2.4.8.4 Byssal thread production 81
2.4.9 Differences in transcript expression in between sites 82
2.5 Conclusions: 83

Chapter 3. Evaluating blue mussels (*Mytilus edulis*) responses to acute hyposalinity using transcriptomics, heart rate and neutral red assay 85

3.1 Introduction 85

3.2 Materials and methods 87

3.2.1 Mussel sites and sizes 87

3.2.2 Hyposalinity trial 88

3.2.3 Heart rate monitoring 88

3.2.4 Neutral Red Assay 88

3.2.5 Statistical analysis of heart rate and neutral red assay 89

3.2.6 Sample preservation, RNA extractions and sequencing 90

3.2.7 *De novo* transcriptome assembly and differential expression analysis 91

3.2.8 Annotation and functional analysis 92

3.3 Results 92

3.3.1 Heart rate and neutral red assay 92

3.3.2 Differential transcript expression analysis 94

3.3.3 Functional analysis 98

3.4 Discussion 112

3.4.1 Heart rate and transcript expression associated with metabolism 112

3.4.2 Transcripts associated with osmoconformation and metabolism 113

3.4.3 Lysosome destabilization and stress related expression 116

3.4.4 Differences in sizes and sites 117

3.5 Conclusions 120

Chapter 4. Evaluating blue mussels (*Mytilus edulis*) responses to different levels of food availability using transcriptomics, heart rate and neutral red assay 121

4.1 Introduction 121

4.2 Materials and Methods 126
4.2.1 Mussel sites and sizes 126
4.2.2 Food availability trials 126
4.2.3 Heart rate monitoring 127
4.2.4 Neutral red assay 127
4.2.5 Statistical analysis of heart rate and neutral red assay 128
4.2.6 Sample preservation, RNA extractions and sequencing 129
4.2.7 *De novo* transcriptome assembly and differential expression analysis 130
4.2.8 Annotation and functional analysis 131
4.3 Results 131
4.3.1 Heart rate and neutral red assay 131
4.3.2 Differential expression analysis 133
4.3.3 Functional analysis 138
4.4 Discussion 155
4.4.1 Physiological and transcriptomic response to food availability 155
4.4.2 Transcripts associated with metabolism 156
4.4.3 Transcripts associated with immune response 156
4.4.4 Transcripts associated with feeding physiology and digestion 158
4.4.5 Differences between mussel sites and sizes 161
4.5 Conclusions 162
Chapter 5: Marker discovery in the blue mussel (*Mytilus edulis*) associated with hypoxia, hyposalinity and food availability stress. 164
5.1 Introduction 164
5.2 Materials and methods 167
5.2.1 Mussel samples and trials 167

5.2.2 Sample preservation, RNA extractions and sequencing 168
5.2.3 Transcriptome assembly and differential expression analysis 168
5.2.4 Marker discovery and primer design 169
5.2.5 cDNA synthesis and controls 170
5.2.6 Primer optimization and validation 170
5.2.7 Statistical analysis of RT-qPCR validation step 172
5.3 Results 172
5.3.1 Differential expression, markers and primer design 172
5.3.2 Primer optimization, verification and normalization 180
5.3.3 Statistical analysis 181
5.4 Discussion 185
5.5 Conclusions 189
Chapter 6: Discussion 190
6.1 Conclusions 190
6.2 Differences in transcriptomic responses between sites and sizes 191
6.3 Future directions 194
Appendix 1 197
Appendix 2 198
Appendix 3 202
Appendix 4 205
Appendix 5 206
Appendix 6 207
Appendix 7 208
Appendix 8 209
Appendix 9 210

Appendix 10 211

Appendix 11 212

Appendix 12 213

Bibliography: 214

List of Tables

Table 1. Differential expression analysis comparisons utilized in experiment.. 43

Table 2. Total number of differentially expressed transcripts (DE) (FDR p-value = < 0.05) for each pairwise comparison (March Water (MW), St. Mary's Bay (StM), adult (A), seed (S)), for both DEseq2, and edgeR. 47

Table 3. KEGG pathways associated with differentially expressed transcripts from each pairwise comparison (MW = March Water; StM = St. Mary's Bay; A = adult; S = seed). 51

Table 4. Differentially expressed transcripts found mutually expressed between different pairwise comparisons (MW = March Water; StM = St. Mary's Bay; A = adult; S = seed). 52

Table 5. Functions/pathway of transcripts found differentially expressed from the March Water adult (MW A) through pairwise comparison. 58

Table 6. Functions/pathway of transcripts found differentially expressed from the St. Mary's Bay adult (StM A) through pairwise comparison. 59

Table 7. Functions/pathway of transcripts found differentially expressed from the March Water seed (MW S) through pairwise comparison. 60

Table 8. Functions/pathway of transcripts found differentially expressed from the St. Mary's Bay seed (StM S) through pairwise comparison. 62

Table 9. Functions/pathway of transcripts found differentially expressed from adult (A) through pairwise comparison. 63

Table 10. Functions/pathway of transcripts found differentially expressed from the seed (S) through pairwise comparison. 65

Table 11. Differential expression analysis comparisons utilized in experiment. 91

Table 12. Estimates from final statistical model of heart rate from mussels held at each salinity (16, 27 ‰).. 93

Table 13. Total number of differentially expressed transcripts (FDR p-value = < 0.05) for each pairwise comparison in each site and size for both DEseq2 and edgeR..... 96

Table 14. KEGG pathways associated with differentially expressed transcripts from each pairwise comparison (MW = March Water; StM = St. Mary's Bay; A = adult; S = seed). 99

Table 15. Differentially expressed transcripts found mutually expressed between different pairwise comparisons (MW = March Water; StM = St. Mary's Bay; A = adult; S, = seed). 100

Table 16. Functions/pathway of transcripts found differentially expressed from the March Water adult (MW A) through pairwise comparison. 103

Table 17. Functions/pathway of transcripts found differentially expressed from the St. Mary's Bay adult (StM A) through pairwise comparison. 103

Table 18. Functions/pathway of transcripts found differentially expressed from the March Water seed (MW S) through pairwise comparison. 106

Table 19. Functions/pathway of transcripts found differentially expressed from the St. Mary's Bay seed (StM S) through pairwise comparison. 107

Table 20. Functions/pathway of transcripts found differentially expressed from the adults (A) through pairwise comparison. 108

Table 21. Functions/pathway of transcripts found differentially expressed from the seed (S) through pairwise comparison. 109

Table 22. Comparisons of Differential expression analyses utilized in experiment..... 130

Table 23. Total number of differentially expressed transcripts (FDR p-value = < 0.05) for each pairwise comparison in each site and size for both DEseq2 and edgeR..... 135

Table 24. KEGG pathways associated with differentially expressed transcripts from each 1 vs 5% pairwise comparisons (MW = March Water; StM = St. Mary's Bay; A = adult; S = seed)..... 140

Table 25. KEGG pathways associated with differentially expressed transcripts from each 1 vs 10% pairwise comparisons (MW = March Water; StM = St. Mary's Bay; A = adult; S = seed)..... 141

Table 26. Differentially expressed transcripts found mutually expressed between different mussel groups within pairwise comparisons (MW = March Water; StM = St. Mary's Bay; A = adult; S, = seed). 142

Table 27. Functions/pathway of transcripts found differentially expressed from the March Water adult (MW A) through different pairwise comparisons. 142

Table 28. Functions/pathway of transcripts found differentially expressed from the St. Mary's Bay adult (StM A) through different pairwise comparisons. 146

Table 29. Functions/pathway of transcripts found differentially expressed from the March Water seed (MW S) through different pairwise comparisons. 148

Table 30. Functions/pathway of transcripts found differentially expressed from the St. Mary's Bay seed (StM S) through different pairwise comparisons. 149

Table 31. Differentially expressed transcripts found mutually expressed within two different pairwise comparisons within one mussel group (MW = March Water; StM = St. Mary's Bay; A = adult; S, = seed).. 152

Table 32. Summary of types of pairwise comparisons utilized for hypoxia, hyposalinity and food availability marker discovery in two mussel sizes (adult and seed) and two sites March Water (MW), and St. Mary's Bay (StM). 169

Table 33. Total number of differentially expressed (DE; FDR p-value = < 0.05) transcripts in the hypoxia trial for treatment (O2 ~ 2 mg/L) vs control (O2 ~ 7–8 mg/L) in each comparison, for both DEseq2, and edgeR. 173

Table 34. Total number of differentially expressed (DE; FDR p-value = < 0.05) transcripts in hyposalinity trial for treatment (16 ‰) vs control (27 ‰) in each comparison, for both DEseq2 (A), and edgeR (B). 173

Table 35. Total number of differentially expressed (DE; FDR p-value = < 0.05) transcripts in low food availability trial for treatment (1%) vs control (5%) in each comparison, for both DEseq2 (A) and edgeR (B). 173

Table 36. Total number of differentially expressed (DE; FDR p-value = < 0.05) transcripts in high food availability trial for treatment (10%) vs control (5%) in each comparison, for both DEseq2 (A) and edgeR (B). 174

Table 37. Candidate markers considered for primer design in the hypoxia trial 174

Table 38. Candidate markers considered for primer design in the hyposalinity trial. 175

Table 39. Candidate markers considered for primer design in the low food availability trial 177

Table 40. Candidate markers considered for primer design in the high food availability trial 178

Table 41. Summary of primers designed from markers in each trial..... 178

Table 42. Primers that passed optimization steps 181

Table 43. All KEGG pathways associated with differentially expressed transcripts in the hypoxia trial (Chapter 2) from different sizes and populations (A = adult; S = seed; MW = March Water; StM = St. Mary's Bay). 198

Table 44. All KEGG pathways associated with differentially expressed transcripts in the hyposalinity trial (Chapter 2) from different sizes and populations (A = adult; S = seed; MW = March Water; StM = St. Mary's Bay). 202

Table 45. concentration of food being fed to adult and seed mussel every hour for each food ration (1%, 5%, 10%) in food availability trials (Chapter 4). 205

List of Figures

Figure 1. General anaerobic pathways in bivalve molluscs. 25

Figure 2. Map of Prince Edward Island showing sampling locations of each site (March Water and St. Mary's Bay).. 39

Figure 3. Estimates from statistical model for: (A) mean hourly HR (1, 2, 3, 4 h) of mussels in acute hypoxia treatment (O2 ~ 2 mg/L) vs control (O2 ~ 7–8 mg/L) (n = 16 replicates per point); and (B) timing (during and after) the hypoxia trial for mussels in control and acute hypoxia treatment.. 44

Figure 4. Preliminary principal component analysis plot of all expressed transcripts in hypoxia trial.). 46

Figure 5. Volcano plots for differentially expressed transcripts identified in DESeq2 for each pairwise comparison 47

Figure 6.Venn Diagram of differentially expressed transcripts found uniquely or mutually between different pairwise comparison 48

Figure 7. Heatmap of all differentially expressed transcripts identified by the DESeq2 statistical packages in each pairwise comparison 49

Figure 8. Subset of differentially expressed transcripts plotted using their subsequent Log_2 Fold change for each pairwise comparison..... 68

Figure 9. Least square means ± SE of heart rate for hyposalinity (16 ‰) and control (27 ‰) from final statistical model for (A) 1, 2, 3, 4, 6 h (n = 3 per point); (B) during, after (n = 3 per bar).. 93

Figure 10. Least square means ± SE of lysosome destabilization index (LDI) from final statistical model for hyposalinity (16 ‰) and control (27 ‰) with time (3, 6 h) in (A) adults and (B) seeds..... 94

Figure 11. Preliminary principal component analysis plot of all expressed transcripts in hyposalinity trial.. 95

Figure 12. Volcano plots for differentially expressed transcripts identified in DESeq2 for each pairwise comparison..... 96

Figure 13. Venn diagram of differentially expressed transcripts found uniquely or mutually between different pairwise comparisons..... 97

Figure 14. Heatmap of all differentially expressed transcripts identified by the DESeq2 statistical packages in each pairwise comparison. 98

Figure 15. Subset of differentially expressed transcripts plotted using their subsequent Log_2 Fold change for each pairwise comparison. 111

Figure 16: Least square mean ± SE of heart rate from final statistical model for adult mussels at: (A) 1, 5, 10, 19, 25, 32, 44, 48 h (n = 24 per point); (B) during, after (n = 24 per bar).). 132

Figure 17. Estimates from final statistical model for lysosomal destabilization indices (LDI) of adult mussels from each site (MW, StM) and (B) of seed mussels at each sampling time (24, 48 h). 132

Figure 18. Preliminary principal component analysis plot of all expressed transcripts in food availability trial.. 134

Figure 19. Volcano plots for differentially expressed transcripts identified in DESeq2 for each pairwise comparison (MW = March Water; StM = St. Mary's Bay; A = adult; S, = seed).. 135

Figure 20. Heatmap of all differentially expressed transcripts identified by the DESeq2 statistical package.. 137

Figure 21. Venn diagram of differentially expressed transcripts found uniquely or mutually between different pairwise comparison of different mussel groups 138

Figure 22. Subset of differentially expressed transcripts plotted using their subsequent Log_2 Fold change for each pairwise comparison. 154

Figure 23. Boxplots showing the results of the test of medians. 183

Figure 24. Estimates from the one-way ANOVA showing the mean Log_{10}(NQR+1) and confidence intervals of each primer set for each mussel group. 184

Figure 25. Standard curve of efficiency, melt peak and melt curve of each successfully verified primer associated with acute hypoxia..... 206

Figure 26. Standard curve of efficiency, melt peak and melt curve of each successfully verified primer associated with acute hyposalinity..... 207

Figure 27. Standard curve of efficiency, melt peak and melt curve of each successfully verified primer associated with low food availability..... 208

Figure 28. Standard curve of efficiency, melt peak and melt curve of each successfully verified primer associated with high food availability 209

Figure 29. GeNorm algorithm indicating the ideal number of reference genes to utilize for normalization of RT-qPCR data for hypoxia primers..... 210

Figure 30. GeNorm algorithm indicating the ideal number of reference genes to utilize for normalization of RT-qPCR data in the hyposalinity primers 211

Figure 31. GeNorm algorithm indicating the ideal number of reference genes to utilize for normalization of RT-qPCR data for low food availability primers 212

Figure 32. GeNorm algorithm indicating the ideal number of reference genes to utilize for normalization of RT-qPCR data for high food availability primers 213

Abstract

The Prince Edward Island blue mussel (*Mytilus edulis*) aquaculture industry is being challenged by climate change induced environmental stressors, that is impacting mussel health and survival. Physiological responses of mussels to stress have been evaluated in many studies, however, less is known about how transcriptomic response leads to physiology. The present thesis aimed to first, study the transcriptomic response of acute stress related to hypoxia, hyposalinity, food availability (low/high), then to design markers capable of detecting early stress response. Two sizes (adult, seed) and sites (March Water, St. Mary's Bay) of mussels from PEI were evaluated to understand similarities and differences in transcriptomic response to stress. Transcriptomic response in each stressor was evaluated using an RNA-seq approach, to understand total mRNA expression occurring during acute stress. Specific markers were discovered associated with each stressor, and underwent optimization and validation, using RT-qPCR. RT-qPCR expression of markers was normalized, and then statistical analysis was completed to understand the expression between the treatments and different mussel sizes and sites. The results of this study found that transcriptomic response was highly variable between sizes, sites and individuals in each stressor evaluated. Marker optimization, verification and statistical analysis further validated this, as expression was found variable between mussel sizes and sites. Markers should be further evaluated in a real world setting to see if they could be effective in detecting the stressors at different time points. Variability in transcriptomics uncovered the complexity related to stress response and was hypothesized to be related to baseline differences between the sizes and environmental differences between the two sites.

List of Abbreviations used

Abbreviation	Definition
~	approximately
°C	degree Celsius
µL	microliter
‰	parts per thousand
A	adult
ADP	adenosine diphosphate
Ar	argon
Arach	arachidonate 5-Lipoxygenase
ATF	activating transcription factor
ATP	adenosine triphosphate
bp	base pair
BPM	beats per minute
BW	dry body tissue weight
bZIP	basic leucine zipper family
C/EBPG	CCAAT/enhance-binding proteins
C1q	compliment 1
Ca^{2+}	calcium
CAD	Canadian dollar
CASP	CASP8 and FADD-like
CAT	catalase
CHAT	choline O-acetyltransferase
Cl^{+}	chorine

chl a	chlorophyl a
cm	centimeter
CO_2	carbon dioxide
CO_3^{2-}	carbonate
CREB	cAMP-response element binding protein
CREB	CREB-binding protein
Cq	cycle quantification value
eif	EIF2B5
ER	endoplasmic reticulum
ETC	electron transport chain
Family	stanniocalcin-like protein
FC	fold change
FOS	FOS proto-oncogene
GPX	glutathione peroxidase
GST	glutathione S-Transferase
h	hour
H^+	hydrogen ion
H_2CO_3	carbonic acid
H_2O	water
HCO_3^-	bicarbonate
hexo	hexosaminidase
HIF	hypoxia inducible factor
HR	heart rate
IL4Il	Interleukin 4 Induced 1

IR	infrared red-light
JUN	JUN proto-oncogene
K^+	potassium
KCTD7	potassium channel tetramerization domain containing 14
KLHL	Kelch Like Family Member 17
L	liter
LDI	lysosome destabilization index
LSM	least square means
M	million
Macro	macrophage expressed protein precursor
mg	milligram
Mg^{2+}	magnesium
min	minute
mL	millilitre
Mono	protein mono-ADP-ribosyltransferase PARP14
mt	metric tonnes
Muts	DNA mismatch repair protein MSH4
MW	March Water
N	nitrogen
N_2	nitrogen gas
Na^+	sodium
NFE2	nuclear factor erythroid 2
NF-κB	nuclear factor κB

NH_3	ammonia
NO	nitric oxide
NO_2^-	nitrite
NO_3^-	nitrate
NRA	neutral red assay
NRF2	nuclear factor erythroid factor 2
O_2	dissolved oxygen
OASIS	old astrocyte specifically induced substance
Origin	origin recognition complex subunit 3-like
P	phosphorus
PAMPs	pathogen-associated molecular patterns
PAR	protease-activated receptors
PCA	principal component analysis
PE	paired end
PEI	Prince Edward Island
Perl	perlucin-like protein
Phospho	phosphoinositide-3-kinase, regulatory subunit 4
Plexin	Plexin
Potass	potassium voltage-gated channel subfamily C member 4 (KCNC4)
PRRs	pattern recognition receptors
RNS	reactive nitrogen species
ROS	reactive oxygen species
RSS	reactive sulphur species

S	Seed
s	seconds
Sacsin	sacsin-like isoform X2
SE	standard error
SH	shell height
SMAF	small musculoaponeurotic fibrosarcoma
SOD	superoxide dismutase
StM	St. Mary's Bay
TFF	trefoil factor 2
TRPM3	transient receptor potential cation channel subfamily M member
USA	United States of America
VIF	variance inflation factor
XBP1	X-box binding protein 1

Acknowledgements

I would like to thank my supervisor's Dr. Fraser Clark and Dr. Sarah Stewart-Clark for all their support, guidance, feedback, and mentorship in my PhD research. Thank you to my supervisory committee member Dr. Denise Méthé for her mentorship, guidance, support, and feedback through out my PhD. Thank you to my supervisory committee member Dr. Christophe Herbinger for his mentorship, feedback and insights that helped to shape my PhD research. I'm extremely fortunate to have had amazing supervisors and supervisory committee, whose guidance and expertise has been vital for the success of this research. I'm forever grateful for the opportunity to complete this PhD at Dalhousie University and be a part of a research project/team that has allowed me to grow as a person and develop as a scientist.

I would like to thank Gillian Tobin-Huxley for their technical assistance and help in running my PhD research experiments at the Dalhousie Aquatron. I would like to thank the staff at the Dalhousie Aquatron, for their work in implementing systems to conduct the experiments. I would also like to extend thanks to my lab members for all their support.

I would like to extend a special thank you to Fisheries and Oceans Canada, Aquaculture Collaborative Research and Development Program (ACRDP) and Prince Edward Island Aquaculture Alliance for funding this research. In addition, a special thank you to Atlantic Aqua Farms and Prince Edward Aqua Farms for supplying the mussels that were used in this research. Thank you to all scientists and staff at Fisheries and Oceans in the Aquaculture and Coastal Ecosystem Section for being so helpful to me during my PhD.

I would like to personally thank my partner Greg, family and friends for their unconditional support. I'm so very lucky to have such amazing family, friends, and partner who have always been there for me. Thank you for always listening to me, making me laugh and encouraging me to take time to relax when things got stressful.

Chapter 1: Introduction

1.1 The blue mussel (*Mytilus edulis*)

1.1.1 Distribution

Environmental conditions dictate distribution of molluscs such as the blue mussel (*Mytilus edulis*) (Seed 1976). The genus *Mytilus* distribution ranges from the littoral to sublittoral zone but can also be found in deeper water in the open ocean and in estuaries (brackish water) with high water circulation (Seed 1976). Blue mussels are gregarious settlers that tend to settle in clumps, where competition for food is often high (Seed 1969; Fisheries and Oceans Canada 2003). The juvenile and adult stages are mostly sessile, but mussels are able to detach byssal threads, particularly at juvenile stages, to allow movement of short distances to a more suitable location (Seed 1969; Fisheries and Oceans Canada 2003).

The blue mussel has a large native geographical range and is found both in the northern and southern hemispheres (Soot-Ryen 1955; Seed 1976). Its most northern location is the Arctic region (Seed 1976). On the Atlantic Coast of North America, its traditional distribution was from the Arctic southward along the Atlantic Coast, until Cape Hatteras, North Carolina, USA (Seed 1976). However, this range has receded 350 km poleward to Lewes, Delaware, USA due to high temperatures (Jones et al. 2010). In Europe, blue mussels are found as far north as Greenland and White Sea to the Mediterranean Sea (Seed 1976).

1.1.2 Morphological and physiological features of blue mussels

Mytilus edulis are bivalves with its shells considered to be mytiliform, meaning that the shells are triangular in shape. The narrow end is the anterior, and wide is the posterior and flattens along the ventral side (Morton 1992). The shell is composed of layers of aragonite and calcite (Morton 1992), with their colour ranging from brown, blue and black (Seed 1976) with annual growth rings (Morton 1992). Along the inside of the shell, there is a large adductor muscle scar on the posterior end, and two byssal retractor muscle scars (one posterior and anterior) (Morton 1992). The adductor muscle is involved with valve movement, while the byssal retractor muscles are involved with the attachment of byssal

threads to a substrate (Sugi et al. 2020). Byssal threads are secreted by a gland in the foot (Silverman and Roberto 2010). The foot is associated with locomotion, and is located on the anterior side of the mantle where it can protrude out of the ventral side of the mussel (Silverman and Roberto 2010).

The mantle encloses the visceral organ systems and consists of three folds. Within the mantle are the gonads and glands responsible for secretion of mucus and shell (Bubel 1976; Morton 1992). The mantle is also highly ciliated and is involved with filter feeding behaviour and rejection of pseudofaeces (Morton 1992). Mussels contain gills, also known as ctenidia, which are involved with both respiration and feeding. Each gill filament contains an inner and outer demibranch, that consists of two lamellae that are joined by connective tissue (Morton 1992). Lamellae are composed of gill filaments which are connected by cilia, which create a current that brings water through laterofrontal cirri into the gills (Morton 1992). In terms of circulation, mussels have an open circulatory system, meaning that haemolymph is not circulated into tissues in defined vessels. Deoxygenated haemolymph is brought from the kidneys (on the anterior side) to the gills by the afferent gill vein, where gas exchange with gill filaments occurs, resulting in oxygenation (Gosling 2003). The oxygenated haemolymph is taken to the efferent gill vein that goes to the pericardial sac (Gosling 2003). The pericardial sac (located posterior to the kidneys) consists of a single ventricle with two lateral auricles. Haemolymph moves from the auricles to ventricle then into the anterior aorta, which divides into many small arteries that leads to pallial cavities and organs. Pallial cavities and organs contain veins that carry the haemolymph to the kidneys and then finally back to the gills for reoxygenation (Gosling 2003).

Feeding also occurs via currents established by the gills. Food particles are caught by the frontal side of the gills and transported to the marginal food groove (Riisgård et al. 1996; Riisgård and Larsen 2001). Attached to the marginal food groove are labial palps which are involved with sorting particles and either accept particles for digestion or reject particles as pseudofaeces (Foster-Smith 1978; Jørgensen 1981; Beninger et al. 1999). Particles are accepted or rejected based on size, whether they are biotic or abiotic and by species. Accepted food is passed through the mouth into the esophagus that opens into the

stomach. When food is plentiful, the stomach contains a crystalline style that mechanically turns and releases enzymes that aid in digestion (Graham 1949; Morton 1992). When food availability is low, the crystalline style is resorbed back into the stomach lining. The stomach is ciliated with a network of sorting areas where food is accepted or rejected. In the stomach, there are ducts that lead to the digestive diverticula where intracellular digestion occurs (Graham 1949; Morton 1992). Mussels have two digestive processes, and form two kinds of faeces: intestinal and glandular. Intestinal faeces are formed when food is not fully digested and bypasses the digestive diverticula, while glandular faeces are the result of well digested food that move through the digestive diverticular (Owen 1955; Van Weel 1961). Inside the digestive diverticular are a network of lysosomes that are involved with intracellular heterotrophic digestion of food and absorption of nutrients (Owen 1972).

1.1.3 Reproductive physiology

Mussels are broadcast spawners, which means that spawning and fertilization occurs externally in the water column. They have two distinct sexes (male and female), with the occasional hermaphrodite (Seed 1969; Fisheries and Oceans Canada 2003). Blue mussels are very fecund species, adult females (Shell height (SH) 42 mm) can store 2 x 10^6 eggs/female (Atlantic Canada population) (Thompson 1979). The amount of energy allocated into reproduction (reproductive effort) varies annually in association with environmental conditions (Seed 1969, 1976), with one of the main factors being annual fluctuation of food availability (Freeman 1974). Over the winter months, gametogenesis occurs until the spring when gonad maturation is high and spawning occurs predominantly from June to August (Atlantic Canada population), with multiple spawning events possible (Battle 1932). Although many factors such as salinity and wave action are known to be involved with the spawning period, temperature is considered to be the key factor at determining spawning (Seed 1976).

After spawning, pelagic larvae develop in the water column. The first phase in development is fertilization, followed by cleavage and extrusion of polar bodies. At four to five hours post-fertilization (18 °C), cilia develop and larvae are motile but non-feeding (trochophore stage) (Bayne 1976). After this phase, the trochophore develop into the feeding veliger

larvae, and shell gland develops giving rise to the prodissoconch (first shell). Once the prodissoconch develops, the larvae are at the veliconcha stage, where significant amounts of growth occur, resulting in larvae between 110–250 μm shell length. When larvae reach between 220–260 μm an eye spot develops, and a foot shortly after (pediveliger stage) (Bayne 1976). At three to four weeks post fertilization, larvae will undergo settlement and metamorphosis. The duration and successful development through the larval phases of settling is dependent on environmental conditions such as salinity and temperature (Brenko and Calabrese 1969). When metamorphosis occurs, several changes develop morphologically including byssal thread, disappearance of velum and formation of labial palps (Bayne 1976). After this point, newly settled individuals are called spat/seed, and continue to grow rapidly. In Atlantic Canada, settling of seed usually occurs in mid-June to late-July (Fisheries and Oceans Canada 2003). Mussels can sexually mature within the first year of growth (Seed 1969), however, small mussels put very little energy into reproductive effort and put more energy into somatic growth until they reach ~ 35 mm SH (Thompson 1979; Guyondet et al. 2015).

1.2 Mussel aquaculture in Prince Edward Island

1.2.1 Mussel aquaculture overview

In Canada, mussels are the top shellfish species grown in aquaculture by volume and second only to oysters in farm gate value. Prince Edward Island (PEI) produces 75% of the total quantity of mussels grown in Canada (Statistics Canada 2021). In 2020, the PEI mussel aquaculture industry produced 12,756 metric tonnes (mt), of mussels, valued at ~ $20M (CAD) (Statistics Canada 2021). In PEI there are two mussel species in the *Mytilus* genus: *Mytilus edulis* and *Mytilus trossolus.* While both species and hybrids have been documented on aquaculture leases in other locations (Tremblay et al. 2011), studies by Tremblay et al. (2011) and Wenne et al. (2020) have found that 100% of the cultivated stock on several sites in PEI were of the *M. edulis* species. Therefore, the PEI aquaculture stock is considered to be *M. edulis,* and in the context of this research, the species that will be discussed in the following sections is *M. edulis*.

1.2.2 Seed collection

The first step to mussel production is seed collection, which occurs during the natural setting season (mid-June to late July) from wild and aquaculture populations of mussels. Some growers have their own seed leases, while others purchase seed from growers. During this time, mussel growers' lower collectors into the water column so that the pelagic mussel larvae can settle and attach to the substrate when they complete the pediveliger stage. Mussel larvae attach to collectors via their byssal thread. Seed collector material can range from old ropes, vexar bags, socking material and nylon bags (Fisheries and Oceans Canada 2003). Once attached, seed will be grown for 3–4 months, until ~ 15 mm and are then transferred to a longline system for grow-out in the fall. Mussel larvae are susceptible to fluctuations in water quality parameters; therefore, the number of seed captured varies from year to year depending on weather conditions (Fisheries and Oceans Canada 2003).

1.2.3 Grow-out

In Atlantic Canada, the long-line system is the most common grow-out method for producing blue mussel in aquaculture. This method is preferable over other methods, such as on-bottom culture, because there is less contact with debris that cause pearl formation and more access to food resources (Fisheries and Oceans Canada 2003). This system consists of a series of ropes that are anchored to bottom at both ends of the system. Socks made of vexar mesh are hung vertically from the horizontal long line. Buoys are used to keep the longline and socks from touching bottom. As mussels grow, more buoys are needed to maintain buoyancy in the water. At time of harvest, mussel socks can weigh around 15–30 kg. Mussels are considered to be at market size between 55–65 mm (18–24 months) (Fisheries and Oceans Canada 2003). The mussel production cycle is a very natural process that relies on few inputs, with the exception of infrastructure, and is highly reliant on suitable growing conditions and food availability in their natural ecosystem.

1.2.4 Industry challenges for mussel aquaculture

The PEI mussel aquaculture industry has experienced several challenges relating to cost of production and productivity. In PEI, the mussel monitoring program has been established by the provincial government's Department of Fisheries and Communities to monitor

mussel productivity by parameters including annual spatfall predictions and mussel meat yield. The PEI mussel monitoring program also monitors ongoing challenges including fouling, predation, and environmental stressors (Smith and Ramsay 2021). In PEI, fouling from invasive tunicates, including violet (*Botrylloides violaceus*), golden star (*Botryllus schlosseri*) vase (*Ciona intestinalis*) and club (*Styela clava*) tunicates (MacNair 2005; Locke et al. 2007; Ramsay et al. 2008, 2009) has resulted in economic losses through increased cost of maintenance by processing machines, waste removal, labor of harvesting, transporting and processing of mussels (Fisheries and Oceans Canada 2006). Predation also represents a loss for the mussel aquaculture industry particularly by diving ducks: Greater Scaup (*Aythya marila*) and Long-tailed duck (*Clangula hyemalis*) (Dionne 2004; Smith and Ramsay 2014). Diving ducks can strip mussel lines very quickly and represent a huge loss for the industry (Dionne 2004; Dionne et al. 2006; Smith and Ramsay 2014).

Suboptimal environmental conditions are also a challenge for the PEI mussel aquaculture industry. Challenges relating to the environment are associated with toxic algae blooms, high temperatures, salinity changes from extreme precipitation events, low food availability, eutrophication and hypoxia/anoxia, all of which can impact the productivity of the industry. Additionally, in PEI and surrounding Gulf of St. Lawrence, summer mass mortality events have been a documented problem for years, and have links to the overlap of high temperatures and spawning behaviour (Mallet et al. 1990; Myrand et al. 2000; Leblanc et al. 2010; Tremblay et al. 2011). Moreover, anthropogenic climate change is resulting in major fluctuations in the aquatic ecosystem and increases the risk for more frequent and prolonged stressful environmental conditions (Rhein et al. 2013; Hoegh-Guldberg et al. 2014; Bernier et al. 2018; Bindoff et al. 2019). For this reason, anthropogenic climate change is considered a major threat to the productivity of the mussel aquaculture industry.

1.3 Natural and climate change induced fluctuations in environmental conditions

Environmental and geographical properties of a marine ecosystem are highly influenced by physical and chemical properties and the Earth's spin and orbit around the sun. These physical and chemical properties drive tides, wind, currents, weather, solar radiation, etc.

which can fluctuate daily, seasonally, and geographically (Stowe 1983). However, as a result of the many anthropogenic activities occurring on earth, climate change is occurring rapidly and is having great impacts on oceans (Stowe 1983; Rhein et al. 2013; Hoegh-Guldberg et al. 2014, 2018; Bindoff et al. 2019). The main driver of climate change is the burning of fossil fuels which has resulted in an intensification of the greenhouse effect through the accumulation of carbon dioxide, methane, and nitrous oxide (Stowe 1983; Mitchell 1989; Cline 1991). The greenhouse effect is a phenomenon which occurs when solar radiation reflects shorter wave radiation (i.e. ultraviolet radiation) into the Earth's atmosphere. This requires the same amount of long wave radiation (i.e. infrared) to be radiated back to space. However, the atmosphere comprised of water vapor, carbon dioxide, ozone, and greenhouse gases are opaque to long wave radiation and trap a portion. Therefore the Earth's atmosphere reradiates some of the energy back to the Earth's surface where it can be absorbed and results in a warming effect (Stowe 1983; Mitchell 1989; Cline 1991). The greenhouse effect is a necessary process vital for Earth to stay hospitable, however, burning of fossil fuels is resulting in excessive retention of gases that result in more infrared radiation being trapped (Stowe 1983; Mitchell 1989; Cline 1991). Climate change threatens the ocean as it stores and transports excess gases and heat into water from the atmosphere and terrestrial habitat (Rhein et al. 2013). The ocean has the capacity to hold 50 times the carbon than the atmosphere, and as a result the ocean is currently absorbing 30% of carbon dioxide emissions (Rhein et al. 2013). As a result, ocean conditions are changing including: increasing temperature, decreases in dissolved oxygen (O_2), acidification, salinity fluctuations, and changes in weather patterns, nutrient cycling, etc. (Rhein et al. 2013; Hoegh-Guldberg et al. 2014; Bindoff et al. 2019).

1.3.1 Temperature

Ocean temperature is a major driver of the marine ecosystem and is highly reliant on solar radiation from the sun, which varies depending on geographical locations (Stowe 1983). For example, in the Northern hemisphere, the Earth's tilt results in great seasonal fluctuations in surface water temperature. In the winter, there is less solar radiation and daylight hours are reduced, hence colder temperatures, while in the summer it's the opposite, more solar radiation, and daylight hours (Stowe 1983). Complex interactions

between the atmosphere, ocean currents, wind, water density and weather patterns lead to natural temperature fluctuations as well (Stowe 1983).

Climate change is resulting in a warming effect due to excess radiation being trapped into the atmosphere (Stowe 1983; Mitchell 1989; Cline 1991; Rhein et al. 2013; Hoegh-Guldberg et al. 2014; Bindoff et al. 2019). Ocean temperatures have been documented to be rising at ~ 0.1 °C/decade in upper layers of the ocean (Rhein, et al. 2013) and the Atlantic Ocean basin has increased more than any other location in the world at ~ 0.3 °C/decade (Hoegh-Guldberg et al. 2014). In the Gulf of St. Lawrence, there has been an increase in average ocean temperatures, with 2012–2016 representing an 100 year record breaking period (Bernier et al. 2018).

1.3.2 Salinity

Salinity in the marine environment is driven mostly by physical processes including evaporation, runoff and precipitation events (Stowe 1983). Coastal environments are more susceptible to fluctuations in salinity (Stowe 1983). In the intertidal zone, water evaporation can increase salinity, while precipitation events can reduce salinity (Geng et al. 2016; Geng and Boufadel 2017). In the subtidal zone and estuaries, tidal fluctuations, spring freshets, and heavy precipitation events can result in fluctuations in salinity (Schmitt 2008; MacCready and Geyer 2010). There are also regional salinity impacts, such as increases in surface salinity in tropical environments from evaporation, while areas with higher precipitation containing lower salinity (Stowe 1983).

Climate change is projected to result in long-term and short-term deviations in salinity. Long-term salinity changes differ depending on geographic location. For example, in the Atlantic Ocean, salinity is increasing from evaporation, while locations in the Pacific Ocean have become less saline from precipitation and runoff (Rhein et al. 2013; Hoegh-Guldberg et al. 2014). Furthermore, melting of sea and glacial ice will also impact ocean salinity (Hoegh-Guldberg et al. 2018). Short term changes are associated with heavy precipitation events, run-off, and flooding (Hoegh-Guldberg et al. 2018). It is anticipated that climate change will strengthen hydrological cycles, from an increase in temperature that results in more saturation in vapor pressure (Held and Soden 2006; Rush et al. 2021).

In Atlantic Canada, precipitation events were reported to have increased ~ 10% between 1948–1995 (Lewis 1997). Extreme precipitation events are projected to increase in Canada, and under high emission projections, extreme events that used to occur once in 20 years will increase to once in five years (Zhang et al. 2019). In addition, the combination of increasing sea levels and tropical cyclones in the US Atlantic has been found to be associated with increased risk of flooding (Marsooli et al. 2019). In the Gulf of St. Lawrence, it is predicted that runoff from precipitation will result in a decline in salinity (Lambert et al. 2013; Long et al. 2016).

1.3.3 Dissolved oxygen

Dissolved oxygen concentrations are driven by several natural factors and as a result O_2 fluctuates regionally, seasonally, and by depth. Dissolved oxygen can enter the marine environment through mixing with the atmosphere in surface waters, or through autotrophic production (Fennel and Testa 2019). In the intertidal zone, tides result in rapid and frequent changes in O_2 through diel oxygen cycling in tide pools which can lead to supersaturation of O_2 in the day, and depletion of oxygen at night through autotrophic consumption of oxygen (Grieshaber et al. 1994). In coastal ecosystems, O_2 reduction can be induced by stratification conditions (Rabalais et al. 2010). Stratification can develop through density changes in water; either through temperature, salinity, or a combination of the two (Rabalais et al. 2010). Temperature stratification can develop during prolonged periods of high temperature, when the upper layer of the water column is calm and has a lower density than the bottom levels of the water column (Grieshaber et al. 1994). Salinity stratification can develop when low saline water interacts with high saline water, such as when two currents meet and cause an overlay of the two sources (Grieshaber et al. 1994). Salinity stratification can also develop during heavy precipitation events when freshwater rapidly accumulates at the surface (Tweedley et al. 2015; Fennel and Testa 2019). During a stratification event, the upper layer of the water column has a higher O_2 content than the bottom layers, due to air-water exchange and high abundance of autotrophic organisms such as phytoplankton (Fennel and Testa 2019). In contrast, the bottom layer contains more heterotrophic bacteria which consume O_2. When stratification occurs and vertical mixing of the upper layer and bottom layer doesn't occur, then O_2 depletion occurs leading to

hypoxia or anoxia in the bottom layers of the water column (Verity et al. 2006; Rabalais et al. 2010). Coastal hypoxic conditions are usually seasonal in nature and will end once vertical mixing occurs between the two layers of different densities in the water column (Fennel and Testa 2019). There are a few exceptions to this rule, where permanent stratification has occurred, such as in the Baltic Sea and the Laurentian Channel in the Gulf of St. Lawrence (Fennel and Testa 2019). There are also locations with long-term low O_2 concentrations within the mid-layer (100–1200 m depth) of the ocean, which are called oxygen minimum zones (Rabalais et al. 2010). Oxygen minimum zones form through a combination of factors including having highly productive upper layers, longstanding water with a high mass age and low circulation (Rabalais et al. 2010). While oxygen minimum zones typically persist for years to decades, natural cycles can cause O_2 levels to fluctuate (Kamykowski and Zentara 1990; Helly and Levin 2004; Paulmier and Ruiz-Pino 2009). For example, upwelling is common in oxygen minimum zones which results in higher heterotrophic/autotrophic concentrations thereby increasing O_2 demand and depleting surrounding O_2 seasonally (Helly and Levin 2004).

Climate change is causing an overall decline in O_2 and increases in events that lead to hypoxia/anoxia (Rabalais et al. 2010). It has been found that the open ocean lost between 0.5–3.3% of dissolved oxygen between 1970–2010 from the ocean surface, and is predicted to continue to decline by 3.2–3.7% by 2081– 2100 (Bindoff et al. 2019). There are several anthropogenic factors contributing to declining O_2 concentrations in the marine environment. Temperature is expected to increase as a result of climate change, and as that occurs O_2 solubility declines (Deutsch et al. 2011; Robinson 2019). Increasing sea surface temperature and stronger weather-related events due to climate change has increased stratification and reduction of dissolved O_2 in bottom layers of the ocean, while disrupting the productivity of autotrophic and heterotrophic microscopic organisms (Hoegh-Guldberg et al. 2014; Robinson 2019). Increases in carbon dioxide (CO_2) and temperature, intensify productivity of autotrophic organisms such as phytoplankton, which leads to more organic material being produced, and increases microbial respiration (Robinson 2019). These climate change driven phenomena are made worse by increased organic matter from anthropogenic activities such as fertilizer runoff and sewage/industrial waste discharge into

aquatic environments leading to eutrophication in coastal ecosystems. This eutrophication leads to rapid localized growth in phytoplankton and microbial populations, and results in further exasperated hypoxic or anoxic events (Rabalais et al. 2010; Tweedley et al. 2015).

Anthropogenic factors have been found to frequently contribute to hypoxic/anoxic events in coastal systems of estuaries and inner-continental shelves (Rabalais et al. 2010). Increases in hypoxic events have led to the spread of dead zones (Diaz and Rosenberg 2008). Additionally, oxygen minimum zones have been found to be increasing in size and may have a link to climate change (Matear et al. 2000; Stramma et al. 2008; Rabalais et al. 2010). Climate change is also predicted to increase upwelling of oxygen minimum zones as well (Keeling et al. 2010; Kämpf and Chapman 2016).

1.3.4 Ocean chemistry/acidity

The atmosphere is made up of ~ 78% Nitrogen (N_2), ~ 21% O_2, ~ 1% argon (Ar), and all other gases are extremely low in abundance, including carbon dioxide (CO_2), which is 0.03% of the atmosphere (Stowe 1983). In contrast, the ocean has a much higher capacity to dissolve CO_2. When one molecule of carbon dioxide CO_2 is dissolved in water it combines with one water molecule (H_2O) to form carbonic acid (H_2CO_3), which disassociates to a hydrogen ion (H^+) and bicarbonate (HCO_3^-) or $2H^+$ and carbonate (CO_3^{2-}) (Stowe 1983). In normal oceanic conditions ~ 90% of CO_2 dissociates to the H^+ and HCO_3^- form and other elements balance out the H^+, which results in a pH of between 7.5 (deep water) to 8.4 (surface water), with an average of pH ~ 7.8. Buffering of seawater occurs by interactions between calcium ions (Ca^{2+}), which interact with CO_3^{2-} to form calcium carbonate ($CaCO_3$), and H^+ with CO_3^{2-} to form HCO_3 (Stowe 1983).

Approximately, 30% of the excess CO_2 being produced through human activity is being absorbed into the ocean (Hoegh-Guldberg et al. 2014), altering seawater equilibrium (Rhein et al. 2013). When excess carbon dioxide is absorbed into the water, a chemical reaction occurs where it is transformed into carbonic acid, which causes the pH of the ocean to decrease and increase CO_3^{2-} and HCO_3^- concentration (Rhein et al. 2013; Hoegh-Guldberg et al. 2014). This influx reduces saturation of calcium carbonate (Rhein et al. 2013), such as calcite and aragonite. Currently, the ocean pH levels have decreased ~ 0.1

units from ambient seawater conditions since the beginning of the industrial revolution (~ 1900 to 2010), and future projection indicate that ocean pH levels will drop additionally by a range of 0.14–0.43 units by 2100 (Hoegh-Guldberg et al. 2014).

1.3.5 Nutrient cycling and phytoplankton

The predominant ocean nutrients are nitrogen (N) and phosphorus (P) (Stowe 1983). These nutrients form the basis of the food chain, where the recycling of nutrients is critical for life. For example, N cycles begin when fecal matter or dead organisms sink to the bottom of an ecosystem (Stowe 1983). Then, decomposition occurs by N fixing bacteria and results in the formation of ammonia (NH_3) and nitrite (NO_2^-) which gets converted to nitrate (NO_3^-) that is utilized by autotrophic organisms (Stowe 1983). Nutrients are often found in sediments at the bottom layer of the water column and need to be brought to the surface where autotrophic organisms live. This often occurs with upwelling, when complex wind-driven currents bring nutrient rich water to surfaces (Kämpf and Chapman 2016). Upwelling typically occurs along continental shelves (Rabalais et al. 2010) and follows seasonal cycles, where nutrients fluctuate along with autotrophic and heterotrophic productivity (Farías and Cornejo 2007; Kämpf and Chapman 2016).

Climate change threatens nutrient cycling through increased stratification, resulting in reduced nutrient mixing in surface waters (Bindoff et al. 2019; Henson et al. 2021). In addition, anthropogenic activities that cause nutrient loading in water and atmospheric nitrogen emissions may result in disruption of N:P balance and result in P limitation (Bindoff et al. 2019). In the Northwest Atlantic Ocean, many locations have seen occurrences of lower nutrient concentration compared to the long-term mean for the region in the past two decades (Bernier et al. 2018).

Phytoplankton concentrations are directly impacted by changes in nutrient levels (Bindoff et al. 2019). Changes in phytoplankton distribution will likely be impacted regionally, but the global trend is predicted to result in the decline of primary producing organisms (Bindoff et al. 2019). Models predict that many species of phytoplankton will make a poleward shift into the North Atlantic Ocean, which will alter community structure and food webs in the region (Barton et al. 2016). In the Northwest Atlantic, phytoplankton

concentrations declined from 1999–2011, which was followed by a recovery period by 2015, and a decline again as of 2016 (Bernier et al. 2018). Anthropogenic nutrient loading from coastal runoff in areas with agriculture has also been found to be a concern in Canadian aquatic ecosystems. Runoff particularly from fertilizer in the form of N and P have been found to result in algae growth and eutrophication (Drury et al. 2016; Reid et al. 2016). Risk assessment by Agriculture and Agri-Food Canada (2016) indicates that the Atlantic Canada region has a moderate to very high risk to water contamination from residual N and low to moderate risk by P in agriculture areas (Drury et al. 2016; Reid et al. 2016). Risk of contamination is highly dependent on weather, and under climate change projections more extreme precipitation events are expected, resulting in an increase in risk of coastal eutrophication (Bindoff et al. 2019).

1.4 Stress response in the blue mussels

Mussels have evolved specialized stress pathways, which has allowed them to survive many mass-extinction events. For example, the order Mytilida (true mussels), was able to survive the Permian-Triassic mass extinction (~ 252 million years ago). The Permian-Triassic was the result of high temperatures and persistent anoxia in the marine environment which wiped out ~ 90% of marine organisms (Song et al. 2014). Mussels' ability to survive means that they have evolved capabilities to adapt in a wide range of environmental stressors. The following section is an overview of stress response adaptations that mussels and other bivalves have acquired to tolerate various environmental stressors.

1.4.1 Behavioural responses

Mussels modify their filtering behaviour and valve gape in response to environmental stress. Valve closure (partial or full closure) and cessation of filtering feeding behaviour can occur in response to environmental cues including: fluctuation in salinity (Gilles 1972; Shumway 1977; Davenport 1979a; Lajus and Sukhotin 1998; Sukhotin et al. 2003; Bayne 2017), low or high food availability (Riisgård and Larsen 2015), hypoxia/anoxia (Wang and Widdows 1993), aerial exposure (Mcmahon 1988; Dowd and Somero 2013), toxins (copper, zinc, cadmium and crude oil) (Davenport and Manley 1978; Redpath and

Davenport 1988; Redmond et al. 2017), and predators (Clements et al. 2020). Valve closure and cessation of filtering behaviour can be associated with metabolic decline and energy conservation particularly in the case of low food availability, hypoxia/anoxia, where energy acquisition is impacted (Jørgensen et al. 1986a, 1986b; Mcmahon 1988; Riisgård et al. 2003; Poulain et al. 2011). In conditions with high food availability, salinity fluctuations, toxins, and predators, the change in filtering behaviour is a protective mechanism to keep the stressor out and mitigate the impacts. In contrast, acute temperature stress has been found to increase filtering behaviour, likely as a mechanism to meet increased metabolic demands, until a critical temperature has been reached (Torossian et al. 2020). Mussels exposed to air have also been found to gape and/or "air gulp" to trap O_2 in their shells to help prolong aerobic respiration (Lent 1968; Coleman and Trueman 1971; Booth et al. 1984).

Mussels can reduce their attachment behaviour via byssal threads in response to environmental stress including hypoxia/anoxia (Wang et al. 2013; Sui et al. 2015), acidification (Li et al. 2015b; Sui et al. 2015; Lassoued et al. 2019), food availability (Babarro et al. 2008; Lassoued et al. 2019) and temperature stress (Van Winkle 1970; Clements et al. 2018). Production of byssal threads is an energy demanding process, therefore, reducing production likely represents energy conservation (metabolic rate depression) (Shin et al. 2009; Wang et al. 2013), or detachment behaviour to move away from stressful environmental conditions (Fisheries and Oceans Canada 2003; Sui et al. 2015). In contrast, other environmental cues increase byssal thread production such as wave action (Babarro and Carrington 2013; Garner and Litvaitis 2013), and predator presence (Reimer and Tedengren 1997; Garner and Litvaitis 2013; Li et al. 2015b). Mussels also utilize vertical byssal thread attachment behaviour to prevent or un-bury themselves out of bottom sediment (Hutchison et al. 2016).

1.4.2 Cellular stress response mechanisms

During initial stress stimuli and subsequent response, transcription factors are recruited to mediate the mechanisms necessary to survive cellular stress in all metazoan organisms (Kültz 2020). There are many families of transcription factors. One of the largest and oldest superfamilies of transcription factors is of basic leucine zipper family (bZIP), which is

involved with cell proliferation, differentiation, stress response and homeostasis (Jindrich and Degnan 2016; Kültz 2020). There are many subfamilies of bZIP transcription factors including: activating transcription factor (ATF), protease-activated receptors (PAR), X-box binding protein 1 (XBP1), old astrocyte specifically induced substance (OASIS), cAMP-response element binding protein (CREB), CCAAT/enhance-binding proteins (C/EBP), nuclear factor erythroid 2 (NFE2), small musculoaponeurotic fibrosarcoma (SMAF), FOS proto-oncogene (FOS), JUN proto-oncogene (JUN), etc, (Reinke et al. 2013). In mussels, many bZIP transcription factors are expressed in response to stress. Mussels (*Mytilus californianus*) have been found to express JUN, FOS, and C/EBP during stretches of low cardiac activity and is hypothesized to result in anaerobic respiration (Gracey and Connor 2016). The mussel (*Mytilus coruscus*) has also been found to express the bZIP transcript factor: NFE2 in association with pollution (benzo(a)pyrene), which is known to trigger antioxidant defence (Qi and Tang 2020). Toxic dinoflagellate exposure has also been found to increase NFE2 expression in green mussels *(Perna viridis*) (Dou et al. 2020). Transcription factors in the bZIP family are responsible for activating genes involved in survival. For example, NFE2 regulates antioxidant production by activating the antioxidant response, which causes gene expression of enzymes such as catalase (CAT), superoxide dismutase (SOD), Glutathione peroxidase (GPX), Glutathione S-transferase (GST), thioredoxin, and peroxiredoxin (Kaspar et al. 2009).

Hypoxia inducible factor (HIF) is another group of transcription factors that are specifically stimulated in the presence of low oxygen. In invertebrates, HIF is responsible for restoring homeostasis and energy in the absence of O_2 through upregulation of anaerobic pathways and increasing oxygenation (Gorr et al. 2006). In the Mediterranean mussel *(Mytilus galloprovincialis*) HIF is expressed in aerial exposure, which results in intracellular hypoxia (Giannetto et al. 2015). Bivalve HIF also has a role as a transcription factor, O_2 sensing and adaptation to hypoxic conditions (Giannetto et al. 2015; Artigaud et al. 2015; Kotsyuba 2017).

Heat shock factors (HSF) are another important family of transcription factors. During a normal cellular state HSF form a complex with heat shock proteins and other chaperones but disassociate when cellular stress is present. Activated HSF initiate gene expression of

heat shock proteins (Kassahn et al. 2009). Heat shock factors are usually activated in response to elevated temperatures, but are also activated by many other stressors. While few studies on bivalves have discovered expression of HSF, many studies on mussels have found over-expression of HSP in response to stressors (i.e. Chapple et al. 1998; Lockwood et al. 2010; Tomanek and Zuzow 2010; Negri et al. 2013; Péden et al. 2014; Nielsen et al. 2021; Clark et al. 2021; Barrett et al. 2022).

Other transcription factors such as nuclear factor κB (NF-κB) have been found to be involved with inflammation, immune response and proliferation in vertebrates (Mitchell and Carmody 2018). Studies in bivalves including mussels have found NF-κB expressed in association with immune response and toxin exposure (Canesi et al. 2006; Meng et al. 2020; Saco et al. 2021). The p53 protein is an important transcription factor associated with control over cell cycle and apoptosis in vertebrates, and has a major role in cancer in vertebrates (Belyi et al. 2010). In the mussel (*M. edulis)* p53 has been over-expressed after exposure to lead and zinc oxide and therefore may have a similar role in mussels as in vertebrates (Guerreiro et al. 2018; Wu et al. 2021). FoxO transcription factors are also involved in gene expression associated with metabolism, cell cycle arrest, differentiation, detoxification, DNA damage and apoptosis in vertebrates (Salih and Brunet 2008). While vertebrates have four gene isoforms associated with FoxO transcription factors, only one has been found in invertebrates (Kültz 2020). While little is known about its expression in bivalves, recent research implicates a role in growth control in Pacific oysters (*Crassostrea gigas*) (Li et al. 2021).

Transcription factors ultimately result in the expression of genes that are involved with homeostasis and protection mechanisms, which are prioritized over other proteins during times of stress (Feder et al. 1992; Chapple et al. 1998; Kültz 2020). It is vital that proteins are folded in three dimensional shapes to function correctly in biological systems (Vabulas et al. 2010; Zhang et al. 2016). However, cellular stress can result in accumulation of misfolded and damaged proteins. Cells have an amazing capacity to control the quality of proteins. The endoplasmic reticulum (ER) is the site of protein synthesis and quality control. During stressful conditions, the ER can signal that it's under stress and this results in the appropriate level of response, which either results in protective mechanisms or

apoptosis (Salminen and Kaarniranta 2010). The ER has three types of stress transducers: protein kinase R-like ER kinase (PERK), activating transcription factor 6 (ATF6), and inositol-requiring enzyme 1 (IRE1). These transducers ultimately lead to the unfolded protein response that can lead to responses such as the expression of NF-κB, inhibition of protein synthesis, metabolism changes, and induction of apoptosis pathways (Salminen and Kaarniranta 2010). Protein damaged by stress results in the expression of molecular chaperones. Molecular chaperones (ie. HSP) are often over-expressed, to help stabilize and refold damaged proteins back to their original conformation (Vabulas et al. 2010). Numerous experiments on environmental stress in mussels have found the induction of HSP including: temperature (i.e. Chapple et al. 1998; Lockwood et al. 2010; Tomanek and Zuzow 2010; Negri et al. 2013; Péden et al. 2014; Nielsen et al. 2021; Clark et al. 2021; Barrett et al. 2022), salinity (ie. Tomanek et al. 2012), hypoxia/anoxia (i.e. Halpin et al. 2004; Gracey et al. 2008; Anestis et al. 2010), toxins/pollution (i.e. Hamer et al. 2004; La Porte 2005; Liu et al. 2014, 2016), and pathogen presence (i.e. Wu et al. 2013). However, when the amount of protein damage exceeds capacity to fix it, then it may result in degradation by the ubiquitin–proteasome system and lysosomal autophagy system (Kültz 2020).

Antioxidant systems have also evolved to prevent oxidative damage of proteins and other macromolecules (ie. DNA and RNA) (Kültz 2020). Free radicals in the form of reactive species (reactive oxygen species (ROS), reactive nitrogen species (RNS), reactive sulphur species (RSS)) are often formed during stress and interact with proteins and macromolecules that have electrophilic side chains, ultimately causing damage (Kültz 2020). There are many sources of reactive species associated with stress. Increases in metabolism can cause increased formation of ROS on the mitochondrial electron transport chain (ETC). In addition, lipid peroxidation, arachidonic acid metabolism, respiratory bursts, and stress induced cellular oxidases (i.e. through processes like purine metabolism) can produce ROS during stress (Nappi and Ottaviani 2000; Kültz 2020; Furuhashi 2020). The role of antioxidant systems is to enzymatically convert ROS (O_2^-, H_2O_2, HO^-) to a more stable form that does not cause oxidative damage. For example, SOD converts O_2^- to H_2O_2, which is then used to oxidize substrates by peroxidases or converted to water by

CAT (Storey 1996; Abele and Puntarulo 2004). In addition, metals (such as iron or copper) can easily cause the transition of H_2O_2 to HO^- through Fenton reactions which are highly damaging. To avoid this, metal binding enzymes known as metallothioneins accumulate in tissues and bind to metals, which makes them unavailable to react with ROS (Halliwell and Gutteridge 1999; Freire et al. 2011). Mussels can increase their antioxidant capacity in response to stress caused by environmental conditions including: temperature changes (i.e. Lesser et al. 2010; Fernández et al. 2010; Matozzo et al. 2013; Hu et al. 2015; Coppola et al. 2017, 2018; Rahman et al. 2019; Andrade et al. 2019; Freitas et al. 2019; Leite et al. 2020; Khan et al. 2021), acidification (i.e. Matozzo et al. 2013; Hu et al. 2015; Khan et al. 2021), food availability (i.e. Solé et al. 1995; Lesser et al. 2010; Dowd et al. 2013), toxins/pollution (i.e. Solé et al. 1995; Fernández et al. 2010; Attig et al. 2014; Coppola et al. 2017, 2018; Freitas et al. 2019; Leite et al. 2020), pathogen presence (i.e. Canesi et al. 2010; Wu et al. 2013), salinity stress (i.e. Matozzo et al. 2013; Freitas et al. 2019), and hypoxia/anoxia (i.e. Andrade et al. 2019; Khan et al. 2021) .

In addition to chaperones and antioxidant systems, there are also chemical cytoprotective metabolites that are involved with the structural and functional homeostasis of cells, which stabilize proteins and membranes (Kültz 2020). These compounds are considered organic osmolytes and include amino acids, polyols, sugars, methylamines, and methylsulfonium, and urea (Yancey 2005). Mussels are osmoconformers and maintain intra- and extracellular osmolyte concentrations that are isosmotic or slightly hyperosmotic with their aquatic environment (Gilles 1972; Zurburg and De Zwaan 1981; Yancey 2005). Osmolytes are hypothesized to be neutral in that they don't interact with macromolecules, and therefore don't disturb cellular function. However, these osmolytes are not inactive and can protect cells, act as antioxidants, protect against hypoxia, and may stabilize macromolecules (Yancey 2005). It has been found that mussels (*M. edulis*) accumulate the amino acids glycine and taurine in tissues in response to hypoxia, which could be related to protective mechanisms associated with these amino acids (Haider et al. 2020a). Osmolytes are also impacted by stressors such as temperature and salinity (Yancey 2005). In mussels the best-known mechanism that osmolytes protect against stress is during a change in salinity, which results in a change in osmolality. After a change in osmolality in extracellular fluid,

mussels will osmoconform by an increase or decrease of water into the cells resulting in cell swelling or shrinking (Florkin 1962; Freire and Sampaio 2021). Euryhaline bivalves such as mussel (*M. edulis*) can prevent cell rupture or shrinkage by maintenance of osmolytes within cells (Yancey 2005). Membranes can also restructure to prevent cell damage in stressful environmental conditions. Changes in temperature and salinity have been found to result in the changes of phospholipid content (Nemova et al. 2013). In blue mussels (*M. edulis*) temperature increases has been found to decrease unsaturation index in gills (Pernet et al. 2007), while hyposalinity also results in changes in lipid structure to aid in fluidity of membranes in response to osmoconformation processes (Nemova et al. 2013).

If stress results in irreversible cellular damage, apoptosis will occur. Apoptosis is a highly important process that causes programmed cell death, and occurs during development/aging, or as a response to cell damage from pathogens or stress (Romero et al. 2015). In molluscs, there are two pathways for apoptosis (1) extrinsic (death receptor pathway) (2) intrinsic (mitochondrial pathway). Caspases (cysteine-dependent aspartate-directed proteases) are an important component of apoptosis and can either be classified as initiators (ie. caspase 2, 8, 9, 10), effectors (caspase 3,6,7) or inflammatory (caspase 1, 4, 5) (Romero et al. 2015). In the Mediterranean mussel (*M. galloprovincialis*) the initiator caspase for apoptosis (caspase-2 and caspase-8) have been described (Romero et al. 2011). Effector caspases (caspase-3) have also been found in mussels (*M. galloprovincialis*), and upregulated in response to acute exposure to thermal stress and heavy metals (Kefaloyianni et al. 2005). Caspases are activated and either undergo extrinsic or intrinsic apoptosis pathways. The extrinsic pathways involves activation of the death domain, which is in the tumor necrosis factor (TNF) gene family that activates caspases (Romero et al. 2015). In mussels (*M. edulis*) the TNF-α has been identified, and has been found activated by lipopolysaccharide-induced TNF-α (Philipp et al. 2012). In contrast, the intrinsic pathway is activated by the absence of growth factors, hormones, cytokines, or presence of ROS and RNS, DNA damage, ER stress, UV radiation, pathogens, or environmental pollutants/toxins (Romero et al. 2015). This stimuli results in mitochondrial damage and the release of pro-apoptotic proteins such as cytochrome c, apoptosis inducing factor and

IAP binding protein, and is under control by Bcl-2 family, and Bax inhibitor-1 which have been characterized in mussels (*M. galloprovincialis*) (Romero et al. 2011; Châtel et al. 2011; Estévez-Calvar et al. 2013). The p53 transcription factors have a role in regulating the Bcl-2 family (Romero et al. 2015). Ultimately the process of apoptosis results in the removal of dying cells by the process of phagocytosis by surrounding cells (Romero et al. 2015). In mussels, apoptosis has been found activated in response to maintaining homeostasis, and associated with several stressors including pathogens (Romero et al. 2011), pollution/toxins (Pruski and Dixon 2002; Romero et al. 2011; Granger Joly de Boissel et al. 2017), hypoxia (Falfushynska et al. 2020), temperature stress (Yao and Somero 2012).

1.4.3 Immune system

Bivalve molluscs are filter feeding organisms that utilize filtration for their main feeding and respiratory mechanisms (Gosling 2003). In relation to these mechanisms, water is constantly being brought in through the gills into their body cavity. Therefore, mussels rely on a healthy ecosystem and clean water, because bacteria, virus, pesticide, industrial waste, toxic metal and petroleum derivatives present in the water can become retained inside the bivalve's internal cavity and impact their health (Song et al. 2010).

Haemolymph, the circulating fluid of bivalves, has an active role in gas exchange, osmoconformation, nutrient distribution, waste elimination and internal defence. Like all invertebrates, bivalve molluscs only contain an innate immune system. The cellular components of haemolymph are haemocytes, and they form the cellular components involved in immune responses (Song et al. 2010). The haemocytes are classified into two categories, hyalinocytes and granulocytes. Granulocytes are further classified into eosinophilic and basophilic cells (Song et al. 2010).

Immune recognition is mediated through pattern recognition receptors (PRRs), that bind to pathogen-associated molecular patterns (PAMPs) and are either secreted, membrane-bound, or cytosolic PRRs (Song et al. 2010). Immune cells produce secreted PRRs, which circulate in haemolymph and tissues waiting to encounter non-self molecules. Secreted PRRs include Complement 1 (C1q) domain-containing proteins, C-type lectins,

fibrinogen-related proteins, galectins, R-type lectins, F-type lectins, Gram-negative binding protein , apextrin- related proteins and thioester-containing proteins (Song et al. 2010; Gerdol and Venier 2015). The second type of PRRs in bivalve molluscs are membrane-bound, which are found in cell membranes of immune cells, either externally or internally. Membrane-bound PRRs appear to be less abundant compared to the secreted forms, and examples include toll-like receptors, peptidoglycan recognition proteins, and scavenger receptor cysteine-rich superfamily (Gerdol and Venier 2015). The third type of PRR in bivalve molluscs are cytosolic, these are PRRs that are found within the cytosol of haemocytes. Examples of cytosolic PRRs include NOD-like receptors (NLRs) and retinoic acid inducible factors (Gerdol and Venier 2015).

Ultimately, the role of PRRs in the immune system is to aid in activation, by binding to PAMPs, and then stimulating the innate immune system to respond. Transcription factors are often upregulated through pathways such as NF-κB, interferon-regulatory factors (IRFs). These transcription factors lead to the expression of inflammatory cytokines, chemokines, and antimicrobial peptides being produced that stimulate an immune response. There are many types of antimicrobial peptides in bivalves. For example, in the *Mytilus sp.* antimicrobial peptides include defensins, big defensins, mytilins, mytichitins, myticins, and mytimycins (Gerdol and Venier 2015).

Once activation of the immune system has occurred through PRRs, recruitment of haemocytes to the site of infection occurs. Haemocytes can respond to infection in a variety of ways, but most commonly through phagocytosis or encapsulation (Song et al. 2010). Phagocytosis is a process of recognizing, engulfing and degrading of non-self molecules/organisms through merging of lysosomes with phagosomes. Target molecules/organisms are destroyed in phagolysosomes through enzymes, ROS, and nitric oxide (NO) via respiratory bursts (Song et al. 2010). Additionally, phagocytosis can be enhanced by other hemolymph factors such as lectins and antimicrobial peptides. If the molecules/organisms are too big to undergo phagocytosis, the haemocytes use encapsulation. In the process of encapsulation, haemocytes surround the foreign molecule and release cytotoxic enzymes and free radicals which act to destroy non-self molecules/organisms (Song et al. 2010).

Mucous is highly important in the immune system of mussels and all bivalves, as it lines the majority of pallial surfaces and digestive tract of bivalves (Allam and Pales Espinosa 2016). Along the pallial surfaces and digestive tract the mucous acts as an important barrier, that contains glycoprotein cross-links that traps microorganisms (Russell et al. 2015; Allam and Pales Espinosa 2016). Gill mucous also contains many immune effectors including lectins, C1q-domains, thioester-containing proteins, lysozymes, proteases and protease inhibitors (McDade and Tripp 1967; Brun et al. 2000; Pales Espinosa et al. 2016; Allam and Pales Espinosa 2016)

While mussels launch an immune response when exposed to pathogens, other environmental stressors may also influence expression. For example, toxic algae (*Prorocentrum minimum*) trigger an inflammatory response and increase diapedesis of haemocytes into the alimentary canal. However, this response eventually depletes haemocytes and leaves mussels immunocompromised (Galimany et al. 2008). Increases in temperature can change the microbiome of mussels, leaving them more exposed to opportunistic pathogens (Li et al. 2018, 2019). Environmental stress can also impact haemocytes and immune factors. Rahman et al. (2019) demonstrated that exposure to high temperatures in mussels significantly increased haemocyte levels and phagocytic activity during the period of temperature stress (Rahman et al. 2019). In contrast, other research has found that mussel immune response is compromised during environmental stress including low salinity (Wu et al. 2018), low food availability (Delaporte et al. 2006; Xu et al. 2008; Parisi et al. 2017), hypoxia/anoxia (Pampanin et al. 2002; Matozzo et al. 2005; Chen et al. 2007a, 2007b; Wang et al. 2011a, 2012b), and ocean acidification (Wu et al. 2018).

1.4.4 Anaerobiosis

Mussels, like most bivalves, have the ability to utilize anaerobic respiration strategies in association with prolonged valve closure (i.e. aerial exposure), hypoxia/anoxia or when aerobic respiration is not sufficient to handle metabolic demand (Sokolova 2013). Anaerobiosis occurs through several substrate-level phosphorylation mechanisms so that enough adenosine triphosphate (ATP) can be produced to maintain a baseline energy requirement for survival. One of the first anaerobic mechanisms that can be utilized is

through the production opines including octopine, strombine, and alanopine (De Zwaan and Wijsman 1976; De Zwaan et al. 1982; De Zwaan 1983, 1991; Grieshaber et al. 1994; Müller et al. 2012). The production of opines occurs when pyruvate is condensed through dehydrogenases with the addition of an amino acid and reduced using NADH (Figure 1). For example, octopine is produced using pyruvate and arginine, while strombine is produced with pyruvate and glycine (Guyon et al. 1980; Müller et al. 2012). The net reaction of this pathway is 2 moles of ATP for every mole of glucose/glycogen used. Opines are stored and not excreted as they can be oxidized back to their original state once aerobic conditions return, and this is very beneficial as bivalves maintain a large supply of free amino acid for their osmotic balance (De Zwaan and Wijsman 1976; Grieshaber et al. 1994; Müller et al. 2012).

The second mechanism, and the most important pathway in bivalve anaerobiosis, is through the production of malate (De Zwaan 1983, 1991; Tielens 2000; Müller et al. 2012). There are two mechanisms to produce malate. The first involves transamination of pyruvate to form alanine using an amino group from aspartate (deamination). The deamination of aspartate results in the formation of oxaloacetate, which is reduced to malate (Collicutt and Hochachka 1977; De Zwaan et al. 1981; De Zwaan et al. 1982; Foreman and Ellington 1983; De Zwaan et al. 1983; De Zwaan 1991; Larade et al. 2002) (Figure 1). This type of malate dismutation often coincides with the production of opines but ceases once aspartate pools have been depleted (De Zwaan 1983, 1991). The second method of malate production uses phosphoenolpyruvate. Phosphoenolpyruvate is the last product produced before pyruvate in glycolysis; however, in anaerobic modifications phosphoenolpyruvate can be converted directly to oxaloacetate and then reduced to malate by re-oxidizing NADH (De Zwaan 1983, 1991; De Zwaan et al. 1983; Tielens 2000; Müller et al. 2012) (Figure 1). This type of malate production is associated with prolonged periods of hypoxia/anoxia and there is a gradual shift to this type of malate production if anaerobic conditions persists and aspartate pools become depleted.

Malate, regardless of the production method, is then transported into the mitochondria where it undergoes malate metabolism (De Zwaan and Wijsman 1976; De Zwaan 1983; De Zwaan 1991; Tielens 2000; Müller et al. 2012). This can occur via two pathways:

through the oxidation of malate to pyruvate, or through malate dismutation and reversal of the Krebs cycle to form succinate. The malate oxidation pathway produces pyruvate from malate oxidation, then pyruvate is oxidized to acetyl-coA by pyruvate dehydrogenase. Finally, coenzyme A (CoA) from acetyl-CoA is removed and acetate is produced as an end-product (De Zwaan and Wijsman 1976; De Zwaan et al. 1981; De Zwaan 1983; De Zwaan 1991; Tielens 2000; Müller et al. 2012) (Figure 1). The net production of this substrate level phosphorylation results in 1 mole of ATP and 2 moles of NADH through malate oxidation.

The second method of malate metabolism involves reversing the Krebs cycle, where malate is converted to fumarate, then reduced to succinate. The reduction of succinate only occurs through the transfer of electrons from NADH, which is produced in the first malate oxidation step. This reduction is completed through a modified ETC, where complex I (NADH reductase) and II (fumarate reductase) is utilized. Complex I removes electrons from NADH with rhodoquinone completing the transport to Complex II, which then transfers electrons to fumarate and causes a reduction to succinate (Figure 1) (Holwerda and De Zwaan 1980; De Zwaan et al. 1981; Schulz and Kluytmans 1983; De Zwaan et al. 1983; De Zwaan 1991; Grieshaber et al. 1994; Van Hellemond et al. 1995; Tielens 2000; Müller et al. 2012). During prolonged periods of hypoxia/anoxia, succinate undergoes a cyclic transformation to propionate and creates 1 additional mole of ATP (Figure 1). This reaction takes time to complete in the blue mussel *M. edulis,* in which it has been found to take 16 hours at 12 °C in anoxic conditions (Kluytmans et al. 1977). Overall, it has been found that the addition of malate dismutation pathways create 2.14 times higher ATP yield compared to traditional glycolysis pathways (De Zwaan 1983, 1991).

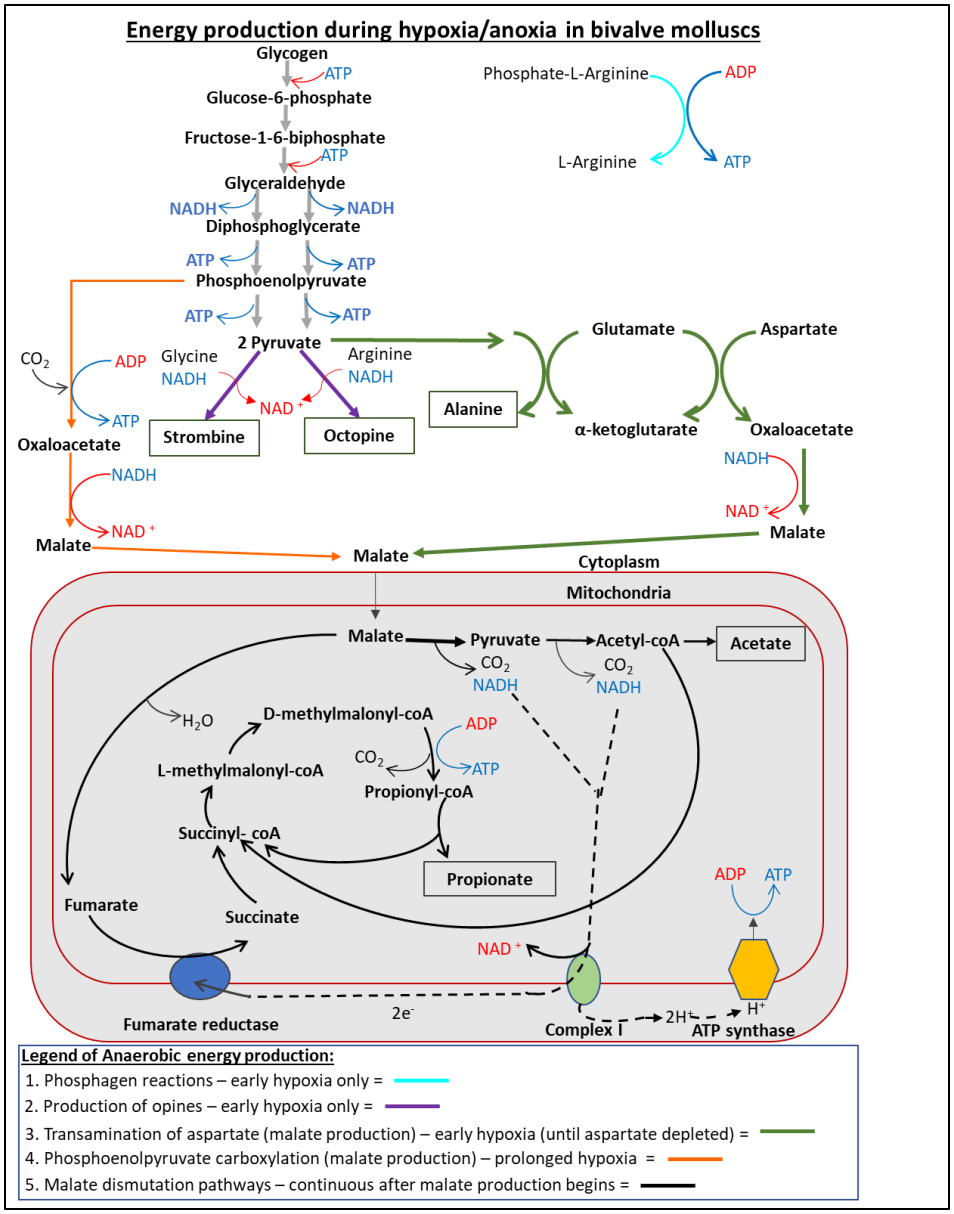

Figure 1. General anaerobic pathways in bivalve molluscs. This map is redrawn based on the data reported by De Zwaan 1991; Grieshaber et al. 1994; Müller et al. 2012. 1. Phosphagens provide a source of ATP during early hypoxia. 2. Opine production via glycolysis occurs during early hypoxia only. 3.Transamination of aspartate forms malate in early hypoxia until aspartate is depleted. 4. Phosphoenolpyruvate is converted to malate during prolonged hypoxia/anoxia. 5. Malate production occurs in two ways concurrently. Electron transport chain utilizes fumarate as terminal electron acceptor with rhodoquinone completing the electron transport to fumarate reductase, which transforms fumarate to succinate. Complex 1 = NADH reductase. Blue arrows/font = higher energy state, Red arrows/font = lower energy state.

1.4.5 Catabolism of energy reserves

Sokolova (2013) describes a concept of energy-limited tolerance to stress. In optimal environmental condition, there is a balance between energy input and expenditure, with both enough energy to cover maintenance metabolism and energy for increasing fitness such as growth and reproduction (Sokolova 2013). As the environment transforms from optimal to stressful, the aerobic scope of metabolism declines, as energy requirements increase, resulting in less energy for fitness related traits. When stress is moderate, aerobic scope can still be maintained, and survival occurs with a trade-off for growth and reproduction; however, beyond this point maintenance demands may not be met fully by aerobic metabolism, and anaerobic metabolism may ensue to compensate (see section 1.4.4 Anaerobiosis) along with metabolic rate depression (see below section 1.4.6. Metabolic decline and energy conservation) (Sokolova 2013). During declining environmental conditions depletion of energy reserves occurs by catabolizing glycogen and lipid reserves (Sokolova 2013).

Food availability has a major role in protection against stress. Several studies in mussels have found that high food quality and availability is important for mussels to maintain health during stressful environmental conditions, (Hatcher et al. 1997; Tremblay et al. 1998; Freites et al. 2003; Delaporte et al. 2006; Babarro et al. 2008; Lesser et al. 2010; Dowd et al. 2013; Lassoued et al. 2019). If low food availability is also present in combination with other stressors, catabolism of energy reserves occurs to satisfy maintenance requirements (Hummel et al. 1989; Encomio and Chu 2000; Clements et al. 2018; Freitas et al. 2019).

When stressful conditions are at a level where anaerobic respiration is utilized, such as when maintenance requirements exceed aerobic requirements (Sokolova 2013) or during times where aerobic respiration is not possible (i.e. hypoxia/anoxia), catabolism of energy stores must occur. In this case, glycogen and free amino acids are the main substrates used (Storey and Storey 2004). Bivalves store large quantities of free amino acids for their osmotic balance (De Zwaan and Wijsman 1976; Grieshaber et al. 1994). Some of these amino acids are utilized in the production of opines (i.e. glycine and arginine, see Figure

1.) (Grieshaber et al. 1994; Müller et al. 2012), while others, such as aspartate, can be depleted due to the production of malate (See Figure 1.) (de Zwaan and Wijsman 1976; Grieshaber et al. 1994; Larade and Storey 2002a; Müller et al. 2012). Depletion of amino acid pools in bivalves can have negative consequences for homeostasis (Grieshaber et al. 1994; Soldatov et al. 2009; Haider et al. 2020a) so protein catabolism is utilised to maintain levels of free amino acids. Bivalves strictly rely on glycogen stores in the later stages of anaerobiosis, indicating that glycogen stores are key for their survival. Bivalves store a significant amount of glycogen, between 10–35% of their dry weight (De Zwaan and Zandee 1972). Glycogen storage is a major physiological stress adaptation in bivalves where bivalves that contain more glycogen are often more stress resilient (Zhang et al. 2016). For example, triploid oysters store more glycogen and are more stress resilient compared to diploid oysters (Akashige and Fushimi 1992; Nell et al. 1994).

1.4.6 Metabolic decline and energy conservation

In stressful environmental conditions that impact energy acquisition or result in valve closure, metabolic decline is necessary. Metabolic rate depression occurs to supress energy demand and is defined as a decrease in pathways that either consume or produce ATP to conserve energy (Hochachka et al. 1996; Sokolova et al. 2012; Haider et al. 2020a). Metabolic rate depression can be achieved through a coordinated shutdown of activities that are energy consuming, such as through suppression of muscle movement, respiration and heartrate (Storey and Storey 2004). Metabolic rate depression also supresses the immune system in bivalves, and the building of macromolecules such as DNA, RNA, proteins and membrane phospholipids (Storey and Storey 2004; Larade and Storey 2009).

Metabolic decline is particularly common when anaerobiosis is the main source of respiration occurring such as in hypoxia/anoxia. In such a case anaerobic respiration would have to occur at a 5–12-fold greater rate, and large quantities of glycogen would be used up rapidly (Grieshaber et al. 1994). If metabolic rate stayed at the same rate as aerobic conditions in the mussel *M. edulis*, there would only be enough glycogen stores to survive for a few days (De Zwaan and Wijsman 1976). In addition, high levels of toxic anaerobic end-products would also lead to cell damage and self-poisoning (De Zwaan 1991).

However, if metabolic rate depression occurs, mussels can survive for up to a few weeks (Storey 1985). Therefore, metabolic rate depression is a key mechanism for survival in hypoxia/anoxia.

Metabolic decline also occurs in association with other stressors. High temperatures increase metabolic rate in mussels (Matoo et al. 2021) until a critical threshold is reached, and then decline occurs (Anestis et al. 2007; Lesser et al. 2010; Torossian et al. 2020). Acute exposure to low salinity results in valve closure to prevent abrupt changes in osmolytes and mitigate stress (Gilles 1972; Shumway 1977; Bayne 2017), and this is associated with decline of metabolism and heart rate (Bahmet et al. 2005; Braby and Somero 2006; Wang et al. 2011b). Low food availability also causes metabolic decline, when food ration is below maintenance ratio (Jørgensen et al. 1986a, 1986b; Newell et al. 2001; Riisgård et al. 2003, 2011; Pascoe et al. 2015).

1.4.7 Shell repair and dissolution

A mussel's shell is a critical part of bivalve morphology and acts as armor that protects their organ systems. During times of stress, mussels are able to close and seal their shell as a protection mechanism from their environment (See 1.4.1 Behaviour section for more details) (ie. Shumway 1977; Davenport and Manley 1978; Davenport 1979; Wang and Widdows 1993b; Lajus and Sukhotin 1998; Riisgård and Larsen 2015). However, their shell also protects them from predators that crush them (ie. fish, bird, and mammals) or drilling organisms (ie. gastropods and cephalopods) (Johnson 2020). In mussels (*Mytilus* spp.), shell strength and thickness varies by species, size, population, season and environment (Smith and Jennings 2000; Beadman et al. 2003; Nagarajan et al. 2006; Penney et al. 2007).

Mussels have mechanisms that control shell growth, repair, and dissolution (Melzner et al. 2011; Clark et al. 2020; Crane et al. 2021). The mechanisms of shell biomineralization are not fully understood; however, recently there has been more research conducted to characterize shell mineralization in mussels (Hüning et al. 2016; Arivalagan et al. 2017, 2020; Yarra et al. 2021a, 2021b). Recent research has found shell repair occurs in stages with the first 20 days after shell injury being a time of organic sheet synthesis and increases

in calcite crystals followed by deposition of aragonite tablets in later stages of healing. Gene expression also changes during this time, with increases in tyrosinase isoforms being upregulated in early stages, and nacrein-like protein being expressed in later stages (Hüning et al. 2016).

When pH decreases (extracellularly or intracellularly), shell dissolution of calcium carbonate occurs increasing buffering capacity (Collip 1920, 1921; Crenshaw and Neff 1969; De Zwaan and Wijsman 1976; Storey and Storey 1990; Grieshaber et al. 1994; Michaelidis et al. 2005; Rafrafi and Uglow 2009; Thomsen and Melzner 2010b; Melzner et al. 2011; Fitzer et al. 2014, 2016, 2018). Changes in shell structure has also been found in research aimed to understand the impacts of ocean acidification on the shell of mussels. Several studies found that ocean acidification scenarios reduce shell growth, reduce shell thickness, and result in more brittle shells (Thomsen and Melzner 2010; Melzner et al. 2011; Fitzer et al. 2014, 2016, 2018; Sadler et al. 2018) which is concerning for mussel health.

1.5 Differences in response to environmental stress between mussel sizes and locations

1.5.1 Inter-individual variability in phenotypes in a single population

Phenotypic variation of wild populations are often found to be relatively small, which is the result of suppression of phenotypic variation due to canalization (Waddington 1942). This means that genotypic impacts that lead to variations can be buffered by physiological processes capable of neutralizing genetic capacitors (Takahashi 2019). However, recent studies in molluscs have found that variability between individuals can be directly observable with gene expression, even if not visible at the phenotype level (Peck et al. 2015; Collins et al. 2021). However, bivalves have been found to exhibit variation in fitness traits that can be related to genetic diversity within the population (Gosling 1992). The best-known example of this in bivalves is the concept of heterozygosity. Heterozygosity at several loci in mussels is linked with growth, fertility and survival (Koehn and Gaffney 1984; Diehl et al. 1985; Hawkins et al. 1986; Bayne and Hawkins 1997; LeBlanc et al. 2008; Myrand et al. 2009). Multiple studies have found that adult mussels that are

heterozygous for various locus may have lower metabolic requirements, more efficient protein turnover and a better capacity to survive starvation (Koehn and Gaffney 1984; Diehl et al. 1985; Hawkins et al. 1986; Bayne and Hawkins 1997; LeBlanc et al. 2008). Bayne and Hawkins (1997) found that heterozygosity had a large influence in how mussels behaved during different feed rations and these differences resulted from cost associated with protein turnover and deposition in association with growth. LeBlanc et al. (2008) found that elevated temperature and aerial exposure could be used as a way of selecting for heterozygosity in mussel (*M. edulis*) aquaculture, as mortality occurred earlier in homozygous mussels. Selecting for heterozygosity resulted in significantly lower metabolic rate and larger mussels compared to the control group after 10 months of growing in the field (LeBlanc et al. 2008).

1.5.2 Population/site differences

At the population level, environmental conditions contribute to genetic selection and epigenetics, which play a role in adaptation (Gosling 1992). For example, a reciprocal transplant study in mussels (*M. edulis*) from the North Sea with high salinity (20–30 ‰) to the Baltic Sea with low salinity (6–7 ‰) resulted in large mortality, and only mussels with similar phenotype as the native population in the Baltic Sea were able to survive indicating a genetic conspecific more suited for the environment (Kautsky et al. 1990). However, mussels have the ability to acclimate to different environmental conditions through plasticity in physiology. For example, acclimation to differences in phytoplankton levels has occurred in some populations of mussels, such as in locations with low food availability, where mussels have become acclimated to filter at extremely low levels of phytoplankton while still maintaining growth (Strohmeier et al. 2009). Mussels have also been found to adapt to environmental conditions by changing their feeding morphology in the gills and/or labial palps (Capelle et al. 2021). Mussels from different oceanic zones may also exhibit differences in physiological traits (Watson et al. 2018). Nemova et al. (2013) found that the lipid membranes of the mussel (*M. edulis*) were different between the intertidal mussels and subtidal mussels. Mussels in the intertidal zone contained higher levels of baseline cholesterol levels compared to the aquaculture mussels which had more saturated fatty acids, n-6 polyunsaturated fatty acids and 22 non-methylene interrupted

fatty acids (Nemova et al. 2013). In addition, the intertidal zone is known to be a more stressful environment for mussels, as it experiences daily tidal cycles that can drastically impact oxygen and temperature (Freire et al. 2011), and mussels that live in the intertidal zone have been found more resilient to environmental fluctuations (Widdows and Shick 1985; Altieri 2006; Petes et al. 2008; Meng et al. 2018).

Gene expression patterns has also been found to vary between sites and populations. Place et al. (2008) analyzed gene expression of the mussel *M. californianus* in different populations along the Pacific coast as far North as Bamfield, British Columbia (Canada) and as far South as Punta San Isidro (Mexico) and found that there were major differences in gene expression patterns associated with each population. Similarly, a study by Counihan et al. (2019) in *M. trossulus* found baseline gene expression patterns varied between six sites in Alaska in two National parks and was hypothesized to be related to local environmental factors. Environmental differences can result in differences in energy reserves, reproductive output and growth in mussels (Freeman 1974; Bayne et al. 1983; Narváez et al. 2008), which can impact gene expression.

1.5.3 Age/size related differences

Mussels of different age/sizes respond differently to environmental conditions. Zilberberg et al. (2011) looked at the impacts of size on biomarker pp38 mitogen activated protein kinase as a marker for osmotic and hypoxic stress in the mussel *Perna perna* and found that mussel size significantly impacted its expression, with smaller mussels having lower levels of the marker compared to larger mussels. Izagirre et al. (2014) also found that biomarkers were dependent on size/age of the mussel *M. galloprovincialis*. Sukhotin et al. (2003) found that mussel's (*M. edulis*) physiological responses to low salinity, high temperature, and aerial exposure are significantly impacted by mussel size. Older mussels (*M. edulis*) have also been found to have a lower capacity to recover after exposure to various stressors (hypoxia, high temperatures, pollution/toxins) compared to younger mussels (Hole et al. 1992, 1993, 1995). A recent study by Wu et al. (2017) found that mussels (*M. galloprovincialis*) at three life stages (D-stage, juvenile and adult) had differential responses to pollution exposure (cadmium), and that D-stage larvae were more susceptible. In addition, each size used a different set of pathways to respond to the stress.

Differences in responses to stress in different size mussels may result due to variation in baseline physiological processes occurring. Seed mussels have been found to allocate their energy to development and rapid growth and allocate very little into reproduction, whereas adults put more energy in reproduction (Thompson 1979). Somatic growth occurs rapidly after settlement, then slows after the first year of development due to increased energy allocation to reproduction (Hawkins and Bayne 1992). Energy reserves in bivalves also differ between size classes, with adult mussels having overall higher energy reserves compared to seed mussels (Holland and Spencer 1973; Mann and Gallager 1985; Widdows et al. 1989). In addition, larval bivalves primarily store lipids and proteins, whereas adults store predominantly glycogen as their main source of energy substrate (Holland and Spencer 1973; Holland and Hannant 1976; Mann and Gallager 1985; Widdows et al. 1989). Furthermore, epigenetics plays a role regulating gene expression associated with growth and development at different stages (Riviere et al. 2013; Li et al. 2015c; Riviere et al. 2017).

1.6 Monitoring stress in mussels

1.6.1 Heart rate

Heart rate is a proven tool in understanding physiology and stress in mollusc species. The first method of studying heart rate involved drilling a single hole above the pericardial sac and inserting of electrodes (Trueman 1967; Hoggarth & Trueman 1967). Since this time, non-invasive methods of infrared phototplethymogram (IR-PPG) heart rate monitoring have since been developed by Depledge & Andersen (1990). This method uses a computer-aided physiological monitoring system (CAPMON) to measure heartbeat in invertebrates and rely on infra-red phototransducers that attach with minimal disturbance to the organism. The original method has been improved and simplified (Burnett *et al*. 2013). The basis of this method is an infrared light emitting diode (LED) coupled with a phototransistor detector that reflects the movement of a heartbeat over time. In many studies heart rate has been used to measure stress response in mussels including salinity (Bahmet et al. 2005; Braby and Somero 2006), temperature (Widdows 1973a; Braby and Somero 2006; Tagliarolo and McQuaid 2015; Zittier et al. 2015; Olabarria et al. 2016), hypoxia (Coleman and Trueman 1971; Bayne 1971; Seo et al. 2016), predation (Rovero et

al. 1999), toxins/pollution/chemicals (Curtis et al. 2000; Nicholson 2003; Comeau et al. 2017b; Shen and Nugegoda 2022), parasite infection (Bakhmet et al. 2019), and food availability (Widdows 1973; Bakhmet 2017).

1.6.2 Neutral red assay

Lysosomes are an important cellular organelle in molluscs, that play important roles in many systems including digestive and immune (Owen 1955, 1972; Hauton et al. 2001). However, lysosomes are also a well-established bioindicator of stress in molluscs. When under stress, the lysosomal membrane becomes unstable and leaky, which is one of the first signs of cellular stress (Moore 1976; Thompson et al. 1978; Moore et al. 1979; Lowe et al. 1992, 1995; Tremblay et al. 1998; Harding et al. 2004). As a result, Neutral Red Retention Assay (NRA) was developed as a tool to detect stress in molluscs (Moore 1976; Borenfreund and Puerner 1985; Lowe et al. 1992, 1995; Lowe and Pipe 1994; Ringwood et al. 1998). Since this time, this method has been used to detect stressors involving salinity (Bayne et al. 1981; Hauton et al. 1998; Méthé, et al. 2015), temperature (Hauton et al. 1998; Matozzo et al. 2012; Mayrand et al. 2015), mechanical stress (Harding 2003), bacterial pathogens (Hauton et al. 2001), ocean acidity (Matozzo et al. 2012), and pollutants/toxins (Ringwood et al. 1998; Viarengo et al. 2007).

1.6.3 Omics tools for monitoring stress

Responses to environmental stress first involves the recognition of stimuli, which results in transcription of mRNA that are then translated to proteins with various post-translational modification. These proteins ultimately lead to physiological responses to the stress (Welch 1993; Rein 2020). The development of omics technologies has allowed for the characterization of (1) genes and proteins that drive physiological responses to stress, and (2) metabolites that are signatures of physiological processes. Omics technologies such as transcriptomics, proteomics are used to visualize and better understand biology and expression in different tissues, life stages, and/or condition of a given organism (Lowe et al. 2017; Nguyen and Alfaro 2020).

The transcriptome of an organism is the total quantity of mRNA transcripts being expressed by a cell at any given moment. The study of transcriptomics is a relatively new field of

genomic technology that began in the early 1990s (Lowe et al. 2017). Since this time, transcriptomics has been applied in many aspects of science, one being the ability to understand and identify biological pathways relating to environmental stressors. Transcriptomics has used multiple methods since it was established, including the serial analysis of gene expression (SAGE) using Sanger sequencing; however, this method has become obsolete since high-throughput technologies have been established (Lowe et al. 2017). Microarrays are another tool used in transcriptomics which allows for thousands of transcript's expression to be studied (Lowe et al. 2017). Since the development of high-throughput sequencing technologies such as RNA-seq, it is now possible to sequence the total quantity of RNA transcripts being expressed in a tissue sample or single cell (Saliba et al. 2014; Lowe et al. 2017).

The proteome is the study of the total sum of proteins present in cells or tissues of an organism at one time. Techniques for proteomics include gel based approaches including two-dimensional gel electrophoresis (2-DE), SDS-polyacrylamide gel electrophoresis (SDS-PAGE), mass spectrometry and liquid chromatography (LC-MS) (Nguyen and Alfaro 2020). Metabolomics is the study of metabolites in a tissue, or organism, and represent the end-products of gene-expression associated with the phenotype of an organism at one time (Nguyen and Alfaro 2020). This type of analysis can use a variety of approaches including infrared spectroscopy (IR), Raman spectroscopy, nuclear magnetic resonance (NMR), and mass spectrometry technologies (Nguyen and Alfaro 2020). Overall, Transcriptomic, proteomic, and metabolomic tools are highly useful for gaining an understanding of the physiological condition of an organism and the impacts of environmental stress.

1.7 **Project**

1.7.1 Rationale and objectives

The PEI mussel aquaculture industry is being challenged by climate change induced environmental stressors, that despite *M. edulis'* remarkable ability to adapt can lead to mortality. One of the major challenges to the mussel aquaculture industry is the lack of visual stress behavior exhibited by mussels. Often the first observable sign of stress is mass

mortality, which represents a loss for the industry. When poor growth and meat yields are observed in mussel production, often the causative reason can only be speculated due to lack of available testing. Recently, the PEI mussel aquaculture industry identified the need to develop a test using an omics approach to detect specific environmental stressors, to determine causative reasons of underperforming mussel populations and reduce mortality.

Development of specific molecular testing relies on gaining knowledge of genomic information, such as gene expression patterns to identify markers that are unique to specific stress responses. Many studies have been published on physiological responses of mussels to stress (i.e. Bayne 1971, 1972; Bayne et al. 1973, 1981; Shumway 1977; Davenport 1979a, 1979b; Widdows et al. 1979, 1989; Holwerda and De Zwaan 1980; De Zwaan et al. 1982; Hawkins et al. 1993; Clements et al. 2018, 2021); however, still, a lot is unknown about how gene expression leads to observable physiological response. Therefore, the goal of this research aimed to discover markers for mussels experiencing acute stress from hypoxia, hyposalinity, and food availability (low/high). It was hypothesized that by studying the acute stress response, markers could be discovered to detect early onset of stress before it leads to major impacts to mussel health. Differences and similarities in transcriptome expression in different sites and sizes of mussels from PEI were also explored, to better understand if markers could be developed that are applicable on a broader scale.

Chapter 2: Evaluating blue mussels (*Mytilus edulis*) responses to acute hypoxia using transcriptomics and heart rate

2.1 Introduction

Anthropogenic climate change has been identified as a major concern for the blue mussel (*Mytilus edulis*) aquaculture industry in Prince Edward Island (PEI). One of the concerns of climate change, is declining oxygen concentrations in the ocean (Bindoff et al. 2019). The open ocean has lost between 0.5–3.3% of dissolved oxygen between 1970–2010 from the ocean surface, and will likely continue to decline by 3.2–3.7% by 2081–2100 (Bindoff et al. 2019). Dissolved oxygen losses are projected to impact ~ 59–80% of the ocean by 2031–2050 (Bindoff et al. 2019). Climate change models predict dissolved oxygen losses are due to increases in oceanic temperatures, stratification, upwelling, algae blooms and microbial respiration (Hoegh-Guldberg et al. 2014; Bindoff et al. 2019). Impacts of low dissolved oxygen (hypoxia) and the complete depletion of oxygen (anoxia) on marine organisms are of concern.

The blue mussel is found within intertidal and subtidal zones that can experience recurrent hypoxia/anoxia events. In the intertidal zone, low tides can result in hypoxic/anoxic events in mussels by oxygen depletion in tide pools, or aerial exposure that results in valve closure and cessation of filtering behaviour (Grieshaber et al. 1994). In subtidal areas, stratification events are the main driver of hypoxia/anoxia. Stratification develops through density changes in water, either by temperature, salinity or a combination of the two (Rabalais et al. 2010). Runoff from fertilizer and sewage/industrial waste contamination can lead to rapid growth of phytoplankton and microbial populations that can exacerbate hypoxic/anoxic events (Diaz and Rosenberg 2008; Tweedley et al. 2015).

Like most bivalves, mussels are facultative anaerobes and hypoxia/anoxia tolerant (Collip 1920; De Zwaan and Wijsman 1976; Larade et al 2002). Initially, mussels respond to declining oxygen concentrations in their environment by increasing ventilation rate, heart rate and respiration rate; while maintaining aerobic respiration (oxyregulation) (Bayne 1971; Grieshaber et al. 1994). Once a critical oxygen level is reached, anaerobic respiration and metabolic rate depression begin to develop, along with other physiological modifications (oxyconformation) (Bayne 1971; Grieshaber et al. 1994). Onset of anaerobic

pathways results in the catabolism of glycogen and amino acids for energy (De Zwaan and Wijsman 1976; Collicutt and Hochachka 1977; Foreman and Ellington 1983; De Zwaan et al. 1983, 1992; De Zwaan 1991; Grieshaber et al. 1994; Larade et al. 2002; Storey and Storey 2004), while metabolic rate depression results in a shutdown of pathways that consume and produce energy (Storey and Storey 2004). Hypoxia/anoxia has also been found to result in the expression of stress and antioxidant genes in mussels to mitigate damages associated with accumulation of toxic end-products and damaged proteins (Halpin et al. 2004; Almeida et al. 2005; Gracey et al. 2008; Anestis et al. 2010; Woo et al. 2013; Andrade et al. 2018, 2019; Falfushynska et al. 2020). Falfushynska et al. (2020) looked at the blue mussel's response to intermittent hypoxia in terms of the expression of inflammatory and apoptosis associated genes to determine the utility of these genes as markers for hypoxia stress in the bivalves. They found inflammatory responses through caspases, and apoptotic genes might be important in understanding sublethal stress response in the blue mussel (Falfushynska et al. 2020). Recently, Haider et al. (2020a) examined how blue mussel homeostasis is maintained during hypoxia and reoxygenation in the blue mussel. This study highlights shifts in amino acids and intermediate metabolites involved with urea cycling and purine metabolism that may be crucial for homeostasis maintenance during short-term and prolonged hypoxia and reoxygenation (Haider et al. 2020a). However, there are still many unknowns associated with principles of homeostasis maintenance during an abrupt change in oxygen in blue mussels.

Variation in responses of bivalves to hypoxia/anoxia has been found between experimental conditions, environment, size, season, and exposure time (De Zwaan 1991; Wang and Widdows 1993; Altieri 2006; Clark et al. 2013; Meng et al. 2018). For example, Altieri (2006) found that intertidal mussels are more tolerant than subtidal mussels, which may be associated with previous exposures to hypoxia. In addition, Wang and Widdows (1993) found that smaller (~ 5 mm seed) mussels can maintain aerobic respiration longer than larger (~ 33 mm adult) mussels, which could be due to larger surface area on the gills in comparison to body size; however, larval mussels have faster mortality. Another study by Clark et al. (2013) found that transcription profiles of young and adults clams (*Laternula*

elliptica) experiencing hypoxia were different, and indicated that the adults were more susceptible to declining oxygen compared to the young clams.

The cellular mechanisms that lead to these differences in phenotypic responses to hypoxia/anoxia have not been well studied; especially those associated with how transcriptomic response leads to the observed physiological response in mussels. This is especially true between sizes and sites of blue mussels. Therefore, the present study evaluated the acute response of hypoxia exposure in blue mussels in two sizes (adult, seed) and from two sites in PEI, Canada (March Water and St. Mary's Bay). Heart rate was evaluated to better understand the status of metabolic rate depression, as heart rate during metabolic rate depression is expected to decline (Coleman and Trueman 1971; Bayne 1971; Seo et al. 2016). It was hypothesized that major shifts in transcriptomic response would be observed within the first four hours of exposure, even if metabolic rate depression hadn't developed. This study also measured changes in transcriptomic response to understand similarities and differences between the two sizes and the two sites.

2.2 Materials and methods

2.2.1 Mussel sites and sizes

Adult and seed mussels (*M. edulis*) were collected (one sock per size) on January 27, 2017, from two off-bottom aquaculture leases located in PEI: March Water (MW) (N 46° 31' 18.8", W 63° 43' 12.9") and St. Mary's Bay (StM) (N 46° 07' 37.2", W 62° 31' 14.2") (Figure *2*). Both adult and seed originated from wild seed collections in PEI. Shell height (SH; mean ± SE) ranged between site and size: MW adult 52.6 ± 0.7 mm, MW seed 20.4 ± 0.5 mm, StM adult 48.3 ± 1.3 mm, and StM seed 31.7 ± 1.2 mm. A total of 2,400 mussels were collected (600 per site and size). At the time of collection, MW had a water temperature of 0.3 °C and a salinity of 25.4 ‰, while StM had a temperature of 0.5 °C and a salinity of 27 ‰. Mussels were immediately placed in a cooler containing ice and transferred to the Dalhousie Aquatron (Halifax, Nova Scotia) on the day of collection. Mussels were transferred to a flow-through holding system at 0.5 °C and salinity of 27 ‰ and slowly acclimated over a month (~ 0.5 °C daily increase) to 16 °C and salinity 27 ‰. Mussels were fed daily during acclimation using an algal blend of *Isochrysis galbana* (T.ISO) and *Chaetoceros mulleri*, at a concentration of 100 cells/µL per individual.

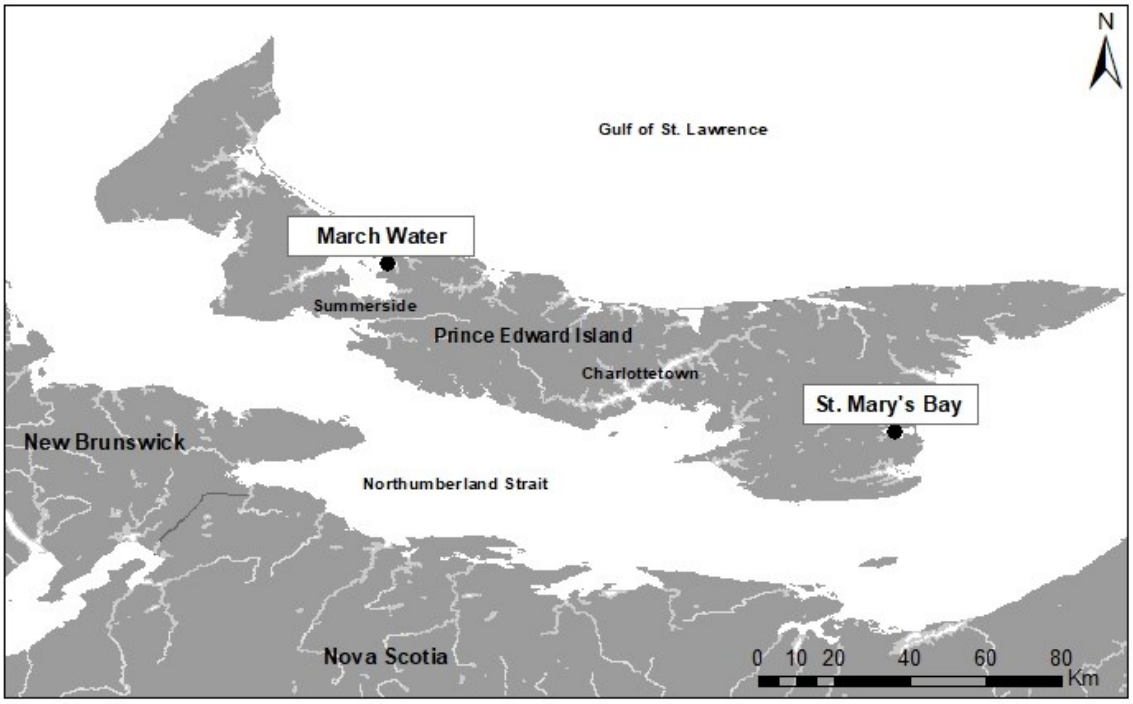

Figure 2. Map of Prince Edward Island showing sampling locations of each site (March Water and St. Mary's Bay). March Water (N 46° 31' 18.8", W 63° 43' 12.9") and St. Mary's Bay (N 46° 07' 37.2", W 62° 31' 14.2").

2.2.2 Hypoxia trial

The hypoxia trial was completed in custom-made sealable respirometer chambers (4.5 L) that were encased into two units containing four chambers each (eight total). Respirometer chambers were allocated either as a treatment (hypoxia) at dissolved oxygen concentration (O_2) ~ 2 mg/L and control at O_2 ~ 7–8 mg/L (four chamber per treatment). Separate hypoxia trials were completed for each size (MW, StM), with the first trial consisting of adults and the second trial consisting of seed. Both hypoxia trials were completed over a 4 h period. In each trial, four mussels from both sites were placed in each chamber (eight per tank N = 64 total).

The water inside the respirometry chambers was static with water temperature maintained at 16 °C and salinity at 27 ‰. Temperature was maintained by circulating water around the outside of the respirometer chambers within the units, by fitting the units with an inlet and outlet water hose. Hypoxia was induced in the treatment group by displacing oxygen in the water through bubbling nitrogen gas for ~ 12 min. To ensure oxygen was evenly distributed

in the respirometer, a mesh false bottom was installed at the bottom of the tank, with magnetic stirring beads and stir plates placed underneath.

2.2.3 Heart rate monitoring

Heart rate (HR) was monitored in the adult size trial, and not in the seed trial as sensors were too big for seed size mussels. To measure HR, non-invasive infrared red-light (IR) sensors were manufactured by Dr. K Fraser Clark using a slightly modified method based on Burnett et al. (2013). The HR sensors were attached to the mussel over the approximate location of the heart, and plumbers' putty (PlumbShop®, Masco Canada Limited, Ontario, Canada) was placed around the sensor to seal it to the mussel and reduce IR signal fluctuations. After initial attachment of IR sensor, mussels were placed back into their holding tank for 24 h to acclimatize to the sensor. Heart rate of four mussel per treatment, two from each site (eight total) were monitored continuously over the 4 h hypoxia trial and for 1 h after the trial. Real-time HR was visualized using the software Makerplot (SelmaWare Solutions, LLC) and then analyzed further by importation into Microsoft Excel 365, to visualize the HR data. Heart rate was interpreted by manually counting the total number of heartbeats in one-minute intervals (beats per minute (BPM)) every 15 minutes, and then calculating the mean of the four intervals for each hour in the trial.

2.2.4 Statistical analysis of heart rate monitoring

Heart rate data was analysed using a General Mixed Effect Model, with repeated measures treated as a hierarchal structure (split-plot): mussels as large units (whole plots) and time as sub-units (subplots). Treatment (hypoxia (O_2 ~ 2 mg/L), control (O_2 ~ 7–8 mg/L)), site (MW, StM), and time (1, 2, 3, 4 h) or (during, after) were considered fixed variables. The mussels were considered a random variable, and nested within treatment and site, as mussels were unique to each group. Separate statistical analyses were completed for time (1) mean hourly HR (1, 2, 3, 4 h) and (2) categories (during, after) as in the mean HR during the last 2 h and 1 h post-treatment once placed back into the acclimation tank. The model included all significant main effects and interactions, with the non-significant main effects (and interactions) being collapsed from the model to give final model estimates. Variance inflation factor (VIF) was calculated to test multicollinearity of the model.

In both statistical analyses, assumptions of normality and homoscedasticity were assessed for the error terms by conducting a normal probability plot of standardized residuals of error terms and equal variance by plotting the residuals of error terms versus fitted. For all analyses, the significance level was set at *p-value* = < 0.05. In the presence of a significant interaction between the various factors, a Bonferroni simultaneous test of means was performed to identify differences between groups. All estimates are reported as least squares mean (LSM) ± standard error (SE), unless otherwise specified.

2.2.5 Sample preservation, RNA extraction and sequencing

Following each hypoxia trial, mussels were collected for RNA preservation. Six mussels per size (adult, seed) and site (MW and StM) in each treatment (control O_2 ~ 7–8 mg/L; hypoxia O_2 ~ 2 mg/L) were collected. Whole mussel tissue was homogenized into RNAlater® solution (Cat. No. 76106, QIAGEN GmbH, Hilden, Germany) using an Omni tissue homogenizer (Omni International, Kennesaw, GA, USA), at a ratio of 1 g tissue per 10 mL of RNAlater®. RNA was isolated using Qiagen RNeasy® Mini Kit (Cat. No: 74104, QIAGEN GmbH, Hilden, Germany) following the manufacture's protocol. An additional on-column DNase I (Cat. No. 79254, QIAGEN GmbH, Hilden, Germany) treatment was applied during the RNA isolation process, to ensure no DNA contamination was present. Concentration and quality of RNA was assessed using Nanodrop spectrophotometry (Thermo Fisher Scientific, Waltham, MA, USA) and Bioanalyzer (Agilent Bioanalyzer, RNA 6000 nano kit, Santa Clara, CA, United States). High quality RNA was shipped to Genome Quebec (Montreal Quebec) where Truseq library preparation was completed on each sample. Then, Hiseq2000 Illumina (sequencing by synthesis) was completed (PE 100), to give a sequencing read depth of 15–20 million reads per sample (eight samples per sequencing lane).

2.2.6 *De novo* transcriptome assembly

Transcriptome assembly was completed by the Canadian Centre for Computation Genomics, McGill University (Montreal, Quebec). The transcriptome assembled in this study was built using mussel samples from the hypoxia (present chapter), salinity (chapter 3), food availability (chapter 4) trials, and resulted in one large transcriptome. Assembly

of one large transcriptome was used to aid in marker discovery (chapter 5), to find markers specific to one particular stressor. Sequencing read quality was assessed using FastQC (Andrews 2018). Trimmomatic software (Bolger et al. 2014) was then used to trim from the 3'end to remove adapter sequences and remove poor quality regions. Only sequences with read length equal to or greater than 50 base pairs (bp) were utilized in transcriptome assembly. Normalization of reads were performed to reduce memory and decrease assembly runtime by reducing the number of reads, using the *in-silico* normalization within Trinity software package (Grabherr et al. 2011; Haas et al. 2013). Transcriptome assembly was completed using *de novo* alignment using Trinity software (Grabherr et al. 2011; Haas et al. 2013).

2.2.7 Differential expression analysis

After transcriptome assembly, raw abundances and normalization of counts were completed using the software kallisto (Bray et al. 2016). Kallisto quantifies abundances and uses a method of *pseudoalignment* for quickly determining the compatibility of reads with targets (Bray et al. 2016). Differential expression analysis was completed in both DESeq2 (Love et al. 2014; Afgan et al. 2018) and edgeR (Robinson et al. 2010; Afgan et al. 2018) (Galaxy Version 3.24.1 + galaxy1). The use of both differential expression analysis packages (DESeq2 and edgeR) was completed to ensure that the analysis was robust. In both methods, *p-value* was adjusted to control for false discovery rate (FDR *p-value*). Several pairwise comparisons were completed to understand the nature of the transcript expression of the different sites and sizes (Table 1). In both differential expression packages, Log_2 fold change (FC) was used to visualize the relative expression of control versus hypoxia. Trends in differential expression analysis results were visualized using volcano plots, Venn diagrams, heatmaps and principal component analysis (PCA). PCA analysis was completed on transcripts that had expression level of 10 across all samples in the hypoxia trials.

Table 1. Differential expression analysis comparisons utilized in experiment. For each comparison, two different methods of differential expression were utilized, DESeq2 and edgeR. Comparisons were laid out as Treatment (O_2 2 mg/L) vs control (O_2 7-8 mg/L) for each size (A = adult; S = seed) and site (MW = March Water; StM = St. Mary's Bay).

Pairwise comparison group	Number of comparisons	Comparison name
Adult by site	2	StM A MW A
Seed by site	2	StM S MW S
Size (MW & StM)	2	A S

2.2.8 Annotation and functional analysis

Whole transcriptome sequence ontology annotation was completed using NCBI BLAST + blastx algorithm (Camacho et al. 2009; Cock et al. 2015) in Galaxy using the NCBI non-redundant (nr) protein database (E-value $\leq 1e^{-10}$; downloaded in July 2018). Differentially expressed transcripts underwent additional annotation (FDR *p-value* < 0.05) using Trinnotate (Bryant et al. 2017) and Blast2GO (basic) software (Version 5.2.5) using NCBI Blast service (blastx), with an E-value set at $1e^{-5}$, and with a taxonomy filter selective to only bivalves (taxa: 6544, Bivalvia) (Conesa et al. 2005; Conesa and Götz 2008; Götz et al. 2008, 2011). The Kyoto Encyclopedia of Genes and Genomes (KEGG) Automatic Annotation Server (KAAS) (Moriya et al. 2007) was used to annotate differentially expressed transcripts as well. Then, annotation assignment of differentially expressed transcripts was used in pathway assignment using KEGG Mapper (Kanehisa and Sato 2020) using the organism-specific search mode. KEGG mapping was assigned using the only two bivalve species within the KEGG server, Pacific oyster (*Crassostrea gigas*) and Yesso scallop (*Mizuhopecten yessoensis*) to receive pathways only relevant to bivalves. Annotation, ortholog, and pathway assignment aided in facilitating functional understanding of differentially expressed transcripts.

2.3 Results

2.3.1 Heart rate monitoring

The main effect of hourly HR (1, 2, 3, 4 h) had a significant impact on HR (*p-value* = 0.009; *F* = 4.05). Site, hypoxia treatment and its interactions were not significant. Figure *3*A shows gradual decline in mean HR over the 4 h acute hypoxia trial. Bonferroni simultaneous test of means found that the 1 h (22.4 ± 1.1 BPM) and 4 h (21.4 ± 1.1 BPM) time points were significantly different. For the categories (during, after), the interactions of acute hypoxia treatment*timing (*p-value* = 0.001) had significant impact on mean HR. Site was not significant. Figure *3*B **s**hows the mean estimates of the interaction of acute hypoxia treatment*timing. It was found that the mean HR in acute hypoxia treatment (O_2 ~ 2 mg/L) significantly decreased after returning to the acclimation tank from 21.6 ± 1.6 to 19.4 ± 1.6 BPM (Figure 3B).

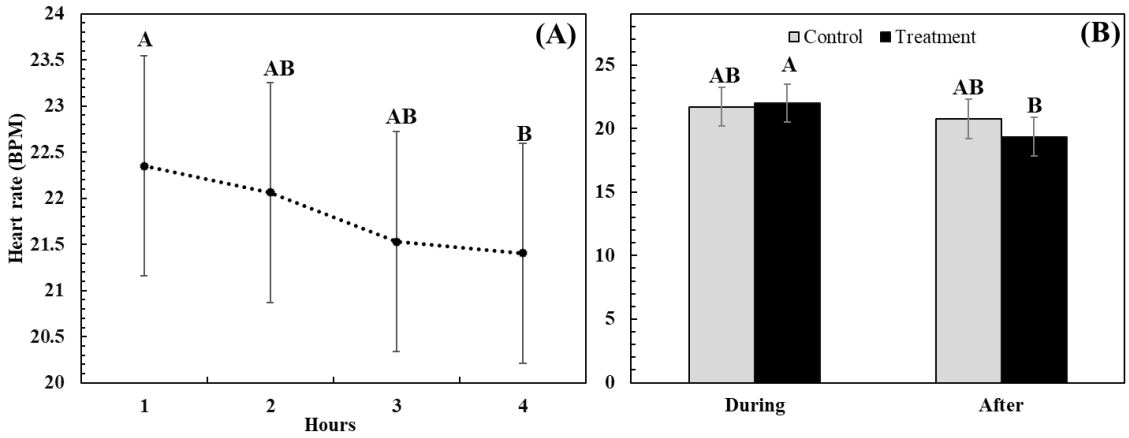

Figure 3. Estimates from statistical model for: (A) mean hourly HR (1, 2, 3, 4 h) of mussels in acute hypoxia treatment (O2 ~ 2 mg/L) vs control (O2 ~ 7–8 mg/L) (n = 16 replicates per point); and (B) timing (during and after) the hypoxia trial for mussels in control and acute hypoxia treatment. The values are expressed as Least square mean (LSM) ± Standard Error (SE). LSM's without a common script were significantly different (*p-value* = < 0.05) (n = 32 replicates per bar 'during': n = 16 replicates per bar 'after').

2.3.2 Transcriptome assembly and annotation

Sequencing resulted in 2,917,849,670 reads after *in silico* normalization. Trinity assembly resulted in a total of 2,861,652 assembled transcripts with a maximum transcript length of

29,956 bp, minimum transcript length of 201 bp, mean transcript length of 498 bp, and N50 of 576 bp.

2.3.3 Differential expression analysis

Preliminary PCA of all expressed transcripts in mussels from the hypoxia trial, indicated there was a lot of variability in expression between individuals; however, some separation between the two sizes (adult, seed) was apparent (Figure 4). Seed size transcriptomic response was highly variable between individuals, with some distinction between the two sites as well. Differential expression analysis resulted in hundreds of over- and under-expressed transcripts being discovered (Figure *5*;Table *2*). Figure *5* shows the differential expression analysis, with statistically significant transcripts (FDR *p-value* = < 0.05) plotted relative to the FC, where over-expressed and under-expressed transcripts are individually represented in red and blue dots for each pairwise comparison. Positive FC was attributed to over-expressed transcripts whereas, negative FC was attributed to under-expressed transcripts in the hypoxia treatment. The numerical results of the differential expression analysis for each statistical package (DESeq2 and edgeR) are also displayed in Table *2*. The edgeR statistical software package resulted in very few differentially expressed transcripts being discovered and all transcripts found by edgeR were also significant through analysis with the DESeq2 statistical package. Figure 6 displays a Venn diagram summary of the differentially expressed transcripts found unique or mutually within their size category. Most transcripts were found unique to their respective pairwise comparisons, confirming that there were differences in expression patterns between different sizes and sites. Heatmaps of mussels with differentially expressed transcripts between pairwise comparisons are shown in Figure *7* and shows the variation of expression between samples.

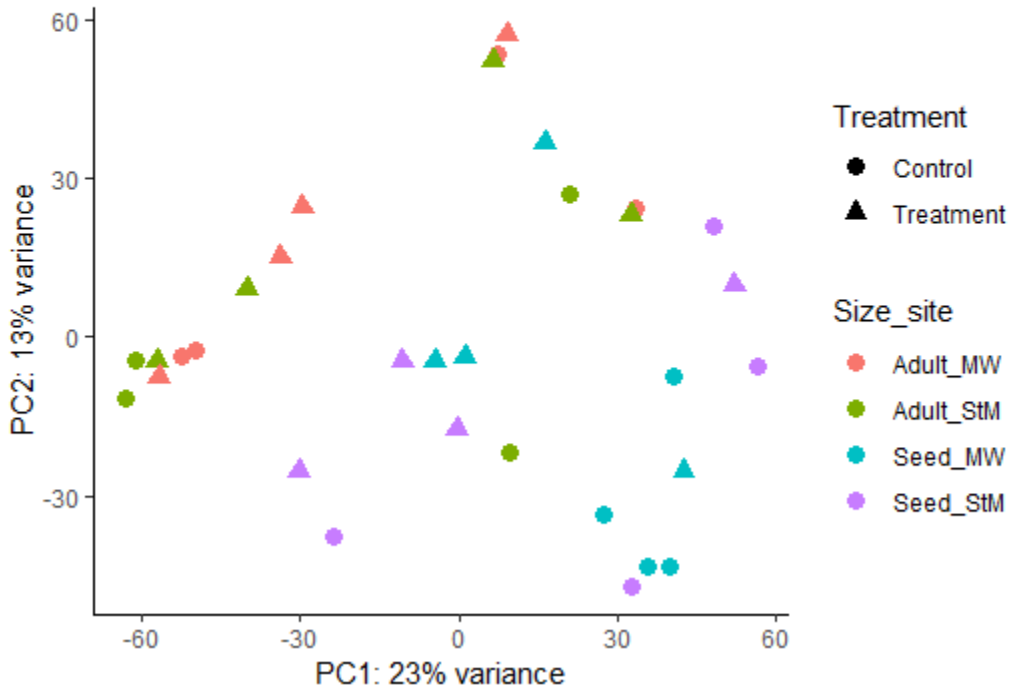

Figure 4. Preliminary principal component analysis plot of all expressed transcripts in the hypoxia trial. Plot shows each mussel sample from both site (MW = March Water, StM = St. Mary's Bay), size (adult, seed), treatment (O_2 ~ 2 mg/L) and control (O_2 ~ 7-8 mg/L).

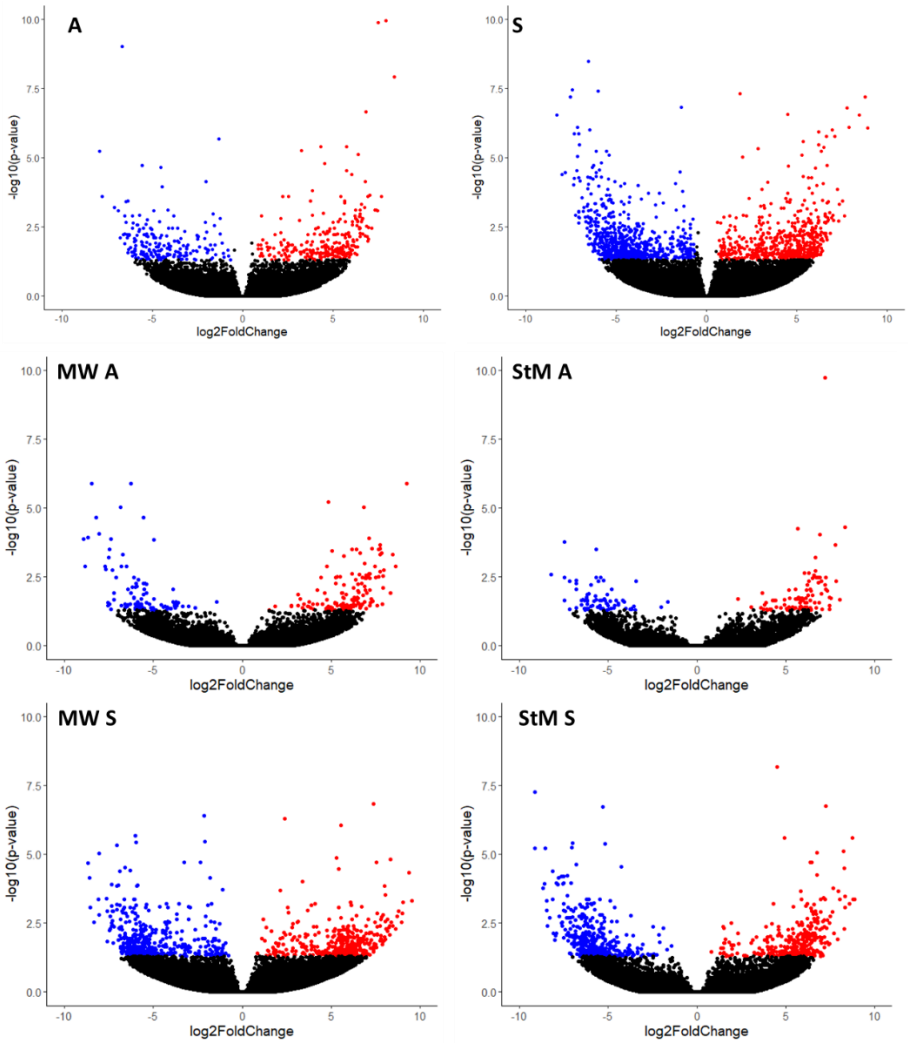

Figure 5. Volcano plots for differentially expressed transcripts identified in DESeq2 for each pairwise comparison (MW = March Water; StM = St. Mary's Bay; A = adult; S = seed). Fold change is expressed as hypoxia treatment (O_2 ~ 2 mg/L) relative to control (O_2 ~ 7–8 mg/L). Transcripts that are differentially expressed (FDR p-value = < 0.05) are indicated by either red (over-expressed) or blue circles (under-expressed).

Table 2. Total number of differentially expressed transcripts (DE) (FDR p-value = < 0.05) for each pairwise comparison (March Water (MW), St. Mary's Bay (StM), adult (A), seed (S)), for both DEseq2, and edgeR.

Comparison name	Total DE DESeq2	Total DE edgeR
MW A	232	0
StM A	172	0
MW S	777	3

Comparison name	Total DE DESeq2	Total DE edgeR
StM S	703	0
A	478	2
S	1291	5

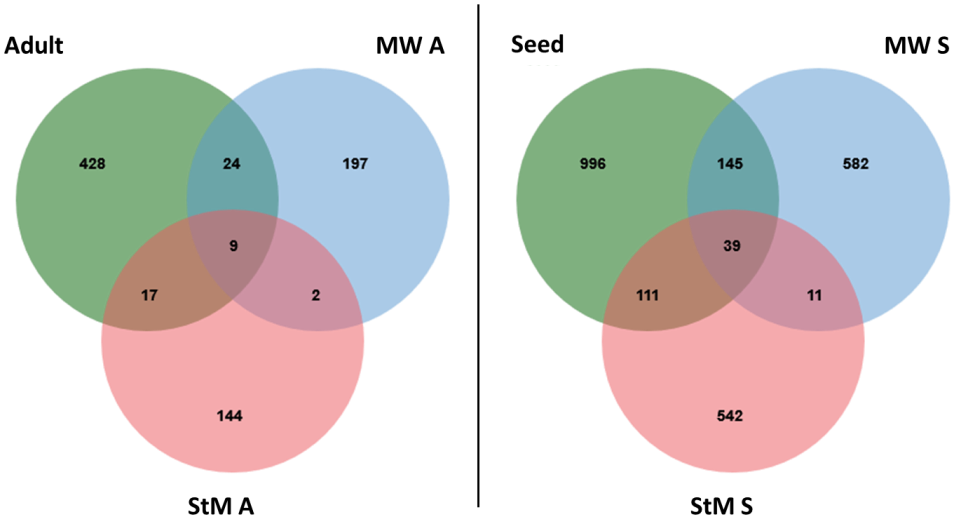

Figure 6. Venn Diagram of differentially expressed transcripts found uniquely or mutually between different pairwise comparison (MW = March Water; StM = St. Mary's Bay; A = Adult; S, = Seed).

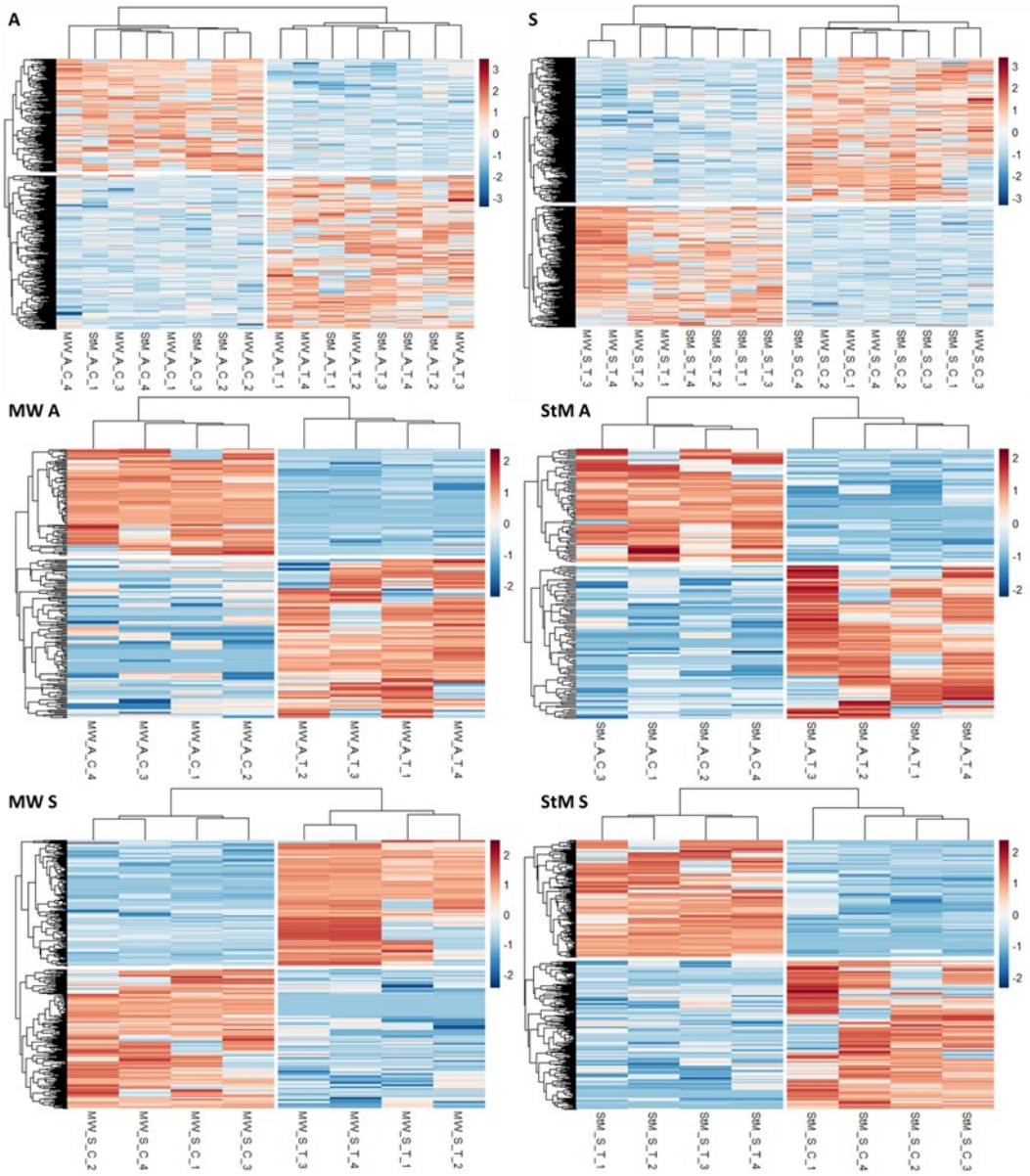

Figure 7. Heatmap of all differentially expressed transcripts identified by the DESeq2 statistical packages in each pairwise comparison (MW = March Water; StM = St. Mary's Bay; A = adult; S = seed; T = treatment (O_2 ~ 2 mg/L) and C = control (O_2 ~ 7-8 mg/L)).

2.3.4 Functional analysis

KEGG pathway assignment of differentially expressed transcripts are shown in Table *3* Only pathways with transcripts assigned to multiple mussel groups are shown (see Appendix 2, for a full list of KEGG pathways). From this analysis, it appeared there were many differentially expressed transcripts associated with metabolic pathways, which could be broadly categorized as carbohydrate metabolism; amino acid metabolism; glycan

metabolism; and other metabolic pathways. Many pathways had both over- and under-expressed transcripts indicating that the mussels were responding to hypoxia by undergoing changes to metabolism. There were also several transcripts associated with cellular processes, environmental information processing, and genetic information processing. Cellular processes involving lysosomes, autophagy, endocytosis, peroxisomes, phagosomes, and spliceosomes, were highly over- and under-expressed by many mussel groups, indicating that these cellular processes were highly important in responding to hypoxia. There were several pathways that were only differentially expressed in seed mussels. Glycan metabolism pathways were entirely differentially expressed by seed mussels. Amino acid metabolism pathways including taurine and hypotaurine metabolism; beta-alanine metabolism; lysine degradation, arginine and proline metabolism; and valine, leucine, and isoleucine degradation were only differentially expressed in seed mussel groups. Seed mussels also had more differentially expressed transcripts related to environmental information processing.

Table 3. KEGG pathways associated with differentially expressed transcripts from each pairwise comparison (MW = March Water; StM = St. Mary's Bay; A = adult; S = seed). Table shows the number of over-expressed (+) transcripts and under-expressed (-)

Category	Pathway	A		MW A		StM A		S		MW S		StM S	
		+	-	+	-	+	-	+	-	+	-	+	-
Amino acid metabolism	Taurine and hypotaurine metabolism	0	0	0	0	0	0	1	0	0	-1	0	0
	beta-Alanine metabolism	0	0	0	0	0	0	2	-1	0	0	1	-1
	Lysine degradation	0	0	0	0	0	0	2	-2	0	0	1	-2
	Arginine and proline metabolism	0	0	0	0	0	0	2	-2	0	-1	1	0
	Valine, leucine and isoleucine degradation	0	0	0	0	0	0	2	-1	0	-2	2	0
	Biosynthesis of amino acids	1	-2	0	-1	1	0	0	-3	0	-4	1	-2
	Amino sugar and nucleotide sugar metabolism	2	0	1	-1	1	0	0	-1	0	-1	1	0
	Cysteine and methionine metabolism	1	0	1	0	0	0	0	-1	0	-1	0	0
	Glycine, serine and threonine metabolism	1	0	1	0	0	0	0	-3	0	0	1	0
Carbohydrate metabolism	Glycolysis / Gluconeogenesis	1	-2	1	-1	1	-1	1	-3	0	-1	3	-3
	Fructose and mannose metabolism	0	0	1	0	1	-1	0	-1	0	0	1	-1
	Pyruvate metabolism	0	-2	0	-1	0	-1	1	-1	0	0	2	-2
	Citrate cycle (TCA cycle)	0	-2	0	-2	0	0	0	0	0	-1	1	-2
	Butanoate metabolism	0	0	0	0	0	0	1	0	0	-1	1	0
	Ascorbate and aldarate metabolism	0	0	0	0	0	0	1	-1	0	0	1	0
	Glycosaminoglycan biosynthesis-heparan sulfate	0	0	0	0	0	0	1	-1	1	-1	1	0
Glycan metabolism	Mannose type O-glycan biosynthesis	0	0	0	0	0	0	1	-1	0	0	0	0
	Various types of N-glycan biosynthesis	0	0	0	0	0	0	1	-1	0	-1	0	-1
	Glycosaminoglycan biosynthesis-chondroitin sulfate	0	0	0	0	0	0	1	0	1	0	1	0
	Glycosphingolipid biosynthesis-globo & isoglobo	0	0	0	0	0	0	1	0	0	-2	1	-1
	Glycosphingolipid biosynthesis-lacto & neolacto	0	0	0	0	0	0	0	-1	0	-1	1	0
	Glycosaminoglycan degradation	0	0	0	0	0	0	0	-1	0	-1	1	0
Lipid metabolism	Fatty acid degradation	0	-1	1	0	0	-1	1	-2	0	-1	2	0
	Arachidonic acid metabolism	1	-1	1	0	0	0	0	-5	0	-1	0	0
	Sphingolipid metabolism	1	0	0	0	0	0	2	0	1	-1	0	0
	Glycerophospholipid metabolism	2	-1	0	0	0	0	0	-2	0	-2	1	0
	Ether lipid metabolism	0	-1	0	0	0	0	0	-2	0	0	0	0
	Linoleic acid metabolism	0	-1	0	0	0	0	0	-3	0	0	0	0
	Glycerolipid metabolism	0	0	0	0	0	0	1	-1	0	0	2	0
	Fatty acid metabolism	0	0	0	0	0	0	0	-2	0	-2	0	0
Other metabolism	Oxidative phosphorylation	2	0	1	-1	1	0	0	0	1	0	2	0
	Drug metabolism-cytochrome P450	0	0	0	0	1	-1	1	0	0	-1	1	-1
	Drug metabolism-other enzymes	0	0	0	-1	0	0	1	-2	0	-3	2	0
	Pyrimidine metabolism	0	0	0	0	1	0	0	-1	0	-1	0	0
	Purine metabolism	0	0	2	-1	1	0	0	-1	0	-2	0	0
	Metabolism of xenobiotics by cytochrome P450	0	-2	0	0	1	-1	1	-1	0	-2	1	-1
	Glutathione metabolism	0	-1	0	0	1	0	2	-5	0	-3	1	0
Cellular Process	Lysosome	2	-1	1	-1	3	0	5	-4	3	-6	2	-7
	Autophagy-animal	1	0	1	-1	1	-1	4	-4	0	-4	0	-1
	Endocytosis	1	0	1	0	1	-2	1	-2	0	0	1	-2
	Peroxisome	1	-1	1	0	0	0	0	-2	0	-3	1	-3
	Proteasome	1	0	1	-1	0	-1	0	0	1	0	0	-1
	Phagosome	2	-1	0	-3	2	-1	2	-1	4	-5	1	-1
	Spliceosome	0	-2	1	0	0	-1	0	-2	1	0	0	-1
Environmental Information Processing	Wnt signaling pathway	1	0	0	0	0	0	1	0	0	0	0	0
	FoxO signaling pathway	2	0	0	0	0	0	2	-3	1	-3	1	0
	mTOR signaling pathway	2	0	0	-1	0	-1	1	-2	0	-3	0	-1
	Neuroactive ligand-receptor interaction	1	0	0	0	0	0	0	-2	1	-1	0	0
	ECM-receptor interaction	0	0	0	0	0	0	0	-1	1	-1	0	-2
	Phosphatidylinositol signaling system	0	0	0	0	0	0	0	-2	0	-2	1	0
	TGF-beta signaling pathway	0	0	0	0	0	0	1	-2	0	0	0	0
Genetic Information Processing	Ribosome	5	-2	1	0	1	-1	2	-2	0	-1	1	-2
	Ribosome biogenesis in eukaryotes	0	-1	0	-1	0	0	1	0	1	-1	3	0
	Ubiquitin mediated proteolysis	1	-2	0	0	1	0	2	-3	3	-1	2	0
	Protein export	0	-1	0	0	0	0	0	-3	0	-2	0	0
	RNA transport	0	0	1	0	0	0	0	0	1	-1	0	0
	Homologous recombination	0	0	0	0	0	-1	0	-1	1	0	0	-1
	Protein processing in endoplasmic reticulum	0	0	0	0	0	-1	0	-5	0	-6	0	-1

Only ~ 20–30% of transcripts were successfully annotated to known proteins relating to Bivalvia in the NCBI nr database, indicating that 70–80% were completely novel or associated with hypothetical or unnamed proteins in bivalves. Table *4*–10 display a subset of differentially expressed transcripts that were successfully annotated (See Appendix 1: Supplemental file 1 for full list). Table 4 displays a subset of differentially expressed transcripts with their sequence ontology and their potential function/pathway that were found mutually between different pairwise comparisons. The majority of differentially expressed transcripts were unique to their pairwise comparison (Table 5–10). Many common themes emerged including most mussel sites and sizes containing transcripts that were associated with metabolism, byssal thread, immune response, stress response, signalling, antioxidant, growth, and development. A subset of commonly expressed differentially expressed transcripts were graphed using their FC, to better understand the expression in other groups not found significant (Figure 8). In the majority of cases, when a transcript was not considered significantly differentially expressed, FC was much smaller compared to those found significant. However, in many of the groups not found significant, the FC was still showing the similar direction (positive/negative FC) as the groups that were found significant.

Table 4. Differentially expressed transcripts found mutually expressed between different pairwise comparisons (MW = March Water; StM = St. Mary's Bay; A = adult; S = seed). Fold change (FC) is shown for each comparison.

Transcript	Sequence Ontology	Function/ Pathway	FC 1	FC 2	FC 3
S; StM A; MW S			**S**	**StM A**	**MW S**
mussels_DN618186_c1_g4_i1	Myticalin C2	Immune	6.5	7.5	7.8
A; MW A; StM A			**A**	**MW A**	**StM A**
mussels_DN589309_c6_g1_i2	Nuclear factor interleukin-3-regulated protein-like	Transcription	3.2	3.3	3.1
mussels_DN624924_c1_g2_i5	Putative C1q domain containing protein MgC1q27	Immune	6.8	6.8	6.3
mussels_DN624924_c1_g2_i3	Putative C1q domain containing protein MgC1q27	Immune	7.5	7.3	6.6

Transcript	Sequence Ontology	Function/ Pathway	FC 1	FC 2	FC 3
mussels_DN652127_c0_g1_i1	Heat shock 90	Chaperone	8.4	7.8	7.0
A; MW A; MW S			**A**	**MW A**	**MW S**
mussels_DN687944_c1_g1_i5	Haloacid dehalogenase-like hydrolase domain-containing 5	Metabolism	2.4	3.5	3.8
mussels_DN690397_c1_g1_i2	Isocitrate dehydrogenase	Metabolism	-2.6	-5.0	-3.6
S; MW S; StM S			**S**	**MW S**	**StM S**
mussels_DN580304_c1_g2_i1	Origin recognition complex subunit 3-like	DNA replication	6.3	5.7	5.7
mussels_DN690013_c0_g2_i3	Origin recognition complex subunit 3	DNA replication	6.5	5.7	6.0
mussels_DN659102_c1_g1_i9	5'-AMP-activated protein kinase, regulatory beta subunit	Energy Sensor	6.7	5.7	7.3
mussels_DN693047_c4_g1_i2	Galactosylgalactosylxylosyl -protein 3-beta-glucuronosyltransferase 3-like	Metabolism	7.6	7.4	7.2
mussels_DN681037_c3_g1_i4	Distal byssal thread collagen	Byssal thread	-6.5	-6.2	-6.6
mussels_DN659012_c0_g1_i3	YGH-rich protein-1	Byssal thread	-6.3	-5.9	-5.7
mussels_DN679162_c1_g1_i6	Byssal peroxidase-like protein 2	Byssal thread	-6.0	-5.8	-5.7
mussels_DN585516_c0_g5_i1	Periostin-like isoform X2	Growth/ Development	-7.5	-5.1	-8.1
mussels_DN617980_c1_g1_i2	Chorion peroxidase-like	Growth/ Development	-6.1	-7.3	-5.0
mussels_DN667690_c4_g1_i13	Putative C1q domain containing protein MgC1q48	Immune	-7.2	-6.8	-6.0
mussels_DN636800_c2_g9_i1	Conodipine-M alpha chain	Metabolism	-7.4	-6.9	-6.8
S; A			**S**	**A**	
mussels_DN678065_c1_g1_i6	Ceramide kinase	Metabolism	2.0	2.1	
mussels_DN652954_c0_g1_i3	Ceramide kinase	Metabolism	3.0	2.7	
mussels_DN702115_c3_g1_i5	CD109	Immune	-3.8	-3.5	

Transcript	Sequence Ontology	Function/ Pathway	FC 1	FC 2	FC 3
mussels_DN672373_c3_g3_i2	U2 small nuclear ribonucleoprotein A'-like	Protein turnover	-1.2	-1.2	
	S; StM A		**S**	**StM A**	
mussels_DN684341_c2_g1_i7	Lipopolysaccharide-induced TNF factor 3	Stress Response	3.3	4.7	
	S; MW S		**S**	**MW S**	
mussels_DN704062_c8_g2_i5	Baculoviral IAP repeat-containing protein 7/8	Apoptosis	2.0	2.3	
mussels_DN696971_c6_g3_i5	Galectin-6-like, partial	Immune	5.3	5.2	
mussels_DN598293_c7_g1_i7	Mytimycin precursor	Immune	6.4	9.1	
mussels_DN678065_c1_g1_i4	Ceramide kinase-like	Metabolism	2.8	3.2	
mussels_DN676839_c1_g5_i1	Von Hippel-Lindau disease tumor suppressor-like	Transcription regulation	0.8	1.2	
mussels_DN645324_c2_g1_i3	cAMP-responsive element-binding protein-like 2 isoform X1	Transcription regulation	2.2	2.8	
mussels_DN699269_c0_g1_i3	Programmed 7 cell death protein, partial	Apoptosis	-4.5	-4.6	
mussels_DN646480_c1_g1_i5	b(0,+)-type amino acid transporter 1-like isoform X1	amino acid transport	-1.2	-1.7	
mussels_DN686978_c0_g1_i2	Foot protein 12	Byssal thread	-7.8	-6.8	
mussels_DN653883_c0_g1_i8	Foot protein 15	Byssal thread	-5.3	-7.3	
mussels_DN681791_c2_g2_i4	Byssal protein-1	Byssal thread	-3.9	-5.6	
mussels_DN683183_c5_g3_i4	Byssal HSP-like protein 1	Byssal thread	-1.0	-1.8	
mussels_DN699204_c2_g1_i4	BiP (heat shock 70)	Chaperone	-1.3	-2.2	
mussels_DN646806_c3_g1_i2	BiP (heat shock 70)	Chaperone	-1.2	-2.1	
mussels_DN642641_c2_g1_i2	Growth arrest and DNA damage-inducible protein GADD45 beta-like	FoxO	-1.3	-2.1	
mussels_DN701354_c5_g3_i1	Sonic hedgehog protein A-like	Growth/Development	-6.9	-6.2	
mussels_DN683160_c0_g2_i3	Inhibin beta A chain	Hormone secretion	-1.7	-2.4	

Transcript	Sequence Ontology	Function/ Pathway	FC 1	FC 2	FC 3
mussels_DN672207_c2_g2_i5	Putative C1q domain containing protein MgC1q48	Immune	-5.8	-8.6	
mussels_DN604786_c0_g3_i1	Lysozyme, partial	Immune	-5.5	-7.3	
mussels_DN604786_c0_g1_i1	I-type lysozyme	Immune	-4.4	-6.5	
mussels_DN631630_c0_g1_i1	Lipopolysaccharide-induced tumor necrosis factor-alpha factor homolog isoform X2	Stress Response	-1.9	-2.1	
mussels_DN698583_c0_g1_i4	Long-chain-fatty-acid--CoA ligase 5-like isoform X2	Metabolism	-1.0	-1.4	
mussels_DN702106_c3_g1_i3	Probable phytanoyl-CoA dioxygenase	Metabolism	-4.9	-6.6	
mussels_DN693047_c4_g1_i1	Galactosylgalactosylxylosyl -protein 3-beta-glucuronosyltransferase 3	Metabolism	-4.6	-5.7	
mussels_DN689356_c2_g1_i4	Elongation of very long chain fatty acids protein 2-like	Metabolism	-1.4	-1.7	
mussels_DN665039_c1_g1_i11	Secretory phospholipase A2	Metabolism	-4.0	-5.8	
mussels_DN678936_c0_g1_i5	Alternative oxidase, mitochondrial-like	Metabolism	-2.8	-3.4	
mussels_DN597817_c2_g1_i1	Alternative oxidase, mitochondrial-like	Metabolism	-2.8	-3.7	
mussels_DN643207_c0_g1_i4	Cytochrome P450 2C8-like	Metabolism	-1.8	-2.5	
mussels_DN659289_c0_g2_i1	Phosphatidylinositol 3-kinase regulatory subunit alpha	mTOR	-1.1	-1.5	
mussels_DN667469_c0_g1_i1	Probable 18S rRNA (guanine-N(7))-methyltransferase	Protein turnover	-3.2	-3.9	
mussels_DN611238_c0_g3_i1	Prolyl-tRNA editing protein ProX	Protein turnover	-2.9	-3.7	
mussels_DN690695_c0_g1_i2	NEDD8-conjugating enzyme ubc12	Protein turnover	-2.4	-3.7	
mussels_DN703733_c3_g1_i2	Protein transport protein Sec24C-like isoform X1	Protein turnover	-0.7	-1.1	

Transcript	Sequence Ontology	Function/ Pathway	FC 1	FC 2	FC 3
mussels_DN623718_c5_g2_i1	Acetylcholine receptor subunit beta-like	Receptor activity	-1.2	-1.4	
mussels_DN624611_c2_g1_i1	Neuronal acetylcholine receptor subunit alpha-10-like	Receptor activity	-0.9	-1.1	
mussels_DN659289_c0_g2_i2	Phosphoinositide-3-kinase, regulatory subunit	Signaling	-1.3	-1.6	
mussels_DN671658_c0_g2_i2	Activating transcription factor 3	Transcription regulation	-2.7	-3.8	
	A; MW A		**A**	**MW A**	
mussels_DN649101_c2_g1_i6	C-type lectin 4	Immune	5.7	6.2	
mussels_DN683349_c2_g1_i1	ATP synthase subunit alpha, mitochondrial-like	Metabolism	4.5	5.4	
mussels_DN566796_c0_g1_i5	Translation initiation factor eIF-2B subunit epsilon-like	Protein turnover	5.7	5.8	
mussels_DN689909_c1_g2_i3	26S proteasome regulatory subunit 4-like	Protein turnover	6.0	5.8	
mussels_DN680994_c6_g2_i1	Phosphatidylcholine protein transfer	Metabolism	4.3	4.5	
mussels_DN685272_c0_g1_i3	Leukotriene-A4 hydrolase	Immune	5.6	7.4	
mussels_DN668624_c1_g1_i1	Peptidylglycine monooxygenase	Potential signalling	6.9	7.2	
	A; StM A		**A**	**StM A**	
mussels_DN700365_c1_g4_i1	Acidic mammalian chitinase-like protein	Metabolism	3.8	3.9	
mussels_DN499915_c0_g1_i1	NADH dehydrogenase subunit 5 (mitochondrion)	Metabolism	4.7	6.4	
mussels_DN690036_c4_g1_i3	Vitelline coat lysin M6 precursor, partial	Reproduction	-7.9	-8.2	
mussels_DN673094_c0_g1_i2	S-(hydroxymethyl)glutathione dehydrogenase	Antioxidant	-4.9	-6.3	
mussels_DN673094_c0_g1_i3	S-(hydroxymethyl)glutathione dehydrogenase	Antioxidant	-1.6	-2.0	
	A; MW S		**A**	**MW S**	

Transcript	Sequence Ontology	Function/ Pathway	FC 1	FC 2	FC 3
mussels_DN606685_c0_g1_i2	Growth arrest and DNA damage-inducible protein GADD45 alpha-like	Growth/Development	1.8	2.5	
	S; StM S		**S**	**StM S**	
mussels_DN689769_c2_g1_i1	Copper chaperone	Chaperone	5.4	6.4	
mussels_DN684544_c4_g1_i8	L-rhamnose-binding lectin CSL3-like	Immune	1.0	1.5	
mussels_DN637045_c7_g2_i1	Nacre apextrin-like protein 1	Immune	5.3	5.3	
mussels_DN656842_c0_g1_i5	Phosphatidylinositol transfer protein alpha isoform	Metabolism	2.8	5.8	
mussels_DN641044_c0_g1_i1	Beta,beta-carotene 15,15'-dioxygenase-like	Metabolism	4.6	5.9	
mussels_DN536948_c0_g1_i1	40S ribosomal protein S3, partial	Protein turnover	4.2	6.6	
mussels_DN669251_c7_g1_i2	E3 ubiquitin-protein ligase TRIM71-like	Protein turnover	6.6	7.6	
mussels_DN628848_c3_g2_i1	Peroxidase-like	Antioxidant	-4.7	-4.8	
mussels_DN690079_c2_g1_i1	Peroxisomal sarcosine oxidase-like	Antioxidant	-4.6	-6.4	
mussels_DN675558_c0_g1_i1	Byssal glycosyl-hydrolase-like protein 2	Byssal thread	-7.3	-7.8	
mussels_DN679162_c1_g1_i3	Byssal peroxidase-like protein 2	Byssal thread	-5.9	-6.7	
mussels_DN693198_c0_g1_i1	Byssal protein-1	Byssal thread	-5.6	-6.0	
mussels_DN675558_c0_g1_i4	Byssal glycosyl-hydrolase-like protein 2	Byssal thread	-5.4	-5.9	
mussels_DN675558_c0_g1_i2	Byssal glycosyl-hydrolase-like protein 2	Byssal thread	-4.7	-6.2	
mussels_DN701015_c1_g5_i1	Byssal tyrosinase-like protein-1 precursor	Byssal thread	-4.7	-5.9	
mussels_DN672206_c3_g1_i4	Byssal protein-1	Byssal thread	-4.4	-7.5	
mussels_DN653538_c4_g1_i2	Proximal thread matrix protein 1 variant a	Byssal thread	-3.9	-6.0	

Transcript	Sequence Ontology	Function/ Pathway	FC 1	FC 2	FC 3
mussels_DN699204_c2_g1_i1	BiP (heat shock 70)	Chaperone	-4.2	-5.2	
mussels_DN665482_c2_g1_i9	Perlucin-like protein	Immune	-3.5	-5.3	
mussels_DN644683_c2_g2_i7	Retinol dehydrogenase 13	Metabolism	-7.0	-7.6	
mussels_DN687445_c1_g1_i6	Aldehyde dehydrogenase, mitochondrial-like	Metabolism	-3.4	-3.9	
mussels_DN663674_c0_g2_i6	39S ribosomal protein L28, mitochondrial-like	Protein turnover	-6.5	-7.1	
	A; StM S		**A**	**StM S**	
mussels_DN592499_c0_g1_i8	foot protein 1	Byssal thread	-5.0	-6.1	

Table 5. Functions/pathway of transcripts found differentially expressed from the March Water adult (MW A) through pairwise comparison. FC = Fold change

Transcript	Sequence Ontology	Function/Pathway	DESeq2 FC
mussels_DN655139_c0_g1_i7	Betaine--homocysteine S-methyltransferase 1 isoform X2	Metabolism	6.9
mussels_DN698229_c0_g1_i6	GDP-mannose 4,6 dehydratase-like isoform X2	Metabolism	6.1
mussels_DN686208_c1_g2_i1	Aldose 1-epimerase-like	Metabolism	5.8
mussels_DN658606_c1_g1_i1	Enoyl-CoA hydratase / long-chain 3-hydroxyacyl-CoA dehydrogenase	Metabolism	5.7
mussels_DN682596_c0_g1_i1	Adenosine deaminase 2-like, partial	Metabolism	4.4
mussels_DN693766_c1_g1_i2	UDP-glucose 4-epimerase	Metabolism	-3.0
mussels_DN701591_c4_g2_i4	Pyruvate dehydrogenase E1 component alpha subunit	Metabolism	-4.0
mussels_DN659959_c1_g2_i3	Ubiquinone biosynthesis monooxygenase COQ6	Metabolism	-7.1
mussels_DN638875_c2_g2_i4	Hypoxanthine-guanine phosphoribosyltransferase	Metabolism	-8.2
mussels_DN666362_c2_g3_i2	Peptidylglycine monooxygenase	Potential signalling	8.6
mussels_DN668624_c1_g1_i6	Peptidylglycine monooxygenase	Potential signalling	7.0
mussels_DN604711_c1_g3_i1	NOTCH2	Notch signalling	4.2
mussels_DN641377_c0_g1_i4	V-type proton ATPase subunit F-like	mTOR pathway	-8.1

Transcript	Sequence Ontology	Function/Pathway	DESeq2 FC
mussels_DN633309_c0_g1_i3	Cathepsin-like protein-4, partial	Autophagy	5.7
mussels_DN682018_c4_g1_i2	Cathepsin L	Autophagy	-5.0
mussels_DN677313_c5_g1_i10	Putative C1q domain containing protein MgC1q83	Compliment immune response	6.4
mussels_DN697621_c4_g2_i1	Peroxisomal membrane protein PEX14-like isoform X1	Peroxisome membrane	6.8
mussels_DN691030_c3_g1_i5	Cell division protein kinase 10	Cell cycle progression	-4.3

Table 6. Functions/pathway of transcripts found differentially expressed from the St. Mary's Bay adult (StM A) through pairwise comparison. FC = Fold change

Transcript	Sequence Ontology	Function/Pathway	DESeq2 FC
mussels_DN494709_c0_g1_i1	Cytochrome b, partial (mitochondrion)	Metabolism	6.4
mussels_DN516426_c1_g1_i1	NADH dehydrogenase subunit 6 (mitochondrion)	Metabolism	6.3
mussels_DN684789_c0_g1_i6	Acidic mammalian chitinase	Metabolism	6.2
mussels_DN469318_c0_g1_i2	Fructose bisphosphate aldolase, partial	Metabolism	6.0
mussels_DN539229_c0_g1_i1	NADH dehydrogenase subunit 2, partial (mitochondrion)	Metabolism	4.4
mussels_DN684951_c1_g1_i6	Sorbitol dehydrogenase-like	Metabolism	-4.2
mussels_DN667886_c2_g1_i3	GTP-binding protein Rheb-like	mTOR	-5.9
mussels_DN632922_c2_g1_i1	26S protease regulatory subunit 6A-B	Protein degradation	-5.5
mussels_DN599943_c1_g1_i4	Byssal protein-1	Byssal thread	-6.5
mussels_DN652134_c2_g1_i1	Cathepsin L2 cysteine protease	Autophagy	6.6
mussels_DN656927_c0_g1_i5	Baculoviral cra_a iap repeat-containing isoform, partial	Apoptosis	5.8
mussels_DN670534_c2_g1_i6	Transcriptional regulator Erg-like isoform X2	Transcription factor	5.6
mussels_DN562587_c1_g2_i6	Heat shock protein 70 kDa 1a	Molecular chaperone	-5.1
mussels_DN680663_c0_g3_i1	Complement component 1 Q subcomponent-binding protein, mitochondrial-like	Compliment immune response	-5.6

Transcript	Sequence Ontology	Function/Pathway	DESeq2 FC
mussels_DN693532_c0_g1_i5	Hepatocyte growth factor-regulated tyrosine kinase substrate	Regulation of growth factor-receptor complexes	7.2
mussels_DN641159_c0_g2_i2	Vitelline envelope zona pellucida domain 9, partial	Egg surface protein	6.6

Table 7. Functions/pathway of transcripts found differentially expressed from the March Water seed (MW S) through pairwise comparison. FC = Fold change

Transcript	Sequence Ontology	Function/Pathway	DESeq2 FC
mussels_DN656275_c0_g2_i4	Temptin-like isoform X1	Metabolism	6.3
mussels_DN642111_c1_g2_i4	Carbonic anhydrase II	Metabolism	6.2
mussels_DN681012_c1_g2_i1	Glycogenin-1-like isoform X3	Metabolism	6.2
mussels_DN623285_c0_g1_i1	Asparagine synthetase (glutamine-hydrolysing)	Metabolism	-2.4
mussels_DN591996_c2_g2_i7	Sulfinoalanine decarboxylase	Metabolism	-4.2
mussels_DN682789_c0_g2_i2	Beta-hexosaminidase subunit beta-like	Metabolism	-5.0
mussels_DN656688_c0_g1_i2	Hydroxymethylglutaryl-CoA synthase 1-like isoform X1	Metabolism	-5.2
mussels_DN672458_c1_g1_i1	Glyceraldehyde-3-phosphate dehydrogenase, partial	Metabolism	-5.4
mussels_DN693047_c4_g1_i1	Galactosylgalactosylxylosyl-protein 3-beta-glucuronosyltransferase 3	Metabolism	-5.7
mussels_DN668463_c0_g1_i5	High affinity cAMP-specific and IBMX-insensitive 3'	Metabolism	-6.5
mussels_DN675645_c0_g1_i8	Galactoside 2-L-fucosyltransferase 1/2	Metabolism	-7.0
mussels_DN605599_c4_g1_i1	Translation initiation factor 4E	Protein turnover	5.9
mussels_DN556153_c2_g1_i2	26S protease regulatory subunit 4	Protein turnover	5.5
mussels_DN703647_c0_g1_i2	Serine/threonine-protein kinase mTOR-like	mTOR	-6.2
mussels_DN640208_c0_g2_i2	translocon-associated protein subunit delta-like	Protein turnover	-6.4
mussels_DN617670_c0_g1_i2	Foot protein 10	Byssal thread	-6.0

Transcript	Sequence Ontology	Function/Pathway	DESeq2 FC
mussels_DN700911_c4_g1_i2	Byssal protein-1	Byssal thread	-4.9
mussels_DN681845_c2_g1_i1	YGH-rich protein-2, partial	Byssal thread	-7.5
mussels_DN671899_c2_g1_i8	Lipopolysaccharide-induced tumor necrosis factor-alpha factor	Stress Response	6.6
mussels_DN687286_c0_g1_i4	Transcription termination factor 3, mitochondrial-like	Transcription Factor	6.0
mussels_DN637563_c5_g1_i1	10 kDa heat shock protein, mitochondrial-like	Molecular Chaperone	-1.9
mussels_DN670756_c3_g2_i2	Caspase 7	Apoptosis	-5.1
mussels_DN662966_c0_g4_i1	Interferon-induced very large GTPase 1-like	Immune Response	8.3
mussels_DN594838_c0_g1_i5	C-type lysozyme 3	Immune Response	7.9
mussels_DN631593_c3_g3_i1	Putative C1q domain containing protein MgC1q5	Compliment Immune Response	7.7
mussels_DN598495_c2_g3_i2	Mytimycin precursor	Antimicrobial Peptide	7.5
mussels_DN667363_c0_g1_i3	Putative C1q domain containing protein MgC1q12	Compliment Immune Response	5.9
mussels_DN668882_c2_g1_i4	Putative C1q domain containing protein MgC1q96	Compliment Immune Response	5.7
mussels_DN622784_c3_g4_i4	Putative C1q domain containing protein MgC1q21	Compliment Immune Response	-4.5
mussels_DN612545_c4_g1_i1	Copper/zinc superoxide dismutase	Antioxidant	-5.5
mussels_DN657070_c0_g1_i7	Glutaredoxin-1-like	Antioxidant	-5.7
mussels_DN665349_c0_g1_i13	C-type lectin 2	Immune Response	-6.0
mussels_DN615776_c3_g2_i8	Nacre protein	Shell development	6.1
mussels_DN636671_c1_g1_i2	Multiple epidermal growth factor-like domains protein 10 isoform X2	Growth factor	3.7
mussels_DN668816_c0_g2_i5	Myosin-1B-like	Muscle Cell Development	-5.2
mussels_DN661679_c2_g1_i1	EF-Hand 1, calcium-binding site	Shell Development	-5.6
mussels_DN604055_c1_g1_i2	Shell protein-2	Shell Development	-6.5

Table 8. Functions/pathway of transcripts found differentially expressed from the St. Mary's Bay seed (StM S) through pairwise comparison. FC = Fold change

Transcript	Sequence Ontology	Function/Pathway	DESeq2 FC
mussels_DN676325_c1_g1_i1	ATP synthase subunit delta, mitochondrial-like	Metabolism	7.0
mussels_DN668019_c3_g4_i1	Succinyl-CoA:3-ketoacid-coenzyme A transferase 1, mitochondrial, partial	Metabolism	6.4
mussels_DN632682_c0_g1_i5	3-hydroxybutyryl-CoA dehydratase-like protein, mitochondrial	Metabolism	6.3
mussels_DN678684_c1_g1_i6	Probable phosphoglycerate mutase	Metabolism	5.7
mussels_DN673785_c0_g1_i2	Retinol dehydrogenase 13	Metabolism	5.2
mussels_DN432810_c0_g1_i1	Cytochrome c oxidase subunit I (mitochondrion)	Metabolism	4.9
mussels_DN590872_c1_g1_i8	Phosphoenolpyruvate carboxykinase	Metabolism	1.9
mussels_DN782059_c0_g1_i1	Aldehyde dehydrogenase: cytosolic 2-like protein, partial	Metabolism	1.6
mussels_DN702394_c4_g4_i2	Fructose-bisphosphate aldolase-like, partial	Metabolism	-4.5
mussels_DN469318_c0_g1_i1	Fructose bisphosphate aldolase, partial	Metabolism	-4.7
mussels_DN673039_c1_g1_i1	Cytochrome c oxidase assembly factor 4 homolog, mitochondrial-like	Metabolism	-5.5
mussels_DN688427_c1_g4_i4	Allene oxide synthase-lipoxygenase protein	Metabolism	-5.5
mussels_DN679147_c0_g3_i3	Alpha-(1,3)-fucosyltransferase fut-1-like	Metabolism	-5.7
mussels_DN690397_c1_g1_i6	Isocitrate dehydrogenase NADP-dependent	Metabolism	-6.0
mussels_DN683873_c3_g1_i4	Pyruvate dehydrogenase E1 component subunit beta, mitochondrial	Metabolism	-6.9
mussels_DN673785_c0_g1_i5	Retinol dehydrogenase 13	Metabolism	-7.6
mussels_DN630521_c3_g1_i4	Proteasome subunit alpha type-3-like	Protein turnover	-4.4
mussels_DN519243_c0_g1_i1	Proteasome-associated protein ECM29 homolog	Protein turnover	-5.2
mussels_DN586392_c3_g1_i4	Byssal protein-3	Byssal thread	-6.4
mussels_DN592499_c0_g1_i11	Foot protein 1	Byssal thread	-5.7

Transcript	Sequence Ontology	Function/Pathway	DESeq2 FC
mussels_DN607202_c3_g1_i1	Foot protein 18	Byssal thread	-6.3
mussels_DN657299_c0_g2_i13	Foot protein-4 variant-1	Byssal thread	-6.9
mussels_DN632599_c3_g2_i21	Byssal HSP-like protein 1	Byssal thread	-5.2
mussels_DN676759_c0_g2_i4	Baculoviral IAP repeat-containing protein 7/8	Apoptosis	7.1
mussels_DN702967_c2_g2_i3	Apoptosis-inducing factor 3	Apoptosis	6.2
mussels_DN703665_c4_g1_i4	Cathepsin D	Autophagy	-3.8
mussels_DN649837_c1_g1_i1	Putative C1q domain containing protein MgC1q84	Compliment immune response	5.5
mussels_DN674262_c0_g2_i2	Putative C1q domain containing protein MgC1q24	Compliment immune response	6.0
mussels_DN582865_c2_g1_i9	Putative C1q domain containing protein MgC1q97	Compliment immune response	6.4
mussels_DN678963_c1_g1_i8	Putative C1q domain containing protein MgC1q4	Compliment immune response	6.8
mussels_DN657021_c1_g1_i13	Glutathione S-transferase U19	Antioxidant	6.0
mussels_DN689730_c2_g2_i4	Superoxide dismutase, Cu-Zn family	Antioxidant	-8.6
mussels_DN658206_c5_g1_i4	Growth/differentiation factor 8-like	Inhibits skeletal muscle growth	5.9
mussels_DN681543_c2_g2_i5	Fibroblast growth factor receptor 2-like isoform X4	Growth	4.5
mussels_DN703304_c2_g1_i1	Myosin-G heavy chain-like isoform X2	Muscle cell development	-5.2

Table 9. Functions/pathway of transcripts found differentially expressed from adult (A) through pairwise comparison. FC = Fold change

Transcript	Sequence Ontology	Function/Pathway	DESeq2 FC
mussels_DN676399_c2_g2_i2	Multiple inositol-polyphosphate phosphatase	Metabolism	4.9
mussels_DN682713_c0_g1_i4	Acidic mammalian chitinase isoform X1	Metabolism	4.3
mussels_DN693252_c3_g2_i2	Cystathionine gamma-lyase-like	Metabolism	5.4
mussels_DN666983_c1_g1_i1	Cytochrome c oxidase subunit II	Metabolism	4.3
mussels_DN671312_c1_g1_i2	Choline/ethanolamine kinase	Metabolism	7.5

Transcript	Sequence Ontology	Function/Pathway	DESeq2 FC
mussels_DN599065_c3_g1_i2	Choline/ethanolamine kinase	Metabolism	5.9
mussels_DN683479_c1_g1_i2	Trans-1,2-dihydrobenzene-1,2-diol dehydrogenase-like	Metabolism	-4.6
mussels_DN569118_c0_g1_i1	Pyruvate dehydrogenase E1 component alpha subunit	Metabolism	-4.8
mussels_DN661401_c0_g2_i4	Ribose-5-phosphate isomerase-like	Metabolism	-4.1
mussels_DN646473_c0_g1_i1	NADH dehydrogenase subunit 2	Metabolism	-4.8
mussels_DN668272_c4_g2_i5	Small subunit ribosomal protein S15	Protein turnover	6.1
mussels_DN657791_c2_g3_i2	60S ribosomal protein L6-like	Protein turnover	5.7
mussels_DN293390_c0_g1_i1	60S ribosomal protein L15-like	Protein turnover	4.1
mussels_DN694172_c2_g2_i2	Methionine aminopeptidase 1D, mitochondrial-like	Protein turnover	6.0
mussels_DN687020_c2_g1_i13	Polyglutamine-binding protein 1-like	Protein turnover	-6.0
mussels_DN693585_c1_g2_i1	60S ribosomal protein L23a-like	Protein turnover	-3.6
mussels_DN603048_c0_g1_i6	UBB protein	Protein turnover	-3.1
mussels_DN664968_c0_g2_i1	Trafficking protein particle complex subunit 4-like	Protein turnover	-5.6
mussels_DN670865_c0_g1_i3	Clathrin light chain B-like isoform X2	Endocytosis	5.6
mussels_DN703051_c4_g2_i2	Serine/threonine-protein kinase Sgk1-like isoform X2	FoxO	6.9
mussels_DN623169_c0_g3_i3	Ganglioside GM2 activator-like	Lysosome	-5.9
mussels_DN641843_c1_g1_i1	Cyclic AMP-dependent transcription factor ATF-4	Transcription	-6.1
mussels_DN641843_c0_g3_i1	Cyclic AMP-dependent transcription factor ATF-4	Transcription	-5.9
mussels_DN677220_c1_g5_i3	Peroxiredoxin-5, mitochondrial-like	Antioxidant	6.5
mussels_DN647445_c3_g1_i8	Cathepsin L	Autophagy	4.6
mussels_DN599221_c4_g1_i2	Defensin gallicin	Immune	5.6
mussels_DN471561_c0_g1_i1	CD206	Immune	-5.4
mussels_DN593596_c0_g1_i9	Macrophage-expressed gene 1 protein	Immune	-4.8

Table 10. Functions/pathway of transcripts found differentially expressed from the seed (S) through pairwise comparison. FC = Fold change

Transcript	Sequence Ontology	Function/Pathway	DESeq2 FC
mussels_DN702705_c2_g2_i2	Probable 2-oxoglutarate dehydrogenase E1 component DHKTD1, mitochondrial	Metabolism	4.3
mussels_DN679015_c0_g3_i3	Hydroxymethylglutaryl-CoA synthase 1-like isoform X1	Metabolism	4.8
mussels_DN693125_c0_g2_i8	UDP-N-acetylglucosamine--peptide N-acetylglucosaminyltransferase 110 kDa subunit-like isoform X1	Metabolism	6.0
mussels_DN560925_c0_g1_i1	Aldehyde dehydrogenase family 16 member A1-like	Metabolism	4.0
mussels_DN652954_c0_g1_i6	Ceramide kinase	Metabolism	2.9
mussels_DN703202_c7_g1_i4	ATP synthase F0 subunit 6	Metabolism	2.9
mussels_DN687911_c2_g1_i8	Ubiquinol-cytochrome c reductase subunit 8	Metabolism	2.8
mussels_DN672777_c0_g1_i1	Ceramide kinase-like	Metabolism	1.2
mussels_DN662050_c3_g4_i5	Secretory phospholipase A2	Metabolism	-5.0
mussels_DN672597_c1_g1_i3	Glutathione S-transferase theta-3-like	Metabolism	-4.8
mussels_DN691230_c1_g1_i5	Glutathione peroxidase-like	Metabolism	-5.9
mussels_DN693009_c1_g1_i6	Alpha-aminoadipic semialdehyde dehydrogenase-like	Metabolism	-4.0
mussels_DN683145_c0_g1_i4	Fukutin-related protein-like	Metabolism	-4.9
mussels_DN697358_c2_g1_i3	Aminopeptidase N	Metabolism	-5.1
mussels_DN665990_c1_g3_i1	Aminopeptidase N	Metabolism	-4.4
mussels_DN625332_c0_g1_i1	Phosphatidylcholine-retinol O-acyltransferase [EC:2.3.1.135]	Metabolism	-6.4
mussels_DN647779_c0_g2_i6	Dopamine beta-monooxygenase [EC:1.14.17.1]	Metabolism	-5.5
mussels_DN699606_c2_g1_i4	40S ribosomal protein S3	Protein turnover	2.9
mussels_DN667362_c4_g2_i4	60S ribosomal protein L3-like	Protein turnover	2.1
mussels_DN664132_c0_g1_i4	Serine/arginine-rich splicing factor 7-like	Protein turnover	-4.4
mussels_DN663674_c0_g1_i5	39S ribosomal protein L28, mitochondrial-like	Protein turnover	-4.7

Transcript	Sequence Ontology	Function/Pathway	DESeq2 FC
mussels_DN683106_c0_g1_i1	eIF-2-alpha kinase GCN2-like	Protein turnover	-5.3
mussels_DN651976_c1_g1_i2	E3 ubiquitin-protein ligase RFWD2	Protein turnover	-5.5
mussels_DN664363_c0_g1_i12	Cullin-1-like isoform X1	Protein turnover	-5.7
mussels_DN642705_c1_g3_i5	40S ribosomal protein S21-like	Protein turnover	-5.8
mussels_DN692191_c3_g3_i1	Cathepsin C	Lysosomes	3.7
mussels_DN684650_c1_g1_i7	Cathepsin L	Autophagy	6.9
mussels_DN599622_c0_g1_i3	Cathepsin L	Autophagy	5.9
mussels_DN618186_c1_g1_i7	Myticalin C7	Immune	5.6
mussels_DN619204_c2_g1_i4	Complement C1q tumor necrosis factor-related protein 6	Immune	5.3
mussels_DN596058_c1_g2_i1	Putative C1q domain containing protein MgC1q87	Immune	4.2
mussels_DN649988_c0_g1_i2	Toll-like receptor 13	Immune	4.1
mussels_DN598495_c2_g2_i5	Mytimycin precursor	Immune	-4.7
mussels_DN637636_c6_g2_i2	Mytimycin precursor	Immune	-6.1
mussels_DN682662_c1_g1_i6	Cyclin C	Transcription regulation	6.9
mussels_DN572550_c7_g1_i1	CREB-binding protein-like	FoxO	6.1
mussels_DN472474_c1_g1_i1	Pre-mRNA 3'-end-processing factor FIP1	mRNA surveillance pathway	6.1
mussels_DN667144_c0_g2_i3	Cyclic GMP-AMP synthase	Cytosolic DNA Sensor	5.5
mussels_DN661855_c1_g1_i5	Peptidylglycine monooxygenase	Potential Signalling	5.7
mussels_DN681297_c0_g1_i12	Cleavage and polyadenylation specificity factor subunit 2-like	mRNA surveillance pathway	5.4
mussels_DN700353_c0_g1_i4	Insulin-like peptide receptor	FoxO	1.0
mussels_DN681670_c0_g5_i3	Rho-associated protein kinase 1	TGF-beta signaling pathway	-6.5
mussels_DN592499_c0_g1_i6	Foot protein 1	Byssal thread	-6.0
mussels_DN592499_c0_g1_i4	Mytilus adhesive protein	Byssal thread	-5.2

Transcript	Sequence Ontology	Function/Pathway	DESeq2 FC
mussels_DN690106_c1_g3_i2	Caspase activity and apoptosis inhibitor 1-like	Apoptosis	5.2
mussels_DN675177_c5_g1_i3	Baculoviral IAP repeat-containing protein 7/8	Apoptosis	4.2
mussels_DN623604_c0_g1_i15	Microsomal glutathione S-transferase 3	Antioxidant	6.0
mussels_DN669476_c1_g1_i4	Selenoprotein W-related protein	Antioxidant	5.7
mussels_DN593810_c0_g1_i1	Sacsin-like isoform X2	Chaperone	5.4

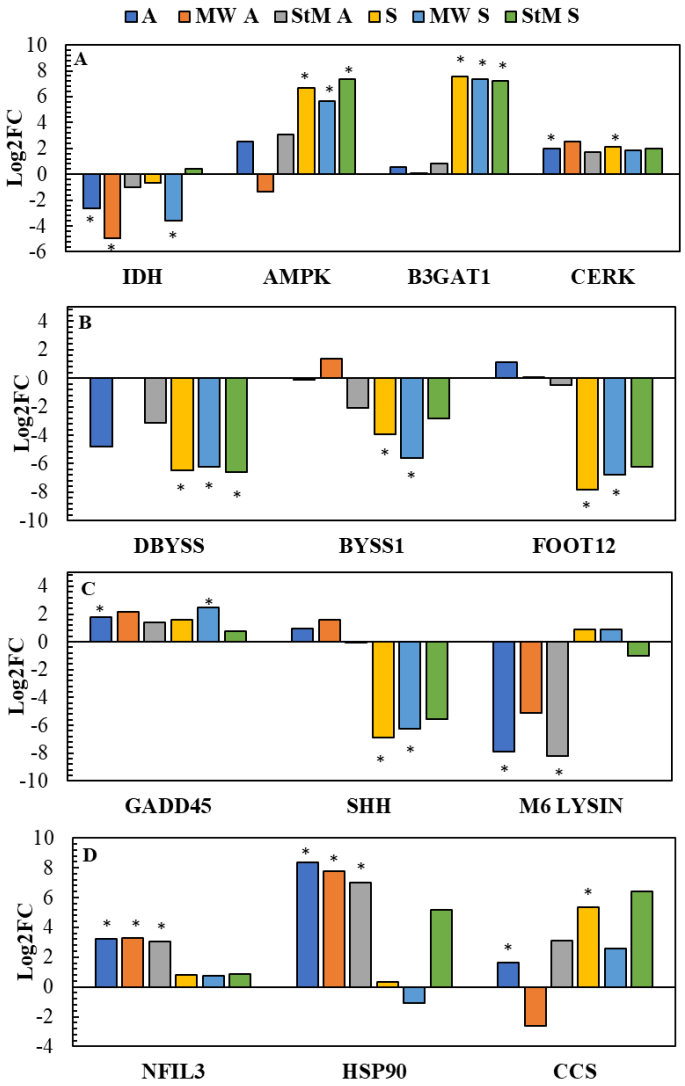

Figure 8. Subset of differentially expressed transcripts plotted using their subsequent Log_2 fold change for each pairwise comparison. Plots are associated with (A) metabolism and energy sensing; (B) byssal thread; (C) growth, development, and reproduction; and (D) stress response. Differentially expressed transcripts were found mutually between pairwise comparisons (MW = March Water; StM = St. Mary's Bay; A = adult; S = seed. IDH = Isocitrate dehydrogenase; AMPK = 5'-AMP-activated protein kinase; B3GAT1 = Galactosylgalactosylxylosyl-protein 3-beta-glucuronosyltransferase 3-like, CERK = Ceramide kinase; DBYSS = Distal byssal thread collagen; BYSS1 = Byssal protein-1; FOOT12 = Foot protein 12; GADD45 = Growth arrest and DNA damage-inducible protein GADD45 alpha-like; SHH = Sonic hedgehog protein A-like; M6 LYSIN = Vitelline coat lysin M6 precursor, partial; NFIL3 = Nuclear factor interleukin-3-regulated protein-like; HSP90 = Heat shock 90; CCS = Copper chaperone.

2.4 Discussion

This study examined the physiological and transcriptomic responses of acute (4 h) hypoxia of blue mussels (*M. edulis*) from two different size classes (seed, adult) and two sites (St. Mary's Bay, March Water, PEI). It was found that acute hypoxia resulted in rapid shifts in transcript expression, as needed to cope with the low oxygen environment. Many transcripts were identified and could be broadly categorized as being related to metabolism, byssal thread, immune, stress response, signalling, antioxidant, growth, development and reproduction. However, the majority of differentially expressed transcripts were considered novel and could not be annotated, indicating the need for more research to be done to identify genes relating to stress response in mussels. The shifts in transcriptomic response found in this study show that response to hypoxia occurs rapidly.

2.4.1 Heart rate monitoring

Mean heart rate of mussels in both treatment (O_2 ~ 2 mg/L) and control (O_2 ~ 7-8 mg/L) conditions were significantly decreased between the first and last hour of the hypoxia trial (Figure *3*A). Several studies have found that during hypoxic/anoxic conditions heart rate of mussels declines (Coleman and Trueman 1971; Bayne 1971; Seo et al. 2016). Bayne (1971) found that the heart rate of *M. edulis* initially regulated to declining oxygen by slightly increasing heart rate, but eventually heart rate began to slow, demonstrating that the mussels conformed to the low oxygen. Similarly, Coleman and Trueman (1971) found that heart rate of *M. edulis* declined during aerial exposure (intracellular hypoxia). Seo et al. (2016) found that heart rate declined to ~ 5 BPM over a 6 h period in *M. galloprovincialis.* The present study also found that heart rate in the hypoxia treatment went down, however, heart rate in the control group also went down as well. Therefore, it is more likely that the initial shock of moving the mussels to the respirometer resulted in the change in heart rate, and more time would be needed to understand the trend of heart rate.

The mean heart rate during the trial was significantly higher in the acute hypoxia treatment (O_2 ~ 2 mg/L) compared with an hour after. Studies have found that heart rate recovers to normal values after transfer back to normoxic conditions, after a brief compensatory period

of rapid heart rate (Coleman and Trueman 1971; Bayne 1971). Normal resting heart rate in mussels has been found to vary depending on environment. For example, in *M. galloprovincialis* at temperatures of 20 °C heart rate was observed between 20–35 BPM, and at temperatures of 10 °C the heart rate was found between 10–25 BPM, therefore dependent on environmental conditions (Seo et al. 2016). At 14 °C it was observed that *M. edulis* has a resting heart rate of 21.30 ± 0.87 BPM (Braby and Somero 2006). The present study found that when mussels were exposed to the treatment (O_2 ~ 2 mg/L) heart rate ranged from 22.4 ± 1.1 to 21.40 ± 1.1 BPM, but declined to 19.4 ± 1.6 BPM after returning to normoxic conditions. This range would be considered normal for mussels and indicates that the mussel's recovery after the trial was rapid, and compensation was not required.

2.4.2 Transcript expression associated with metabolism and anaerobiosis:

Bivalves have evolved specialized strategies to survive hypoxic/anoxic events in their environment, including the switch from aerobic respiration to anaerobic respiration. The present study found that exposing mussels to acute hypoxia resulted in rapid changes to metabolic pathways, as illustrated by many differentially expressed metabolic transcripts. Metabolic pathways with the most differentially expressed transcripts could be broadly categorized as carbohydrate, amino acid, lipid, glycan and other pathways. This finding was expected as bivalves will gradually shift from aerobic respiration to anaerobic respiration during hypoxic conditions (De Zwaan et al. 1983; De Zwaan 1991; Grieshaber et al. 1994; Müller et al. 2012).

During early hypoxia, carbohydrates and amino acids are the main metabolites used for energy. Glycolysis results in the production of pyruvate that can be utilized in two ways during hypoxia. Pyruvate can be condensed using specific dehydrogenases and the addition of amino acids to form opines (strombine (glycine), alanopine (alanine), octopine (arginine) (De Zwaan and Wijsman 1976; De Zwaan et al. 1982, 1983; De Zwaan 1983, 1991; Grieshaber et al. 1994; Müller et al. 2012). Pyruvate can also undergo transamination reactions with aspartate, that forms alanine and oxaloacetate. Oxaloacetate is then reduced to malate and is utilised in the mitochondria to produce additional moles of ATP (Collicutt and Hochachka 1977; De Zwaan et al. 1981; De Zwaan et al. 1982, 1983; Foreman and

Ellington 1983; De Zwaan 1991; Larade et al. 2002). During prolonged hypoxia/anoxia, a switch to malate metabolism occurs in the mitochondria, resulting in succinate, acetate and propionate as end-products (De Zwaan and Wijsman 1976; De Zwaan 1983, 1991; Müller et al. 2012). The mitochondrial electron transport chain will also undergo modification, where fumarate becomes the terminal electron acceptor instead of oxygen (Holwerda and De Zwaan 1980; De Zwaan et al. 1981; De Zwaan 1983, 1991; Schulz and Kluytmans 1983; Grieshaber et al. 1994; Van Hellemond et al. 1995; Müller et al. 2012).

In the present study, there were no significantly expressed dehydrogenase transcripts found involved with the production of opines or transamination reactions occurring (alanine aminotransferase; aspartate transferase). However, the adult mussel groups and St. Mary's Bay seed had under-expressed transcripts annotated as Pyruvate dehydrogenases E1 components, which is associated with pyruvate metabolism and the citric acid cycle. Other transcripts were associated with the citric acid cycle, including isocitrate dehydrogenase which was under-expressed in all mussel groups. The under-expression of pyruvate metabolism and citric acid cycle is an important finding, as both pathways are associated with aerobic respiration (Raven et al. 2008). Therefore, the under-expression of the transcripts associated with these pathways could signify the transition from aerobic to early anaerobic pathways.

In this study, transcripts associated with enzymes involved in amino acid metabolism were differentially expressed. Amino acids, particularly glycine, alanine, arginine, and aspartate have an important role in anaerobic metabolism in bivalves (De Zwaan and Wijsman 1976; De Zwaan et al. 1982, 1983; De Zwaan 1983, 1991; Grieshaber et al. 1994; Müller et al. 2012). There were a few trends discovered associated with amino acids that could be considered important for anaerobiosis. For example, a transcript annotated as asparagine synthase (glutamine-hydrolysing) was under-expressed in March Water seed mussels. Asparagine synthase (glutamine-hydrolysing) is involved with the conversion of aspartate to asparagine (Patterson and Orr 1968; Lomelino et al. 2017). Since aspartate commonly becomes depleted during transamination reactions (De Zwaan 1983, 1991), this under-expression of the asparagine synthase enzyme might be involved with conservation of aspartate pools. In addition, seed mussels had more amino acid metabolism pathways

differentially expressed compared to adults. Amino acid pools are also important for osmotic balance (Grieshaber et al. 1994). Catabolism of proteins during hypoxia has been demonstrated in bivalves as a potential mechanism to maintain these amino acid pools (Soldatov et al. 2009; Haider et al. 2020a). Therefore, differential expression of amino acid pathways in this study may be associated with the maintenance of free amino acids as an important strategy for survival in hypoxic conditions.

There were also several differentially expressed transcripts associated with oxidative phosphorylation pathways in all mussel groups in this study, which may have a role in hypoxia tolerance mechanisms. For example, a ubiquinone biosynthesis monooxygenase Coq6 transcript was under-expressed in the March Water adults. Ubiquinone biosynthesis monooxygenase Coq6 is involved with the production of ubiquinol-n that gets utilized during oxidative phosphorylation in the electron transport chain (ETC) (Kawamukai 2016). In addition, there were also several significantly differentially expressed transcripts associated with the ETC in all mussel groups including ATP synthase subunits (March Water adult, St. Mary's Bay seed), cytochrome b, partial (mitochondrion) (St. Mary's Bay adult), multiple cytochrome c oxidase subunits (all mussel groups), NADH dehydrogenase subunit 2 (adult mussels), and NADH dehydrogenase subunit 6 (St. Mary's Bay adult). It is well established that some complexes in ETC stay active, such as complex I and II but less is known about the other complexes during hypoxia (Holwerda and De Zwaan 1980; De Zwaan et al. 1981; De Zwaan 1983, 1991; Müller et al. 2012). However, a study by Ivanina et al. (2016) in hard shell clams (*Mercenaria mercenaria*) found that during hypoxia there was enhancement of substrate oxidation capacity, and it was hypothesized to be associated with modifications to the electron transport complexes. Therefore, differential expression of these transcripts in this study may be associated with changes occurring in the ETC and enhancement of substrate oxidative capacity.

2.4.3 Transcript expression associated with metabolic rate depression

A second strategy to survive hypoxia/anoxia is metabolic rate depression. Metabolic rate depression can be defined as a coordinated shutdown of pathways that either consume or produce ATP to conserve energy (Grieshaber et al. 1994; Hochachka et al. 1996). This

shutdown occurs when there is a disruption in energy balance, such as when more ATP is being consumed than produced (Larade et al. 2002). Metabolic rate depression results in shutdown of many physiological systems and processes including muscle movement, energetics, respiration, heart rate, immune system, and building of macromolecules such as DNA, RNA, proteins and membrane phospholipids (Storey and Storey 2004; Larade and Storey 2009). As previously discussed, the trend in heart rate in the present study indicates that metabolic rate depression had not fully developed in the mussels. However, this study found that there were some changes in transcriptomic response patterns indicating that metabolic depression could be developing; including differential expression of transcripts associated with metabolic regulation. For example, seed mussels had a common transcript over-expressed annotated as 5'-AMP-activated protein kinase, regulatory beta subunit. This protein is a well-known energy sensor in vertebrates that is activated by detecting low ATP levels, such as in hypoxia, and leads to suppression of ATP-consuming processes (Hardie and Hawley 2001). A recent study by Wang et al. (2020) has validated this pathway is associated with energy metabolism in the clam *Ruditapes philippinarum* in response to aerial exposure. The over-expression of this transcript was likely associated with the transition to metabolic rate depression in the present study. The mTOR signalling pathway was also under-expressed in this study. This pathway is involved in signalling and regulating stress, survival, metabolism, growth and development (Laplante and Sabatini 2009; Sabatini 2017). The present study found that there were several differentially expressed transcripts associated with the mTOR pathway and may have a potential role in metabolic rate depression. For example, in the St. Mary's Bay adult group, there was an under-expressed transcript annotated as "GTP-binding protein Rheb-like". This protein is involved in regulation of mTOR pathways. GTP-binding protein Rheb-like is regulated by several external stimuli, one of which is an energy deficit or hypoxia. When there is a low ATP:ADP ratio the GTP-binding protein Rheb-like is under-expressed and mTOR pathway becomes inhibited (Laplante and Sabatini 2009). This downregulation in mTOR can result in changes to metabolism, angiogenesis, autophagy, and endoplasmic reticulum homeostasis (Wouters and Koritzinsky 2008). The March Water adult group also had an under-expressed transcript associated with mTOR which was annotated as V-type proton ATPase, subunit F, this is a transcript that has a role

in amino acid sensing pathways. Decreasing amino acids may trigger suppression of mTOR and result in autophagy (Efeyan et al. 2012). Furthermore, the March Water, seed group had an under-expressed transcript annotated as serine/threonine-protein kinase mTOR-like. Serine/threonine-protein kinase mTOR-like is an important complex involved with the mTOR pathway and under-expression of this will result in changes in cellular metabolism, growth and survival (Laplante and Sabatini 2009; Sabatini 2017). The differential expression of these pathways might indicate that the mussels exposed to hypoxia were experiencing a transition period where signalling events had begun the process of shutting down energetic pathways.

2.4.4 Energy conservation mechanisms

Energy conservation mechanisms in association with metabolic rate decline in hypoxia/anoxia tolerant bivalves results in suppression of several basic physiological processes. For example, macromolecules synthesis has been found to be supressed to conserve energy (Hand 1998; Robertson et al. 2001; Larade and Storey 2009). In the gastropod *Littorina littorea,* anoxia resulted in a reduction of protein synthesis of 49% of normoxic conditions (Larade and Storey 2002).

The present study did not show conclusive evidence of protein turnover suppression. This study found that the translation initiation factor eIF-2B subunit epsilon-like, and translation initiation factor 4E were over-expressed in adult mussels, and March Water seed, respectively. Both translation factors are associated with eukaryotic translation initiation factor, which are important complexes involved with protein translation, that have been found significantly supressed in response to hypoxia/anoxia in molluscs (Larade and Storey 2002; Ivanina et al. 2016). Therefore, the significant over-expression of these translation initiation factors in the present study could indicate that protein translation had not yet been supressed.

The present study found components of the 26S proteasome were differentially expressed in all mussel groups. The 26S proteasome is an important complex that is involved with protein turnover, particularly proteolysis (Voges et al. 1999), which has been found to be

supressed in hypoxia/anoxia in molluscs (Ivanina et al. 2016). In the March Water group, two transcripts were over-expressed annotated as 26S proteasome regulatory subunit 4-like (March Water adult), and 26S protease regulatory subunit 4 (March Water seed group), indicating that the proteasome had not been supressed in these mussel groups. In contrast, the St. Mary's Bay adults had under-expression of the 26S protease regulatory subunit 6A-B. The St. Mary's Bay seed also had two under-expressed transcripts associated with proteosomes including proteasome-associated protein ECM29 homolog and proteasome subunit alpha type-3-like. Ivanina et al. (2016), found that the clam (*Mercenaria mercenaria*) was able to suppress the 26S proteasomes (trypsin-like and caspase-like) rapidly whereas, the hypoxia sensitive scallop (*Argopecten irradians)* maintained expression levels, and differences were speculated to be due to differences in tolerances. Therefore, the results of the present study could indicate that St. Mary's Bay mussels were faster at supressing the proteosome, then March Water mussels.

2.4.5 Stress response:

This study found differential expression of transcripts associated with several classes of stress related transcripts including protein integrity mechanisms, transcription factors, apoptosis, stress sensing/signalling, immune and antioxidant. Hypoxia/anoxia can lead to homeostasis disruptions in mussels including intracellular acidosis and accumulation of toxic end-products that can lead to protein damage (Grieshaber et al. 1994; Almeida et al. 2005; Slobodskova et al. 2012; Ivanina et al. 2016), which leads to stress response. Metabolic rate depression and anaerobic respiration may lead to an energy deficiency, which also triggers stress responses (Storey and Storey 2007; Anestis et al. 2010). In addition, some stress related transcripts may be over-expressed in association with stress granules, to prevent damage and allow quick rebound after reoxygenation occurs (Anderson and Kedersha 2002; Rzymski and Harris 2007; Larade and Storey 2009).

In this study, Heat shock protein (HSP) 90 was over-expressed mutually between the adult mussels. The majority of HSP's were under-expressed in seed mussels including three transcripts annotated as Binding immunoglobulin protein (BiP) (heat shock 70). The HSP, BiP, is an important molecular chaperone in the endoplasmic reticulum. However, seed

mussels had over-expression of sacsin, which has been found to be a molecular chaperone (Anderson 2013). Molecular chaperones are involved in interacting with proteins that are misfolded, to help stabilize and refold them back to their original conformation (Vabulas et al. 2010) and have a role in protecting bivalves from cellular damage/stress (Kiang and Tsokos 1998; Sørensen et al. 2003; Nie et al. 2018).

Cathepsin related transcripts were also found differentially expressed. Cathepsin L isoforms were found differentially expressed in all mussel groups: March water adults (under-expressed), St. Mary's Bay adults (over-expressed) and seed mussels (over-expressed). Cathepsin L is a cysteine protease, which is a lysosomal endopeptidase enzyme that is involved with protein degradation and has roles in protein turnover, immune system, proprotein processing and apoptosis (Barrett and Kirschke 1981; Conus 2010; Kumaresan et al. 2014). This study also found that cathepsin D was under-expressed within the St. Mary's Bay seed group. In contrast to the present study, Falfushynska et al. (2020) found that in *M. edulis* there was an increase in free cathepsin D during short-term activity of hypoxia likely due to a release of already existing cathepsin D inside lysosomes, however, at 6-days there was another increase in Cathepsin D (~ 3.5–6 fold increase), indicating an increase in autophagic processes (Falfushynska et al. 2020). This indicates that perhaps more time would be needed for the expression of Cathespin D to be expressed. Cathepsin D has been found to have a well-known role in protein degradation in lysosomes, but also directly involved with autophagy and apoptosis (Benes et al. 2008).

There were several transcripts differentially expressed and annotated to genes associated with apoptosis including caspase 7, baculoviral IAP repeat-containing proteins, programmed 7 cell death protein and apoptosis-inducing factor 3. Seed mussel groups contained over-expressed transcripts annotated as baculoviral IAP-containing proteins which are involved with regulating apoptosis in bivalves (Zhang et al. 2016). In addition, one transcript in the St. Mary's Bay seed group annotated as an apoptosis-inducing factor 3 was over-expressed, which plays a role in caspase-independent cell death (Sevrioukova 2011). The differential expression of these apoptosis-related transcripts is an indicator of cell damage and the need for clearance of damaged cells (Romero et al. 2011).

2.4.6 Immune Response:

This study found there were differentially expressed transcripts annotated associated with the immune system. Immune related transcripts were both over and under-expressed. In hypoxia/anoxia the immune system has been found under-expressed (Pampanin et al. 2002; Matozzo et al. 2005; Chen et al. 2007a, 2007b; Wang et al. 2011a). Therefore, the over-expression of several immune transcripts was not an expected finding. The C1q domain containing family was found differentially expressed in all mussel groups. The family of C1qs plays a role in innate immune response by promoting immune effector recruitment, ending cell-cycle progression, and promotes survival through the NF-kB pathways in vertebrates (Van den Berg et al. 1998; Bordin and Tan 2001; Amanullah et al. 2003; Yamada et al. 2004). In addition, the C1q domain containing proteins have been found in other non-immune related proteins including adiponectin, precerebellin, hibernation protein, etc (Kishore et al. 2004). It is not clear why several immune transcripts were found significantly over-expressed in all mussel groups; however, the expression may be associated with an early stress response and likely would be under-expressed in the later stages of hypoxia/anoxia exposure due to metabolic depression.

2.4.7 Antioxidant:

Antioxidant associated transcripts were also found significantly differentially expressed including peroxidases, superoxide dismutase (SOD), glutaredoxin (Grx), gluthathone-S-tranferase (GST), etc. Reactive oxidative species (ROS) can be generated during hypoxia and cause oxidative damage to some bivalves (Almeida et al. 2005; Slobodskova et al. 2012; Zhang et al. 2017). In addition, the transition back to aerobic respiration after hypoxia/anoxia can generate ROS and lead to further oxidative stress. Oxidative damage during hypoxia/reoxygenation appears to be linked to tolerance. Bivalves that are considered hypoxia tolerant do not appear to develop oxidative damage as demonstrated by Rivera-Ingraham et al. (2013) in *M. edulis*. In contrast, bivalves considered hypoxia sensitive appear to develop tissue damage to gills and the digestive gland/hepatopancreas during hypoxia (Almeida et al. 2005; Slobodskova et al. 2012). There is still some debate whether antioxidants are over-expressed in response to hypoxia stress in bivalves. Several

studies in the Mediterranean mussel (*M. galloprovincialis*) have found that hypoxia/anoxia have increased SOD, Gpx and lipid peroxidase (Woo et al. 2013; Andrade et al. 2018, 2019). In the present study, antioxidant expression was both over- and under-expressed. Adults had little differential expression of antioxidants, with exception of over-expression of Peroxiredoxin-5, mitochondrial-like (adults) and Peroxisomal membrane protein PEX14-like isoform X1(March Water adult group) and under-expression of two transcript isoforms identified as S-(hydroxymethyl)glutathione dehydrogenase (adult mussels). Seed mussels had over-expression of a copper chaperone, microsomal glutathione S-transferase 3, Selenoprotein W-related protein and under-expression of a Peroxidase and Peroxisomal sarcosine oxidase. Seed mussels also had other antioxidants unique to their site and size including over-expression of Glutathione S-transferase U19 (St. Mary's Bay seed) and under-expression of Superoxide dismutase (St. Mary's Bay seed), Copper/zinc superoxide dismutase (March Water seed), and Glutaredoxin-1-like (March Water seed)

2.4.8 Differences in transcriptomic response in different size mussels

This study found that there were differences in the transcriptomic response to hypoxia between the size of mussels and sites. Functional analysis in adult and seed indicates that hypoxia treatment resulted in differential expression of similar functional groups including metabolism, signalling, protein turnover, stress response, immune etc. However, there were differences in expression as discussed in previous sections. Overall, the seed size had more differentially expressed transcripts compared to the adults. Differences in expression between seed and adult mussels during exposure to hypoxia is likely associated with the differences in development stage between the adult and seed mussels. Clark et al. (2016) found that in the clam (*Laternula elliptics*), younger individuals' transcriptomic response was more active and were in better physiological condition, compared to adults. This could indicate the higher level of transcriptomic expression in the present study may be resulting from seed mussels responding faster to mitigate damages, compared to adults.

2.4.8.1 Reproductive response

One of the reasons why differences may emerge in transcript expression between mussel size is reproductive status. Mussels have been found to put more energy in their first year of development to rapid growth and put very little energy in reproduction (Thompson 1979). As mussels reach adulthood there is a gradual shift to place more energy into reproduction than somatic growth (Thompson 1979). This study found two reproductive transcripts differentially expressed in adults, one over-expressed (Vitelline envelope zona pellucida domain 9, partial) (St. Mary's Bay adults) and one under-expressed (Vitelline coat lysin M6 precursor, partial) (adults). The seed mussels did not contain any reproductive transcripts differentially expressed. It has been found that mussel reproductive effort is a function of body size, ranging from zero to ~ 80% of total growth (dry weight) between the first year to four-year-old mussels (Thompson 1979). Gametogenesis begins when mussels reach ~ 35 mm in PEI (Guyondet et al. 2015), indicating the seed size mussels were likely allocating more energy to somatic growth compared to the adults. This trend is visualized with more growth and developmental transcripts differentially expressed in the seed mussel groups compared to the adult.

2.4.8.2 Growth Response:

This study found that seed mussels had many differentially expressed transcript associated with growth and development. Although variation was found in transcriptomic response in growth transcripts between the two sites within the seed group, there was a subset of potential growth-related transcripts commonly differentially expressed between the two groups. Sonic hedgehog protein A-like was found significantly under-expressed in the seed mussels. The hedgehog gene family are important regulators of development, growth and morphogenesis in both vertebrates and invertebrates (Shimeld 1999; Ingham and McMahon 2001; Nederbragt et al. 2002; Grimaldi et al. 2008; Li et al. 2018; Nie et al. 2021). Sonic hedgehog has been found to have key roles in myogenesis in vertebrates and have a determinant role of fast and slow muscle growth (Blagden et al. 1997; Grimaldi et al. 2004). More recent studies in invertebrates have found that hedgehog signalling may also play an important role in growth and development in molluscs such as *Sepia officinalis*

(Grimaldi et al. 2008), and *Ruditapes philippinarum* (Nie et al. 2021). Chorion peroxidase-like was also found commonly significantly under-expressed in seed mussels and may have a role in shell biomineralization in *Mytilus sp.* mussels (Hüning et al. 2016; Malachowicz and Wenne 2019). Periostin-like isoform X2 was also found to be commonly significantly under-expressed in seed mussels and has been found to be a mesenchymal protein that may have a role in development, and cell repair in vertebrates particularly in bone and cardiac cells (Kudo et al. 2007; Conway et al. 2014). In zebrafish (*Danio rerio*), periostin has been found to be important for repairing cardiac damage (Ito et al. 2014). Periostin has been found differentially expressed in developing molluscs including *Meretrix meretrix* (Huan et al. 2012) and *Babylonia areolata* (Shen et al. 2018). Sonic hedgehog protein A-like, chorion peroxidase-like, and periostin-like isoform X2 were only significantly expressed in the seed group and not within the adult (Figure 8) and this could indicate that this subset of transcripts were of high importance to the stage of development that the seed were in compared to the adults.

Two myosin related transcripts were also found under-expressed in the seed mussels including Myosin 1B-like (March Water seed) and Myosin-G heavy chain-like isoform X2 (St. Mary's Bay seed). Myosin has been found to be important for muscle ontogenesis within the contractile "catch" muscles in the larval stages of mussel *M. trossulus* and oyster *C. gigas* (Dyachuk et al. 2005; Dyachuk and Odintsova 2009; Yu et al. 2017). The differential expression of myosin related transcripts in the seed and not in adult mussels might be an indicator that the expression of these transcripts is developmental/growth related. Hypoxia has been found to result in metabolic rate shutdown to conserve energy in bivalves (De Zwaan et al. 1991; Larade et al. 2002, Storey and Storey 2004). This metabolic rate depression results in suppression of many physiological pathways including growth (Norkko et al. 2005; Larade and Storey 2009). In addition, a study by Wang and Widdows (1993) found that juvenile *M. edulis* (~ 13 mm) are not able to allocate energy into growth below PO_2 of 10 kPa (~ 4 mg/L). This indicates that the seed mussels were showing similarities in terms of their shut-down of growth pathways within the first four-hours of hypoxia exposure.

2.4.8.3 Metabolism:

Metabolism might also play a role in differences in responses to hypoxia between different sizes. The current study found that there were more transcripts under-expressed associated with metabolism in seed compared to adults. This could indicate that the seed mussels might have been responding faster to the hypoxia treatment resulting in an earlier metabolic rate shutdown. However, this can only be speculated, as metabolic rate was not measured in this study. Differences in metabolic responses have been documented in different sizes of mussel. A study by Sukhotin et al. (2003) on *M. edulis* found that there were size related differences in how long a mussel could survive. Mussels that were smaller (mean tissue wet weight 0.12 g), and medium size (mean tissue wet weight 0.39 g) could survive longer exposed to aerial exposure than larger mussels (mean tissue wet weight 0.78 g). This difference was speculated to be due to higher absolute metabolic rates in the larger mussels (Sukhotin et al. 2003). Energy reserves have been found to differ between sizes, with younger bivalves having overall lower energy reserves than adults (Holland and Spencer 1973; Mann and Gallager 1985; Widdows et al. 1989). Therefore, the differences in metabolic pathways might be associated with conserving energy reserves. Anaerobic responses in bivalves are highly variable depending on the energy reserves available; therefore, intra-individual variability can result in differing types of end-products and ratios associated with anaerobic pathways (De Zwaan 1991).

2.4.8.4 Byssal thread production

Byssal thread production transcripts were found entirely under-expressed in seed mussels. The under-expression found in this study could be indicative that byssal thread production is decreasing in response to acute hypoxia. Climate change stressors such as high temperature, acidification and hypoxia have been found to reduce the byssal thread attachment in mussels (Wang et al. 2013; O'Donnell et al. 2013; Sui et al. 2015; Clements et al. 2018). Several mussel species have been found to reduce their attachment behaviour via byssal threads during hypoxia (Wang et al. 2013; Sui et al. 2015). Byssal thread production suppression is likely associated with energy conservation such as in metabolic rate depression (Shin et al. 2009; Wang et al. 2013). Roberts et al. (2021) found that the

cost of production of byssal thread in the mussel *M. trossulus* was between 2–47% of a mussel's total energy budget depending on season and need to form byssus. Therefore, the suppression of byssal threads might be one of the first mechanisms that occurs to conserve energy in hypoxia/anoxia conditions. Suppression of byssal threads during anoxic events in coastal ecosystems could have negative consequences including dislodgment of mussels and mortality (Roberts et al. 2021). Seed mussel detachment in long-line systems has been a issue for the mussel aquaculture industry, and while this issue is not fully understood it may be associated with stressful conditions, predation, migratory behaviour, and competition of food resources (Comeau et al. 2017a; South et al. 2022). If mussel attachment becomes weaker during stressful environmental conditions as well, climate change associated increases in hypoxic/anoxic conditions could further increase this issue and lead to more losses.

2.4.9 Differences in transcript expression in between sites

Differences in transcriptomics between sites were also apparent in this study. It has been found that mussels from different areas in Atlantic Canada show genetic diversity, particularly between areas where there would be differences in environmental fluctuations and little gene flow (Gartner-Kepkay et al. 1980; Koehn et al. 1984). However, in locations where there is mixing of larvae from dispersal, similarities in genetics have been observed (Gartner-Kepkay et al. 1980). Due to likely larval dispersal in PEI estuaries, it would not be expected that the mussels from March Water and St. Mary's Bay would be significantly genetically different. Gene expression has also been found variable between mussel sites. For example, a study by Place et al. (2008) analyzed gene expression of the mussel *M. californianus* in different populations along the Pacific coast as far North as Bamfield, British Columbia and as South as Punta San Isidro, Mexico and found that there were major differences in gene expression patterns associated with each population. Interestingly, this difference in gene expression was not associated with temperature gradient from north to south and it was speculated that it might have been associated with other factors such as nutrient availability, hypoxia, salinity, or predator abundance. A recent report by Poirier et al. (2021) monitored environmental differences over three years (2016–2018) in six locations within PEI including: Brudenell River, March Water, Murray River, New London

Bay, Nine Mile Creek, and Tracadie Bay. The environmental data in this report is highly relevant to this research as the sites covered in this study were monitored directly (March Water) or nearby (Brudenell River is in the same watershed as St. Mary's Bay). In addition, the mussels in this study were collected in 2017, therefore would have been exposed to the same environmental conditions. Poirier et al. (2021) found that water parameters trends and growth appear similar between sites; however, some interesting anomalies were observed. In 2017, March Water mussels seed was smaller compared to all other sites, this trend was observed in this study as well, as seed from March Water used in this study were smaller. Size related differences between the two sites could have resulted in some of the differences in transcriptome responses found between these two groups, as intra-individual variability can result in differing types of end-products and ratios associated with anaerobic pathways (De Zwaan 1991). Poirier et al. (2021) found that the majority of water parameters including mean monthly temperatures, salinity and pH were similar between the two locations, with some differences in daily fluctuations visible. Other studies have found that the frequency of hypoxia exposure may result in intraspecies tolerance differences in bivalves (Altieri 2006; Meng et al. 2018). However, since dissolved oxygen concentrations were so similar between the two sites, it is unlikely that this was a factor contributing to the differences in transcript expression. Interestingly, spring bloom timings were different between March Water, Brudenell River, with March Water having an earlier bloom and more peaks of chlorophyl A in 2016 and 2017 (Poirier et al. 2021). Therefore, there could be links between differences in transcriptome expression exhibited between March Water and St. Mary's Bay in relation to small differences in their environment.

2.5 Conclusions:

Overall, this study found that there were significant changes in heart rate and transcript expression patterns in short-term hypoxia exposure in mussels. Overall major shifts in transcript expression were observed in association with metabolism, signalling, protein turnover, byssal thread production, stress response, immune, growth and development after the four-hour hypoxia exposure. While heart rate did not show conclusive decline, as would be expected in metabolic rate depression, transcript expression patterns indicate a switch

to anaerobic metabolism and signalling indicative to metabolic rate changes which would likely translate into phenotypic changes.

This study found differences in transcript expression between size classes of mussels and sites. Differences in the size classes of mussels could have resulted due to differences in physiological status, growth, metabolism and development in the seed compared to adults. Furthermore, the site differences could again have resulted from differences in size between the seed mussels and potentially differences in the environmental conditions that they originated from.

Long-term anoxic events can result in mass mortality events in bivalves (Steimle and Sindermann 1978; Santos and Simon 1980; Lenihan and Peterson 1998; Buzzelli et al. 2002; Uzaki et al. 2003; Lim et al. 2006; Van Colen et al. 2010; Kozuki et al. 2013; Tweedley et al. 2015; Coffin et al. 2021). However, the results of this study show that after the first few hours of hypoxia exposure, shifts in transcriptome expression occurs that would likely lead to major physiological changes. In the seed mussels, there was under-expression of several growth, development, and byssal thread transcripts that could have implications for mussel aquaculture, as fast growth and development is important for productivity of the industry. Further, byssal thread production decline could result in increases in detachment from mussels socks and increases in predation. Overall, more research is needed to follow up on these findings to determine if these changes relate to long-term physiological impacts.

Chapter 3. Evaluating blue mussels (*Mytilus edulis*) responses to acute hyposalinity using transcriptomics, heart rate and neutral red assay

3.1 Introduction

Anthropogenic climate change has been identified as a major concern for the blue mussel (*Mytilus edulis*) aquaculture industry in Prince Edward Island (PEI). One of the concerns of climate change, is both long-term and short-term deviations in salinity (Rhein et al. 2013; Hoegh-Guldberg et al. 2014). Long-term salinity changes have been found to differ depending on geographic location. For instance, salinity is increasing from evaporation in parts of the Atlantic Ocean, while it has become less saline due to increased precipitation and runoff in the Pacific Ocean (Rhein et al. 2013; Hoegh-Guldberg et al. 2014). Melting of sea and glacial ice also impacts ocean salinity (Hoegh-Guldberg et al. 2018). Short term changes are associated with heavy precipitation events, run-off, and flooding (Hoegh-Guldberg et al. 2018). It is anticipated that climate change will strengthen hydrological cycles, from an increase in temperature that results in more saturation in vapor pressure (Held and Soden 2006; Rush et al. 2021). In Atlantic Canada, precipitation increased ~ 10% between 1948–1995 (Lewis 1997; Lambert et al. 2013) . Extreme precipitation events are projected to increase in Canada, and under high emission projections, extreme events that use to occur once in 20 years will increase to once in five years (Zhang et al. 2019). In the Gulf of St. Lawrence, climate projections are predicting that there will be a substantial decrease in sea ice and salinity by late 2060's due to runoff from precipitation events (Long et al. 2016).

In Atlantic Canada, blue mussels are found within the intertidal and subtidal zones, where frequent salinity fluctuations occur (Schmitt 2008; MacCready and Geyer 2010; Geng et al. 2016; Geng and Boufadel 2017). Blue mussels are euryhaline, meaning they can tolerate a wide range of salinities between ~ 35–5 ‰, but can handle short periods of salinity outside this range as well (Gilles 1972; Shumway 1977; Davenport 1979a; Vuorinen et al. 2002; Duarte et al. 2020); however, abrupt changes in salinity is a source of osmotic stress (Schmitt 2008; Bayne 2017). Blue mussels are osmoconformers, meaning that they maintain intra- and extracellular osmolyte concentrations that are isosmotic or slightly

hyperosmotic to their environment (Gilles 1972; Zurburg and De Zwaan 1981; Yancey 2005). Osmoconformation in hyposaline environments results in the decline of osmolyte concentration to match that of its environment (Zurburg and De Zwaan 1981; Yancey 2005). The process involves passive osmotic transport of inorganic ions from extracellular fluid, followed by an uptake of water into cells and subsequent degradation or expulsion of osmolytes (i.e. free amino acids) from the cells to the environment (Florkin 1962; Lang et al. 1998; Freire and Sampaio 2021). In addition, blue mussels have been found to change the structure of their phospholipid membranes in response to hyposalinity stress to aid in fluidity (Nemova et al. 2013). Valve closure can also occur as an early response to hyposalinity stress to prevent abrupt changes in osmolytes and mitigate osmotic stress (Gilles 1972; Shumway 1977; Bayne 2017); which is often associated with a significant slowdown of metabolism and heart rate (Bahmet et al. 2005; Braby and Somero 2006). While the blue mussel is tolerant to hyposalinity, the process of osmoconformation can be stressful and energetically costly to bivalves. Bivalves are generally smaller and have less energy to put into somatic growth and calcification in areas of prolonged hyposalinity (Riisgård et al. 2013; Sanders et al. 2018). Temperature increases along with declining salinity, as predicted in climate change scenarios, may further impact growth and calcification (Hiebenthal et al. 2013; Filgueira et al. 2016; Nielsen et al. 2021).

At the cellular level, adapting to hyposaline conditions in mussels has been found to result in changes in ion channels, ion exchangers, aquaporins, ATPase pumps, osmolyte transporters, which all aid in the osmoconformation process (Lockwood and Somero 2011; Barrett et al. 2022). Expression of genes associated with stress response such as heat shock proteins (HSP) and antioxidants has also been found (Lockwood and Somero 2011; Nielsen et al. 2021; Barrett et al. 2022). Changes in gene expression associated with signalling, metabolism, proteolysis, and cell cytoskeleton organization has also been found in mussels (Hamer et al. 2008; Lockwood and Somero 2011). Other studies in oysters have found that hyposalinity stress results in changes of expression of genes associated with metabolism, osmoconformation, membranes, immune effectors, stress response, and antioxidant defence (Lockwood and Somero 2011; Zhao et al. 2012, 2014; Meng et al. 2013; Nie et al. 2017; Xiao et al. 2018; Ertl et al. 2019). These studies showcase the well adapted

mechanisms that bivalves can utilize to regain homeostasis and osmoconform to their environment.

Despite several studies dedicated to understanding physiological and genotypic responses of mussels to hyposaline conditions, there are still many unknowns, especially associated with how genetic response results in observable changes in their physiology. Studies have found variances in physiological responses in hyposaline conditions between bivalves of different size classes and populations (Pierce and Greenberg 1973; Pierce et al. 1995; Qiu et al. 2002; Sukhotin et al. 2003; Hosoi et al. 2005; Nemova et al. 2013; Bayne 2017; May et al. 2017). While studies have been completed to understand the transcriptomic mechanisms involved with osmoconformation (Lockwood and Somero 2011; Nielsen et al. 2021; Barrett et al. 2022), no studies (to my knowledge) have been completed to understand how transcriptomics vary between sizes and sites. Therefore, this study evaluated the acute response of hyposalinity exposure in two sizes (adult, seed) of blue mussel from two sites (March Water, St. Mary's Bay, PEI, Canada). Heart rate and lysosomal destabilization were evaluated to understand the physiological responses during the hyposalinity exposure. It was hypothesized that major shifts in transcript expression, heart rate, and lysosomal destabilization would be observed within the first six-hours of exposure to hyposalinity, and that there would be substantial differences in the transcriptomic response between the two sizes and sites of mussels.

3.2 Materials and methods

3.2.1 Mussel sites and sizes

Adult and seed mussels (*M. edulis*) were obtained from two aquaculture leases located in PEI: March Water (MW) (N 46° 31' 18.8", W 63° 43' 12.9") and St. Mary's Bay (StM) (N 46° 07' 37.2", W 62° 31' 14.2") (Figure *2*(Chapter 2)). For a detailed summary of mussel sites, sizes and acclimation used in this trial please refer to Chapter 2 (2.2.1 Mussel sites and sizes).

3.2.2 Hyposalinity trial

Separate salinity trials were completed for each size group (MW, StM), with the first consisting of adults and the second consisting of seed mussels. The salinity trial was completed in a flow-through (120 mL/min) zebra tank (9 L) set-up. A total of eight zebra tanks divided into two groups (4 replicates): control (27 ‰) and treatment (hyposalinity: 16 ‰). Both salinity trials were completed over a 6 h period. In each trial, a total of 14 mussels from both sites were placed in each tank (28 per tank; N = 224 total). Temperature was maintained at 16 °C.

3.2.3 Heart rate monitoring

Heart rate (HR) was monitored only in the adult trial, and not in the seed trial as sensors were too big for seed size mussels. To measure HR, non-invasive infrared red-light (IR) sensors were manufactured by Dr. K Fraser Clark using a slightly modified method based on Burnett et al. (2013). The HR sensors were attached to the mussel over the approximate location of the heart, and plumbers' putty (PlumbShop®, Masco Canada Limited, Ontario, Canada) was placed around the sensor to seal it to the mussel and reduce IR signal fluctuations. After initial attachment of IR sensor, mussels were placed back into their holding tank for 24 h to acclimatize to the sensor. Heart rate of three mussel per treatment (six total) were monitored continuously over the 6 h salinity trial and for 1 h after the trial. Real-time HR was visualized using the software Makerplot (SelmaWare Solutions, LLC) and then analyzed further by importation into Microsoft Excel 365, to visualize the HR data. Heart rate was interpreted by manually counting the total number of heartbeats in one-minute intervals (beats per minute (BPM)) every 15 minutes, and then calculating the mean in 1 h time intervals.

3.2.4 Neutral Red Assay

Neutral red assay (NRA) was conducted in the adult and seed trials at three time points: 0 h (pre-treatment), 3 h, 6 h. For the adult trial, one mussel from each site (MW, StM) was used at 0 h (pre-treatment). During the trial (3, 6 h) one mussel from each tank per site was used. For the seed trial, seed mussels were too small to collect a sufficient haemolymph and mantle fluid sample from, therefore, four individuals were pooled during each NRA

reading. The pre-treatment (0 h) reading consisted of a pooled sample from each site (MW and StM), and during the trial (3, 6 h) a pooled sample from each site per tank was used. Lysosome destabilization index (LDI) was calculated using the method developed by Hauton et al. (2001); Harding et al. (2004); Methe et al. (2015).

Briefly, a stock solution was prepared using 2.28 mg of neutral red dye (3-amino-7-dimethylamino-2-methylphenazine hydrochloride) (F1631: Sigma-Aldrich, St. Louis, MO) dissolved in 1 mL of dimethyl sulfoxide (DMSO) (D128, Thermo Fisher Scientific, Waltham, MA, USA). Approximately 500 µL of mantle fluid was collected from the mussels (pooled sample for seed mussels) and filtered through a 0.2 µm Progene cellulose acetate membrane (Ultident, St. Laurent, QC, Canada). Then, a working solution was prepared by dissolving 8.5 µL of stock solution into the mantle fluid. A 0.2 mL haemolymph sample was then collected from the pericardial sac region and mixed with 0.2 mL of mantle fluid in a low-retention 1.5 mL microtube (Eppendorf, Thermo Fisher Scientific). An aliquot of 40 µL was transferred to a microscope slide and incubated (dark) for 15 minutes at 20 °C, then 20 µL of working solution was added to the slide and incubated for an additional 45 minutes. The microscope slide was read under a compound microscope (630x magnification) by counting 50 haemocyte cells total and expressing them as LDI.

3.2.5 Statistical analysis of heart rate and neutral red assay

Separate statistical analysis was completed for HR and LDI. Two statistical analyses were completed for HR: (1) mean hourly HR (1, 2, 3, 4, 5, 6 h) and (2) trial timing categories of the mean HR during the last two hours of the trial and mean HR of the one-hour post-treatment when mussels were placed back into acclimation tank. Heart rate differences between sites could not be analysed due to insufficient replication. To analyse HR, a General Mixed Effect Model was used with repeated measures treated as hierarchal structure (split-plot) with mussels as large units (whole plots) and time as sub-units (subplots). In the HR analysis, the salinity (control 27 ‰, treatment 16 ‰), and time (1, 2, 3, 4, 5, 6 h) or (during, after) were considered fixed variables. The mussels were considered a random variable with salinity nested within. Variance inflation factor was calculated to test multicollinearity of the model. The model included all significant main effects and

interactions, with the insignificant main effects and interactions being collapsed from the model to give final model estimates.

Neutral red assay's LDI was analysed separately for each size (adult, seed) at time 3 h and 6 h. To analyse LDI, a General Mixed Effect Model was used. Salinity (control 27 ‰, treatment 16 ‰), site (MW, StM), and time (3 h, 6 h) were considered fixed variables. Tank effect was considered random with salinity and site nested within. The model included all significant main effects and interactions.

In both analysis of HR and LDI, assumptions of normality and homoscedasticity were assessed for the error terms by conducting a normal probability plot of standardized residuals of error terms and variance by plotting the residuals of error terms versus fitted. For all analyses, the significance level was set at *p-value* = < 0.05. In the presence of a significant interaction between the various factors, a Bonferroni simultaneous test of means was performed to identify differences between groups. All estimates are reported as least square mean (LSM) ± standard error (SE), unless otherwise specified.

3.2.6 Sample preservation, RNA extractions and sequencing

Six mussels per size (adult, seed) and site (MW and StM) in each salinity treatment (control (27 ‰), hyposalinity (16 ‰)), were collected following the 6 h salinity trials. Whole mussel tissue from individual animals was homogenized into RNAlater® solution (Cat. No. 76106, QIAGEN GmbH, Hilden, Germany) using an Omni tissue homogenizer (Omni International, Kennesaw, GA, USA), at a ratio of 1g tissue per 10 mL of RNAlater®. RNA was isolated using Qiagen RNeasy® Mini Kit (Cat. No: 74104, QIAGEN GmbH, Hilden, Germany) following the manufacture protocol. An additional on-column DNase I (Cat. No. 79254, QIAGEN GmbH, Hilden, Germany) treatment was applied during the RNA isolation process, to ensure no DNA contamination was present. Concentration and quality of RNA was assessed using Nanodrop spectrophotometry (Thermo Fisher Scientific, Waltham, MA, USA) and Bioanalyzer (Agilent Bioanalyzer, RNA 6000 nano kit, Santa Clara, CA, United States), respectively. High quality RNA was shipped to Genome Quebec (Montreal Quebec) where Truseq library preparation was completed on each

sample. Then, Hiseq2000 Illumina (sequencing by synthesis) was completed (PE 100), to give 15–20 million reads per sample (eight samples per sequencing lane).

3.2.7 *De novo* transcriptome assembly and differential expression analysis

The transcriptome assembled in this study was built using mussel samples from the hypoxia (chapter 2), salinity (present chapter), food availability (chapter 4) trials, and resulted in one large transcriptome. For detailed description of assembly and differential expression analysis, see Chapter 2 (2.2.6 *De novo* transcriptome assembly; 2.2.7 Differential expression analysis).

Differential expression analysis was completed using both DESeq2 (Love et al. 2014; Afgan et al. 2018) and edgeR (Afgan et al. 2018; Robinson 2019) (Galaxy Version 3.24.1 + galaxy1) algorithms. In both methods, *p-value* was adjusted to control for false discovery rate (FDR *p-value*). Several pairwise comparisons were completed to understand the nature of the transcript expression of the different sites and sizes, and this is summarized in Table 11. Log_2 fold change (FC) was used to visualize the relative expression of control (27 ‰) versus treatment (16 ‰). Trends in differential expression analysis results were visualized using volcano plots, Venn diagrams, heatmaps and principal component analysis (PCA) analysis. PCA analysis was completed on transcripts that had expression level of 10 across all samples in the hyposalinity trials.

Table 11. Differential expression analysis comparisons utilized in experiment. For each comparison, two different methods of differential expression were used, DESeq2 and edgeR. Comparisons were laid out as control (27 ‰) vs hyposalinity (16 ‰) for each size (A = adult; S =seed) and site (MW = March Water; StM = St. Mary's Bay).

Pairwise comparison group	Number of comparisons	Comparison name
Adult by site	2	StM A MW A
Seed by site	2	StM S MW S
Size (MW & StM)	2	A S

3.2.8 Annotation and functional analysis

Differentially expressed transcripts underwent annotation (FDR *p-value* < 0.05) using Trinnotate (Bryant et al. 2017) and Blast2GO (basic) software (Version 5.2.5) using NCBI Blast service (blastx), with an E-value cut-off set at $1e^{-5}$, and with a taxonomy filter selective to only bivalves (taxa: 6544, Bivalvia) (Conesa et al. 2005; Conesa and Götz 2008; Götz et al. 2008, 2011). The Kyoto Encyclopedia of Genes and Genomes (KEGG) Automatic Annotation Server (KAAS) (Moriya et al. 2007) was used to annotate differentially expressed transcripts as well. Then, annotation assignment of differentially expressed transcripts was used in pathway assignment using KEGG Mapper (Kanehisa and Sato 2020) using the organism-specific search mode. KEGG mapping was assigned using the only two bivalve species within the KEGG server, Pacific oyster (*Crassostrea gigas*) and Yesso scallop (*Mizuhopecten yessoensis*) to receive pathways only relevant to bivalves. Annotation, ortholog, and pathway assignment aided in facilitating functional understanding of differentially expressed transcripts.

3.3 Results

3.3.1 Heart rate and neutral red assay

For the mean hourly HR (1, 2, 3, 4, 5, 6 h) statistical analysis, the interaction of salinity*hour had a significant impact on HR (*p-value* = <0.001; *F* = 30.74). Figure 9A shows the gradual increase in HR over the 6 h salinity trial. Bonferroni simultaneous test of means found that the 6 h time point at salinity 16 ‰ (hyposalinity), HR was significantly different than several other time points in both salinities (hyposalinity, control) (Table 12). The 3 h mark appeared to show a significant increase in mean HR at 16 ‰ (hyposalinity) from 1 h and 2 h, and this increasing trend continued throughout the remainder of the trial. For the timing categories (during, after), statistical analysis found that the interactions of salinity*timing (*p-value* = < 0.001; *F* = 7.62) had significant impacts on mean HR in this study (Figure 9B). It was found that HR at 16 ‰ (hyposalinity) significantly decreased after returning to the acclimation tank from 20.6 ± 0.6 to 16.6 ± 0.5 BPM. The results of the analysis of NRA found that LDI was not significantly impacted by salinity (*p-value* = 0.213), time (*p-value* = 0.904), or site (*p-value* = 0.763) (Figure 10).

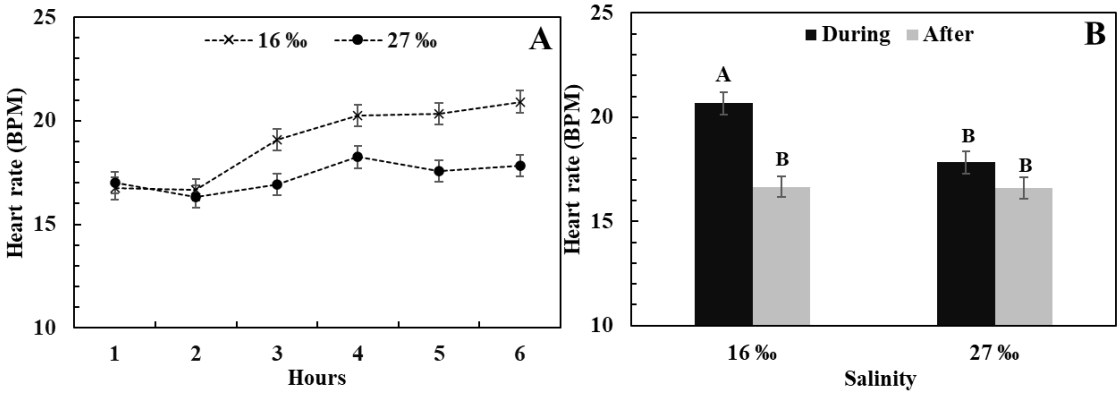

Figure 9. Least square means (LSM) ± Standard error (SE) of heart rate for hyposalinity (16 ‰) and control (27 ‰) from final statistical model for (A) 1, 2, 3, 4, 6 h (n = 3 per point); (B) during, after (n = 3 per bar). LSMs without a mutual script were significantly different (*p-value* < 0.05).

Table 12. Estimates from final statistical model of heart rate from mussels held at each salinity (16, 27 ‰). Bonferroni Pairwise Comparison of the interactional effect of Salinity*Hour. LSM's that don't share a letter are considered statistically significant (*p-value* < 0.05).

Salinity *Hour	N	Mean	SE	Grouping			
16 ‰–6h	3	20.9	0.53	A			
16 ‰–5h	3	20.3	0.53	A	B		
16 ‰–4h	3	20.3	0.53	A	B		
16 ‰–3h	3	19.1	0.53	A	B	C	
27 ‰–4h	3	18.2	0.53	A	B	C	D
27 ‰–6h	3	17.8	0.53		B	C	D
27 ‰–5h	3	17.6	0.53		B	C	D
27‰–1h	3	17.0	0.53			C	D
27 ‰–3h	3	16.9	0.53			C	D
16 ‰–1h	3	16.7	0.53				D
16 ‰–2h	3	16.6	0.53				D
27 ‰–2h	3	16.3	0.53			C	D

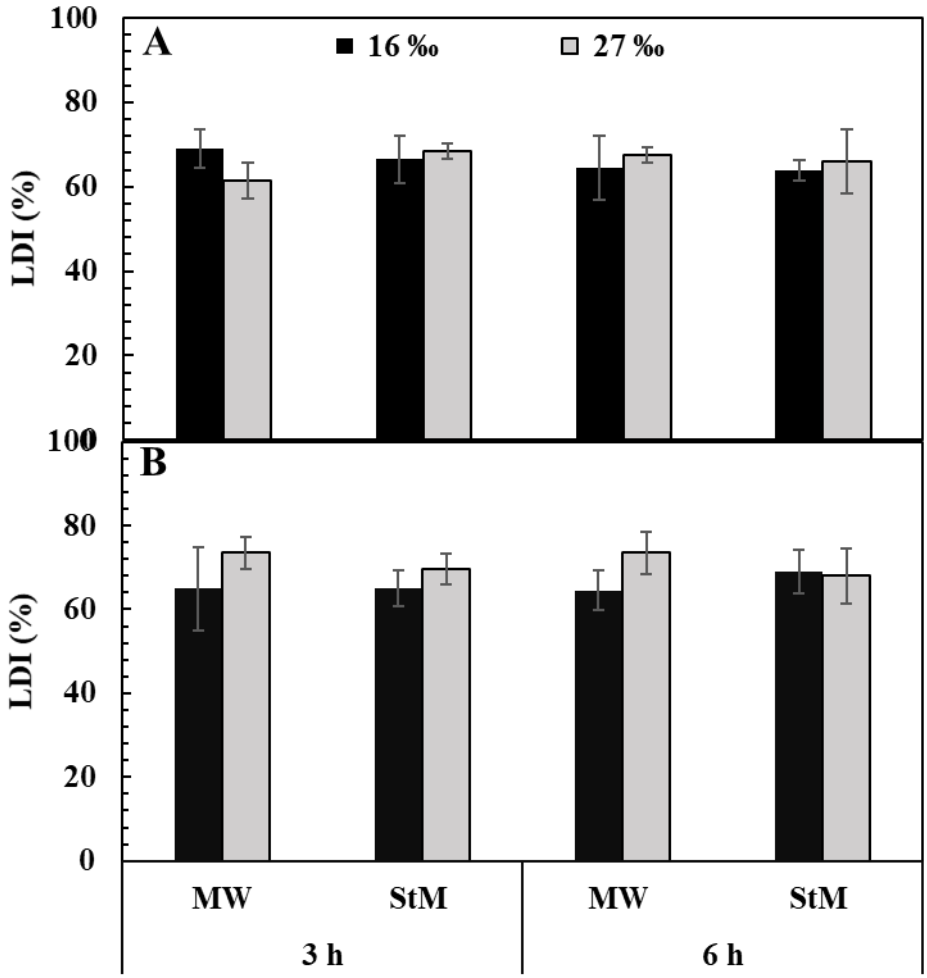

Figure 10. Least square means (LSM) ± Standard error (SE) of lysosome destabilization index (LDI) from final statistical model for hyposalinity (16 ‰) and control (27 ‰) with time (3, 6 h) in (A) adults and (B) seeds (MW, March Water; StM, St. Mary's Bay; n = 4 per bar).

3.3.2 Differential transcript expression analysis

Preliminary PCA of transcripts expressed in mussels from the hyposalinity trial, indicated that there was a lot of variability between individuals; however, some separation could be visualized between different sizes and sites (Figure *11*). Differential expression analysis resulted in hundreds of over-expressed and under-expressed transcripts being discovered (Figure *12*; Table 13). Figure 11 highlights the differential expression analysis, with statistically significant transcripts (FDR *p-value* = < 0.05) plotted relative to the FC, where over-expressed and under-expressed transcripts are individually represented in red and blue

dots for each pairwise comparison. Positive FC was attributed to over-expressed transcripts whereas, negative FC was attributed to under-expressed transcripts in the hyposalinity treatment. The edgeR statistical software package resulted in only a few differentially expressed transcripts being discovered, compared to DESeq2, and all transcripts identified by edgeR were also identified by DESeq2 (Table 13).

Venn diagrams of the differentially expressed transcripts found unique or mutually between pairwise comparison is displayed in Figure 13. Most transcripts were found to be unique to their respective pairwise comparisons, indicating that there were differences in expression patterns between sizes and sites. Heatmaps of mussels with differentially expressed transcripts between pairwise comparisons are shown in Figure 14 and shows the variation of expression between samples.

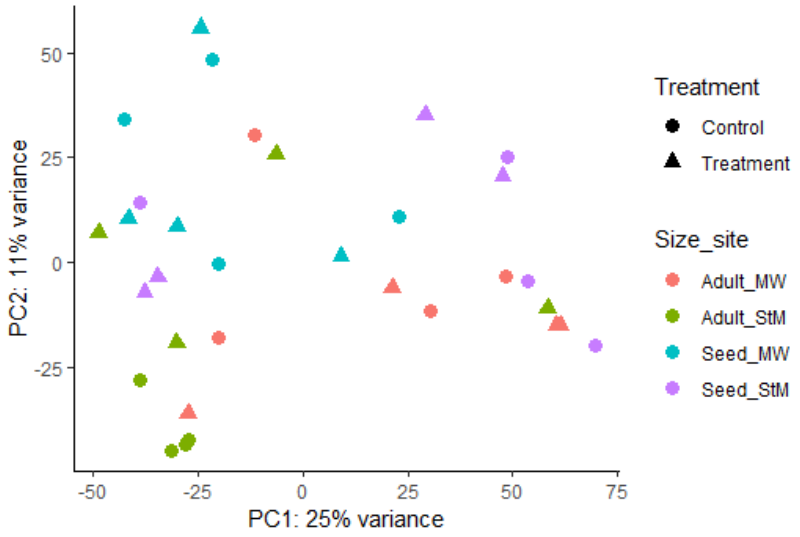

Figure 11. Preliminary principal component analysis plot of all expressed transcripts in hyposalinity trial. Plot shows each mussel sample from both sites (MW = March Water, StM = St. Mary's Bay) size (adult, seed), hyposalinity (16 ‰) and control (27 ‰).

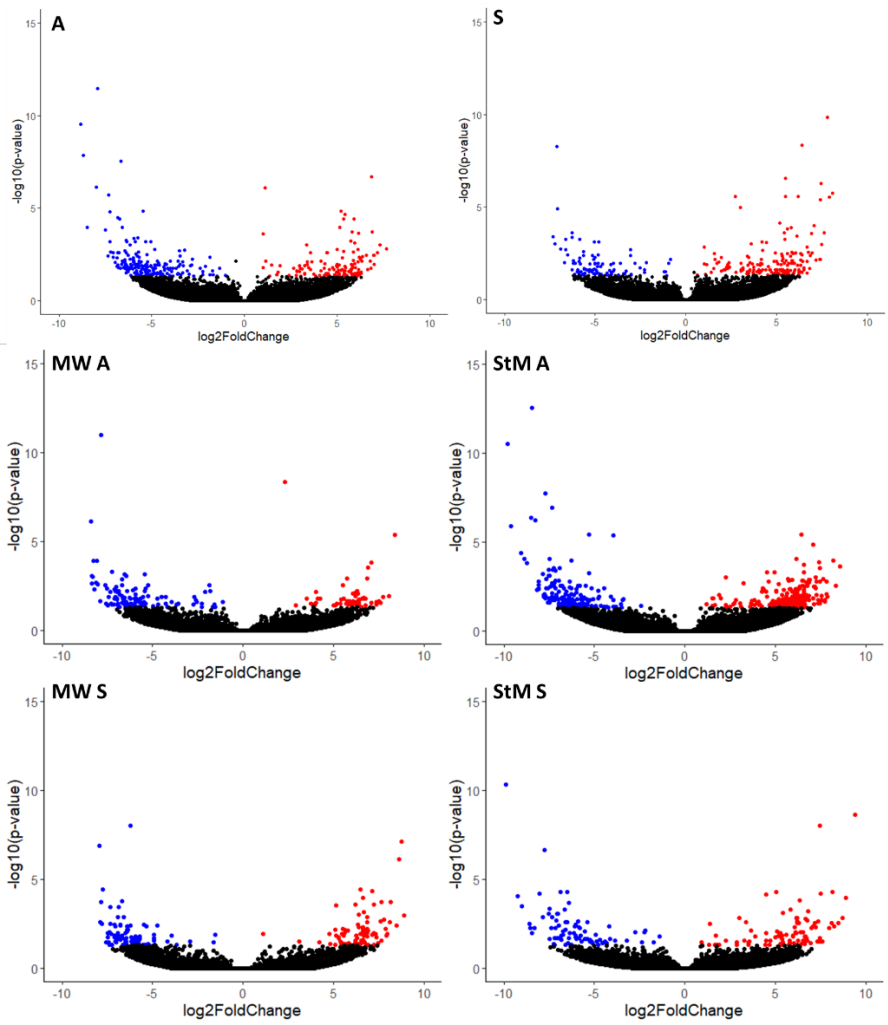

Figure 12. Volcano plots for differentially expressed transcripts identified in DESeq2 for each pairwise comparison (MW = March Water; StM = St. Mary's Bay; A = adult; S, = seed). Fold change is expressed as hyposalinity (16 ‰) vs control (27 ‰). Transcripts that are differentially expressed (FDR p-value = < 0.05) are indicated by either red (over-expressed) or blue (under-expressed) circles.

Table 13. Total number of differentially expressed transcripts (FDR p-value = < 0.05) for each pairwise comparison in each site and size for both DEseq2 and edgeR.

Comparison name	Total DE DESeq2	Total DE edgeR
MW A	442	7
StM A	178	0
MW S	175	0
StM S	167	1

Comparison name	Total DE DESeq2	Total DE edgeR
A	335	1
S	268	2

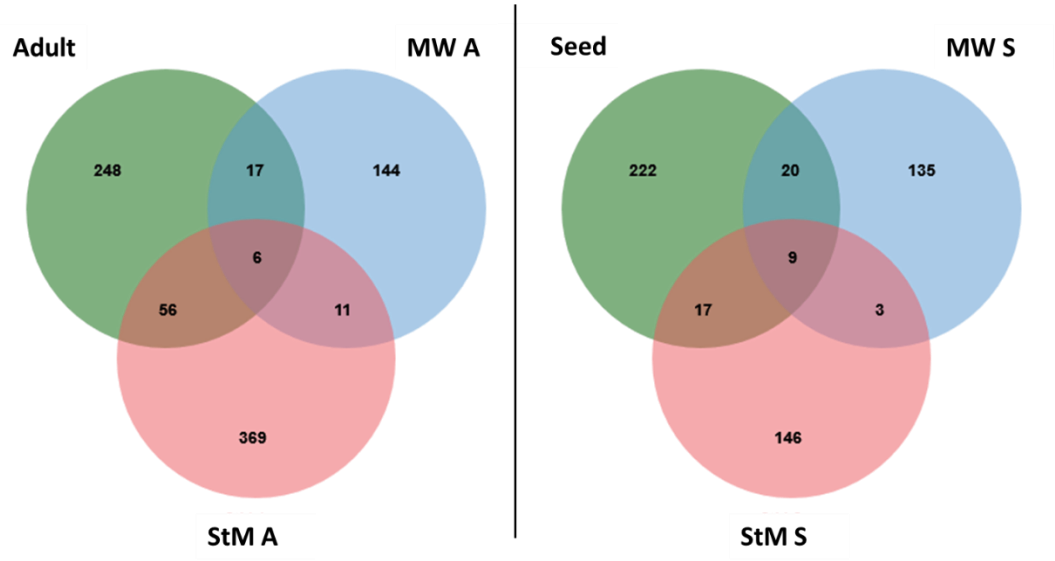

Figure 13. Venn diagram of differentially expressed transcripts found uniquely or mutually between different pairwise comparisons (MW = March Water; StM = St. Mary's Bay; A = adult; S, = seed)

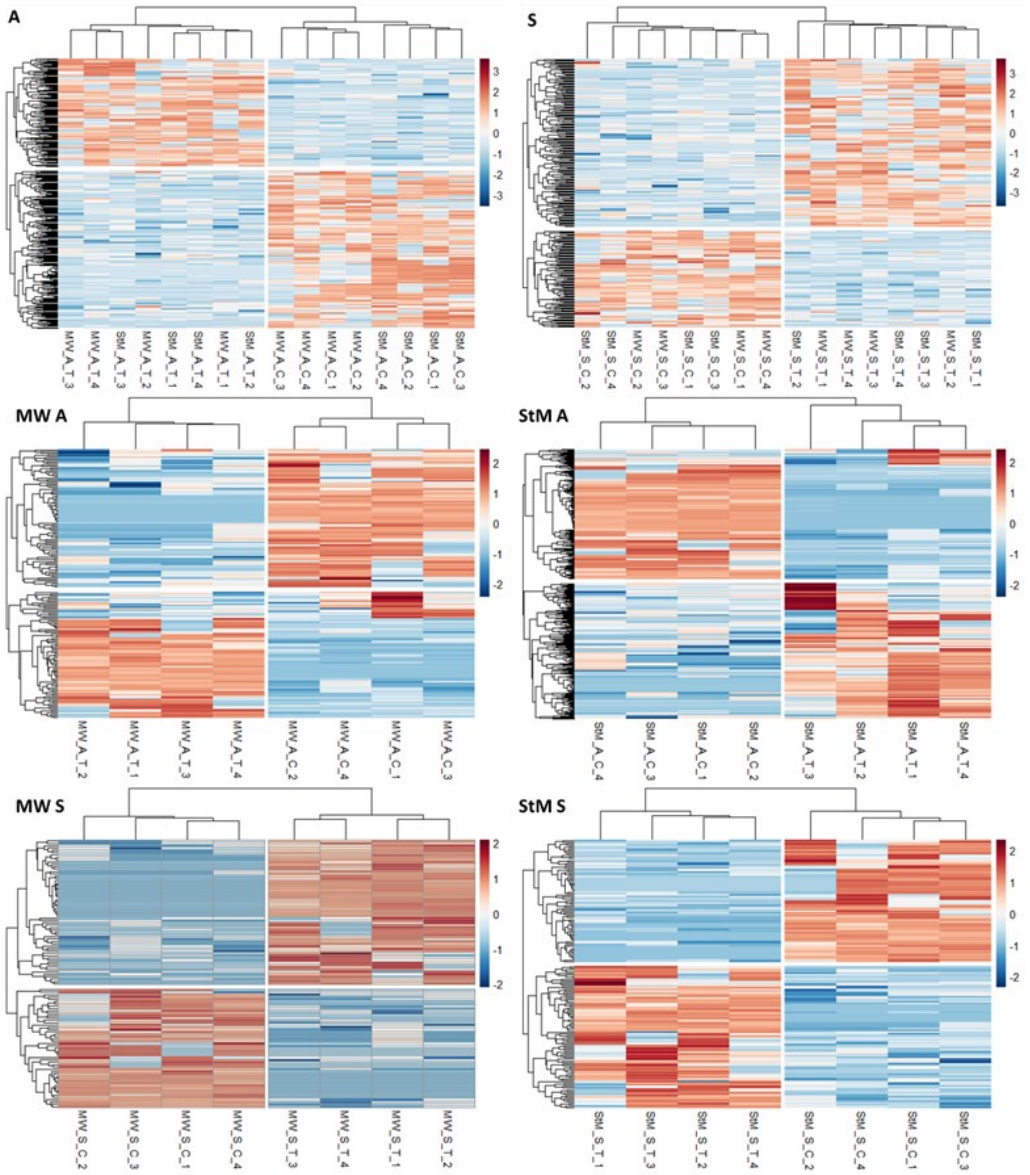

Figure 14. Heatmap of all differentially expressed transcripts identified by the DESeq2 statistical packages in each pairwise comparison (MW = March Water; StM = St. Mary's Bay; A = adult; T = hyposalinity (16 ‰); and C = control (27 ‰)).

3.3.3 Functional analysis

A subset of KEGG pathways assigned to differentially expressed transcripts are shown in Table 14 (See Appendix 3 for a full list). Table 14 shows differentially expressed transcripts associated with metabolic pathways which were broadly categorized as: amino acid metabolism; carbohydrate metabolism; glycan metabolism; lipid metabolism; and other metabolic pathways. KEGG pathways that were not associated with metabolism were related to cellular processes, environmental information processing, and genetic

information processing. The adult mussels appear to have more pathways with differentially expressed transcripts. Particularly, StM A appeared to have many transcripts over-expressed in many categories, compared with all other mussel groups. Several amino acid pathways were only differentially expressed in adult mussels including arginine and proline metabolism; biosynthesis of amino acids; tyrosine metabolism; and glycine, serine and threonine metabolism.

Table 14. KEGG pathways associated with differentially expressed transcripts from each pairwise comparison (MW = March Water; StM = St. Mary's Bay; A = adult; S = seed). Table shows the number of over-expressed (+) transcripts and under-expressed (-).

Category	Pathway	A		MW A		StM A		S		MW S		StM S	
		+	-	+	-	+	-	+	-	+	-	+	-
Amino acid metabolism	Arginine and proline metabolism	0	0	0	0	2	0	0	0	0	0	0	0
	Biosynthesis of amino acids	0	0	1	0	1	0	0	0	0	0	0	0
	Tyrosine metabolism	0	0	0	-1	1	0	0	0	0	0	0	0
	Glycine, serine and threonine metabolism	0	0	0	-1	0	0	0	0	0	0	0	0
	Cysteine and methionine metabolism	0	0	0	-1	0	0	0	-1	1	0	0	-1
Carbohydrate metabolism	Glycolysis / Gluconeogenesis	0	0	0	0	1	0	0	0	0	0	0	0
	Starch and sucrose metabolism	0	0	0	0	1	0	0	0	0	0	0	0
	Citrate cycle (TCA cycle)	0	0	1	0	0	-1	0	0	1	0	0	0
	Pyruvate metabolism	0	0	0	0	0	-1	0	0	1	0	0	0
Glycan metabolism	Other glycan degradation	1	0	0	-1	1	0	0	0	0	0	0	0
	Glycosphingolipid biosynthesis-globo & isoglobo	0	0	0	-1	1	0	0	0	0	0	0	0
	Glycosphingolipid biosynthesis-lacto & neolacto	0	-1	0	0	1	0	0	0	0	0	0	0
	Various types of N-glycan biosynthesis	0	-1	1	-1	0	0	0	0	0	0	0	0
Lipid metabolism	alpha-Linolenic acid metabolism	0	0	0	0	2	0	0	0	0	0	0	0
	Sphingolipid metabolism	1	0	0	0	0	0	1	0	0	0	0	0
	Arachidonic acid metabolism	0	0	0	0	1	0	0	0	0	-1	0	0
	Ether lipid metabolism	0	0	0	0	1	0	0	0	0	0	0	-1
	Glycerophospholipid metabolism	0	-1	0	0	1	0	0	0	0	0	0	-1
Other metabolism	Oxidative phosphorylation	1	-1	0	0	9	-1	0	0	0	0	0	0
	Drug metabolism-other enzymes	2	0	0	0	2	0	1	0	0	0	0	0
	Metabolism of xenobiotics by cytochrome P450	1	0	0	0	0	0	1	0	1	0	0	0
	Purine metabolism	0	-1	0	0	1	0	0	0	0	0	0	-1
	Drug metabolism-cytochrome P450	0	0	0	0	0	0	1	0	1	0	0	0
	Glutathione metabolism	0	0	0	0	0	0	1	0	2	0	0	0
Cellular Process	Lysosome	2	0	1	-1	6	0	2	0	1	0	0	0
	Phagosome	1	-1	0	0	5	0	1	0	0	0	0	0
	Endocytosis	0	0	0	0	3	-1	2	0	0	0	0	0
	Proteasome	0	0	0	0	2	0	0	0	0	0	0	0
	Peroxisome	0	-1	0	0	2	0	0	0	0	0	0	-1
Environmental Information Processing	FoxO signaling pathway	0	0	0	0	1	0	0	0	0	0	0	0
	TGF-beta signaling pathway	0	0	0	0	1	0	0	0	0	0	0	0
	Notch signaling pathway	0	0	0	-1	1	0	0	0	0	0	1	0
	mTOR signaling pathway	0	-1	0	0	1	0	0	0	1	0	0	0
	Phosphatidylinositol signaling system	0	0	0	0	0	0	0	0	0	-1	1	0
	mRNA surveillance pathway	0	0	0	0	0	0	1	-1	0	0	0	0
Genetic Information Processing	Ubiquitin mediated proteolysis	0	0	0	-1	5	-2	2	0	0	-1	0	0
	Protein processing in endoplasmic reticulum	0	0	1	0	2	-2	2	0	0	0	0	0
	ECM-receptor interaction	0	0	0	0	1	0	1	0	0	0	0	-1
	Spliceosome	0	-1	0	0	1	-1	1	0	0	0	0	0
	Neuroactive ligand-receptor interaction	0	0	0	0	0	0	1	0	0	-1	0	0
	DNA replication	0	-1	0	0	1	-1	0	0	0	0	0	0
	Ribosome	0	-4	0	0	3	-2	0	0	0	0	1	0
	Nucleocytoplasmic transport	0	-2	0	0	0	0	1	0	0	0	0	0

Only ~ 30–35% of transcripts were successfully annotated to known proteins relating to Bivalvia in the NCBI nr database, indicating that 65–70% were completely novel or associated with hypothetical or unnamed proteins in bivalves. Table 15– 21 contain a subset of differentially expressed transcripts that were successfully annotated (See Appendix 1: Supplemental file 2 for full list). Table 15 contains a subset of differentially expressed transcripts with their sequence ontology and their potential function/pathway that were found mutually between different pairwise comparisons. Transcripts found mutually expressed between pairwise comparisons were found to be associated with metabolism, protein turnover, immune, stress response, membranes, antioxidant, etc. The majority of transcripts that were differentially expressed were unique to their pairwise comparison. Many transcripts were annotated associated with metabolism, immune, osmoconformation, membranes, protein turnover, stress response, antioxidants, etc. and are displayed in Table 16–21. Transcripts with a potential role in osmoconformation and membrane were displayed in bar charts in Figure 15, to better understand the expression in other groups not found significant. In the majority of cases, when a transcript was not considered significantly differentially expressed, FC was much smaller in other mussel groups, indicating its expression was unique to the group found significant within.

Table 15. Differentially expressed transcripts found mutually expressed between different pairwise comparisons (MW = March Water; StM = St. Mary's Bay; A = adult; S, = seed). Fold change (FC) is shown for each comparison.

Transcript	Sequence Ontology	Function/ Pathway	FC 1	FC 2	FC 3
A; MW A; StM A			**A**	**MW A**	**StM A**
mussels_DN678477_c1_g1_i10	Cholesterol desaturase daf-36	Metabolism	6.8	6.1	6.3
mussels_DN674515_c0_g2_i4	40S ribosomal protein S7-like	Protein turnover	-7.9	-4.5	-8.5
S; MW S; StM S			**S**	**MW S**	**StM S**
mussels_DN661051_c0_g2_i3	F-box protein 39	Protein turnover	6.4	5.8	6.2
mussels_DN645762_c4_g1_i1	Putative C1q domain containing protein MgC1q48	Immune	6.2	5.6	6.0
S; StM A; StM S			**S**	**StM A**	**StM S**

Transcript	Sequence Ontology	Function/ Pathway	FC 1	FC 2	FC 3
mussels_DN639667_c1_g1_i1	putative period clock protein, partial	Regulator of homeostasis	-7.1	-6.2	-7.7
	A; MW A		**A**	**MW A**	
mussels_DN686145_c1_g1_i2	Ubiquitin-fold modifier 1	Protein turnover	5.1	6.3	
mussels_DN693270_c4_g3_i6	Fibrinogen-like protein A protein 1	Immune	-2.9	-3.7	
mussels_DN616850_c2_g1_i13	Low-density lipoprotein receptor-related protein 4-like	mTOR	-5.7	-7.1	
	A; StM A		**A**	**StM A**	
mussels_DN671899_c2_g1_i8	Lipopolysaccharide-induced tumor necrosis factor-alpha factor	Lysosomes	6.9	6.5	
mussels_DN674838_c1_g1_i2	Serine pats1 threonine-protein kinase, partial	Cytokinesis	6.6	6.5	
mussels_DN655063_c0_g1_i4	Probable thiopurine S-methyltransferase	Metabolism	6.3	6.5	
mussels_DN685058_c0_g1_i4	Interferon-inducible GTPase 5-like	Immune	5.9	6.4	
mussels_DN659858_c1_g2_i5	Pleiotrophin	Growth factor	4.1	5.1	
mussels_DN674591_c0_g3_i4	Heavy metal-binding protein HIP	Metal binding	2.8	4.5	
mussels_DN683349_c2_g1_i1	ATP synthase subunit alpha, mitochondrial-like	Metabolism	-4.2	-5.3	
mussels_DN682925_c0_g1_i5	Forkhead box protein N	Transcription regulator	-5.2	-6.3	
mussels_DN661767_c0_g3_i3	Lysine-specific demethylase 4C-like	Methylation	-5.5	-6.3	
mussels_DN513011_c0_g1_i2	Tctex1 domain-containing protein 1-B-like	Cilia	-5.8	-6.9	
mussels_DN599146_c1_g2_i2	Stanniocalcin-like protein, partial	Calcium homeostasis	-6.0	-6.7	
mussels_DN650842_c1_g1_i1	SOSS complex subunit C-like	DNA repair	-6.3	-7.3	
mussels_DN696494_c1_g1_i6	Exocyst complex component 2	Exocytic vesicles docking	-6.4	-6.4	

Transcript	Sequence Ontology	Function/ Pathway	FC 1	FC 2	FC 3
mussels_DN662836_c1_g2_i1	Annexin A7/11	Membrane	-6.4	-8.5	
mussels_DN464391_c0_g1_i1	E3 ubiquitin-protein ligase UHRF1-like	Epigenetic regulator	-6.5	-7.4	
mussels_DN684808_c1_g2_i8	Ribonuclease H1-like	DNA replication	-6.9	-7.7	
mussels_DN534774_c1_g1_i4	Lens fiber membrane intrinsic protein-like isoform X2	Membrane	-7.3	-6.5	
mussels_DN642388_c0_g2_i5	CRP-I 21	Immune	-7.3	-7.8	
mussels_DN674515_c0_g1_i1	40S ribosomal protein S7-like	Protein turnover	-8.8	-9.8	
	S; MW S		**S**	**MW S**	
mussels_DN657323_c0_g1_i2	Proto-oncogene serine/threonine-protein kinase Pim-3	Apoptosis	1.0	1.1	
	S; StM S		**S**	**StM S**	
mussels_DN682696_c2_g3_i2	Carboxypeptidase B-like	Metabolism	8.1	8.1	
mussels_DN613656_c1_g1_i5	Putative C1q domain containing protein MgC1q55	Immune	6.7	7.0	
mussels_DN594152_c1_g1_i2	Interferon-induced helicase C domain-containing protein 1	Immune	5.4	6.2	
mussels_DN649258_c2_g2_i3	Putative C1q domain containing protein MgC1q48	Immune	5.0	6.6	
mussels_DN645853_c2_g4_i5	Non-structural maintenance of chromosomes element 3 homolog	Chromosome maintenance	5.0	5.8	
mussels_DN689730_c2_g2_i4	Superoxide dismutase, Cu-Zn family	Antioxidant	-5.3	-8.0	
mussels_DN689662_c1_g1_i6	Translation initiation factor eIF-2B subunit alpha-like	Protein turnover	-5.6	-6.0	

Table 16. Functions/pathway of transcripts found differentially expressed from the March Water adult (MW A) through pairwise comparison. FC = Fold change

Transcript	Sequence Ontology	Function/Pathway	DESeq2 FC
mussels_DN642733_c0_g1_i2	Dolichyl-Diphosphooligosaccharide--Protein Glycosyltransferase 48 Kda Subunit-Like	Metabolism	8.2
mussels_DN666138_c1_g1_i3	Phospholipid Phosphatase 3-Like	Metabolism	-10.3
mussels_DN651880_c0_g1_i8	Putative Neutral Sphingomyelinase	Metabolism	-10.9
mussels_DN681500_c1_g1_i10	Sodium/myo-inositol cotransporter 2-like	Osmoconformation	6.7
mussels_DN681258_c2_g3_i4	Sodium/potassium-transporting ATPase subunit beta-1-interacting protein 3 isoform X3	Osmoconformation	6.3
mussels_DN703044_c2_g1_i3	MAP kinase-activating death domain protein	Stress response	7.1
mussels_DN688649_c3_g1_i6	Ataxin-2-like protein isoform X5	Stress granule	6.4
mussels_DN701907_c2_g1_i2	Baculoviral IAP repeat-containing protein 2-like	Apoptosis	-6.8
mussels_DN641631_c0_g1_i1	Putative C1Q Domain Containing Protein MgC1Q21	Immune	5.4
mussels_DN696668_c3_g2_i3	C-Type Lectin Domain Family 6 Member A	Immune	-4.7
mussels_DN611570_c4_g1_i7	Myticin B Precursor	Immune	-5.6
mussels_DN657027_c0_g1_i2	Putative C1Q Domain Containing Protein MgC1Q3	Immune	-5.9
mussels_DN661999_c6_g1_i3	C-Type Lectin 5	Immune	-6.7
mussels_DN639705_c4_g1_i1	Putative C1Q Domain Containing Protein MgC1Q35	Immune	-7.2
mussels_DN605599_c5_g1_i1	Peroxisomal Biogenesis Factor 19-Like	Antioxidant	-7.0

Table 17. Functions/pathway of transcripts found differentially expressed from the St. Mary's Bay adult (StM A) through pairwise comparison. FC = Fold change

Transcript	Sequence Ontology	Function/Pathway	DESeq2 FC
mussels_DN603778_c0_g2_i2	ATP Synthase F0 Subunit 8 (Mitochondrion)	Metabolism	6.8

Transcript	Sequence Ontology	Function/Pathway	DESeq2 FC
mussels_DN684875_c1_g2_i1	Glycoprotein-N-Acetylgalactosamine 3-Beta-Galactosyltransferase 1-Like Isoform X1	Metabolism	6.7
mussels_DN666983_c2_g1_i2	Cytochrome B (Mitochondrion)	Metabolism	6.3
mussels_DN669585_c1_g3_i1	Cytochrome C Oxidase Subunit I (Mitochondrion)	Metabolism	6.1
mussels_DN669585_c1_g4_i1	Cytochrome C Oxidase Subunit 1 (Mitochondrion)	Metabolism	6.1
mussels_DN667082_c1_g2_i1	NADH Dehydrogenase Subunit 5 (Mitochondrion)	Metabolism	5.9
mussels_DN676325_c1_g1_i3	ATP Synthase Subunit Delta, Mitochondrial-Like	Metabolism	5.9
mussels_DN646473_c0_g2_i1	NADH Dehydrogenase Subunit 2, Partial (Mitochondrion)	Metabolism	5.8
mussels_DN603778_c0_g1_i2	NADH Dehydrogenase Subunit 3 (Mitochondrion)	Metabolism	5.8
mussels_DN628796_c3_g4_i1	Glycogen Phosphorylase, Muscle Form-Like Isoform X3	Metabolism	5.8
mussels_DN689495_c2_g1_i1	ATP Synthase F0 Subunit 6 (Mitochondrion)	Metabolism	5.7
mussels_DN687709_c0_g2_i1	Arginine Kinase	Metabolism	5.7
mussels_DN677778_c0_g2_i3	Pancreatic Lipase-Related Protein 2-Like	Metabolism	5.7
mussels_DN593628_c0_g1_i1	NADH Dehydrogenase Subunit 1 (Mitochondrion)	Metabolism	5.7
mussels_DN667082_c1_g4_i1	NADH Dehydrogenase Subunit 6 (Mitochondrion)	Metabolism	5.5
mussels_DN692116_c2_g2_i4	V-Type Proton Atpase Subunit D 1-Like	Metabolism	3.7
mussels_DN672458_c1_g3_i2	Glyceraldehyde-3-Phosphate Dehydrogenase, Partial	Metabolism	1.5
mussels_DN697099_c1_g2_i3	Fumarate Hydratase Class I, Aerobic	Metabolism	-4.2
mussels_DN623322_c1_g1_i7	Cytochrome B561 Domain-Containing Protein 2-Like	Metabolism	-5.8
mussels_DN661599_c1_g2_i4	Transmembrane Protein 50B-Like	Membrane homeostasis	6.5

Transcript	Sequence Ontology	Function/Pathway	DESeq2 FC
mussels_DN688655_c2_g1_i7	Solute Carrier Family 35 Member F6-Like	Osmoconformation	4.2
mussels_DN652917_c2_g1_i2	Transmembrane Protein 68-Like Isoform X1	Membrane homeostasis	3.2
mussels_DN688107_c2_g2_i3	Phospholipid Scramblase 1-Like	Membrane homeostasis	-6.6
mussels_DN681271_c0_g2_i6	Heat shock 70 Kda Protein 12A-Like	Chaperone	6.2
mussels_DN685821_c0_g2_i4	UV Excision Repair Protein Rad23 Homolog B-Like	DNA repair	1.5
mussels_DN698582_c11_g1_i3	Baculoviral Iap Repeat-Containing Protein 3-Like	Apoptosis	-3.4
mussels_DN693339_c1_g2_i3	Heat Shock 70 Kda Protein 12B-Like	Molecular chaperone	-6.1
mussels_DN648962_c0_g3_i3	Putative C1Q Domain Containing Protein MgC1Q95	Immune	8.6
mussels_DN665248_c6_g2_i1	Ladderlectin-Like	Immune	7.1
mussels_DN641210_c6_g1_i3	Putative C1Q Domain Containing Protein MgC1Q76	Immune	4.1
mussels_DN678963_c1_g1_i8	Putative C1Q Domain Containing Protein MgC1Q4	Immune	-5.4
mussels_DN639430_c1_g3_i1	Putative C1Q Domain Containing Protein MgC1Q35	Immune	-5.5
mussels_DN593960_c2_g1_i4	Lysozyme 2	Immune	-5.8
mussels_DN611570_c3_g1_i2	Myticin-A	Immune	-6.3
mussels_DN636434_c0_g2_i2	Myticalin D6	Immune	-6.4
mussels_DN676052_c0_g3_i8	Protein Unc-93 Homolog A-Like	Immune	-6.5
mussels_DN649101_c2_g1_i7	C-Type Lectin 2	Immune	-7.7
mussels_DN687690_c7_g2_i3	Methionine-R-Sulfoxide Reductase B2, Mitochondrial-Like	Antioxidant	7.5

Table 18. Functions/pathway of transcripts found differentially expressed from the March Water seed (MW S) through pairwise comparison. FC = Fold change

Transcript	Sequence Ontology	Function/Pathway	DESeq2 FC
mussels_DN692477_c1_g1_i4	Cystathionine Gamma-Lyase-Like	Metabolism	6.9
mussels_DN527900_c0_g1_i2	Inositol Polyphosphate 5-Phosphatase Inpp5E	Metabolism	6.8
mussels_DN672840_c0_g4_i3	Cytosolic Malate Dehydrogenase	Metabolism	6.7
mussels_DN702418_c6_g2_i2	Phosphatidylinositol Phosphatase Ptprq-Like, Partial	Metabolism	6.3
mussels_DN648275_c5_g1_i1	Leucyl Aminopeptidase	Metabolism	5.7
mussels_DN597647_c1_g1_i1	Cytochrome C Oxidase Subunit 6B-Like	Metabolism	-6.1
mussels_DN685272_c0_g1_i8	Leukotriene A-4 Hydrolase-Like Isoform X1	Metabolism	-6.6
mussels_DN617160_c1_g2_i1	Stanniocalcin-Like Protein, Partial	Calcium homeostasis	6.4
mussels_DN650923_c5_g1_i1	Acetylcholine Receptor Subunit Alpha-1-B-Like	Osmoconformation	-4.8
mussels_DN656357_c0_g1_i2	Putative Calmodulin-3 Isoform X2	Calcium homeostasis	-5.9
mussels_DN662408_c2_g1_i3	Caspase 7	Apoptosis	7.2
mussels_DN686401_c0_g1_i6	Cathepsin B-Like	Autophagy	5.1
mussels_DN692706_c3_g1_i7	Cathepsin L, Partial	Autophagy	-5.4
mussels_DN651326_c1_g3_i1	Heat shock 70 Kda Protein 12A-Like	Chaperone	-6.5
mussels_DN695389_c5_g2_i1	Heat shock 70 Kda Protein 12B-Like	Chaperone	-6.8
mussels_DN628753_c0_g1_i4	Small Heat Shock Protein 24	Chaperone	-10.4
mussels_DN644027_c2_g1_i6	Immune-4 Lectin-Like Receptor, Partial	Immune	7.9
mussels_DN688116_c1_g3_i2	Defensin	Immune	6.7
mussels_DN639137_c1_g2_i2	Putative C1Q Domain Containing Protein MgC1Q32	Immune	6.6
mussels_DN633181_c3_g2_i2	Putative C1Q Domain Containing Protein MgC1Q84	Immune	6.5
mussels_DN555836_c0_g1_i2	Putative C1Q Domain Containing Protein MgC1Q3	Immune	6.4
mussels_DN674947_c1_g1_i1	Myticin C Precursor	Immune	5.9

Transcript	Sequence Ontology	Function/Pathway	DESeq2 FC
mussels_DN598495_c2_g6_i1	Mytimycin Precursor	Immune	-6.6
mussels_DN641204_c0_g3_i6	Putative C1Q Domain Containing Protein MgC1Q48	Immune	-7.5
mussels_DN618186_c1_g1_i15	Myticalin C3	Immune	-7.9
mussels_DN647860_c2_g1_i3	Nadph--Cytochrome P450 Reductase	Antioxidant	6.6
mussels_DN676483_c1_g2_i2	Glutathione S-Transferase A-Like	Antioxidant	5.2

Table 19. Functions/pathway of transcripts found differentially expressed from the St. Mary's Bay seed (StM S) through pairwise comparison. FC = Fold change

Transcript	Sequence Ontology	Function/Pathway	DESeq2 FC
mussels_DN681086_c1_g1_i2	Isopentenyl-Diphosphate Delta-Isomerase 1-Like	Metabolism	4.5
mussels_DN696088_c1_g1_i1	Delta(14)-Sterol Reductase-Like Isoform X1	Metabolism	-2.4
mussels_DN690870_c4_g1_i7	Phospholipase D3-Like Isoform X1	Metabolism	-5.1
mussels_DN668463_c0_g1_i4	High Affinity Camp-Specific And Ibmx-Insensitive 3',5'-Cyclic Phosphodiesterase 8	Metabolism	-6.0
mussels_DN516426_c1_g1_i2	NADH Dehydrogenase Subunit 6 (Mitochondrion)	Metabolism	-6.1
mussels_DN674243_c0_g2_i3	Inhibitor Of Nuclear Factor Kappa B-1	Stress response	6.7
mussels_DN686195_c0_g1_i10	Baculoviral Iap Repeat-Containing Protein 7-B-Like, Partial	Apoptosis	6.1
mussels_DN653314_c3_g2_i2	C-Type Lectin Domain Family 4 Member E-Like Isoform X3	Immune	5.8
mussels_DN654744_c0_g1_i2	Putative C1Q Domain Containing Protein MgC1Q69	Immune	-4.8
mussels_DN630649_c1_g3_i1	I-Type Lysozyme	Immune	-9.0
mussels_DN689730_c2_g1_i3	Superoxide Dismutase	Antioxidant	-9.9

Table 20. Functions/pathway of transcripts found differentially expressed from the adults (A) through pairwise comparison. FC = Fold change

Transcript	Sequence Ontology	Function/Pathway	DESeq2 FC
mussels_DN698781_c5_g3_i5	Bifunctional polynucleotide phosphatase/kinase	Metabolism	6.8
mussels_DN623771_c2_g1_i2	FUCA	Metabolism	6.1
mussels_DN655063_c0_g1_i3	Probable thiopurine S-methyltransferase	Metabolism	6.1
mussels_DN667082_c1_g1_i2	NADH dehydrogenase subunit 6	Metabolism	5.2
mussels_DN664196_c2_g3_i5	Trans-1,2-dihydrobenzene-1,2-diol dehydrogenase-like	Metabolism	5.0
mussels_DN597647_c1_g1_i5	Cytochrome c oxidase subunit 6B-like	Metabolism	4.6
mussels_DN646473_c0_g1_i2	NADH dehydrogenase subunit 2	Metabolism	4.0
mussels_DN658154_c2_g1_i2	Cytochrome P450 3A6-like	Metabolism	1.0
mussels_DN698222_c1_g2_i1	Succinate dehydrogenase assembly factor 2, mitochondrial-like	Metabolism	-4.7
mussels_DN695124_c2_g1_i7	Manganese-dependent ADP-ribose/CDP-alcohol diphosphatase-like	Metabolism	-5.7
mussels_DN675757_c0_g1_i5	Isoamyl acetate-hydrolyzing esterase 1 homolog isoform X2	Membrane	4.8
mussels_DN674805_c0_g2_i1	Transmembrane protein 107-like isoform X2	Membrane	-5.8
mussels_DN679878_c1_g1_i1	RCC1 and BTB domain-containing protein 1-like	Protein turnover	-5.4
mussels_DN642705_c1_g2_i1	40S ribosomal protein S21-like	Protein turnover	-4.4
mussels_DN593581_c1_g3_i2	Selenocysteine-specific elongation factor	Protein turnover	-4.6
mussels_DN601446_c5_g1_i3	Probable ribosome biogenesis protein RLP24	Protein turnover	-5.7
mussels_DN672837_c0_g2_i7	Translation initiation factor 3 subunit J	Protein turnover	-5.9
mussels_DN621451_c5_g1_i2	28S ribosomal protein S2, mitochondrial-like	Protein turnover	-6.8
mussels_DN636434_c0_g7_i1	Myticalin C1	Immune	7.0
mussels_DN650186_c3_g2_i1	Serum amyloid A protein	Immune	5.0
mussels_DN664493_c0_g1_i9	Complement C1q-like protein 4	Immune	-5.9

Transcript	Sequence Ontology	Function/Pathway	DESeq2 FC
mussels_DN652539_c0_g1_i6	Macrophage migration inhibitory factor	Immune	-6.0
mussels_DN689441_c0_g1_i3	Spindle and centriole-associated protein 1-like	Mitotic division	5.9
mussels_DN685009_c1_g3_i2	Cyclic GMP-AMP synthase-like	Cytosolic DNA sensor	5.0
mussels_DN697869_c8_g2_i3	Kinesin-associated protein 3	Lysosome	4.5
mussels_DN697082_c1_g1_i2	Mitochondrial glycine transporter-like isoform X7	Mitochondrial	1.3
mussels_DN501070_c0_g1_i1	Importin subunit beta-1	Nucleocytoplasmic transport	-5.4
mussels_DN692954_c1_g2_i2	Heat shock 70 kDa protein 12A-like	Chaperone	5.1
mussels_DN437254_c1_g1_i1	dnaJ homolog subfamily B member 4-like	Chaperone	1.8
mussels_DN487582_c0_g1_i1	Peroxisomal membrane protein PEX14-like isoform X1	Antioxidant	-4.3
mussels_DN577524_c2_g1_i2	Major vault protein	transport process	-2.4
mussels_DN679069_c1_g3_i1	Intraflagellar transport protein 52 homolog isoform X2	Cilia	-4.7
mussels_DN667372_c6_g1_i2	Vitelline membrane outer layer protein 1-like	Reproduction	-4.7

Table 21. Functions/pathway of transcripts found differentially expressed from the seed (S) through pairwise comparison. FC = Fold change

Transcript	Sequence Ontology	Function/Pathway	DESeq2 FC
mussels_DN598237_c0_g1_i1	Sulfite oxidase-like	Metabolism	7.5
mussels_DN682696_c2_g1_i3	Carboxypeptidase B-like	Metabolism	5.9
mussels_DN616145_c1_g1_i2	Prostaglandin-H2 D-isomerase / glutathione transferase	Metabolism	5.0
mussels_DN564268_c0_g1_i1	Chitin synthase	Metabolism	4.8
mussels_DN678065_c1_g1_i6	Ceramide kinase	Metabolism	1.8
mussels_DN646473_c0_g1_i1	NADH dehydrogenase subunit 2	Metabolism	-4.8
mussels_DN543381_c0_g1_i2	Sulfite oxidase-like	Metabolism	-5.0
mussels_DN688983_c5_g1_i3	Cysteine dioxygenase	Metabolism	-5.6

Transcript	Sequence Ontology	Function/Pathway	DESeq2 FC
mussels_DN628499_c9_g3_i1	Ubiquitin-conjugating enzyme E2 G2	Protein turnover	6.2
mussels_DN699151_c1_g1_i11	RNA exonuclease 1	Protein turnover	6.8
mussels_DN697719_c1_g1_i7	NEDD8-conjugating enzyme Ubc12	Protein turnover	6.4
mussels_DN568821_c0_g1_i4	Dipeptidyl-peptidase III	Protein turnover	5.5
mussels_DN581315_c2_g1_i2	Elongation factor 1 alpha	Protein turnover	4.2
mussels_DN588409_c1_g2_i4	Major vault protein-like	transport process	4.9
mussels_DN675767_c0_g1_i11	Calcyphosin-like protein isoform X1	Calcium homeostasis	-5.3
mussels_DN692505_c2_g1_i2	Heat shock protein 70	Chaperone	3.8
mussels_DN687575_c1_g1_i7	Heat shock protein 70	Chaperone	3.7
mussels_DN692505_c2_g2_i5	Heat shock protein 70	Chaperone	3.5
mussels_DN671554_c0_g1_i5	Putative C1q domain containing protein MgC1q29	Immune	6.5
mussels_DN647150_c2_g1_i2	Perlucin-like protein	Immune	5.3
mussels_DN651440_c1_g3_i1	2'-5'-oligoadenylate synthetase	Immune	5.2
mussels_DN677352_c2_g2_i6	Myticin C	Immune	4.9
mussels_DN674947_c1_g1_i1	Myticin C	Immune	4.7
mussels_DN701734_c2_g3_i1	CD109 antigen	Immune	-4.3
mussels_DN634430_c3_g3_i2	Antimicrobial peptide MGD2b precursor	Immune	-4.7
mussels_DN674007_c4_g3_i5	Poly [ADP-ribose] polymerase 2-like	Base excision repair	7.2
mussels_DN654375_c0_g1_i8	Ganglioside GM2 activator-like	Lysosome	7.1
mussels_DN646763_c0_g1_i2	Protein pelota-like	mRNA surveillance pathway	6.4
mussels_DN696895_c2_g1_i1	Charged multivesicular body protein 2a-like	Endocytosis	6.3
mussels_DN677970_c1_g1_i3	Mitochondrial fission 1 protein-like	Mitophagy	5.6
mussels_DN648453_c0_g1_i2	Orexin receptor type 2-like	Neuroactive ligand-receptor interaction	5.3
mussels_DN678541_c0_g1_i1	DNA repair protein RAD50	DNA repair	4.6

Transcript	Sequence Ontology	Function/Pathway	DESeq2 FC
mussels_DN637542_c5_g1_i2	Lipopolysaccharide-induced tumor necrosis factor-alpha factor	Lysosome	2.2
mussels_DN701199_c0_g2_i2	Serine/threonine-protein phosphatase PP1-beta catalytic subunit	mRNA surveillance pathway	-4.9

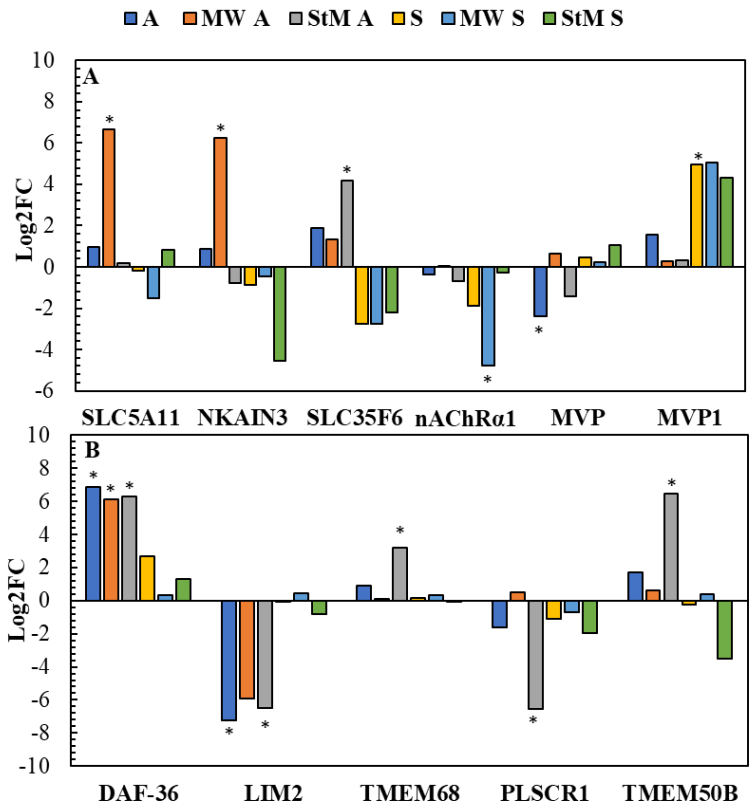

Figure 15. Subset of differentially expressed transcripts plotted using their subsequent Log_2 Fold change for each pairwise comparison. Plots are associated with (A) osmoconformation; (B) membranes. (MW = March Water; StM = St. Mary's Bay; A = adult; S = seed. SLC5A11 = Sodium/myo-inositol cotransporter 2-like; NKAIN3 = Sodium/potassium-transporting ATPase subunit beta-1-interacting protein 3 isoform X3; SLC35F6 = Solute Carrier Family 35 Member F6-Like; nAChRα1 = Acetylcholine Receptor Subunit Alpha-1-B-Like; MVP = major vault protein; MVP1 = major vault protein-like; DAF-36 = Cholesterol desaturase daf-36; LIM2 = Lens Fiber Membrane Intrinsic Protein-Like Isoform X2; TMEM68 = Transmembrane Protein 68-Like Isoform X1; PLSCR1 = Phospholipid Scramblase 1-Like; TMEM50B = Transmembrane Protein 50B-Like

3.4 Discussion

3.4.1 Heart rate and transcript expression associated with metabolism

This study found that abrupt hyposalinity exposure resulted in a significant increase in heart rate over the 6 h exposure period. This is contrary to most studies, which report a decline in heart rate due to hyposalinity (Bakhmet et al. 2005; Braby and Somero 2006). Braby and Somero (2006) found that as salinity declined, heart rate of mussels (*Mytilus* sp.) declined until a critical salinity was reached, and then heart rate dropped abruptly. Bakhmet et al. (2005) examined the effects of long-term hyposalinity (15 ‰) on sublittoral and littoral zone mussels (*M. edulis*) and found that heart rate decreased gradually over nine days; with the littoral zone mussels having less of a decline than the sublittoral zone mussels. Decline in heart rate has been found associated with valve closure, reduction in filtration, and metabolic decline (Bakhmet et al. 2005; Braby and Somero 2006). There is a possibility that the six-hour hyposalinity exposure in this study may not have been sufficient to result in a full metabolic decline. Regardless, the results show that the first hours of exposure to hyposalinity resulted in a significant cardiac response. Cardiac response has been linked to respiratory function (Bayne 1971; Rovero et al. 1999), and therefore the increase in heart rate may be related to an increase in energy demand.

Mussels are osmoconformers, (Gilles 1972; Shumway 1977) and osmoconformation to hyposalinity conditions has been found to be less energetic compared to osmoconformation to hypersalinity or osmoregulation (Willmer 2006; Bayne 2017; Rivera-Ingraham and Lignot 2017). The diffusion of inorganic ions in extracellular fluids occurs passively, while cell volume conformation via changes in intracellular osmolyte is an energetic process, known as isosmotic intracellular cell volume regulation (Florkin 1962; Freire and Sampaio 2021). Studies on osmoconforming copepods have found that hyposalinity shock can result in increased respiration rates, likely resulting from oxidative deamination of free amino acids during osmoconformation (Goolish and Burton 1989; McAllen and Taylor 2001). A study by Shumway (1977) using *M. edulis* found that during the first 6 h of hyposalinity exposure, major changes in osmolality occurs; however, after valve closure, changes in osmolality slowed and eventually stopped. The St. Mary's Bay mussels in this study showed over-expression of oxidative phosphorylation pathways, which could be indicative

of compensation through increased metabolic output. Therefore, the increase in heart rate found in this study could be associated with the initial hyposalinity shock and osmoconformation in adults.

3.4.2 Transcripts associated with osmoconformation and metabolism

The present study found many transcripts that were differentially expressed associated with the process of osmoconformation. Osmoconformation to hyposalinity exposure initially results in a rapid decline of osmolality of extracellular fluids (i.e. haemolymph) (Gilles 1972; Shumway 1977). Seawater and extracellular fluid have several abundant inorganic ions responsible for its osmolality including sodium (Na^+), chlorine (Cl^+), potassium (K^+), magnesium (Mg^{2+}) and calcium (Ca^{2+}). After a decrease in osmolality in extracellular fluid, the mussels will osmoconform by increasing the uptake of water into cells, resulting initially in cell swelling (Florkin 1962; Freire and Sampaio 2021). Euryhaline bivalves such as the blue mussel can prevent cell rupture by maintenance of osmolytes within cells (Yancey 2005). In contrast to extracellular fluid, cells and tissues contain substantial levels of organic osmolytes that contribute to osmotic pressure (Zurburg and De Zwaan 1981). For example, in the adductor muscle of the mussel *M. edulis,* 50% of the osmotic pressure was found to be due to inorganic ions; however, the other 50% is due to organic osmolytes (Potts 1958; Zurburg and De Zwaan 1981). These osmolytes include free amino acids (i.e. taurine, alanine, and glycine), small carbohydrates, polyols (inositols, sorbitol), free methylamines, methylsulfonium solutes, and urea (Yancey et al. 1982; Yancey 2001, 2005). Osmolytes within cells, not including urea, are called “compatibility solutes”, which are safer than inorganic ions, as they don’t interact with macromolecules in ways that impacts cellular function (Brown and Simpson 1972; Yancey et al. 1982; Yancey 2005).

In this study, there were several transcripts that were differentially expressed associated with amino acid metabolism and ion/osmolyte/solute transport. Exposure to hyposalinity, results in the reduction of osmolytes in cells and extracellular fluids to maintain osmotic pressure. Studies on the mussel, *M. edulis,* have found that reduction of free amino acid such as taurine, glycine, and alanine is a common response to hyposaline conditions (Gilles 1972; Shumway et al. 1977; May et al. 2017). This reduction of amino acids is due to both

transport outside of cells, and catabolism due to deamination that results in ammonia excretion (Zurburg and De Zwaan 1981). In the present study, adult mussels had differentially expressed transcripts associated with changes in amino acids metabolism, which is likely involved in maintenance of amino acids needed for osmoconformation. The results of this study are in agreement of other transcript expression studies on bivalves that have found amino acid metabolism pathways were differentially expressed (Meng et al. 2013; Zhao et al. 2014; Xiao et al. 2018; Nie et al. 2018)

This study also found that there were several transcripts differentially expressed that were associated with osmolyte/solute transport. The differential expression of various osmolyte membrane transport transcripts was predominantly found within the adult mussel groups. For example, in the St. Mary's Bay adult group, one solute carrier family gene was over-expressed (solute carrier family 35 member F6-like). The solute carrier family is a group of membrane-bound transporters that transport amino acids, oligopeptides, small carbohydrates, and inorganic ions (He et al. 2009). Several studies have found the solute carrier family differentially expressed in response to hyposalinity stress (Lockwood and Somero 2011; Zhao et al. 2012; Ertl et al. 2019; Barrett et al. 2022). In the March Water adult group sodium/potassium-transporting ATPase subunit beta-1-interacting protein 3 isoform X3 was over-expressed and is likely involved with inorganic ion transport as found in several other marine osmoconformers including oyster *S. glomerata* (Ertl et al. 2019), shrimp *Exopalaemon carinicauda* (Li et al. 2015a), and crab *Carcinus maenas* (Towle et al. 2011). Also in the March Water adult group, sodium/myo-inositol cotransporter 2-like was over-expressed. This gene has been found to have a role in regulating osmotic pressure and salinity tolerance (Kage-Nakadai et al. 2011; Cui et al. 2020). In turbot (*Scophthalmus maximus*), myo-inositol is an osmolyte, which has been found to play an important role in osmoregulatory mechanisms in both hypo- and hypersalinity stress. There were also some transcripts associated with cellular transport that were novel to mussels. In seed and adult mussels, two major vault proteins were found differentially expressed, over-expressed in seed and under-expressed in adult. It is not clear the role they play in hyposalinity stress, however, they may play a role in intracellular transport processes (Van Zon et al. 2003). Acetylcholine receptor subunit alpha-1-B-like was over-expressed in March Water seed,

which are known to be associated with ligand-gated ion channels (Papke and Lindstrom 2020). Overall, the differential expression of the ion/solute transporters found in this study most likely have important roles in osmoconformation processes associated with hyposalinity stress.

In this study there were several transcripts differentially expressed associated with lipid metabolism and membrane changes. One of the initial responses to hyposaline environments is the uptake of water to balance the osmolyte concentration within cells to environment (Florkin 1962; Bayne 2017; Freire and Sampaio 2021). This results in swelling of cells and changes in membrane structure (Freire and Sampaio 2021). In the St. Mary's adult mussels, there were two over-expressed transcripts annotated as transmembrane proteins (50B-Like and 68-like isoform). In addition, transmembrane protein 107-like isoform X2 was under-expressed in adult mussels. Transmembrane protein's role in hyposalinity stress in bivalves are not well defined; however, some may have a functional role as osmosensors involved with regulation of membranes during conformation changes (stretching/warping) (Hohmann 2015). Another transcript found under-expressed in the St. Mary's Bay adult mussels was phospholipid scramblase 1-like. A study on the sea cucumber *Apostichopus japonicus* also found that phospholipid scramblase was under-expressed during exposure to hyposalinity conditions (Tian et al. 2019). Phospholipid scramblases are important for energy-dependent phospholipid movement, such as of removal of apoptotic cells and blood clotting in the plasma membrane of vertebrates (Williamson 2016), but may also have a role in lipid modeling (Wiedmer et al. 2004). Changes to lipid membrane structure has been found to occur in *M. edulis* experiencing fluctuations of salinity (Nemova et al. 2013). Nemova et al. (2013) found cholesterol content within gills membranes decreased in both wild and aquaculture mussels and was associated with increased fluidity in membranes (Nemova et al. 2013). In the adult mussels, a transcript annotated as cholesterol desaturase daf-36 was over-expressed. This enzyme is important for converting cholesterol to 7-dehydrocholesterol and is important for promoting life longevity in the nematode *Caenorhabditis elegans* (Wollam et al. 2011); therefore, it may be involved with removal of cholesterol in membranes and promoting survival in *M. edulis*.

3.4.3 Lysosome destabilization and stress related expression

Lysosomal destabilization index was not impacted by the salinity transfer. Other studies have found that salinity changes can result in changes in lysosomal destabilization; however, these studies were on longer time scales (weeks to months of exposure) (Hauton et al. 1998; Méthé, et al. 2015; Méthé et al. 2017). This indicates that the exposure time was not sufficient to result in destabilization of lysosomes; however, it did result in changes in transcript expression relating to protein integrity mechanisms, apoptosis, immunity and antioxidants. Most mussel groups had both over- and under-expression of these transcripts. Heat shock (HSP) 70 Kda protein 12A (seed) and 12B (St. Mary's Bay seed) were both under-expressed, while three other transcripts identified as HSP 70 were over-expressed in seed mussels. In contrast, adult mussels only had over-expression of HSP 70 protein 12A. Other studies have also found that differential expression of HSP 70 within bivalves experiencing hyposalinity conditions (Werner 2004; Pourmozaffar et al. 2020). The family of heat shock proteins are involved with the stabilization and refolding of misfolded proteins (Vabulas et al. 2010). Many environmental stressors can activate heat shock proteins (Kiang and Tsokos 1998). Heat shock 70 has been found to be activated by changes in intracellular pH, cyclic AMP, Ca^{2+}, Na^{+}, inositol trisphosphate, protein kinase C, and protein phosphatases (Kiang and Tsokos 1998).

All mussel groups, except March Water seed had differential expression of baculoviral IAP-containing proteins. Both adult mussel groups contained under-expressed transcripts annotated as baculoviral IAP-containing proteins, whereas St. Mary's Bay seed mussel had one transcript over-expressed. This gene is involved with inhibiting apoptosis, through interaction with caspases, and therefore the under-expression of this transcript might be associated with an increase in apoptosis activity (Rigato et al. 2020). Caspases are involved with apoptosis pathways in both vertebrates and invertebrate species (Vogeler et al. 2021). Only one differentially expressed transcript was associated with caspases which was found over-expressed in March Water seed (Caspase 7). There were also several other transcripts over-expressed associated with stress response. For example, the March Water adult mussels had one transcript over-expressed annotated as Ataxin-2-like protein isoform X5. Ataxin-2 proteins have been found to have an important role in stress granule formation

which are involved with regulating protein turnover during stressful conditions and diseases in humans (Nonhoff et al. 2007; Ostrowski et al. 2017). The March Water seed also had one transcript over-expressed to Cathespin B, which is involved with autophagy (Mort and Buttle 1997). Overall, the mussel's transcript expression showed indications that the salinity exposure was starting to elicit a stress response.

This study found differentially expressed transcripts annotated to genes associated with the immune system. The most prevalent groups of differentially expressed transcripts were annotated to the family of C1qs, C-type lectins, lysozymes, and various antimicrobial peptides. Immune related transcripts were both over and under-expressed. Several studies have found that hyposalinity results in the downregulation of the immune system (Wang et al. 2012a; Wu et al. 2018). In contrast, other transcriptomic studies have also found over-expression of immune related transcripts such as C1qs and C-type lectins (Zhao et al. 2012; Nie et al. 2017; Xiao et al. 2018; Ertl et al. 2019), indicating that they're involved with an osmotic stress response. The family of C1qs play a role in innate immune response in infection by promoting immune effector recruitment, ending cell-cycle progression, and promote survival through the NF-kB pathways in vertebrates (Van den Berg et al. 1998; Bordin and Tan 2001; Amanullah et al. 2003; Yamada et al. 2004). The C1q domain containing proteins have been found in other non-immune related proteins including adiponectin, precerebellin, hibernation protein, etc (Kishore et al. 2004), which indicates they have other functions aside from being an immune effector. This indicates that the over-expression of the C1q's in this study might have functions outside the immune system that aid in physiological responses to osmotic stress.

3.4.4 Differences in sizes and sites

This study found differences in expression patterns between size and site. This is not an unexpected finding as the responses to salinity are variable depending on amino acid pools, site, season etc. (Bayne 2017). Overall, St. Mary's Bay adult *M. edulis* had more differentially expressed transcripts than all other mussel groups. St. Mary's Bay adults had more transcripts associated with osmoconformation, and oxidative phosphorylation compared to all other mussels after 6 h. A study by Sukhotin et al. (2003) on the mussel *M. edulis* showed that large mussels (0.78 g) were much more likely to stay open and

maintain activities at lower salinity, compared to medium size mussels (0.39 g) and small mussels (0.12 g). This difference was speculated to be due to an increase in resistance to salinity stress or higher metabolic requirements. This could indicate that the St. Mary's Bay adults might be still actively osmoconforming after 6 h. However, all other groups except St. Mary's Bay seed showed differential expression associated with osmoconformation, but each mussel group had a unique set of transcripts.

Figure *15* shows the expression of osmoconformation transcripts found differentially expressed in this study and shows that most transcripts were unique to the site and size. In contrast to the present study, a study on oysters *Ostrea lurida* from three populations from California, reared in a common garden condition in laboratory, over multiple generation showed that transcriptomic responses to hyposalinity varied by population, with a hyposalinity tolerant population showing higher expression of transcripts related to cilia (Maynard et al. 2018). However, Maynard et al. (2018) demonstrated that all populations had a subset of transcripts that were expressed similarly between the three populations, indicating that when different populations are exposed to the same environments over multiple generations there is a conserved response to hyposalinity (Maynard et al. 2018). In the present study, mussels were from two sites, and while it is unlikely that large differences in genetics between the two sites exist, environmental differences between the two sites could have been driving some of the differences in transcription expression. This could be due to differences in osmolyte storage as highlighted by Pierce and Greenberg (1973) and Pierce et al. (1995). Pierce and Greenberg (1973) found that free amino acid concentrations and composition were different between the two populations of oysters (*C. virginica*), and that these differences might be associated with tolerance mechanisms. In addition, Freeman (1974) found that there were differences in growth between *M. edulis* in two embayment's in Nova Scotia: St Margaret's Bay and Bedford basin. This difference was attributed to differences in food supply and not temperature (Freeman 1974). Dietary supply can also influence the amino acid composition of bivalves, particularly taurine (Hosoi et al. 2005; Bayne 2017). Differences also exist in terms of osmotic stress associated with lipid composition in wild (intertidal) and aquaculture (sublittoral) mussels. A study by Nemova et al. (2013) analyzed the lipid membrane of wild and aquaculture *M. edulis*

and found that baseline lipids were different between the two mussel groups. This baseline difference in lipid composition resulted in different responses to hyposalinity. Mussels in the intertidal zone contained higher levels of baseline cholesterol levels compared to the aquaculture mussels, which contained more saturated fatty acids, n-6 polyunsaturated fatty acids and 22 non-methylene interrupted fatty acids. In both wild and aquaculture mussels, hyposalinity from 25 to 15 ‰ resulted in changes in the membrane lipids associated with the gills, including increased content of phosphatidylethanolamine and phosphatidylserine in the membranes.

A recent report by Poirier et al. (2021) monitored environmental differences over three years (2016–2018) in six location with mussel aquaculture including Brudenell River, March Water, Murray River, New London Bay, Nine Mile Creek, and Tracadie Bay. The environmental data in this report is highly relevant to this research as the sites covered in this study were monitored directly (March Water) or nearby (Brudenell River is in the same watershed at St. Mary's Bay), and mussels were present at these locations between 2016 and January 2017. In general, this report found that water parameter trends and growth appear relatively similar between sites; however, some interesting anomalies were observed. March Water *M. edulis* seed was smaller compared to all other sites. This trend was also observed in this study, as seed from March Water were smaller. In addition, spring bloom timings were different between March Water, Brudenell River, with March Water having an earlier and more peaks of chlorophyl A in 2016 and 2017 (Poirier et al. 2021). Salinity did not vary greatly between the two locations (Poirier et al. 2021), which indicates that food availability could have been driving the differences in transcript expression between the mussel sites.

Differences in seed and adult mussels may have been further driven by differences in amount and types of energy reserves. As younger bivalves have been found to have less energy reserves than adults (Holland and Spencer 1973; Mann and Gallager 1985; Widdows et al. 1989). Larval stage bivalves have been found to store more lipids and proteins, and less polysaccharides, and this is the main energy source during this stage of development (Holland and Spencer 1973; Mann and Gallager 1985; Widdows et al. 1989). Adult mussels predominantly store glycogen, which is the main energy source in

metabolism (Holland and Hannant 1976). This could indicate that smaller mussels might need to respond faster to hyposalinity stress, and their osmoconformation strategies could be different due to differences in energy reserves.

3.5 Conclusions

Overall, it was found that abrupt hyposalinity, resulted in major responses both in heart rate and transcript expression. Heart rate increased during the first 6 h of hyposalinity in adult mussels. This could be associated with osmotic shock and increased respiration rates, potentially resulting from oxidative deamination of free amino acids during osmoconformation. Differential expression analysis discovered several transcripts associated with metabolism, osmoconformation, stress response, immune response, and antioxidants. Differences were also found between the two sites and sizes, indicating that there could be differences in environmental factors that could result in variance in responses to hyposalinity. Overall, this means that transcript expression strategies in response to hyposalinity stress may be highly specific to the environment and size of mussels. Food availability may play an important role in stress responses in hyposalinity stress.

Chapter 4. Evaluating blue mussels (*Mytilus edulis*) responses to different levels of food availability using transcriptomics, heart rate and neutral red assay

4.1 Introduction

Mussels (*Mytilus edulis*) are suspension feeding organisms that ingest microorganisms such as phytoplankton as their main source of food (Page and Hubbard 1987; Wong and Levinton 2004). Phytoplankton abundance in a marine ecosystem fluctuates both in short-term (days) and long-term (weeks to months) and is controlled by natural factors including season, which impacts the sunlight and length of daylight, and by other factors including temperature, salinity, currents, precipitation, nutrients etc. (Cranford et al. 2011; Käse and Geuer 2018).

Climate change threatens phytoplankton communities predominantly through ocean acidification, increasing water temperatures and stratification. Stratification blocks nutrients in colder bottom water from mixing into the warmer surface water, where phytoplankton resides (Henson et al. 2021). Changes in phytoplankton distribution will likely be regionally impacted, but the global trend is predicted to result in a decline of primary producing organisms particularly in subtropical and temperate regions of the northern hemisphere (Bindoff et al. 2019; Henson et al. 2021). However, polar areas are projected to have increases in phytoplankton concentration due to retreat of sea ice, increases in growing season and growth rate (Dutkiewicz et al. 2013; Cabré et al. 2015; Kwiatkowski et al. 2020; Henson et al. 2021). In the Northwest Atlantic Ocean, many locations have seen occurrences of lower nutrient concentration compared to the long-term mean for the region in the past two decades (Bernier et al. 2018). Phytoplankton concentrations declined from 1999–2011, which was followed by a recovery period by 2015, and a decline again as of 2016 (Bernier et al. 2018). Spring blooms also fluctuated in magnitude and amplitude from 2011–2016 in the Northwest Atlantic, which are impacted annually by warming, winds, mixing, ice cover, and nutrients (Bernier et al. 2018).

Climate change projections have predicted that phytoplankton species richness will be impacted (Henson et al. 2021). Models predict that many species of phytoplankton will make a poleward shift into the North Atlantic Ocean, which will alter community structure and food webs in the region (Barton et al. 2016). In the Northwestern Atlantic it is predicted that climate change will result in an influx of dinoflagellates and dizaotrophs, and decline of diatoms (Henson et al. 2021).

At the same time, episodic coastal eutrophication is expected to increase as a result of runoff (Bindoff et al. 2019). Nutrient loading from fertilizer, in the form of nitrogen (N) and phosphorus (P), have been found to result in phytoplankton growth and eutrophication (Drury et al. 2016; Reid et al. 2016). Risk assessment by Agriculture and Agri-Food Canada (2016 report) indicates that the Atlantic Canada region has a moderate to very high risk to water contamination from residual N, and low to moderate risk by P in agricultural areas (Drury et al. 2016; Reid et al. 2016). Eutrophication events are often accompanied by hypoxia/anoxic conditions that can be detrimental to aquatic ecosystems (Bindoff et al. 2019). In addition, harmful algae blooms associated with climate change and coastal eutrophication is expected to continue to increase (Gobler et al. 2017; Bindoff et al. 2019; Griffith et al. 2019).

Fluctuations in phytoplankton can have direct impacts to mussels, as mussels rely on it as their main source of food (Page and Hubbard 1987; Wong and Levinton 2004). Mussel's feeding behaviour, physiology and morphology is greatly impacted by food availability. In low food availability conditions, mussel feeding behaviour has been found to cease below 4,000 cells of phytoplankton per mL of seawater (0.5 µg/L Chlorophyl a (chl a)) (Pascoe et al. 2009). Cessation of filtering, is a mechanism for the prevention of tissue loss, as the cost of filtration maybe higher than what could be gained from the concentration of food (Winter and Langton 1975; Hawkins et al. 1999). As food availability increases from a minimum threshold, filtering and clearance rate increases up to a maximal level (Riisgård et al. 2011). Above this maximal level, it has been found that mussels will close their valve or reduce their gape, and clearance rate is reduced (Riisgård et al. 2011). The level of feed that represents the cessation of filtering behaviour in high food availability has been variable between study (Riisgård 1991; Pascoe et al. 2009; Riisgård et al. 2011). Pascoe et

al. (2009) found that mussels of ~ 35 mm shell height (SH), being held at constant conditions of 30,000 cells/mL (6 µg/L chl a; *Isochrysis galbana*) for more than 2 h resulted in cessation of filtration behaviour. In contrast, Riisgård et al. (2011) found that for mussels ~ 21 mm SH, that the cessation of filtering activity occurred at concentrations between 5,000–8,000 cells/mL (~ 6–10 µg/L chl a; *Rhodomonas salina*), and this was associated with the ingestion of ~ 11 x 10^6 cells (Riisgård et al. 2011). It is not clear whether a reduction in filtration rate and valve closure is a mechanism to prevent overloading the gills or due to saturation of digestive tubules (Riisgård et al. 2011).

Mussels, like most bivalves, are highly plastic in feeding behaviour and physiology and have the ability to acclimate to different levels of food concentrations through alterations in both their feeding behaviour and physiology (Fegley et al. 1992). For example, in locations of the Norwegian coast, where phytoplankton concentration are low due to low nutrient levels, mussels living in this location are able to maintain feeding down to 0.01 µg/L (chl a), indicating that they have acclimated to levels of low phytoplankton (Strohmeier et al. 2009). Acclimation to low food environments has been found to result in changes to behaviour, physiology and morphological structures to maintain energy balance in bivalves (Hawkins and Bayne 1992). Mucosal lectins increase in abundance in bivalves exposed to starvation, and has been hypothesized to be associated with aiding in the food selection process (Pales Espinosa and Allam 2013a, 2018; Allam et al. 2021). Steeves et al. (2020) also found that capture efficiency can vary by populations and by environmental cues such as low food availability. Increases in gills size and reduction of labial palps has also been found to result in low food availability, as this aids in increasing clearance of particles per unit time (Honkoop et al. 2003; Capelle et al. 2021). As with low food availability, when mussels are exposed to high food availability, physiological and morphological changes occur to compensate. Morphologically, gills have been found to decrease in size while labial palps have been found to increase their size to aid in sorting behaviour (Honkoop et al. 2003; Capelle et al. 2021). It has been found that the sorting and rejecting of food increases production of pseudofaeces (Foster-Smith 1978; Widdows et al. 1979b; Jørgensen 1981; Beninger et al. 1999). Digestion has also been found to be enhanced during times of high food availability through use of crystalline style and

increases in enzymes α-amylase and laminarinase. (Langton 1977; Hawkins and Bayne 1992). The gut has also been found to be plastic in relation to changes in food concentration. Increases in food concentration has been found to increase gut volume, while decreasing gut passage time in bivalves (Bayne et al. 1984; Navarro et al. 1992, 2009).

There are limitations on a bivalve's ability to acclimate to different diets and food availability. For example, gut volume, and gill/palp size can only increase to a maximal size (Hawkins et al. 1990; Labarta et al. 1997). In addition, behavioural and physiological plasticity may require time to develop. For example, transplant studies have found that it takes weeks to months for clearance rate to adjust to a rate similar to a native population (Okumuş and Stirling 1994; Navarro et al. 2003; Wong and Cheung 2003; Tang et al. 2020). Therefore, despite mussels highly plastic feeding behaviour and physiology, fluctuation in phytoplankton concentrations can directly impact mussel health. Filgueira et al. (2016) modeled the potential impacts of phytoplankton and nutrients under climate change scenarios for the Gulf of St. Lawrence coastal embayments, to understand the impacts of bivalve-phytoplankton trophic interactions. Phytoplankton decreased in several scenarios , however the most resilient bays would be ones that have interactions with large rivers and high exchange with oceans, that replenish nutrients and phytoplankton (Filgueira et al. 2016). Many other environmental conditions are expected to change in relation to climate change including temperature, dissolved oxygen, salinity, acidity (Hoegh-Guldberg et al. 2014; Bindoff et al. 2019). Environmental factors including increases in temperature has been found to result in increased top-down pressure on phytoplankton, by resulting in an increase of bivalve metabolism which increases food requirement to maintain growth (Filgueira et al. 2016). Food availability has been found to be the most important environmental factor in contributing to mussel growth (Freeman 1974; Page and Hubbard 1987). In addition, food availability has a major role in protection against stress. High food availability in combination with stressful environmental conditions, has been found to result in better survival outcomes compared to if the environmental stress was combined with low food availability (Hatcher et al. 1997; Tremblay et al. 1998; Freites et al. 2003; Delaporte et al. 2006; Babarro et al. 2008; Lesser et al. 2010; Dowd et al. 2013;

Lassoued et al. 2019). Overall, nutritive stress can result in catabolism of energy reserves, and can lead to mortality (Thompson et al. 1974; Widdows 1978). Therefore, declines in phytoplankton concentrations, as predicted by climate change models, could negatively impact mussels.

Species richness declines in phytoplankton and zooplankton may also impact mussel health, as optimal growth has been found associated with mixed diets (Wong and Levinton 2004). Research has found that mussels can exhibit selective grazing capacity (Bougrier et al. 1997). Phytoplankton size also impacts retention efficiency, with mussels able to retain larger particles better than smaller (Vahl 1972; Møhlenberg and Riisgård 1978; Riisgård 1988; Sonier et al. 2016); however, picoplankton has also been found to be an important contributor to a mussels energy budget (Sonier et al. 2016). Research has found that shellfish preferentially feed on diatoms, but shape and flexibility may also influence food selection (Bougrier et al. 1997). Climate change projection in the North Atlantic have predicted declines in diatoms and increases in dinoflagellates. There is currently a limited understanding of how climate change driven changes in phytoplankton will impact mussels. However, research by Liang et al. (2019) in scallops (*Patinopecten yessoensis)* found that nutrient limitation associated with silica and P resulted in a transition from diatoms to dinoflagellates and acted as a 'bottle-neck' in the carrying capacity (Liang et al. 2019). Overall, changes to phytoplankton could result in more competition for food resources, which could impact bivalve growth (Fréchette 2005; Lachance-Bernard et al. 2010; Filgueira et al. 2014; Guyondet et al. 2015).

Despite numerous studies on how food availability impacts mussels' health (i.e. Hatcher et al. 1997; Tremblay et al. 1998; Freites et al. 2003; Delaporte et al. 2006; Babarro et al. 2008; Lesser et al. 2010; Dowd et al. 2013; Lassoued et al. 2019), little is known about how gene transcription controls physiological responses to food availability. In addition, it has been found that a mussel's physiological response to food availability can vary between individuals (Bayne and Hawkins 1997; Bayne 2004), size (Winter 1973; Thompson and Bayne 1974; Winter and Langton 1975), and sites/populations (Strohmeier et al. 2009; Steeves et al. 2020). Therefore, an understanding of how transcription patterns vary between mussel groups in response to food availability is an important aspect to

understand. The present study evaluated the acute transcriptomic response of different levels of food availability in mussels to gain knowledge of the types of pathways involved in regulating changes in physiological response. Differences in transcriptomics were also evaluated between two sites in PEI (March Water, and St. Mary's Bay) and sizes (adult, seed) to understand how transcriptomics varies. Heart rate and lysosomal destabilization was evaluated to better understand the physiological response and stress response to different food rations. It was hypothesized that major shifts in transcriptomics, heart rate, and lysosomal destabilization would be observed within the 48 h of exposure to different food rations and that there would be substantial differences in the transcriptomic response between the two sizes and sites of mussels from PEI.

4.2 Materials and Methods

4.2.1 Mussel sites and sizes

Adult and seed mussels (*M. edulis*) were from two aquaculture leases located in PEI, March Water (MW) (N 46° 31' 18.8", W 63° 43' 12.9") and St. Mary's Bay (StM) (N 46° 07' 37.2", W 62° 31' 14.2") (Figure *2* (Chapter 2)). For a detailed summary of mussel sites, sizes and acclimation used in this trial please refer to Chapter 2 (2.2.1 Mussel sites and sizes).

4.2.2 Food availability trials

Separate food availability trials were completed for each size groups (MW, StM), with the first consisting of adults and the second consisting of seed mussels. The food availability trials were completed in 12 flow-through (100 mL/min) zebra tanks (9 L) with salinity and temperature maintained at 16 °C and 27 ‰, respectively. The tanks were divided into three groups (4 replicates): low food ration at 1% dry body tissue weight (BW), intermediate food ration at 5%, and high food ration at 10%. In both trials, each tank contained 14 mussels from each site (28 per tank; N = 336 total).

The % BW was calculated based on a mean of the two sites for each size (adult, seed). It was hypothesized that the 5% ration was optimal and 1% and 10% were low and high food rations, respectively (Thompson and Bayne 1974; Winter and Langton 1975; Connor et al. 2016). The amount of feed given was based on the total biomass in the tank, i.e. 28

individuals. Mussels were fed a 1:1 mixture of *Isochrysis galbana* and *Chaetoceros muelleri*. Food was rationed and fed hourly using an automatic dosing machine (GHL© standalone doser, GHL, Rheinland-Pfalz, Deutschland). The concentration of food in the tank that was administered by the dosing machine on an hourly basis is summarized in Appendix 4.

4.2.3 Heart rate monitoring

Heart rate (HR) was monitored only in the adult trial, and not in the seed trial as sensors were too big for seed size mussels. To measure HR, non-invasive infrared red-light (IR) sensors were manufactured by Dr. K Fraser Clark using a slightly modified method based on Burnett et al. (2013). The HR sensors were attached to the mussel over the approximate location of the heart, and plumbers' putty (PlumbShop®, Masco Canada Limited, Ontario, Canada) was placed around the sensor to seal it to the mussel and reduce IR signal fluctuations. After initial attachment of IR sensor, mussels were placed back into their holding tank for 24 h to acclimatize to the sensor. Heart rate of three mussel per treatment, two from each site (six total) were monitored continuously over the 48 h food availability trial and for 1 h after the trial. Real-time HR was visualized using the software Makerplot (SelmaWare Solutions, LLC) and then analyzed further by importation into Microsoft Excel 365, to visualize the HR data. Heart rate was interpreted by manually counting the total number of heartbeats in one-minute intervals every 15 minutes and calculating the average beats per minute (BPM) for each hour in the 48 h trial.

4.2.4 Neutral red assay

Neutral Red Assay (NRA) was conducted in the adult and seed trials, at three time points; an initial reading (pre-treatment) (0 h). For the adult trial, one mussel from each site (MW, StM) was used as the initial sample (0 h) and during the trial. During the trial (24, 48h) one mussel from each tank per site was used. For the seed trial, seed mussels were too small to collect a sufficient haemolymph and mantle fluid sample from, therefore, four individuals were pooled during each NRA reading. The pre-treatment (0 h) reading consisted of a pooled sample from each site (MW and StM), and during the trial (24, 48 h) a pooled sample from each site per tank was used. Lysosome destabilization index (LDI) was

calculated using the method developed by (Hauton et al. 2001; Harding et al. 2004; Méthé, et al. 2015).

Briefly, a stock solution was prepared using 2.28 mg of neutral red dye (3-amino-7-dimethylamino-2-methylphenazine hydrochloride) (F1631: Sigma-Aldrich, St. Louis, MO) dissolved in 1 mL of dimethyl sulfoxide (DMSO) (D128, Thermo Fisher Scientific, Waltham, MA, USA). Approximately 500 µL of mantle fluid was collected from the mussels (pooled sample for seed mussels) and filtered through a 0.2 µm Progene cellulose acetate membrane (Ultident, St. Laurent, QC, Canada). Then, a working solution was prepared by dissolving 8.5 µL of the stock solution into the mantle fluid. A 0.2 mL haemolymph sample was collected from the mussels directly from the pericardial sac region and mixed with 0.2 mL of its own mantle fluid in a low-retention Eppendorf® (Thermo Fisher Scientific). An aliquot of 40 µL was transferred to a positively charged microscope slide and incubated in the dark for 15 minutes at 20 °C. Working solution (20 µL) was then added to the slide and incubated for an additional 45 minutes. The microscope slide was read under a compound microscope (630x magnification) by counting 50 haemocyte cells total and expressing them as LDI. After the 24 h NRA reading, food concentration was adjusted as needed due to removal of mussels from tanks for LDI reading (Appendix 4).

4.2.5 Statistical analysis of heart rate and neutral red assay

Separate statistical analyses were carried out for HR and LDI. For HR, two statistical analysis was completed: (1) mean hourly HR (1, 5, 10, 19, 25, 32, 44, 48 h) and (2) trial timing categories as in the mean HR during the last two hours of the trial and mean HR of the one-hour post-treatment when placed back into acclimation tank. Heart rate differences between sites could not be analysed due to insufficient replication. To analyse HR, a General Mixed Effect Model with repeated measures treated as hierarchal structure (split-plot): mussels as large units (whole plots) and time as sub-units (subplots). In the HR analysis, food availability (1%, 5%, 10%), and time (1, 5, 10, 19, 25, 32, 44, 48 h) or (during, after) were considered fixed variables. The mussels were considered a random variable with food availability nested within. Variance inflation factor (VIF) was calculated

to test multicollinearity of the model. The model included all significant main effects and interactions, with the nonsignificant main effects and interactions being collapsed from the model to give final model estimates.

Neutral red assay's LDI was analysed separately for each size (adult, seed) at time 24 h and 48 h. To analyse LDI, a General Mixed Effect Model was used. The food availability (1%, 5%, 10%), site (MW, StM), and time (24 h, 48 h) were considered fixed variables. Tank effect was considered random with food availability and site nested within. The model included all significant main effects and interactions.

In both analysis of HR and LDI, the assumptions of normality and homoscedasticity of the models were assessed for the error terms by conducting a normal probability plot of standardized residuals of error terms and variance by plotting the residuals of error terms versus fitted. For all analyses, the significance level was set at *p-value* = < 0.05. In the presence of a significant interaction between the various factors, a Bonferroni simultaneous test of means was performed to identify differences between groups. All estimates are reported as least squares mean (LSM) ± standard error (SE), unless otherwise specified.

4.2.6 Sample preservation, RNA extractions and sequencing

Six mussels per size (adult, seed) and site (MW and StM) in each food availability treatment (1%, 5%, 10%), were collected for RNA preservation directly following the 48 h food availability trials. Whole mussel tissue was homogenized into RNAlater® solution (Cat. No. 76106, QIAGEN GmbH, Hilden, Germany) using an Omni tissue homogenizer (Omni International, Kennesaw, GA, USA), at a ratio of 1g tissue per 10 mL of RNAlater®. RNA was isolated using Qiagen RNeasy® Mini Kit (Cat. No: 74104, QIAGEN GmbH, Hilden, Germany) following the manufacture protocol. An additional on-column DNase I (Cat. No. 79254, QIAGEN GmbH, Hilden, Germany) treatment was applied during the RNA isolation process, to ensure no DNA contamination was present. Concentration and quality of RNA was assessed using Nanodrop spectrophotometry (Thermo Fisher Scientific, Waltham, MA, USA) and Bioanalyzer (Agilent Bioanalyzer, RNA 6000 nano kit, Santa Clara, CA, United States), respectively. High quality RNA was shipped to Genome Quebec (Montreal Quebec) where Truseq library preparation was completed on

each sample. Then, Hiseq2000 Illumina (sequencing by synthesis) was completed (PE 100), to give a sequencing read depth of 15–20 million reads per sample (eight samples per sequencing lane).

4.2.7 *De novo* transcriptome assembly and differential expression analysis

The transcriptome assembled in this study was built using mussel samples from the hypoxia (chapter 2), salinity (chapter 3), food availability (present chapter) trials, and resulted in one large transcriptome. For detailed description of assembly and differential expression analysis, see Chapter 2 (2.2.6 *De novo* transcriptome assembly; 2.2.7 Differential expression analysis)

Differential expression was completed in both DESeq2 (Love et al. 2014; Afgan et al. 2018) and edgeR (Afgan et al. 2018; Robinson 2019) (Galaxy Version 3.24.1 + galaxy1). In both methods, *p-value* was adjusted to control for false discovery rate (FDR *p-value*). Several pairwise comparisons were completed to understand the nature of the transcriptomic response of the different sites and sizes, and this is summarized in Table 22. In both differential expression packages, Log_2 fold change (FC) was used to understand how the expression changed relative to each food ration in each comparison. Trends in differential expression analysis results were visualized using volcano plots, Venn diagrams, heatmaps and principal component analysis (PCA) analysis. PCA analysis was completed on transcripts that had expression level of 10 across all samples in the food availability trials.

Table 22. Comparisons of Differential expression analyses utilized in experiment. For each comparison, two different methods of differential expression were utilized, DESeq2 and edgeR. Two mussel sizes (adult and seed) and two site (March Water (MW), and St. Mary's Bay (StM).

Group	Comparisons
StM adult	10% vs 5%; 1% vs 10%; 1% vs 5%
MW adult	10% vs 5%; 1% vs 10%; 1% vs 5%
StM seed	10% vs 5%; 1% vs 10%; 1% vs 5%
MW seed	10% vs 5%; 1% vs 10%; 1% vs 5%

4.2.8 Annotation and functional analysis

Differentially expressed transcripts underwent annotation (FDR *p-value* < 0.05) using Trinnotate (Bryant et al. 2017) and Blast2GO (basic) software (Version 5.2.5) using NCBI Blast service (blastx), with an E-value set at $1e^{-5}$, and with a taxonomy filter selective to only bivalves (taxa: 6544, Bivalvia) (Conesa et al. 2005; Conesa and Götz 2008; Götz et al. 2008, 2011). The Kyoto Encyclopedia of Genes and Genomes (KEGG) Automatic Annotation Server (KAAS) (Moriya et al. 2007) was used to annotate differentially expressed transcripts as well. Then, annotation assignment of differentially expressed transcripts was used in pathway assignment using KEGG Mapper (Kanehisa and Sato 2020) using the organism-specific search mode. KEGG mapping was assigned using the only two bivalve species within the KEGG server, Pacific oyster (*Crassostrea gigas*) and Yesso scallop (*Mizuhopecten yessoensis*) to receive pathways only relevant to bivalves. Annotation, ortholog, and pathway assignment aided in facilitating functional understanding of differentially expressed transcripts.

4.3 Results

4.3.1 Heart rate and neutral red assay

This study found that HR (adult) was not significantly impacted by food availability, however, the main effects of time (1, 5, 10, 19, 25, 32, 44, 48 h) was found significant (*p-value* = <0.001; *F-value* = 6.6). Overall, heart rate increased in the first 32 h, and Bonferroni simultaneous test of means found that the HR at 1, 5 and 10 h were significantly different from the HR at 32 h (Figure 16A). After 32 h, heart rate declined until the end of the trial, at 48 h. Analysis of timing categories (during, after) found HR significantly increased (*p-value* = 0.002, *F-value* = 11.6) when mussels were returned to the acclimation tank (Figure 16B).

The initial readings of LDI were calculated as 38% (MW) and 48% (StM) in the adults, and 42% (MW) and 50% (StM) in the seed, respectively. During the trial, LDI (adult, seed) was not significantly impacted by food availability. However, LDI in the adult trial found that site (MW, StM) was significantly different (*p-value* = 0.003, *F-value* = 9.7). Figure 17 shows that LDI was significantly higher in the MW (65.5 ± 3.9 %) compared to StM (48.3

± 3.9 %). In the seed trial, LDI was not impacted by food availability (*p-value* = 0.310), time (*p-value* = 0.154), or site (*p-value* = 0.597).

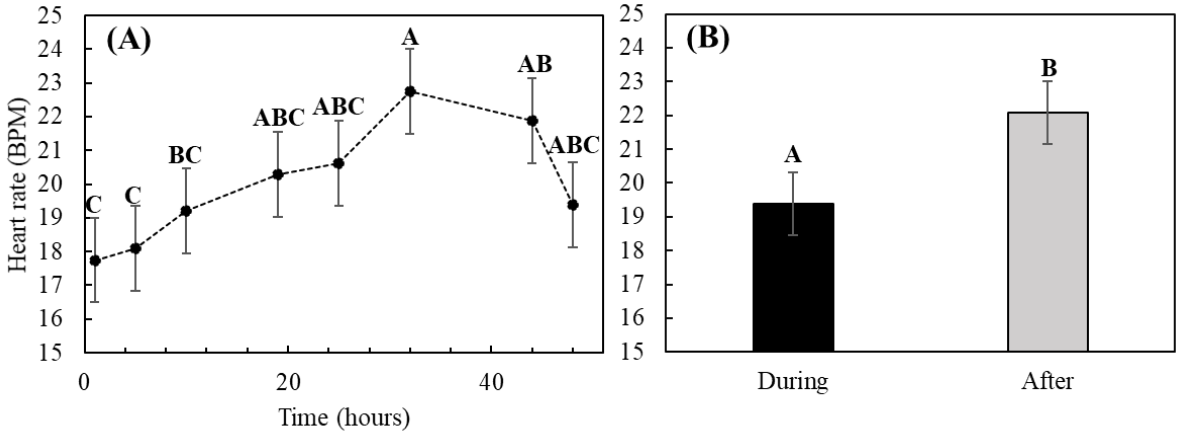

Figure 16: Least square mean (LSM) ± Standard error (SE) of heart rate from final statistical model for adult mussels at: (A) 1, 5, 10, 19, 25, 32, 44, 48 h (n = 24 per point); (B) during, after (n = 24 per bar). LSM's without a common script were significantly different (*p-value* = < 0.05).

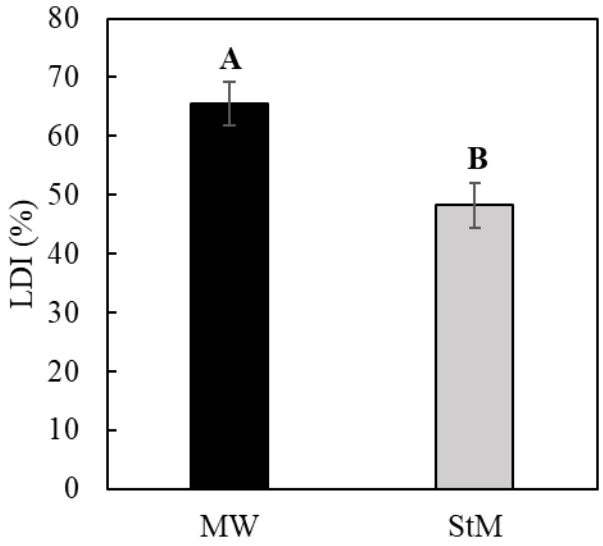

Figure 17. Estimates from final statistical model for lysosomal destabilization indices (LDI) of adult mussels from each site (MW, StM). LSM's without a common script were significantly different (*p-value* = < 0.05).

4.3.2 Differential expression analysis

Preliminary PCA of all highly expressed transcripts in mussels from the food availability trial, indicates that there was a lot of variability between individuals; however, some separation is visible between the two sites and food ration for both the adult and seed PCA plots (Figure *18*). Differential expression analysis resulted in many over-expressed and under-expressed transcripts being discovered in each pairwise comparison (Figure 19; Table 23). Figure 19 shows the differential expression analysis, with statistically significant transcripts (FDR *p-value* = < 0.05) plotted relative to the FC, where over-expressed and under-expressed transcripts are individually represented in red and blue dots for each pairwise comparison. Positive FC was attributed to over-expressed transcripts whereas, negative FC was attributed to under-expressed transcripts in the food availability treatment. Overall DESeq2 resulted in more differentially expressed transcripts being discovered compared to edgeR (Table 23). Only 24 transcripts discovered in MW adults were unique to the edgeR statistical analysis, and the remainder were also found within the DESeq2 statistical package. The March Water adults in all pairwise comparisons resulted in many more differentially expressed transcripts being discovered compared to all other mussel groups. Heatmaps of mussels with differentially expressed transcripts between each mussel group are shown in Figure 20 and shows the variation of expression between samples. Venn diagrams were created to understand the overlap of differentially expressed transcripts between the mussel sites for each pairwise comparison (Figure 21). Adult and seed mussels were not compared in Venn diagrams due to differences in food concentration in the tank between the two trials. It was found that only a few of the transcripts overlapped between different mussel sites, and that most transcripts discovered were unique to their respective mussel group (Figure 21).

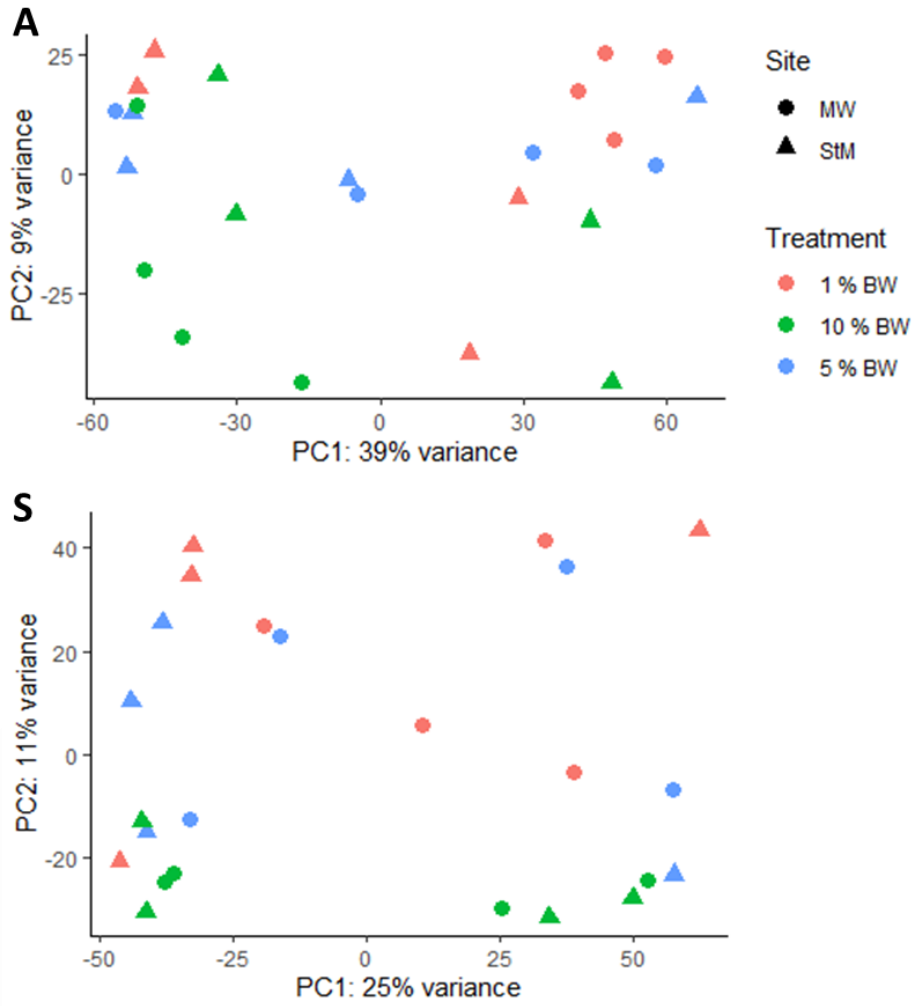

Figure 18. Preliminary principal component analysis plot of all expressed transcripts in food availability trial. Plot A show adults mussel samples, while S shows seed mussel samples from both sites (MW = March Water, StM = St. Mary's Bay) and food availability (1%, 5%, 10%).

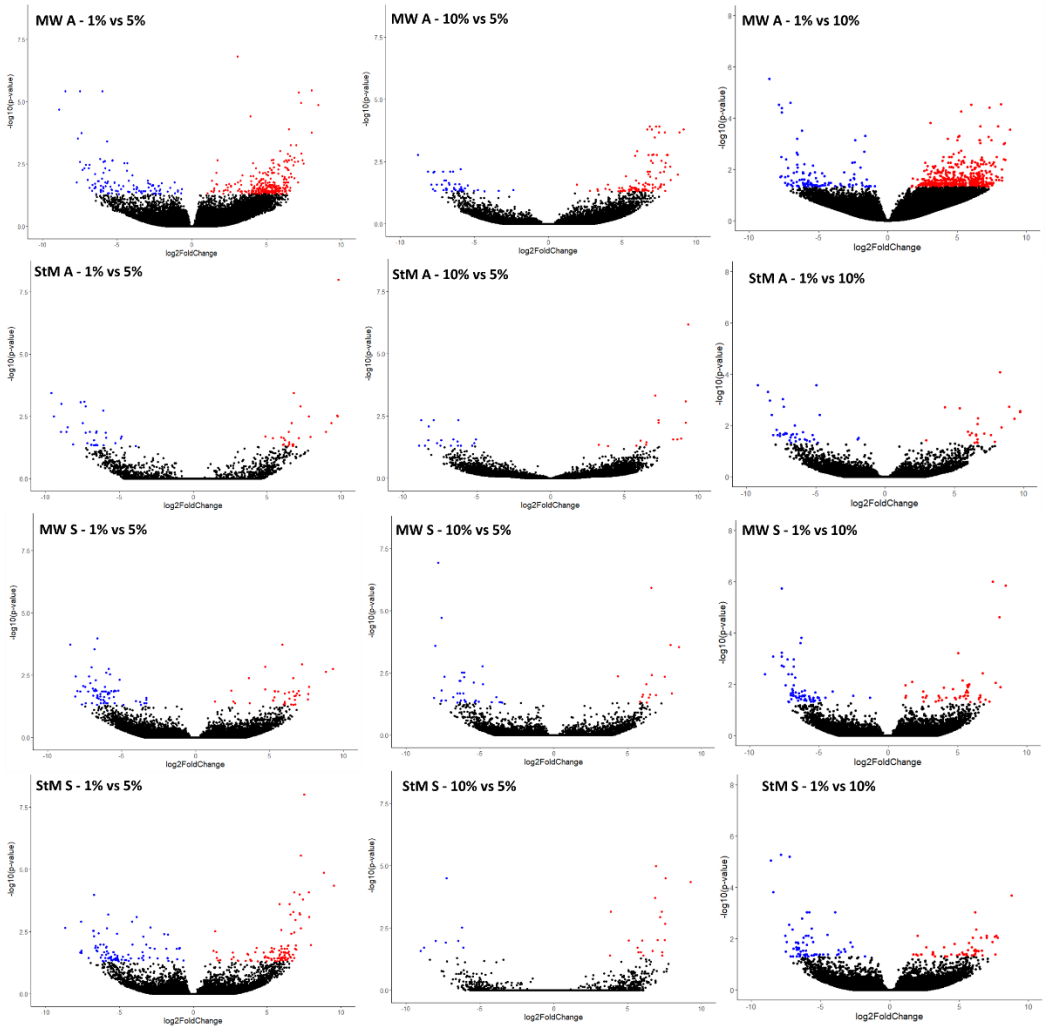

Figure 19. Volcano plots for differentially expressed transcripts identified in DESeq2 for each pairwise comparison (MW = March Water; StM = St. Mary's Bay; A = adult; S, = seed). Fold change is expressed as the first food ration relative to the second (1% vs 5%; 10% vs 5%; 1% vs 10%). Transcripts that are differentially expressed (FDR *p-value* = < 0.05) are indicated by either red (over-expressed) or blue (under-expressed) circles.

Table 23. Total number of differentially expressed transcripts (FDR p-value = < 0.05) for each pairwise comparison in each site and size for both DEseq2 and edgeR.

Pairwise comparison	Mussel group	Total DE DESeq2	Total DE edgeR
1% vs 5%	MW A	593	107
	StM A	57	0
10% vs 5%	MW A	144	0
	StM A	34	0

Pairwise comparison	Mussel group	Total DE DESeq2	Total DE edgeR
1% vs 10%	MW A	629	10
	StM A	60	0
1% vs 5%	MW S	108	0
	StM S	195	1
10% vs 5%	MW S	52	2
	StM S	30	0
1% vs 10%	MW S	112	2
	StM S	115	0

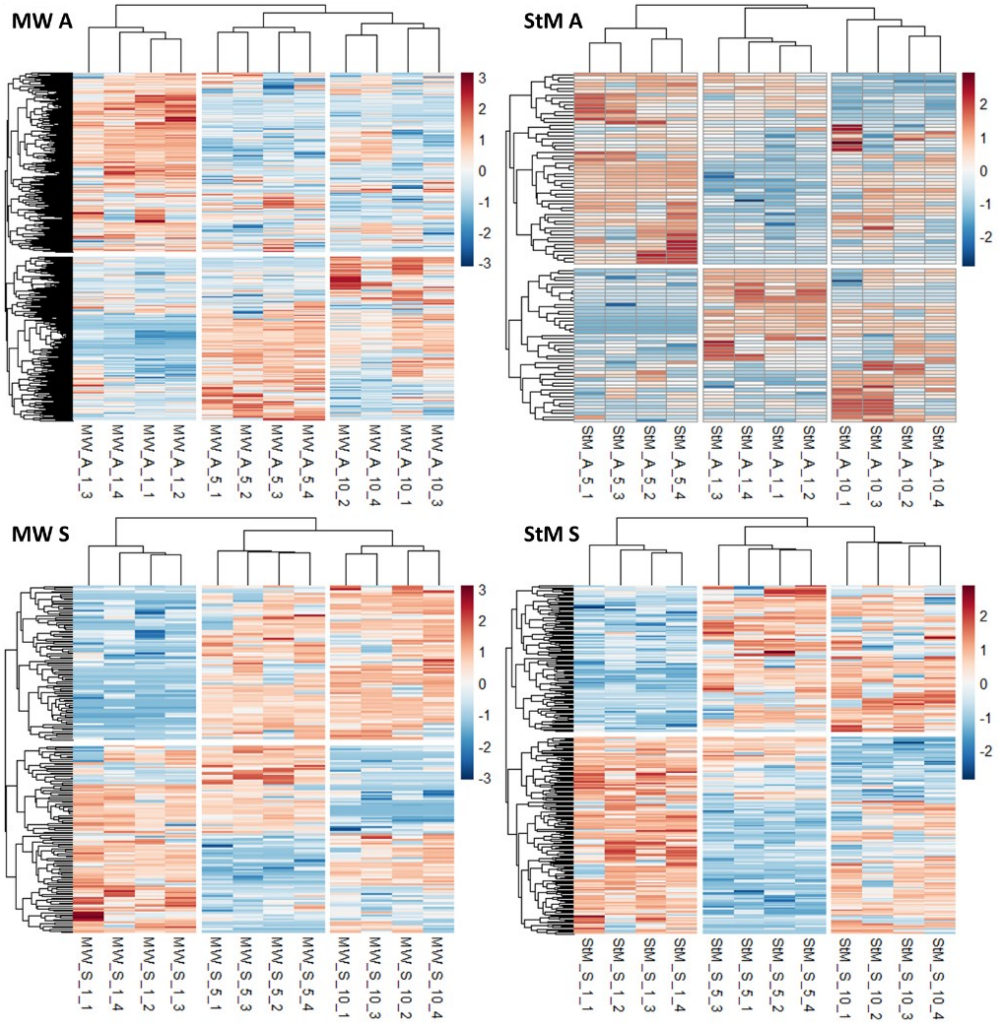

Figure 20. Heatmaps of all differentially expressed transcripts identified by the DESeq2 statistical package. Each heatmap shows one mussel group (MW = March Water; StM = St. Mary's Bay; A = adult; S = seed, with individuals from each food availability (1%, 5%, 10%).

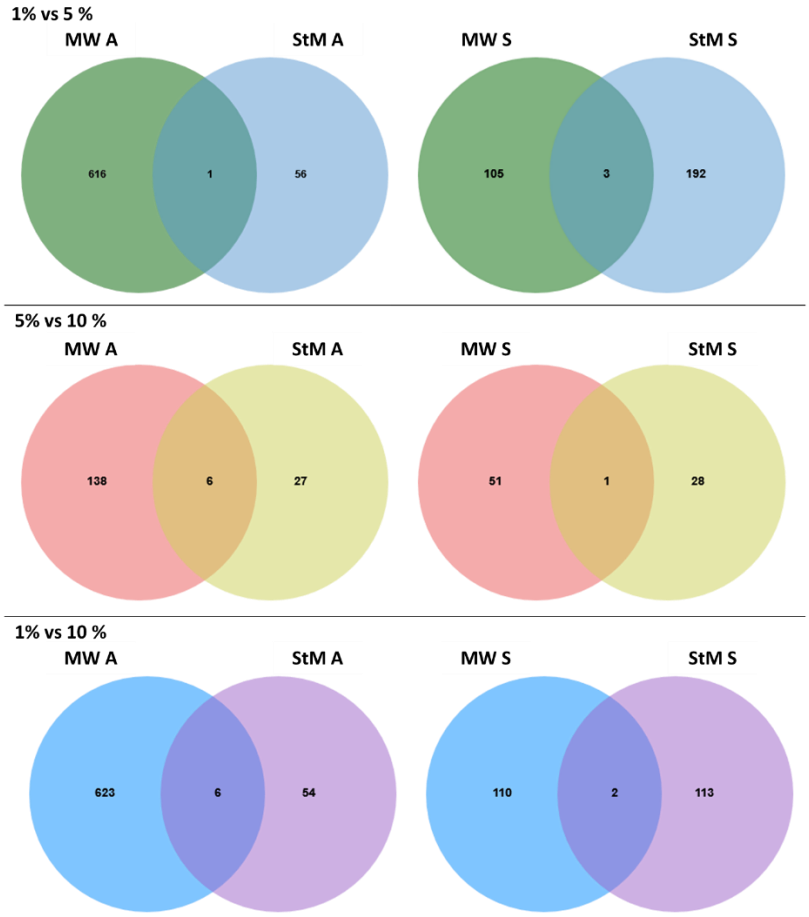

Figure 21. Venn diagram of differentially expressed transcripts found uniquely or mutually between different pairwise comparison of different mussel groups (MW = March Water; StM = St. Mary's Bay; A = adult; S, = seed)

4.3.3 Functional analysis

Pairwise comparisons with the most differentially expressed transcripts were between the 1% vs 5% and 1% vs 10% comparisons, and the least differentially expressed transcript were related to the 10% vs 5%. This indicates that transcript expression was more similar between the mussels being fed at higher rations (10% and 5%) compared to the 1% ration. Therefore, to understand the transcriptomic response of 1% ration on each mussel group, functional analysis will be focused on understanding the transcriptomic response between 1% vs 5% and 1% vs 10% comparisons. KEGG pathways associated with each pairwise comparison is shown in Table 24 and Table 25. In MW mussels (adult, seed), metabolic pathways were mostly under-expressed in the 1% ration. In all pairwise comparison there

were pathways differentially expressed associated with metabolism, genetic information processing, environmental sensing processing, and cellular processes.

Differentially expressed transcripts successfully annotated and found mutually expressed between different sites are shown in Table 26. Differentially expressed transcripts unique to its mussel site and size are shown in Table 27–30. Finally, transcripts found differentially expressed mutually between pairwise comparison (1% vs 5% and 1% vs 10%) within the same mussel group are shown in Table 31. A full list of differentially expressed transcripts can be found in Appendix 1: Supplemental file 3. Overall, several transcripts were annotated associated with links to cilia, immune, ion channels, metabolism, protein turnover, antioxidants, and lysosomes. A subset of transcripts with annotations relating to cilia, digestive enzymes, and immune response were graphed in Figure 22, using their respective fold change compared to other mussel groups in the same pairwise comparison. It was found that expression of transcripts related to cilia and digestive enzymes were different between mussel sites and sizes; however, some similarity in expression was observed in the immune transcripts with several mussel groups showing negative fold change in pairwise comparisons 1% vs 5% and 1% vs10%.

Table 24. KEGG pathways associated with differentially expressed transcripts from each 1 vs 5% pairwise comparisons (MW = March Water; StM = St. Mary's Bay; A = adult; S = seed). Table shows number of over-expressed (+) transcripts and under-expressed (-).

Category	Pathway	MW A		StM A		MW S		StM S	
		+	-	+	-	+	-	+	-
Amino acid metabolism	Histidine metabolism	0	0	0	0	2	-1	0	0
	Valine, leucine and isoleucine degradation	0	0	0	0	0	-1	1	0
	Biosynthesis of amino acids	0	0	0	0	0	-1	1	0
	Lysine degradation	0	-1	0	0	0	-1	0	0
	Arginine and proline metabolism	0	0	0	0	0	-1	0	0
	beta-Alanine metabolism	0	0	0	0	0	-1	0	0
	Cysteine and methionine metabolism	0	0	0	0	0	0	0	-1
	Glycine, serine and threonine metabolism	0	0	0	0	0	0	0	-1
	Tryptophan metabolism	0	0	0	0	0	-1	0	0
Carbohydrate metabolism	Glycolysis / Gluconeogenesis	0	0	0	0	0	-2	1	0
	Pyruvate metabolism	0	-1	0	0	0	-2	0	0
	Inositol phosphate metabolism	0	0	0	0	0	0	0	-1
	Amino sugar and nucleotide sugar metabolism	0	0	0	-1	0	0	0	0
	Ascorbate and aldarate metabolism	0	0	0	0	0	-1	0	0
	Citrate cycle (TCA cycle)	0	0	0	0	0	-1	0	0
Glycan metabolism	Glycosphingolipid biosynthesis	0	0	0	0	2	0	0	0
	Other glycan degradation	0	0	0	0	0	0	0	-1
	Other types of O-glycan biosynthesis	0	0	0	0	0	-1	0	0
Lipid metabolism	Glycerophospholipid metabolism	0	-3	0	0	0	0	0	0
	Fatty acid metabolism	0	0	0	0	0	-1	2	0
	Glycerolipid metabolism	0	0	0	0	0	-1	0	0
	Butanoate metabolism	0	0	0	0	0	0	1	0
	Terpenoid backbone biosynthesis	0	-1	0	0	0	0	0	0
Other metabolism	Oxidative phosphorylation	1	-1	0	0	0	0	0	-1
	Glutathione metabolism	0	0	0	0	0	-1	1	0
	Biosynthesis of cofactors	0	0	0	0	0	-1	0	-1
	2-Oxocarboxylic acid metabolism	0	0	0	0	0	-1	0	0
	Biotin metabolism	0	0	0	0	0	0	0	-1
	Pantothenate and CoA biosynthesis	0	0	0	0	0	-1	0	0
	Porphyrin and chlorophyll metabolism	0	0	0	0	0	0	0	-1
	Selenocompound metabolism	0	-1	0	0	0	0	0	0
Cellular Processes	Lysosome	0	-3	1	0	1	-2	2	-2
	Endocytosis	0	0	0	0	0	-1	1	-1
	Spliceosome	0	0	0	0	1	0	0	-4
	Mitophagy	0	0	0	-1	1	-1	0	0
	Peroxisome	0	-2	0	0	0	-1	0	0
	Phagosome	0	-2	0	0	0	0	0	0
	Autophagy	0	-1	0	0	0	0	0	-1
Environmental Information Processing	ECM-receptor interaction	0	-1	0	-1	0	0	1	-1
	Neuroactive ligand-receptor interaction	0	0	1	0	0	0	0	-1
	mTOR signaling pathway	0	-1	0	0	1	0	0	0
	Wnt signaling pathway	0	-1	1	0	0	0	0	0
	ABC transporters	0	-1	0	0	0	0	0	0
	FoxO signaling pathway	0	0	0	0	1	0	0	0
	Notch signaling pathway	0	0	0	0	0	0	0	-1
	Phosphatidylinositol signaling system	0	0	0	0	0	0	0	-1
Genetic information processing	Protein processing in endoplasmic reticulum	0	-3	0	0	0	0	0	0
	Nucleocytoplasmic transport	0	-1	0	0	0	0	1	0
	Ribosome	0	0	0	0	0	0	2	-1
	Ubiquitin mediated proteolysis	0	-1	0	0	0	0	0	0
	Protein export	0	0	0	0	0	0	1	0
	Ribosome biogenesis in eukaryotes	0	0	1	0	0	0	0	-1
	RNA degradation	0	0	0	0	0	0	1	-1
	SNARE interactions in vesicular transport	0	0	0	0	0	0	0	-1
	DNA replication	0	0	0	0	0	0	1	0
	Mismatch repair	0	0	0	0	0	0	1	0
	mRNA surveillance pathway	0	0	0	0	0	0	0	-1
	Nucleotide excision repair	0	0	0	0	0	0	1	0

Table 25. KEGG pathways associated with differentially expressed transcripts from each 1 vs 10% pairwise comparisons (MW = March Water; StM = St. Mary's Bay; A = adult; S = seed). Table shows number of over-expressed (+) transcripts and under-expressed (-).

Category	Pathway	MW A		StM A		MW S		StM S	
		+	-	+	-	+	-	+	-
Amino acid metabolism	Arginine and proline metabolism	0	-2	0	0	0	-1	1	0
	Lysine degradation	0	-1	0	0	0	-1	0	0
	Amino sugar and nucleotide sugar metabolism	0	0	0	-1	0	0	0	0
	Arginine biosynthesis	0	-1	0	0	0	0	0	0
	beta-Alanine metabolism	0	0	0	0	0	-1	0	0
	Histidine metabolism	0	0	0	0	0	-1	0	0
	Tryptophan metabolism	0	0	0	0	0	-1	0	0
	Valine, leucine and isoleucine degradation	0	0	0	0	0	-1	0	0
	Cysteine and methionine metabolism	0	-1	0	0	0	0	1	0
	Glycine, serine and threonine metabolism	0	0	0	0	0	0	1	0
Carbohydrate metabolism	Glycolysis / Gluconeogenesis	0	-2	0	0	0	-1	0	0
	Inositol phosphate metabolism	0	-2	0	0	0	0	0	0
	Pyruvate metabolism	0	-1	0	0	0	-1	0	0
	Ascorbate and aldarate metabolism	0	0	0	0	0	-1	0	0
	Citrate cycle (TCA cycle)	0	0	0	0	0	-1	0	0
	Starch and sucrose metabolism	0	0	0	0	1	0	0	0
Glycan metabolism	Other types of O-glycan biosynthesis	0	-1	0	0	0	-1	0	0
	Glycosaminoglycan biosynthesis-chondroitin sulfate	0	0	0	0	0	0	0	-1
	Mannose type O-glycan biosynthesis	0	-1	0	0	0	0	0	0
Lipid metabolism	Arachidonic acid metabolism	0	-1	0	0	0	0	0	0
	Glycerolipid metabolism	0	0	0	0	0	-1	0	0
	Glycosaminoglycan biosynthesis-heparan sulfate / heparin	0	0	0	0	0	0	0	-1
	Fatty acid degradation	0	0	0	0	0	-1	0	0
	Glycerophospholipid metabolism	0	-1	1	0	0	0	0	0
	Sphingolipid metabolism	1	0	0	0	0	0	0	0
	Ether lipid metabolism	1	0	1	0	0	0	1	0
Other metabolism	Glutathione metabolism	0	-1	0	0	0	-2	0	0
	Biosynthesis of cofactors	0	-1	0	0	0	-1	0	0
	2-Oxocarboxylic acid metabolism	0	0	0	0	0	-1	0	0
	Drug metabolism-other enzymes	0	-1	0	0	0	0	0	0
	Pantothenate and CoA biosynthesis	0	0	0	0	0	-1	0	0
	Selenocompound metabolism	0	-1	0	0	0	0	0	0
	Ubiquinone and other terpenoid-quinone biosynthesis	0	-1	0	0	0	0	0	0
	Purine metabolism	0	0	0	0	0	0	1	0
	Retinol metabolism	0	0	0	0	0	0	1	0
	Oxidative phosphorylation	3	-1	0	0	0	0	1	0
Cellular processes	Endocytosis	0	0	0	0	1	-1	0	-1
	Lysosome	1	-1	0	-1	2	-1	0	-1
	Mitophagy-animal	0	0	0	-1	0	0	0	0
	Autophagy-animal	1	-1	0	0	1	0	0	-1
	Phagosome	2	-3	1	0	1	0	0	-1
	Spliceosome	0	0	0	0	1	0	1	0
Envrionmental processing	Wnt signaling pathway	0	-3	0	0	0	0	0	0
	ABC transporters	0	-1	0	0	0	0	0	0
	Notch signaling pathway	0	-2	0	0	0	0	1	0
	mTOR signaling pathway	1	-1	0	0	0	0	0	0
	ECM-receptor interaction	0	0	0	0	0	0	1	0
	Neuroactive ligand-receptor interaction	1	-1	0	0	1	0	0	0
Genetic information processing	Protein processing in endoplasmic reticulum	0	-3	0	0	1	0	0	0
	Aminoacyl-tRNA biosynthesis	0	-1	0	0	0	0	0	0
	DNA replication	0	-1	0	0	0	0	0	0
	Mismatch repair	0	-1	0	0	0	0	0	0
	Nucleotide excision repair	0	-1	0	0	0	0	0	0
	Ribosome	0	-1	0	0	1	0	0	0
	Ribosome biogenesis in eukaryotes	0	0	0	0	0	0	1	0
	RNA degradation	0	0	0	0	1	0	0	0
	Ubiquitin mediated proteolysis	0	0	0	0	1	0	0	0

Table 26. Differentially expressed transcripts found mutually expressed between different mussel groups within pairwise comparisons (MW = March Water; StM = St. Mary's Bay; A = adult; S, = seed). Fold change (FC) is shown for each comparison.

Transcript	Sequence Ontology	Function/ Pathway	FC 1	FC 2
	1% vs 5%:		**MW S**	**StM S**
mussels_DN649579_c1_g2_i17	Ganglioside GM2 activator	Lysosome	7.7	6.5
	1% vs 5%:		**StM A**	**StM S**
mussels_DN638984_c4_g3_i2	Countin-3-like isoform X1	Unknown	6.4	6.0
	1% vs 10%:		**MW A**	**StM A**
mussels_DN662906_c0_g3_i2	steroid 17-alpha-hydroxylase/17,20 lyase-like	Metabolism	3.1	3.0

Table 27. Functions/pathway of transcripts found differentially expressed from the March Water adult (MW A) through different pairwise comparisons. FC = Fold change

Transcript	Sequence Ontology	Function/ Pathway	DESeq2 FC
	1% vs 5%		
mussels_DN702217_c2_g1_i6	Copper/zinc superoxide dismutase	Antioxidant	2.0
mussels_DN507775_c1_g1_i1	Heat shock 70 kDa protein 12A-like isoform X1	Chaperone	2.1
mussels_DN680041_c9_g1_i4	Solute carrier family 13 (sodium-dependent dicarboxylate transporter), member 2/3/5	Ion transport	4.3
mussels_DN680041_c9_g1_i3	Solute carrier family 13 (sodium-dependent dicarboxylate transporter), member 2/3/5	Ion transport	3.5
mussels_DN700337_c5_g1_i4	P2X purinoceptor 7	Ligand gated ion channel	3.0
mussels_DN660699_c5_g2_i4	Vacuolar protein sorting-associated protein 52	Lysosome	7.1
mussels_DN700114_c14_g2_i3	Membrane 1-like metallo-endopeptidase-like	Membrane	4.1
mussels_DN644775_c6_g2_i4	Membrane 1-like metallo-endopeptidase-like	Membrane	3.5
mussels_DN687709_c0_g1_i4	Arginine kinase	Metabolism	5.3
mussels_DN696656_c10_g1_i6	Fatty-acyl-CoA synthase	Metabolism	3.2
mussels_DN701631_c11_g1_i2	mRNA export factor	Protein turnover	4.1

Transcript	Sequence Ontology	Function/ Pathway	DESeq2 FC
mussels_DN661506_c10_g1_i2	mRNA export factor	Protein turnover	3.6
mussels_DN671123_c6_g2_i1	40S ribosomal protein S2	Protein turnover	2.7
mussels_DN643857_c6_g2_i2	Receptor-type t tyrosine-protein phosphatase	Signal transduction	4.2
mussels_DN698876_c8_g1_i1	Receptor-type t tyrosine-protein phosphatase	Signal transduction	3.8
mussels_DN700839_c0_g1_i1	Receptor-type t tyrosine-protein phosphatase	Signal transduction	3.6
mussels_DN685524_c2_g2_i1	Cathepsin L1-like	Autophagy	-3.1
mussels_DN699339_c0_g1_i1	Kinesin-like protein KIF23 isoform X2	Cell division	-3.8
mussels_DN697493_c3_g1_i2	Kinesin-like protein KIFC3 isoform X1	Cell division	-5.9
mussels_DN677672_c1_g1_i1	Rhomboid domain-containing protein 1	Cell growth	-5.9
mussels_DN548948_c0_g1_i9	Sialate O-acetylesterase	Immune	-5.0
mussels_DN671799_c2_g3_i7	Multidrug resistance-associated protein 1-like	Immune	-6.0
mussels_DN610186_c1_g1_i9	Macrophage migration inhibitory factor-like protein	Immune	-6.1
mussels_DN551758_c0_g1_i1	Tripartite motif-containing protein 45-like	Immune	-6.4
mussels_DN702651_c1_g1_i2	Nuclear pore complex protein Nup98-Nup96	Immune	-5.9
mussels_DN636434_c0_g2_i5	Myticalin D2	Immune	-6.9
mussels_DN695084_c0_g4_i2	Voltage-gated hydrogen channel 1-like	Ion transport	-5.7
mussels_DN704182_c4_g1_i2	Piezo-type mechanosensitive ion channel component 1-like isoform X1	Ion transport	-5.6
mussels_DN628601_c0_g2_i6	Niemann-Pick C2 protein	Lysosome	-6.9
mussels_DN684374_c2_g1_i4	Transmembrane protein 147	Membrane	-2.9
mussels_DN697589_c1_g1_i14	Protein unc-13 A/B/C	Membrane trafficking	-5.5
mussels_DN689662_c1_g1_i7	Methylthioribose-1-phosphate isomerase	Metabolism	-5.8

Transcript	Sequence Ontology	Function/ Pathway	DESeq2 FC
mussels_DN585180_c0_g1_i1	Phosphomevalonate kinase	Metabolism	-5.7
mussels_DN696754_c4_g2_i4	Phosphoethanolamine N-methyltransferase-like isoform X1	Metabolism	-6.4
mussels_DN607850_c5_g1_i1	Ubiquitin-conjugating enzyme E2 D	Protein turnover	-3.5
mussels_DN698297_c2_g1_i1	Protein lin-28	Protein turnover	-4.7
mussels_DN626634_c1_g1_i2	Phosphatidylinositol phosphatase PTPRQ	Regulation of survival and proliferation	-5.8
mussels_DN636387_c0_g1_i2	Lipopolysaccharide-induced tumor necrosis factor-alpha factor homolog	Stress response/ immune	-5.4
mussels_DN695594_c2_g1_i3	Ral GTPase-activating protein subunit alpha-1	Transcription	-6.2
	1% vs 10%		
mussels_DN633309_c0_g1_i3	Cathepsin L	Autophagy	6.2
mussels_DN687270_c1_g1_i1	cancer susceptibility candidate protein 1	Cilia movement	4.4
mussels_DN701046_c10_g2_i8	dynein assembly factor 2, axonemal	Cilia movement	4.2
mussels_DN680058_c1_g1_i1	dynein heavy chain, axonemal	Cilia movement	4.1
mussels_DN703469_c1_g1_i2	Tetratricopeptide repeat protein 17	Cilliagenesis	6.8
mussels_DN694858_c1_g1_i8	CD220	Immune	2.6
mussels_DN647154_c0_g1_i2	Mannose receptor, C type	Immune	5.2
mussels_DN675256_c0_g3_i1	Sodium/potassium/calcium exchanger 3-like isoform X1	Ion channel	7.4
mussels_DN576252_c1_g1_i1	FAM38	Ion channel	7.2
mussels_DN680553_c3_g1_i1	TWiK family of potassium channels protein 18-like isoform X3	Ion channel	5.5
mussels_DN625141_c3_g2_i1	MFS transporter, OCT family, solute carrier family 22 (organic cation transporter), member 4/5	Ion channel	4.1
mussels_DN646402_c0_g4_i3	AGA (aspartylglucosaminidase)	Lysosome	4.8
mussels_DN585136_c2_g1_i2	Protein unc-13 A/B/C	Lysosome	4.2
mussels_DN696683_c2_g1_i5	Transmembrane protein 272-like	Membrane	3.3
mussels_DN675892_c7_g1_i3	Fatty-acyl-CoA synthase	Metabolism	7.3
mussels_DN557424_c0_g1_i1	Lysine-specific demethylase PHF8	Metabolism	6.8
mussels_DN669585_c1_g3_i2	Cytochrome c oxidase subunit I	Metabolism	6.7
mussels_DN593628_c0_g2_i2	NADH dehydrogenase subunit 1	Metabolism	6.6
mussels_DN603778_c0_g4_i2	ATP synthase F0 subunit 8	Metabolism	6.2
mussels_DN516426_c1_g1_i2	NADH dehydrogenase subunit 6	Metabolism	6.0

Transcript	Sequence Ontology	Function/ Pathway	DESeq2 FC
mussels_DN699338_c5_g1_i1	NADPH-dependent diflavin oxidoreductase 1	Metabolism	5.4
mussels_DN703735_c2_g1_i1	Adenine nucleotide translocator	Metabolism	5.3
mussels_DN687911_c2_g1_i8	Ubiquinol-cytochrome c reductase subunit 8	Metabolism	3.3
mussels_DN616057_c5_g2_i2	Eukaryotic translation initiation factor 2C	Protein turnover	4.2
mussels_DN689428_c0_g1_i1	Large subunit ribosomal protein L31e	Protein turnover	3.2
mussels_DN597831_c7_g1_i3	Translation initiation factor 4E	Protein turnover	6.9
mussels_DN588014_c2_g2_i5	Receptor-type t tyrosine-protein phosphatase	Sonic hedgehog signalling	4.7
mussels_DN704153_c3_g1_i1	Segment polarity protein dishevelled	Wnt signalling	2.8
mussels_DN612948_c2_g1_i1	Zinc finger BED domain-containing protein 1-like	Zinc homeostasis	7.3
mussels_DN695103_c1_g1_i3	Heat shock 70 kDa protein 12A-like	Chaperone	-6.4
mussels_DN566296_c0_g1_i1	Chymotrypsin-like serine proteinase	Digestive enzyme	-6.9
mussels_DN661550_c0_g3_i2	C-Maf-inducing protein	Immune	-5.2
mussels_DN636434_c0_g2_i3	Myticalin D6	Immune	-7.2
mussels_DN611773_c0_g1_i1	NPC intracellular cholesterol transporter 2-like	Lysosome	-7.8
mussels_DN641084_c0_g3_i1	Niemann-Pick C2 protein	Lysosome	-6.5
mussels_DN682818_c2_g7_i1	Transmembrane protein 104 homolog	Membrane	-2.5
mussels_DN608981_c0_g1_i3	Transmembrane protein 104 homolog	Membrane	-2.5
mussels_DN700552_c3_g1_i3	Glycerol-3-phosphate dehydrogenase [NAD(+)], cytoplasmic-like	Metabolism	-1.5
mussels_DN688583_c0_g1_i2	Spermidine synthase-like	Metabolism	-2.4
mussels_DN694683_c2_g2_i2	Nitric oxide synthase, brain-like isoform X1	Metabolism	-2.7
mussels_DN688427_c1_g4_i2	Allene oxide synthase-lipoxygenase protein-like isoform X3	Metabolism	-4.1
mussels_DN664384_c0_g3_i3	Gamma-butyrobetaine dioxygenase-like isoform X3	Metabolism	-4.2
mussels_DN677930_c0_g1_i1	Phenylalanine--tRNA ligase alpha subunit-like	Metabolism	-4.5
mussels_DN693094_c1_g1_i7	Probable phospholipid-transporting ATPase IF isoform X7	Metabolism	-4.7
mussels_DN620097_c4_g7_i1	MINPP1 (Multiple Inositol-Polyphosphate Phosphatase 1)	Metabolism	-4.8

Transcript	Sequence Ontology	Function/ Pathway	DESeq2 FC
mussels_DN649060_c0_g1_i2	Acyl-CoA-binding domain-containing protein 6	Metabolism	-7.0
mussels_DN689904_c3_g5_i1	SDR16C5 (Short Chain Dehydrogenase/Reductase Family 16C Member 5)	Metabolism	-7.7
mussels_DN654430_c0_g2_i1	ER lumen protein-retaining receptor 2 isoform X2	Protein turnover	-1.5
mussels_DN692085_c1_g2_i1	Protein disulfide isomerase family A, member 3	Protein turnover	-1.8
mussels_DN678983_c1_g4_i1	Peptidyl-prolyl cis-trans isomerase FKBP2-like	Protein turnover	-2.0
mussels_DN673643_c10_g3_i2	Protein disulfide-isomerase A3-like	Protein turnover	-2.4
mussels_DN591502_c0_g1_i1	Protein disulfide-isomerase A4-like	Protein turnover	-2.4
mussels_DN622369_c3_g3_i3	Protein O-mannosyl-transferase 1-like	Protein turnover	-4.5
mussels_DN699194_c2_g1_i4	Kyphoscoliosis peptidase	Protein turnover	-5.6
mussels_DN674192_c2_g1_i4	dnaJ homolog subfamily C member 5-like	Protein turnover	-5.8
mussels_DN601446_c5_g1_i3	Probable ribosome biogenesis protein RLP24	Protein turnover	-7.0
mussels_DN698451_c7_g2_i1	28S ribosomal protein S29, mitochondrial-like	Protein turnover	-5.3
mussels_DN677932_c0_g3_i2	60S ribosomal protein L36-like	Protein turnover	-6.0
mussels_DN697847_c1_g1_i1	Vacuolar protein sorting-associated protein 41 homolog	Vacuole	-1.3
mussels_DN687880_c1_g1_i4	Serine/threonine-protein phosphatase 2B catalytic subunit	Wnt signalling	-6.8

Table 28. Functions/pathway of transcripts found differentially expressed from the St. Mary's Bay adult (StM A) through different pairwise comparisons. FC = Fold change

Transcript	Sequence Ontology	Function/ Pathway	DESeq2 FC
1% vs 5%			
mussels_DN641299_c2_g1_i5	Transforming growth factor-beta-induced protein ig-h3-like	Growth	6.8
mussels_DN664600_c0_g1_i2	Splicing factor, arginine/serine-rich 12	Protein turnover	5.4
mussels_DN664600_c0_g1_i10	Splicing factor, arginine/serine-rich 12	Protein turnover	4.9

Transcript	Sequence Ontology	Function/ Pathway	DESeq2 FC
mussels_DN682895_c4_g3_i4	PLXNA	Signaling	6.1
mussels_DN691866_c2_g1_i1	Axin-1-like	Wnt signaling pathway	9.8
mussels_DN664433_c0_g1_i4	Caspase 8	Apoptosis	-9.4
mussels_DN604761_c0_g3_i4	Complement C1q tumor necrosis factor-related protein 6	Immune	-7.2
mussels_DN640390_c1_g2_i2	Mytilin B precursor	Immune	-9.0
mussels_DN661783_c1_g2_i4	Ganglioside GM2 activator-like	Lysosomes	-6.6
mussels_DN699247_c0_g2_i5	F-BAR domain only protein	Membranes	-7.3
mussels_DN646604_c0_g1_i2	Calmodulin	Phosphatidylinositol signaling system	-6.5
mussels_DN697291_c1_g3_i3	Nascent polypeptide-associated complex subunit alpha	Protein turnover	-4.9
mussels_DN675362_c0_g1_i11	Zinc transporter ZIP10-like	Zinc homeostasis	-6.6
	1% vs 10%		
mussels_DN643288_c2_g1_i4	Arthropod defensin-like 1	Immune	9.0
mussels_DN698288_c5_g1_i6	Phosphoinositide 3-kinase adapter protein 1	(PI3K)-Akt signaling pathway	6.7
mussels_DN597033_c2_g1_i1	Phospholipase D3-like	Metabolism	6.7
mussels_DN697918_c0_g1_i3	Regulating synaptic membrane exocytosis protein 2	Protein transport	6.1
mussels_DN611570_c0_g1_i1	Myticin B precursor	Immune	-7.3
mussels_DN661783_c1_g2_i2	Ganglioside GM2 activator	Lysosome	-6.8
mussels_DN671833_c0_g1_i3	Endoplasmic reticulum resident protein 29-like	Protein turnover	-1.9
mussels_DN625549_c0_g1_i4	39S ribosomal protein L53, mitochondrial-like	Ribosome	-7.4
mussels_DN703728_c2_g1_i3	Low-density lipoprotein receptor-related protein 4	Signalling	-7.2

Table 29. Functions/pathway of transcripts found differentially expressed from the March Water seed (MW S) through different pairwise comparisons. FC = Fold change

Transcript	Sequence Ontology	Function/ Pathway	DESeq2 FC
	1% vs 5%		
mussels_DN670701_c2_g1_i3	Peroxidasin homolog	Antioxidant	6.6
mussels_DN498940_c0_g1_i1	Cu+-exporting ATPase	Antioxidant	2.6
mussels_DN618186_c1_g4_i1	Myticalin C2	Immune	8.8
mussels_DN615958_c7_g2_i2	Membrane 1-like metallo-endopeptidase-like	Membrane	6.9
mussels_DN676150_c0_g1_i5	Urocanate hydratase-like	Metabolism	6.8
mussels_DN682394_c0_g1_i2	Histidine ammonia-lyase	Metabolism	6.7
mussels_DN680604_c0_g2_i2	DNA damage-regulated autophagy modulator protein 2-like isoform	Protein turnover	6.0
mussels_DN672824_c1_g1_i5	GTPase HRas	Signaling (FoxO, mTOR)	5.9
mussels_DN638962_c0_g1_i6	U6 snRNA-associated Sm-like protein LSm6	Spliceosome	6.6
mussels_DN685252_c1_g4_i5	Brain protein I3-like	Stress	6.6
mussels_DN608667_c1_g1_i1	Collagen-like protein 2	Structural	5.2
mussels_DN688182_c0_g1_i1	peroxidase-like protein	Antioxidant	-3.3
mussels_DN688182_c0_g2_i3	peroxidase-like protein	Antioxidant	-3.5
mussels_DN600692_c1_g7_i1	GTPase IMAP family member 4-like	Apoptosis	-7.4
mussels_DN668318_c1_g2_i1	cyclin A	Cell cycle	-4.0
mussels_DN704233_c1_g1_i1	Dynein heavy chain, axonemal	Cilia	-6.7
mussels_DN687629_c1_g1_i5	EGF-like repeat and discoidin I-like domain-containing protein 3	Growth	-6.4
mussels_DN612679_c4_g2_i3	Fibrinogen-related protein	Immune	-6.1
mussels_DN623169_c0_g1_i1	Ganglioside GM2 activator-like	Lysosome	-7.8
mussels_DN698539_c2_g1_i1	Dihydrolipoyllysine-residue acetyltransferase component of pyruvate dehydrogenase complex, mitochondrial-like	Metabolism	-5.7
mussels_DN400342_c0_g1_i1	Cytoplasmic FMR1 interacting protein	Protein turnover	-5.1

Transcript	Sequence Ontology	Function/ Pathway	DESeq2 FC
mussels_DN646433_c2_g1_i3	telomeric repeat-binding factor 2-interacting protein 1	Represses transcription	-3.7
mussels_DN681234_c0_g2_i2	Plexin domain-containing protein 1-like isoform X4	Signaling	-5.9
	1% vs 10%		
mussels_DN682018_c4_g2_i3	Cathepsin L	Autophagy	5.7
mussels_DN687575_c1_g1_i7	Heat shock protein 70	Chaperone	5.4
mussels_DN692097_c3_g2_i3	Alpha-amylase	Digestive enzyme	5.7
mussels_DN667704_c4_g2_i3	Cholecystokinin A receptor	Digestive enzyme secretion	5.5
mussels_DN583041_c0_g1_i10	Fos-related antigen 1-like isoform X2	Immune system	3.7
mussels_DN649579_c1_g2_i17	Ganglioside GM2 activator-like	Lysosome	7.7
mussels_DN688905_c1_g1_i3	Regulation of nuclear pre-mRNA domain-containing protein 1B-like	Protein turnover	3.6
mussels_DN703450_c2_g1_i2	CDC-like kinase	Spliceosome	6.6
mussels_DN671412_c0_g1_i2	Peroxiredoxin 6	antioxidant	-6.6
mussels_DN653823_c1_g1_i6	Complement C1q-like protein 4	Immune	-5.9
mussels_DN646531_c0_g2_i3	Perlucin-like protein	Immune	-6.9
mussels_DN695618_c3_g1_i3	Eas-related protein Rab-11B-like	Protein turnover	-5.0

Table 30. Functions/pathway of transcripts found differentially expressed from the St. Mary's Bay seed (StM S) through different pairwise comparisons. FC = Fold change

Transcript	Sequence ontology	Function/ Pathway	DESeq2 FC
	1% vs 5%		
mussels_DN677028_c2_g1_i5	Myticin C	Immune	7.8
mussels_DN611570_c0_g1_i1	Myticin B precursor	Immune	7.5
mussels_DN646531_c0_g2_i3	Perlucin-like protein	Immune	6.1
mussels_DN678111_c0_g2_i4	dynein light chain Tctex-type 1	Cilia	5.1
mussels_DN645663_c0_g1_i1	Trypsin, partial	Digestive enzyme	6.41

Transcript	Sequence ontology	Function/ Pathway	DESeq2 FC
mussels_DN664384_c0_g1_i4	Gamma-butyrobetaine dioxygenase-like isoform X3	Metabolism	6.0
mussels_DN651225_c0_g2_i1	Prohibitin 2	Mitchondrial	5.7
mussels_DN644993_c2_g3_i5	28S ribosomal protein S14, mitochondrial-like	Protein turnover	7.6
mussels_DN672211_c3_g1_i5	Transcriptional activator GLI3-like	Protein turnover	7.3
mussels_DN675086_c1_g1_i5	Elongation factor-1a	Protein turnover	7.0
mussels_DN675086_c4_g3_i1	Elongation factor 1 alpha	Protein turnover	6.9
mussels_DN644993_c2_g3_i1	28S ribosomal protein S14, mitochondrial-like	Protein turnover	5.1
mussels_DN671458_c3_g2_i1	Cysteine/serine-rich nuclear protein 3-like	Apoptosis	-1.7
mussels_DN653823_c1_g1_i6	Complement C1q-like protein 4	Immune	-5.7
mussels_DN663848_c4_g2_i1	Complement component 1, q subcomponent	Immune	-6.1
mussels_DN612679_c4_g2_i3	Fibrinogen-related protein	Immune	-7.3
mussels_DN681586_c5_g5_i2	EHD1	Membrane	-3.8
mussels_DN686093_c1_g1_i2	PRKCA-binding protein	Membrane	-6.2
mussels_DN693272_c3_g5_i3	Prohibitin 2	Mitophagy	-1.8
mussels_DN675281_c0_g4_i2	tRNA pseudouridine synthase Pus10 isoform X2	Protein turnover	-1.8
mussels_DN632388_c1_g2_i3	Vesicle transport protein USE1-like	Protein turnover	-2.0
mussels_DN670354_c1_g1_i4	39S ribosomal protein L4, mitochondrial-like	Protein turnover	-3.4
	1% vs 10%		
mussels_DN641044_c0_g1_i1	Beta,beta-carotene 15,15'-dioxygenase-like	Antioxidant	5.5
mussels_DN600406_c2_g1_i2	Caveolin 3	Endocytosis	2.2
mussels_DN683779_c3_g2_i5	Protein patched homolog 1-like	Hedghog pathway	6.2
mussels_DN652509_c1_g6_i1	Big defensin 1	Immune	8.8
mussels_DN687617_c0_g1_i9	Fibrinogen-related protein	Immune	7.0

Transcript	Sequence ontology	Function/ Pathway	DESeq2 FC
mussels_DN677846_c0_g1_i3	Lysosomal-associated membrane protein 1/2	Lysosomes	6.7
mussels_DN693047_c4_g1_i3	Galactosylgalactosylxylosylprotein 3-beta-glucuronosyltransferase 3-like	Metabolism	6.1
mussels_DN673456_c0_g1_i10	Metalloproteinase inhibitor 3	Antioxidant	-7.2
mussels_DN639444_c1_g1_i1	227 kDa spindle- and centromere-associated protein-like	Cell division	-5.7
mussels_DN673688_c1_g4_i9	Trans-L-3-hydroxyproline dehydratase-like	Digestive	-6.3
mussels_DN693102_c3_g1_i3	Integrin alpha-4-like isoform X1	ECM-receptor interaction	-6.3
mussels_DN689683_c1_g2_i5	Nuclear receptor coactivator 4-like	Immune	-5.9
mussels_DN689683_c1_g2_i4	Nuclear receptor coactivator 4	Immune	-6.1
mussels_DN474678_c0_g1_i1	Galectin-4 isoform X1	Immune	-6.2
mussels_DN681288_c1_g1_i7	Ileal sodium/bile acid cotransporter-like	Ion channel	-6.8
mussels_DN686133_c6_g1_i3	Transmembrane protein 189	Metabolism	-1.8
mussels_DN684435_c0_g2_i1	Multifunctional protein ADE2-like	Metabolism	-3.7
mussels_DN680994_c6_g2_i1	Phosphatidylcholine protein transfer	Metabolism	-5.1
mussels_DN655139_c0_g1_i6	Betaine--homocysteine S-methyltransferase 1-like	Metabolism	-7.0
mussels_DN703044_c2_g1_i4	MAP kinase-activating death domain protein	Metabolism	-7.3
mussels_DN598544_c7_g1_i1	Probable ATP-dependent RNA helicase DDX41	Protein turnover	-4.8
mussels_DN648813_c1_g1_i1	Tyrosyl-DNA phosphodiesterase 2	Protein turnover	-6.7
mussels_DN641964_c1_g2_i11	SNW domain-containing protein 1	Spliceosome	-3.5

Table 31. Differentially expressed transcripts found mutually expressed within two different pairwise comparisons within one mussel group (MW = March Water; StM = St. Mary's Bay; A = adult; S, = seed). Fold change (FC) is shown for each comparison.

Transcript	Sequence Ontology	Function/ Pathway	FC 1	FC 2
Mutual between MW A:			**1 vs 5**	**1 vs 10**
mussels_DN704237_c17_g1_i4	Copper/zinc superoxide dismutase	Antioxidant	3.6	3.2
mussels_DN649471_c6_g1_i1	Copper/zinc superoxide dismutase	Antioxidant	2.9	2.9
mussels_DN704237_c17_g1_i1	Copper/zinc superoxide dismutase	Antioxidant	2.1	2.0
mussels_DN530363_c0_g1_i1	Senescence-associated protein	Cell cycle progression	5.1	5.1
mussels_DN654456_c7_g1_i4	Dynein assembly factor 2, axonemal	Cilia	1.8	1.7
mussels_DN688232_c12_g1_i1	Fyve phosphoinositide finger-containing	Cytoskeleton regulation	4.7	3.5
mussels_DN628525_c3_g1_i1	Thyrostimulin beta-5 subunit	Hormonal	3.9	3.3
mussels_DN632356_c3_g3_i2	P2X purinoceptor 7	Ion channel	4.5	4.0
mussels_DN680041_c9_g1_i7	Solute carrier family 13 (sodium-dependent dicarboxylate transporter), member 2/3/5	Ion transport	4.8	4.2
mussels_DN646473_c0_g1_i3	NADH dehydrogenase subunit 2	Metabolism	5.5	6.9
mussels_DN663824_c5_g5_i1	Fatty-acyl-CoA synthase	Metabolism	2.9	2.7
mussels_DN677531_c2_g2_i1	Peptidyl-prolyl cis-trans isomerase B-like	Chaperone activity	-6.2	-6.2
mussels_DN652539_c0_g1_i2	Macrophage migration inhibitory factor	Immune	-6.3	-6.1
mussels_DN698697_c3_g1_i4	NADP-dependent malic enzyme-like isoform X1	Metabolism	-6.1	-6.6
mussels_DN674530_c0_g2_i1	Distal membrane-arm assembly complex protein 2	mitochondrial	-6.6	-7.3
mussels_DN679433_c1_g1_i3	V-type proton ATPase catalytic subunit A	mTOR	-1.1	-1.6
mussels_DN692085_c1_g3_i2	Protein disulfide-isomerase A3-like	Protein turnover	-1.8	-2.4
mussels_DN673643_c10_g4_i1	Protein disulfide isomerase family A, member 3	Protein turnover	-2.0	-2.6

Transcript	Sequence Ontology	Function/ Pathway	FC 1	FC 2
mussels_DN698786_c3_g1_i6	Cotranscriptional regulator FAM172A isoform X2	Transcription	-6.0	-5.8
mussels_DN589309_c6_g1_i2	Nuclear factor interleukin-3-regulated protein-like	Transcription	-7.5	-7.0
mussels_DN657130_c0_g1_i5	TTF2	Transcription	6.7	5.9
mussels_DN664384_c0_g1_i4	Gamma-butyrobetaine dioxygenase-like isoform X3	Transport of fatty acids	-4.9	-6.5
Mutual between StM A:			**1 vs 5**	**1 vs 10**
mussels_DN693658_c3_g2_i2	next to BRCA1 gene 1 protein-like	Autophagy	-7.6	-7.3
Mutual between MW S:			**1 vs 5**	**1 vs 10**
mussels_DN702678_c2_g3_i1	Nucleobindin	Calcium homeostasis	-5.9	-5.5
mussels_DN677352_c2_g1_i1	Myticin C	Immune	-6.2	-6.2
mussels_DN628039_c1_g1_i6	C-type lectin 8	Immune	-6.3	-6.2
mussels_DN683350_c0_g1_i7	Protein O-glucosyltransferase 1-like	Metabolism	-5.5	-5.0
mussels_DN690397_c1_g1_i4	Isocitrate dehydrogenase	Metabolism	-6.1	-6.8
mussels_DN690207_c2_g2_i6	Aldehyde dehydrogenase, mitochondrial-like	Metabolism	-7.2	-7.6
mussels_DN694799_c4_g2_i3	collagen, type VI, alpha	Structural	-6.2	-6.2

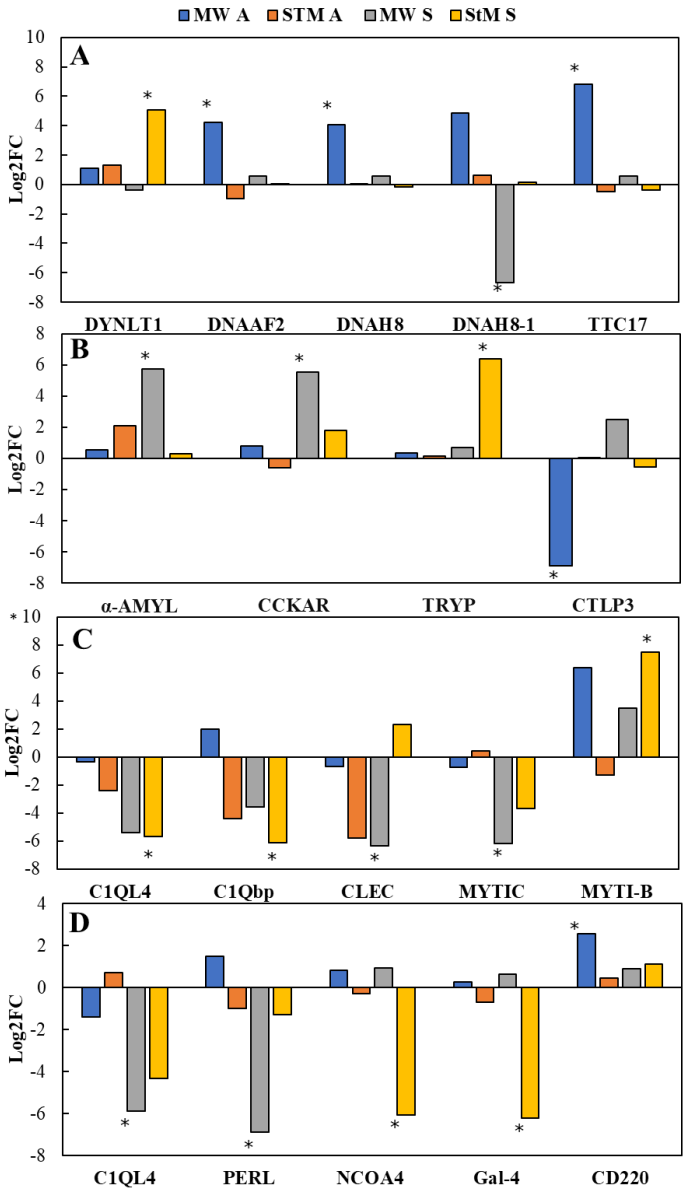

Figure 22. Subset of differentially expressed transcripts plotted using their subsequent Log_2 Fold change for each pairwise comparison. Plots are associated with (A) cilia; (B) digestive enzymes, (C) immune (1% vs 5%) and (D) immune (1% vs 10%). (MW = March Water; StM = St. Mary's Bay; A = adult; S = seed. Asterisk (*) indicates the mussel group that it was found significant. DYNLT1 = Dynein light chain Tctex-type 1; DNAAF2 = Dynein assembly factor 2, axonemal; DNAH8 = Dynein heavy chain, axonemal; DNAH8-1 = Dynein heavy chain, axonemal (1); TTC17 = Tetratricopeptide repeat protein 17; α-AMYL = Alpha-amylase; CCKAR = Cholecystokinin A receptor; TRYP = Trypsin, partial; CTLP3 = Chymotrypsin-like serine proteinase; C1QL4 = Complement C1q-like protein 4; C1Qbp = Complement component 1, q subcomponent; CLEC = C-type lectin 8; MYTIC = Myticin C; MYTI-B = Myticin B precursor; C1QL4 = Complement C1q-like protein 4; PERL = Perlucin-like protein; NCOA4 = Nuclear receptor coactivator 4; Gal-4 = Galectin-4 isoform X1; CD220 = CD220.

4.4 Discussion

4.4.1 Physiological and transcriptomic response to food availability

This study aimed to better understand acute transcriptomic and physiological responses to changes in food availability. Three food rations were fed to mussels over a 48 h period. It was hypothesized that the 5% ration would be an optimal level of feed as described by (Connor et al. 2016) in *M. californianus.* The 1% ration was hypothesized to be potentially below maintenance ration in mussels (Thompson and Bayne 1974; Winter and Langton 1975), while 10% might be too high and result in stress from overloading the gills or digestive tract (Pascoe et al. 2009; Riisgård et al. 2011). However, the results of this study do not support this hypothesis. This study used heart rate and lysosomal destabilization to measure the physiological responses of different food rations on mussels. Overall, the heart rate and lysosomal destabilization were not significantly different between food rations (1%, 5%, 10%). Mean heart rate was found to significantly increase in the first 32 h; however, after this point the heart rate declined until the end of the 48 h trial. Widdows (1973b) studied the heart rate in *M. edulis* in relation to food availability over a 28-day period and found that during starvation, heart rate declined to ~ 14 BPM which coincided with lower oxygen consumption. When mussels were fed, heart rate increased to ~ 22 BPM, which resulted in increases in oxygen consumption and was considered to be "active metabolism" (Widdows 1973b). Thompson and Bayne (1972) found similar findings in *M. edulis* but also found that oxygen consumption eventually declined from "active metabolism" to "routine metabolism" after five days of continuous feeding. Therefore, in the present study, the increase in heart rate, followed by the decline in heart rate after 32 h may indicate adult mussels might have been in an active metabolism state but gradually declined towards routine metabolism. Therefore, this indicates that the 1% and 10% rations were not extreme enough to result in a physiological response or more time would be required to visualize this. In addition, pairwise comparisons between 10% vs 5% rations resulted in the fewest differentially expressed transcripts being identified indicating that mussels in these rations had a transcriptomic response more similar compared to the mussels in the 1% ration.

4.4.2 Transcripts associated with metabolism

In all mussel groups, KEGG pathway assignment resulted in more under-expressed transcripts associated with metabolism in pairwise comparisons 1% vs 5% and 1% vs 10%, indicating that there were less metabolic pathways over-expressed in the 1% ration compared to 5% and 10%. This may indicate that the 5% and 10% ration, was resulting in a higher level of energy acquisition without having to significantly change their physiology (i.e. heart rate), and as a result could indicate an opportunistic higher energy acquisition for the mussels in higher food rations. Metabolic pathways over-expressed in the 1% ration were mostly related to lipid metabolism, amino acid metabolism and oxidative phosphorylation. Lipid and protein metabolism in bivalves experiencing low food availability or starvation has been found in other bivalves as well (Roznere et al. 2014; Haider et al. 2020b), and therefore could indicate that the metabolic strategy was different between mussels in the 1% vs 5% and 10% ration. March Water adults had over-expression of a transcript identified as senescence-associated protein in the 1% ration in both pairwise comparison. Senescence-associated proteins are associated with cell cycle arrest in vertebrates, which can be triggered through aging signals or stress (Frey et al. 2018). While the role it plays in bivalves is not known, its expression in the current study could indicate a role in cell cycle arrest to conserve energy.

4.4.3 Transcripts associated with immune response

In all mussel groups, there were transcripts differentially expressed associated with the immune system. In the March Water mussel group (adult, seed) there was a trend of more transcripts under-expressed associated with the immune system in the 1% ration, indicating that many immune transcripts were over-expressed at higher food rations. In addition, Figure 22C,D shows transcripts associated with the immune system between mussel groups. Each of the immune related transcript displayed in Figure 22 was only differentially expressed in one mussel group; however, most were showing the same fold change direction in several mussel groups, particularly under-expressed within the 1% ration. This is an interesting finding, and there are several reasons why this could have occurred. Bivalves are filter feeding organisms and as a result their gills and

gastrointestinal tract can accumulate bacteria, parasites and viruses (Song et al. 2010; Allam and Pales Espinosa 2016). If the mussels in the 5% and 10% rations are sensing more feed and particles in their environment, it may trigger an increase the production of immune transcripts as a protection mechanism, as the immune system and feeding behaviour may be interconnected, with some hypothesis' suggesting a common origin (Broderick 2015). One parallel between the immune system and feeding is mucous. Mucous lines the gills and gastrointestinal tract of bivalves (Garcia-Garcia et al. 2013) and has multiple roles including acting as a barrier, aiding in immune response, and also plays an important role in feeding (Pales Espinosa and Allam 2013b; Pales Espinosa et al. 2016; Allam and Pales Espinosa 2016). In connection to feeding, there are many reasons for mucus production, including the ability to aid in particle capture and movement from the gills into the mouth and through the gastrointestinal tract (Jørgensen 1981, 1990, 1996; Nielsen et al. 1993; Riisgård et al. 1996). For example, c-type lectins in mucous on feeding apparatus may play a role in particle capture efficiency in low food availability to maximize the acquisition of more nutritious particles (Pales Espinosa and Allam 2013a, 2018; Allam et al. 2021). In the present study, multiple differentially expressed transcripts were annotated to lectins in different food rations, and therefore may have a role in both the immune system and feeding behaviour. Increases in food availability are also associated with the onset of pseudofaeces, which results in rejection of food particles which are enclosed into mucous strings (Jørgensen 1981, 1990, 1996). Mucous in bivalves has also been found to contain many immune effectors including antimicrobial peptides, lysozymes, lectins and C1q domain containing proteins which aid in immune responses of bivalves (Allam and Pales Espinosa 2016; Yang et al. 2022). Therefore, if the mussels in 5% and 10% rations were interacting with more food particles in their environment, it might be necessary to increase production of mucous, and might also inadvertently increase the production of immune transcripts or vice versa (Chen et al. 2003).

In addition, if the 1% ration is resulting in a lower level of energy acquisition, under-expression of immune transcripts may be related to energy conservation. Other studies on bivalves have found that low food availability can result in a decline in immune effectors (Delaporte et al. 2006; Xu et al. 2008; Parisi et al. 2017). Parisi et al. (2017) found that

food availability resulted in changes to immune function in terms of enzymes (esterase, phosphatase, and phenoloxidase), and that high food availability increased the immune effectors in the mussel *M. galloprovincialis* (Parisi et al. 2017). Unfortunately, climate change is expected to result in increases in pathogenic organisms, while reducing the production of phytoplankton (Vezzulli et al. 2013; Hoegh-Guldberg et al. 2014; Barton et al. 2016; Bernier et al. 2018; Bindoff et al. 2019; Henson et al. 2021). If conditions brought on by climate change simultaneously decrease immune function, mussels may be more susceptible to mortality. Therefore, the under-expression of immune transcripts in the 1% ration warrants future investigation.

4.4.4 Transcripts associated with feeding physiology and digestion

The feeding physiology and behaviour of *M. edulis* is highly plastic, and food availability may drive acclimation to maximize energy acquisition (Foster-Smith 1978; Widdows et al. 1979; Jørgensen 1981b; Jørgensen et al. 1986a, 1986b; Beninger et al. 1999; Honkoop et al. 2003; Capelle et al. 2021). Plasticity in feeding physiology include changes to the gastrointestinal tract, feeding apparatus, food digestion time, efficiency of digestion, etc. (Foster-Smith 1978; Widdows et al. 1979; Jørgensen 1981b; Jørgensen et al. 1986a, 1986b; Beninger et al. 1999; Honkoop et al. 2003; Capelle et al. 2021). The present study found several transcripts associated with feeding physiology that indicated the start of acclimation to the changes in food availability. This study found over-expressed transcripts associated with cilia in several mussel groups (Figure 22A). Cilia is a highly important component of the gills and gastrointestinal tract in mussels, and the over-expression in this study could indicate changes occurring in feeding behaviour or physiology (Jørgensen et al. 1984; Riisgård and Larsen 2001). For example, in the 1% ration, March Water adult and St. Mary's Bay seed both had over-expression of transcripts associated with cilia. In both mussel groups, there was over-expression of transcripts associated with dynein complex (March water adult: dynein assembly factor 2, axonemal; dynein heavy chain, axonemal; St. Mary's Bay seed: dynein light chain Tctex-type 1). Dynein complexes are a highly important component of aiding in cilia movement (Kollmar 2016), and have been found differentially expressed in gills of other molluscs (Valenzuela-Miranda et al. 2015; Prieto et al. 2019). In addition, tetratricopeptide repeat protein 17 was found over-expressed in

March Water adults 1% ration, which has been found associated with ciliagenesis in vertebrates (Hayes et al. 2007; Xu et al. 2015). Over-expression of cilia related transcripts in the 1% ration may indicate that the gills of the mussels were responding to low food availability. It has been found that low food availability may trigger a shut down of gills and filtering behaviour (Winter and Langton 1975; Pascoe et al. 2009); however, results of this study show that the 1% ration was not low enough to result in this shut down. Above a critical value it may trigger a higher filtration rate to maximize food capture, and in long-term low food availability it has been found that physiological changes occur in the gill surface area and reduction of palps to maximize their feeding ability (Honkoop et al. 2003; Capelle et al. 2021). Therefore, the over-expression of these transcripts in the present study might indicate that the mussels were compensating for the low food by changing their gill cilia behaviour or abundance.

The present study also found there were several transcripts associated with lysosomes and digestion. Lysosomes are involved with many cellular processes that involve digestion of both exogenous and endogenous materials (Owen 1972). Digestive cells in bivalves contain a network of lysosomes, which are associated with heterotrophic (exogenous) digestion (Owen 1972). In high food availability an increase in digestive cells and lysosome density may be needed to maintain digestion and increase gut volume (Bayne et al. 1984; Navarro et al. 1992, 2009; Ibarrola et al. 2000), whereas in low food availability more autophagic (endogenous) lysosomes may be needed to catabolize energy stores (Scott et al. 2004).

Several transcripts were also associated with digestive enzymes (Figure 22B). Digestive enzymes in bivalves have an important role in digestion and have been found variable between food rations (Hawkins and Bayne 1992; Fernández-Reiriz et al. 2001; Labarta et al. 2002; Connor et al. 2016). In the March Water adults, a transcript identified as Chymotrypsin-like serine proteinase was over-expressed in the 10% ration. Chymotrypsin proteases have been identified in the digestive gland of scallops (*Pecten maximus*) (Le Chevalier et al. 1995), and has been found to have a role in digestion and immune response (Louati et al. 2011). Other digestive enzymes were over-expressed in the 1% ration in seed mussel groups including alpha-amylase, cholecystokinin A receptor (March Water seed)

and Trypsin, partial (St. Mary's Bay seed). Alpha-amylase and trypsin have both been found to play a role in digestion in bivalves (Hawkins and Bayne 1992; Fernández-Reiriz et al. 2001; Labarta et al. 2002; Connor et al. 2016). The cholecystokinin/sulfakinin signalling system has an important role in regulating feeding behaviour, nutritional status, and energy storage in gonads of oysters (*C. gigas*) (Schwartz et al. 2018). Interestingly, the activation of cholecystokinin/sulfakinin system has been found to play a role in the release of alpha-amylase in scallops (*Pecten maximus*) (Nachman et al. 1997), therefore, the over-expression of Cholecystokinin A receptor in the current study maybe related to the change in food availability and over-expression of alpha-amylase. Most research indicates an increase in digestive enzymes secretion during feeding (Hawkins and Bayne 1992; Nachman et al. 1997; Fernández-Reiriz et al. 2001; Labarta et al. 2002; Schwartz et al. 2018). However, Connor et al. (2016) also found that amylase activity was under-expressed at high food availability (5% BW) compared to low food availability (1%), and was hypothesized that it may be due to dietary requirements being met, resulting in a shutdown of specific digestive enzymes. Therefore, it can be hypothesized that the expression of digestive enzymes in the low food availability indicates the potential need to enhance digestion and optimize energy acquisition.

There were also other transcripts over-expressed associated with ion transport in multiple mussel groups and treatments. The functional role of changes in ion channels in this study is not known, but research has implicated ion channel roles in autophagic processes (Abuammar et al. 2021), membrane potential and hormonal secretion (Perry et al. 2020), which could play a role in feeding and digestive behaviour. In the St. Mary's Bay seed 10% rations, there was over-expression of ileal sodium/bile acid cotransporter. This ion channel transporter has been found in the intestines of vertebrates and is involved in bile salt uptake (Montagnani et al. 2006). Bile in vertebrates has an important role in absorption of fats, vitamins, and cholesterol (Montagnani et al. 2006). In addition, in the adults (March Water, St. Mary's Bay) 10% ration there was an over-expression of two transcripts identified as SLC17A5 and MFS transporter, ACS family, solute carrier family 17. Both transcripts are associated with solute carrier family 17, which are involved with the transport of sialic acid out of lysosomes (Tarailo-Graovac et al. 2017). The production of sialic acid could be

associated with the production of lectins which have implication for both immune and feeding behaviour in bivalves (Tunkijjanukij et al. 1998).

4.4.5 Differences between mussel sites and sizes

This study found that there were major differences in transcriptomics between mussel sizes (adult, seed) and sites (March Water and St. Mary's Bay). There are many reasons why this variability could have occurred. First, mussels were fed a ration based on % dry body weight (1%, 5% and 10%), therefore the calculated ration of food in the adult mussels would be much larger compared to the seed mussels. Tank volume between the adult and seed experiments did not change and therefore the concentration of food in the adult mussel group was much higher than the seed mussel tanks, and this concentration may have contributed to differences in transcriptomic response patterns between the adult and seed mussels. Regardless of this detail, mussels have been found to have differences in physiological responses between different sizes. Smaller mussels are known to put more energy into somatic growth compared to adults and have differences in metabolism, and biochemical makeup (Holland and Spencer 1973; Thompson 1979; Mann and Gallager 1985; Widdows et al. 1989).

Differences may also be associated with environmental variability between the two sites. A recent report on the PEI mussel aquaculture industry compared environmental differences between several locations in PEI (Poirier et al. 2021). This environmental assessment included the March Water site used in this study and Brudenell River, which is in the same watershed as the St. Mary's Bay site. In 2016, 2017, there were differences in chl a between the two sites (Poirier et al. 2021). Overall, March Water experienced earlier and more frequent phytoplankton blooms, compared to Brudenell River (Poirier et al. 2021). In the present study, March Water adults, had many more differentially expressed transcripts, and had a significantly higher lysosomal destabilization index compared to all mussel groups, indicating they were more stressed by the change in food availability. In addition, expression of transcripts associated with cilia and digestive enzymes were unique to the mussel group, indicating that each site and size was having a different response to the food availability. Other studies have also found that site/population can result in feeding

plasticity (Fernández-Reiriz et al. 2001; Strohmeier et al. 2009; Steeves et al. 2020; Capelle et al. 2021). Fernández-Reiriz et al. (2001) found that digestive enzymes activity was highly plastic in mussels (*M. chilensis*) from different populations and habitat, and it was hypothesized that the two origins and habitat may differ in diet conditions and result in different enzyme investment. Strohmeier et al. (2009) found that mussels (*M. edulis)* in long-term low food availability, have adapted to continue to filter at extremely low levels of phytoplankton while still maintaining growth (Strohmeier et al. 2009). In addition, mussels have also been found to adapt to environmental conditions by changing their feeding apparatus such as the gills and labial palps (Capelle et al. 2021). Frequency of exposure to stressful environmental conditions may also result in epigenetic changes that ultimately lead to differences in transcript expression patterns or how quickly a response occurs (Watson et al. 2018). Therefore, differences in spring bloom and environmental conditions between the two sites in the present study may be driving the apparent differences in transcripts with links to feeding and digestion. Furthermore, inter-individual differences between mussels can result in differences in feeding and physiology. A study by Bayne and Hawkins (1997) found that heterozygosity had a large difference in how mussels behaved during different feed rations and these differences resulted from cost associated with protein turnover and deposition in association with growth. Heterozygosity levels has been found to differ between sites in PEI (Tremblay et al. 2011), but it is not known if this could have been a factor in this study. Therefore, the differences found in this study may be related to size, environmental, epigenetics, and genetic factors.

4.5 Conclusions

Overall, this study found that 1% and 10% rations were not extreme enough to result in significant changes in heart rate or lysosomal destabilization. Overall, it appeared that the March Water adults had a stronger response to the differences in food rations. Transcriptomic response indicated that the metabolism and immune systems were under-expressed in the 1% ration compared to the 5% and 10% rations. Under-expression of immune related transcripts in the 1% ration should be further investigated to understand if this could make them more susceptible to pathogen outbreaks. In all mussel groups, changes in transcripts were observed at different food rations associated with cilia, mucosal

transcripts, digestive enzymes. Each mussel group had a different transcriptomic response in terms of transcripts related to feeding and digestion, indicating that site and size might play a role in the responses to food availability. In addition, expression of transcripts associated with feeding and digestion indicates that the acclimation process to different food rations can commence as early as 48 h after an acute change in food availability.

Chapter 5: Marker discovery in the blue mussel (*Mytilus edulis*) associated with hypoxia, hyposalinity and food availability stress.

5.1 Introduction

Anthropogenic climate change is resulting in rapid changes to the aquatic ecosystem that will alter both physical and chemical properties of the ocean (Bindoff et al. 2019). Overall, ocean temperature and acidity are increasing, while dissolved oxygen concentrations are decreasing (Hoegh-Guldberg et al. 2014; Bindoff et al. 2019). Increases in extreme precipitation events are resulting in short-term changes in salinity for coastal ecosystems, while long-term deviations in weather patterns are expected to impact long-term salinity patterns resulting in increased or decreased salinity depending on geographic location (Rhein et al. 2013; Hoegh-Guldberg et al. 2014, 2018). These changing conditions are altering distribution and abundance of primary producers such as phytoplankton, which can impact food availability for filter feeding organisms (Hoegh-Guldberg et al. 2014; Barton et al. 2016).

In Prince Edward Island (PEI), the blue mussel (*Mytilus edulis*) aquaculture industry as of 2020 was responsible for the production of 12,756 mt, which represents ~ 75% of the total production in Canada, valued at ~ $20M (CAD) (Statistics Canada 2021). Global production of shellfish landings is predicted to decline by 42–54%, however, these impact will not be evenly distributed and rather regionally specific (Hicke et al. 2022). Cheung et al. (2010) predicts that fisheries potential will redistribute by 2055, with warmer regions seeing decline in catch potential, while increasing poleward. For example, in the Gulf of St. Lawrence, oysters (*Crassostrea virginica*) and mussels (*M. edulis*) are closer to its historical mid or northern range, which indicates that climate change scenarios may increase production in these regions, due to increases in temperature and growing season (Steeves et al. 2018; Wilson et al. 2020). Yet, increases in production are also highly reliant on food availability which has been modeled to potentially decrease under climate change scenarios in the Gulf of St. Lawrence (Filgueira et al. 2016), and mussels may become more susceptible in terms of reduced growth and mortality during the summer when heat stress is present (Steeves et al. 2018). Moreover, extreme weather events including heat

waves, precipitation events, etc. are predicted to increase in occurrence in climate change scenarios (Bindoff et al. 2019; Seuront et al. 2019), indicating it is likely that mussels will experience episodic stress events in their aquatic ecosystem. While mussels are well adapted to stressful environmental conditions, summer mortality events have been documented for many years in PEI and Gulf of St. Lawrence (Mallet et al. 1990; Myrand et al. 2000; Leblanc et al. 2010; Tremblay et al. 2011). Additionally, Seuront et al. (2019) in mussels (*M. edulis)* found that multiple episodic heat waves during the summer can make mussels more susceptible to mortality, which is concerning under climate change scenarios.

One of the major challenges in protecting mussel health is the lack of visual signs exhibited by mussels to stress or disease. Often the only sign of stress observed is mass mortality, which represents a huge economic loss for the industry. When poor growth and meat yields are observed in mussel production post harvest, the causative reason can often only be speculated. While other indicators are available to assess shellfish health (i.e. neutral red assay) (Hauton et al. 1998; Harding 2003; Harding et al. 2004; Méthé, et al. 2015) most are indicative of general stress and can not identify the causative reason. Therefore, the PEI mussel aquaculture industry identified the need to develop a molecular test to detect environmental stress, to determine causative reasons of underperforming mussel sites that can be used as a tool to aid in aquaculture best practices and prevent mortality.

Many studies have used molecular markers in mussels (*M. edulis*) to monitor impacts of environmental stressors on transcript expression particularly associated with detoxification processes (i.e. Metallothionein, catalase, glutathione-*S*-transferase) and molecular chaperones (heat shock proteins) (i.e. Fitzpatrick et al. 1997; Galloway et al. 2002; Rickwood and Galloway 2004; Bocquené et al. 2004; Leiniö and Lehtonen 2005; Gagné et al. 2008; Al-Subiai et al. 2011; Rola et al. 2012; Magara et al. 2019; Falfushynska et al. 2019; Nielsen et al. 2021). Recently, markers have been developed capable of detecting transcripts involved in inflammatory responses of *M. edulis* in hypoxia including caspases (2, 3, 8), B-cell lymphoma 2 (Bcl-2), Bcl-2-associated X protein (BAX), TGF-β-activated kinase 1, nuclear factor kappa B1(NF-κB), inhibitor of NF-κB kinase subunit α and serine/threonine-protein kinase TBK1-like (Falfushynska et al. 2020). While these

studies are excellent examples of how markers can be used to understand if mussels are experiencing stress from their environment, transcripts associated with detoxification, molecular chaperones, inflammation, etc., may be upregulated in response to a variety of different stimuli. The development of specific molecular markers relies on knowledge of how transcript expression patterns lead to physiological responses. While physiological responses to stress have been studied in mussels (i.e. Bayne 1971, 1972; Bayne et al. 1973, 1981; Shumway 1977; Davenport 1979a, 1979b; Widdows et al. 1979, 1989; Holwerda and De Zwaan 1980; De Zwaan et al. 1982; Hawkins et al. 1993; Clements et al. 2018, 2021), there are still a lot of unknowns about how molecular response to stress leads to observed phenotype. Recent studies have focused on making connections between genotypic and phenotypic responses to stress in mussels (Halpin et al. 2004; Gracey et al. 2008; Lockwood and Somero 2011; Woo et al. 2013; Gracey and Connor 2016; Falfushynska et al. 2020; Barrett et al. 2022). As an additional factor, several studies have found variability of responses to stress in bivalves in relation to season (Leiniö and Lehtonen 2005; Kube et al. 2007; Múgica et al. 2015; Lacroix et al. 2017), individuals (Diehl et al. 1985; Bayne and Hawkins 1997; Bayne 2004; Peck et al. 2015; Collins et al. 2021), sizes/age (Sukhotin et al. 2003; Clark et al. 2013, 2016), and sites/populations (Place et al. 2008; Maynard et al. 2018; Counihan et al. 2019), which indicates these differences can influence how a mussel responds to different stressors.

The previous chapters (2–4) have examined the acute responses to hypoxia, hyposalinity, and food availability in blue mussels to gain an understanding of transcriptomic response associated with each of the stressors. Differences in transcriptomics were also evaluated between two sites in PEI (March Water, St. Mary's Bay) and sizes (adult, seed) to gain an understanding about how these factors impacted expression patterns for each stressor. Overall acute stress responses resulted in rapid changes in transcriptomic response, and differentially expressed transcripts were characterized to determine how they could relate to physiology. Differences in transcriptomic responses in each stressor was confirmed between individuals, sites, and sizes, and were hypothesized to be related to differences in development stage between sizes, and environmental variation between the two sites. Overall, it was concluded in each chapter that differences in site and sizes of mussels must

be taken under consideration when developing a molecular test to ensure that the test is robust. Therefore, the goal of this study was to identify and verify markers that could be used to identify acute stress response associated with hypoxia, hyposalinity and food availability stress in blue mussels of different sizes and sites.

5.2 Materials and methods

5.2.1 Mussel samples and trials

For a detailed overview of mussel samples and trials see chapters 2–4. Blue mussels (*M. edulis*) were collected from two sites in Prince Edward Island (PEI) (March Water, St. Mary's Bay) and two sizes (adult, seed). Three stress trials were completed including: hypoxia, hyposalinity and food availability, which are summarized briefly below:

Hypoxia: The hypoxia stress trial occurred in 4.5 L sealable respirometer chambers (8 total), divided into two groups: control group at dissolved oxygen (O_2) ~ 7–8 mg/L and treatment (hypoxia) at O_2 ~ 2 mg/L. Temperature and salinity were held at 16 °C and 27 ‰. Hypoxia was induced in the treatment group by displacing oxygen by bubbling nitrogen gas for ~ 12 minutes. Two 4 h hypoxia trials were conducted to assess adults, and then to assess seeds. Four mussels from both sites (8 total) were placed in individual baskets in each tank. For detailed methodology see: Chapter 2.

Hyposalinity: A flow-through (120 mL/min) zebra tank (9 L) set-up was used to conduct salinity trials. A total of eight zebra tanks divided into two groups: control at salinity 27 ‰ at 16 °C and treatment (hyposalinity) group at salinity 16 ‰ at 16 °C. Two 6 h salinity trials were conducted, the first using adult mussels and the second using seed mussels. A total of 14 mussels from both sites (28 total) were placed in separate baskets in each tank. For detailed methodology see: Chapter 3.

Food availability: Zebra tank set up was also used in the food availability trial. A total of 12 zebra tanks were set up and divided in to three food rations:1%, 5%, 10% dry body tissue weight (BW) daily ration. Other parameters such as salinity and temperature were kept constant at 16 °C and 27 ‰. Feeding occurred using an automatic dosing machine. Two, 48 h feed availability trials were conducted, the first using adult mussels and then the

second using seed mussels. A total of 14 mussels from both sites (28 total) were placed in separate baskets in each tank. For detailed methodology see: Chapter 4.

5.2.2 Sample preservation, RNA extractions and sequencing

Six mussels per size, site, and treatment were collected for RNA preservation directly following each of the stress trials. Whole mussel tissue was homogenized into RNAlater® solution (Cat. No. 76106, QIAGEN GmbH, Hilden, Germany) using an Omni tissue homogenizer (Omni International, Kennesaw, GA, USA), at a ratio of 1g tissue per 10 mL of RNAlater®. RNA was isolated using Qiagen RNeasy® Mini Kit (Cat. No: 74104, QIAGEN GmbH, Hilden, Germany) following the manufacture protocol. An additional on-column DNase I (Cat. No. 79254, QIAGEN GmbH, Hilden, Germany) treatment was applied during the RNA isolation process, to remove DNA contamination if present. Concentration and quality of RNA was assessed using a Nanodrop spectrophotometer (Thermo Fisher Scientific, Waltham, MA, USA) and Bioanalyzer (Agilent Bioanalyzer, RNA 6000 nano kit, Santa Clara, CA, United States). High quality RNA was shipped to Genome Quebec, Montreal Quebec, Canada to undergo RNA-seq. Before sequencing, Trueseq library preparation was completed on each sample. Then, Hiseq2000 Illumina (sequencing by synthesis) was completed (PE 100), to give a sequencing read depth between 15–20 million reads per sample (eight samples per sequencing lane).

5.2.3 Transcriptome assembly and differential expression analysis

One transcriptome was assembled combining the hypoxia, hyposalinity, and food availability trials. For detailed methodology see: Chapters 2 (2.3.1 *De novo* transcriptome assembly). Differential expression analysis was completed for each trial using two different statistical packages: DESeq2 (Love et al. 2014) and edgeR (Robinson et al. 2010). The use of these two differential expression analysis packages (DESeq2 and edgeR) was completed to ensure that the analysis was robust. In both methods, *p-value* was adjusted to control for false discovery rate (FDR *p-value*). Several pairwise comparisons were completed to understand the nature of the transcript expression of the different sites and sizes. In both differential expression packages, Log_2 fold change (FC) was used to visualize the relative expression of control versus treatment in each trial. Multiple comparisons were made to

identify differentially expressed transcripts that could be used as markers between sites and sizes (Table 32). Differentially expressed transcripts underwent annotation (FDR *p-value* < 0.05) using Blast2GO (basic) software (Version 5.2.5) using NCBI Blast service (blastx), with an E-value set at $1e^{-5}$, and with a taxonomy filter selective to only bivalves (taxa: 6544, Bivalvia) (Conesa et al. 2005; Conesa and Götz 2008; Götz et al. 2008, 2011).

Table 32. Summary of types of pairwise comparisons utilized for hypoxia, hyposalinity and food availability marker discovery in two mussel sizes (adult and seed) and two sites March Water (MW), and St. Mary's Bay (StM). For each comparison, two differential expression analysis software were utilized: DESeq2 and edgeR.

Comparison name	Groups in comparisons
Adult (All)	All adult (MW, StM)
Seed (All)	All seed (MW, StM)
Adult and Seed (All)	Both sites (MW and StM) and sizes (adult, seed)

5.2.4 Marker discovery and primer design

Markers were selected from differential expression analysis pairwise comparisons summarized in Table 32. Only transcripts that were found to be significantly differentially expressed FDR *p-value* < 0.05, FC ≥ 4 and successfully annotated in NCBI nr database were considered for marker discovery. Markers that had the highest expression and showed specificity to only the treatment of interest were chosen as candidate markers. Candidate marker sequences were run in a BLAST search against the transcriptome to identify other transcripts that were highly similar. This was completed by using the tool NCBI BLAST + makeblastdb in Galaxy Version 2.10.1 (Camacho et al. 2009; Cock et al. 2015). For marker candidates with more than one match in the transcriptome, the software MEGA-X (Kumar et al. 2018) was used to run a MUSCLE alignment to determine the regions that were unique to the candidate marker. Unique sections of marker sequences were selected to undergo primer development. Primers were developed, using IDT Primer Quest Tool

(Primer3 software (version 2.2.3), Whitehead Institute for Biomedical research). Primers were developed for qPCR with intercalating dyes, using the following parameters: Tm (°C) between 59–65 °C, GC% between 35–65 %, size (nucleotides (nt)) between 17–30 nt, and overall amplicon size (base pairs (bp)) between 70–250 bp.

5.2.5 cDNA synthesis and controls

Total RNA from each mussel sample in the experiment was converted to cDNA using a reverse transcription (RT) step. This was completed using the BIORAD iScript™ Reverse transcription supermix for RT-qPCR. Each cDNA conversion was completed using a 20 µL reaction, using 4 µL of the iScript RT Supermix, 1 µg–1 pg of RNA, and variable amount nuclease-free water (based on RNA concentration). The samples were then run on a Bio-Rad C1000 Touch Thermal Cycler (Bio-Rad Laboratories, Inc, California, USA) for 5 min at 25 °C, 20 min at 46 °C, and then 1 min at 95 °C. Each cDNA reaction was then diluted using 20 µL of nuclease free water, and then divided up into single use 2 µL aliquots, and stored at -80 °C.

5.2.6 Primer optimization and validation

Each primer set underwent optimization to determine the optimal annealing temperature, reaction efficiency, and lowest limit of detection. Melt curve analysis was completed to ensure that the amplification was specific and free of primer dimer. Agarose gel electrophoresis was completed on 1 % gel to ensure that amplicon size was consistent with primer design. Finally, primers were tested on all mussel samples to verify the amplification was specific to the treatment they were designed for. All RT-qPCR was completed using the Bio-Rad iTaq™ Universal SYBR® Green Supermix using a Bio-Rad CFX96™ Real-Time system on a C1000 Touch™ Thermal Cycler. All RT-qPCR was completed using a 10 µL reaction, consisting of 5 µL of Supermix, 2.8 µL of nuclease-water, 0.1 µL Forward primer, 0.1 µL Reverse primer and 2 µL of template cDNA.

Determination of optimal annealing temperature of each primer was completed by running each primer in duplicate against a temperature gradient (53–68 °C) using all cDNA samples (pooled). RT-qPCR reactions were completed using the following protocol: 3 minutes at 95 °C; 40 cycles of 5 s at 95 °C and gradient step for 30 s at each temperature (53–68 °C);

finally, a melt curve analysis was completed by incrementally increasing temperature by 0.5 °C every 5 s from 65 to 95 °C. Optimal annealing temperature was determined by viewing RT-qPCR data at each gradient temperature and finding the lowest cycle quantification value (Cq) associated with each primer. In addition, melt curve data was evaluated to determine if primer dimer, or secondary amplicons were present.

Efficiency of primers were determined by running serial dilution reactions on all samples of pooled cDNA. In total five dilutions were created in triplicate: 1, 1/5, 1/25, 1/125. RT-qPCR reactions were completed using the following protocol: 3 minutes at 95 °C; 40 cycles of 5 s at 95 °C, 20 s at the optimal annealing temperature, followed by a melt curve analysis from 65 to 95 °C incrementally increased by 0.5 °C every 5 s. Efficiency was determined by plotting a graph of Log_{10} dilution (x-axis) vs Cq values (y-axis). The slope of the graph was determined, and the primer amplification efficiency was calculated using the following equation: Amplification Efficiency = -1 + 10^(-1/slope). Amplification efficiency was required to be between 90–110% and linear regression of slope (R^2) 90–100% to be considered good primers.

Finally, primers were verified on four mussel samples per site and size per treatment (32 samples total) and controls (No RT-control and negative control) in duplicate to ensure primer amplification was as expected within each sample in the treatment and control groups. RT-qPCR reactions were completed using the following protocol: 3 minutes at 95 °C; 40 cycles of 5 s at 95 °C, 20 s at optimal annealing temperature, followed by a melt curve analysis from 65 to 95 °C incrementally increased by 0.5 °C every 5 s. Normalization of RT-qPCR was completed using primers designed in this study, that were found to have a relatively stable expression within a particular trial. The software qbase+, version 3.0 (Biogazelle, Zwijnaarde, Belgium - www.qbaseplus.com) was used to run geNorm algorithm (Vandesompele et al. 2002) to determine an optimal number of reference genes to normalize expression data. Relative quantities (RQ) for a primer set were calculated by first calculating the average Cq value across all samples, and then determining the change in expression for a given sample based on the amplification efficiency of the primer set. The RQ is transformed to normalized relative quantity (NRQ) by dividing by the normalization factor as calculated by geNorm algorithm.

5.2.7 Statistical analysis of RT-qPCR validation step

Statistical analyses were completed on NRQ of expression for each successfully optimized and verified primer set in each trial (hypoxia, hyposalinity, food availability (low, high)). Before statistical analysis NRQ is recommended to be transformed by Log_{10} to make NRQ more symmetrical and provide more accurate statistical analysis (Hellemans and Vandesompele 2011); however, due to the presence of samples with no expression of a target gene, the expression was transformed by the following expression $Log_{10}(NRQ +1)$ so that samples with no expression could be included in the analysis. Assumptions of normality and homoscedasticity were assessed using Anderson-Darling test of normality and Levene's test of equal variance. For each primer set, amplification was very low in all samples in the control group (as expected), and this resulted in a non-normal distribution due to several samples with no-expression. Therefore, a non-parametric test of medians in SPSS software version 27 (IBM® SPSS® Statistics) was completed for each primer set to compare the expression between the control and treatment. Then, the control group was excluded from the analysis and a one-way ANOVA using Minitab® 19 was completed to analyze the expression in the treatment groups between each mussel site and size. Pairwise comparisons were completed using a Tukey test to determine differences in expression between the different mussel groups. The mean of $Log_{10}(NRQ +1)$ with confidence interval will be stated unless otherwise specified.

5.3 Results

5.3.1 Differential expression, markers and primer design

Each pairwise comparison resulted in differentially expressed transcripts being discovered. Table 33–36 show the total differentially expressed transcripts found in each trial, and by each statistical package (edgeR and DESeq2). More differentially expressed transcripts were discovered by the DESeq2 statistical package compared to the edgeR. Best candidates for marker design, were chosen based on their FC, annotated sequence ontology, and expression in each sample (Table 37–40). In total, 5–6 markers were chosen to undergo primer design and are summarized to Table 41.

Table 33. Total number of differentially expressed (DE; FDR p-value = < 0.05) transcripts in the hypoxia trial for treatment (O2 ~ 2 mg/L) vs control (O2 ~ 7–8 mg/L) in each comparison, for both DEseq2, and edgeR.

Comparison name	Groups in comparison	Total DE (DESeq2) (#)	Total DE (edgeR) (#)
Adult (All)	All adult (MW, StM)	478	2
Seed (All)	All seed (MW, StM)	1291	5
Adult and Seed (All)	Both sites (MW and StM) and sizes (adult, seed)	1554	811

Table 34. Total number of differentially expressed (DE; FDR p-value = < 0.05) transcripts in hyposalinity trial for treatment (16 ‰) vs control (27 ‰) in each comparison, for both DEseq2 (A), and edgeR (B).

Comparison name	Groups in comparison	Total DE (DESeq2) (#)	Total DE (edgeR) (#)
Adult (All)	All adult (MW, StM)	335	1
Seed (All)	All seed (MW, StM)	270	2
Adult and Seed (All)	Both sites (MW and StM) and sizes (adult, seed)	498	296

Table 35. Total number of differentially expressed (DE; FDR p-value = < 0.05) transcripts in low food availability trial for treatment (1%) vs control (5%) in each comparison, for both DEseq2 (A) and edgeR (B).

Comparison name	Groups in comparison	Total DE (DESeq2) (#)	Total DE (edgeR) (#)
Adult (All)	All adult (MW, StM)	850	2
Seed (All)	All seed (MW, StM)	210	0
Adult and Seed (All)	Both sites (MW and StM) and sizes (adult, seed)	2858	973

Table 36. Total number of differentially expressed (DE; FDR p-value = < 0.05) transcripts in high food availability trial for treatment (10%) vs control (5%) in each comparison, for both DEseq2 (A) and edgeR (B).

Comparison name	Groups in comparison	Total DE (DESeq2) (#)	Total DE (edgeR) (#)
Adult (All)	All adult (MW, StM)	404	2
Seed (All)	All seed (MW, StM)	107	0
Adult and Seed (All)	Both sites (MW and StM) and sizes (adult, seed)	767	5

Table 37. Candidate markers considered for primer design in the hypoxia trial. Table shows the sequence ontology for each candidate marker, the comparison found significant and Log_2 FC for statistical package(s) found significant.

Transcript	Sequence ontology	FC DEseq2	FC edgeR	Comparison
mussels_DN616789_c0_g1_i10	Sacsin-like isoform X2	5.2		All
mussels_DN606395_c0_g1_i1	Choline O-acetyltransferase	5.4		All
mussels_DN693810_c2_g1_i9	Rho guanine nucleotide exchange factor 7-like isoform X10	5.4		All
mussels_DN621230_c1_g1_i22	Deoxynucleoside triphosphate triphosphohydrolase SAMHD1-like	6.6		All
mussels_DN665458_c3_g1_i1	CASP8 and FADD-like apoptosis regulator		7.7	All
mussels_DN637856_c3_g1_i14	Alkylglycerol monooxygenase isoform X1		6.7	All
mussels_DN580304_c1_g2_i1	Origin recognition complex subunit 3-like	6.7	6.6	All
mussels_DN580827_c1_g1_i9	Serine protease A	6.4	4.7	All
mussels_DN647148_c4_g1_i1	Sepiapterin reductase-like		6.7	All
mussels_DN566796_c0_g1_i5	EIF2B5	5.7	6.8	Adult (All)

Transcript	Sequence ontology	FC DEseq2	FC edgeR	Comparison
mussels_DN686855_c2_g1_i4	ALK tyrosine kinase receptor	5.9	7.9	Adult (All)
mussels_DN599065_c3_g1_i2	Choline/ethanolamine kinase-like	5.9	6.9	Adult (All)
mussels_DN693716_c1_g2_i2	Polynucleotide 5'-hydroxyl-kinase NOL9-like	6.6	8.3	Adult (All)
mussels_DN654835_c0_g1_i3	Calpain-6 isoform X2	5.6	6.1	Adult (All)
mussels_DN693125_c0_g2_i8	Ogt UDP-N-acetylglucosamine--peptide N-acetylglucosaminyltransferase 110 kDa subunit-like isoform X1	6.0	7.1	Seed (All)
mussels_DN665412_c0_g2_i6	Tropomyosin-2-like isoform X1	5.5	7.4	Seed (All)
mussels_DN689769_c2_g1_i1	Copper transport protein ATOX1-like	5.4	5.9	Seed (All)
mussels_DN572550_c7_g1_i1	CREB-binding protein	6.1	8.4	Seed (All)

Table 38. Candidate markers considered for primer design in the hyposalinity trial. Table shows the sequence ontology for each candidate marker, the comparison found significant and Log_2 FC for statistical package(s) found significant.

Transcript	Sequence ontology	FC DEseq2	FC edgeR	Comparison
mussels_DN624524_c4_g1_i1	Protein mono-ADP-ribosyltransferase PARP14		7.0	All
mussels_DN621904_c0_g1_i11	Transient receptor potential cation channel subfamily M member 3-like		6.5	All
mussels_DN668024_c0_g2_i13	Potassium channel tetramerization domain containing 14	5.0		All
mussels_DN704202_c6_g3_i5	Proprotein convertase subtilisin/kexin type 5-like	4.0		All

Transcript	Sequence ontology	FC DEseq2	FC edgeR	Comparison
mussels_DN617160_c1_g2_i4	Stanniocalcin family protein		8.4	All
mussels_DN691422_c1_g1_i1	Sodium leak channel non-selective protein-like isoform X2		5.2	All
mussels_DN502204_c0_g1_i1	KCNC4	4.7		All
mussels_DN646069_c0_g1_i5	Perivitellin-2 67 kDa subunit-like	5.4		All
mussels_DN669533_c2_g2_i2	G-protein coupled receptor 157-like	5.6		All
mussels_DN704071_c0_g2_i1	Protocadherin Fat 4-like	5.4		All
mussels_DN681485_c4_g1_i1	UPF0748 protein YngK isoform X1	5.1		All
mussels_DN474547_c0_g1_i1	Sodium- and chloride-dependent glycine transporter 1-like	5.0		All
mussels_DN683815_c0_g1_i1	G-protein coupled receptor 157-like	5.0		All
mussels_DN680385_c5_g1_i3	Beta-1,3-galactosyltransferase 1-like	5.0		All
mussels_DN635950_c0_g1_i2	Sodium-dependent proline transporter-like	4.9		All
mussels_DN632908_c5_g1_i1	Protocadherin Fat 4-like isoform X2	4.9		All
mussels_DN632198_c9_g1_i3	L-xylulose reductase-like	4.5		All
mussels_DN628601_c0_g1_i1	NPC intracellular cholesterol transporter 2	4.1	8.6	All
mussels_DN684804_c1_g1_i5	MICOS complex subunit MIC60-like	4.1		All
mussels_DN589506_c3_g1_i2	Conodipine-M alpha chain	4.7	7.3	All

Table 39. Candidate markers considered for primer design in the low food availability trial. Table shows the sequence ontology for each candidate marker, the comparison found significant and Log_2 FC for statistical package(s) found significant

Transcript	Sequence ontology	FC DEseq2	FC edgeR	Comparison
mussels_DN701809_c4_g3_i3	Dual specificity protein kinase shkA/tyrosine-protein kinase Fer-like isoform X1		9.1	All
mussels_DN699100_c0_g2_i2	DNA mismatch repair protein MSH4		7.8	All
mussels_DN660748_c0_g1_i4	Glyoxal reductase,9,11-endoperoxide prostaglandin H2 reductase	5.7		All
mussels_DN584730_c1_g2_i2	TFFT_putative gastrointestinal growth factor		7.6	All
mussels_DN612601_c5_g1_i2	Mosc mitochondrial domain-containing protein, partial	5.5		All
mussels_DN580436_c0_g1_i1	Arachidonate 5-lipoxygenase-like	6.4		All
mussels_DN652694_c0_g1_i1	Hexosaminidase	8.8		All
mussels_DN689580_c1_g2_i5	Interleukin 4 Induced 1	6.3		All
mussels_DN697358_c3_g2_i6	Aminopeptidase N-like isoform X1	5.6		All
mussels_DN635103_c3_g3_i4	Arachidonate 5-lipoxygenase-like isoform X1	6.9		All
mussels_DN701046_c10_g4_i1	Allene oxide synthases - lipooxygenase like isoform X5	6.5		All
mussels_DN647465_c7_g1_i1	Alpha-N-acetylgalactosaminidase-like isoform X1	6.0		All
mussels_DN650200_c0_g1_i2	Katanin p60 ATPase-containing subunit A-like 1	5.7		All

Table 40. Candidate markers considered for primer design in the high food availability trial. Table shows the sequence ontology for each candidate marker, the comparison found significant and Log_2 FC for statistical package(s) found significant

Transcript	Sequence ontology	FC DEseq2	FC edgeR	Comparison
mussels_DN678118_c1_g7_i1	Killer 1-like cell lectin-like receptor subfamily f member	5.6		All
mussels_DN571023_c0_g1_i1	Macrophage-expressed gene 1 protein-like	5.0		All
mussels_DN535942_c0_g1_i9	phosphoinositide 3-kinase regulatory subunit 4-like	5.3		All
mussels_DN622797_c0_g4_i1	Plexin-B2-like isoform X1		5.3	All
mussels_DN700161_c1_g1_i1	THAP domain-containing protein 2		6.5	All
mussels_DN676474_c0_g2_i1	Ependymin-related protein 1	6.6		All
mussels_DN674496_c1_g1_i4	Serpin B6, Leukocyte elastase inhibitor	5.3		All

Table 41. Summary of primers designed from markers in each trial. Table shows the sequence ontology name, primer name, primer sequence, location in transcript, and size of amplicon (base pairs = bp)

Sequence ontology	Primer name	Primer Sequence	Location	Size (bp)
Hypoxia				
Choline O-acetyltransferase	CHAT	5'-GCGCTTGGCATGTGAATTAG-3' 5'-TTGTGGAACAGTACGGGAAAG-3'	363–382 460–440	98
CASP8 and FADD-like	CASP	5'-CTAGAAGGTTTCTCGGGTTCAG-3' 5'-CGTATCATTTGCCGTGATTGTAG-3'	936–957 1040–1018	105
CREB-binding protein	CREB	5'-ATGGGAGATCATGCCAAGTAAG-3' 5'-CTGGGAAACAGAGAGGACAATC–3'	395–416 493–473	99
Sacsin-like isoform X2	Sacsin	5'-GGGTACAACACAGACACAGTAA-3' 5'-CCCATTAGAGGTTGTGGATCTG-3'	148–169 265–244	118

Sequence ontology	Primer name	Primer Sequence	Location	Size (bp)
EIF2B5	eif	5'-GCCATCTAAACAATACTTGTTCCT-3' 5'-GCCATCTAAACAATACTTGTTCCTC-3'	51 - 72 162 - 138	112
origin recognition complex subunit 3-like	Origin	5'-CAAGGATGACGTTGAGAGGATAA-3' 5'-CCATGTTAATGATTCTGTCCATGAT-3'	18–40 143–119	126
Hyposalinity				
Protein mono-ADP-ribosyltransferase PARP14	Mono	5’-AACTGCAGAAGTGGGTTCTT-3’ 5’-GACCGGGATTTCGTCTCTTT-3’	451–470 532–513	82
Transient Receptor Potential Cation Channel Subfamily M Member	TRPM 3	5’-CAGAACAACACTTTGGCTCTTAC-3’ 5’-CTCAAACAAGATCGCAGTTCAAA-3’	74–96 153–131	80
Potassium channel tetramerization domain containing 14	KCTD 7	5’-ACAAACATCAAGCATTATCCATCTC-3’ 5’-GATTCCTCAGTGGTACAGTCTTC-3’	99–123 201–179	103
Stanniocalcin-like protein	Family	5’-TGGAGCTCTTCATAGTGTGTTT-3’ 5’-TGCTACCCAAGACAACTGTATC-3’	226–247 321–300	96
KCNC4	Potass	5’-ACGGCATGACACTGTTCATAA-3’ 5’-ATAAAGTATCCGCAGTCCTTGG-3’	52–72 152–131	101
Food availability - low				
Trefoil Factor 2	TFF	5’-GAATATCTGCGCCATTCTTCTTG-3’ 5’-TCCTAACCATCCACAATCCTTAC-3’	19–41 124–102	106
Arachidonate 5-Lipoxygenase	Arach	5’-GATGTTGTGTAGCATGTATGAGTTT-3’ 5’-AAGTTGGTGGAAATTGGATTGG-3’	106–130 219–198	114
Interleukin 4 Induced 1	IL4Il	5’-CATGTCTATCATCGTGTCGTTAGT-3’ 5’-TACTGCGCATCAGAACTTATACC-3’	178–201 274–252	97
DNA mismatch repair protein MSH4 [Mytilus galloprovincialis]	Muts	5’-GAGACTCCAGTGAACAACCAA-3’ 5’-CGACCAGTGGTGTATGAAGAA-3’	136–156 233 - 213	98
Hexosaminidase	hexo	5’-CCAACTCTCAGACGTGGAATAA-3’ 5’-GACTGGTTCTCTTGCCATCA-3’	533–554 625–606	93

Sequence ontology	Primer name	Primer Sequence	Location	Size (bp)
Food availability - high				
Perlucin-like protein	Perl	5'-CCGTCATTGTCTGTAGGTTTGA-3' 5'-CATGAGATGTTTGCCACTTGAC-3'	169–190 287–266	119
Macrophage expressed protein precursor	Macro	5'-CTCGCAGCAAAGACACATTC-3' 5'-CGACACCAAGTTCTGCTCTAT-3'	35–50 145–125	111
Kelch Like Family Member 17	KLHL	5'-CACTTACTATGCATCAATTGCCTATC-3' 5'-TTGACATGTTTACCTGGACCAT-3'	4032–4057 4179–4158	148
Plexin	Plexin	5'-GACAAGGAACCATGTCCAATTAC-3' 5'-TCAGTGAGGAAACCACAAGAG-3'	116–138 228–208	113
Phosphoinositide-3-kinase, regulatory subunit 4	Phospho	5'-TGTGAGCTACAGATCTCGTCTA-3' 5'-GCGCGGAATGTCTTCATTTG-3'	59–80 152–133	94

5.3.2 Primer optimization, verification and normalization

For each primer set designed, optimization and verification was completed. In total three primers from each trial (hypoxia, hyposalinity, and food availability (low, high)) were successfully optimized and verified (Table 42). Each of the primer sets in Table 42 were found to be specific to the treatment, and not expressed in mussel samples from other trials. Amplification efficiency graphs and melt curve analysis are located within Appendix 5–8. Other primer sets designed in this study that were not found specific to the trial, and expressed in all mussel samples, were used as reference genes. The geNorm algorithm was run for each trial to calculate geNorm M value and geNorm V value, to determine the optimal number of reference genes to normalize expression data (Appendix 9–12). In the Hypoxia trial, geNorm algorithm found that reference genes were highly stable (geNorm $M < 1$ and geNorm $V < 0.15$) and two reference genes were considered optimal (phospho and potass) and were used to normalize expression of target primers (Appendix 9). For the hyposalinity trial, three reference genes contained geNorm $M < 1$ and was found to be moderately stable, but geNorm V was > 0.15, and was advised by geNorm algorithm to use three candidate reference genes with the lowest M values to normalize (vertnin,

phospho, eif) (Appendix 10). In the food availability trials (low, high) reference gene stability was difficult to achieve and was above geNorm M and V value optimal thresholds (geNorm M > 1; geNorm V > 0.15), therefore it was advised to use five reference genes with lowest geNorm M (family, origin, eif, phosphor, mut) for low food availability and four reference genes for high food availability (eif, mut, origin, phospho) to normalize target genes (Appendix 11, 12).

Table 42. Primers that passed optimization steps. Table shows the primer name, annealing temperature (°C), R^2, and amplification efficiency (%) for each trial hypoxia, hyposalinity, food availability (low, high).

Primer name	Annealing	R^2	Efficiency (%)
	Hypoxia		
CASP	59 °C	0.97	93.3%
CREB	59 °C	0.91	96.0%
Sacsin	59 °C	0.95	97.3%
	Hyposalinity		
Mono	59 °C	0.91	92.0%
TRPM3	59 °C	0.96	94.8%
KCTD7	59 °C	0.94	90.4%
	Food availability–low		
TFF	59 °C	0.94	99.3%
Arach	59 °C	0.96	95.6%
IL4IlF	59 °C	0.93	92.0%
	Food availability–high		
Perl	59 °C	0.91	98.2%
Macro	59 °C	0.97	91.1%
Plex	59 °C	0.98	90.3%

5.3.3 Statistical analysis

In this study, primers that were verified had either no amplification in the control or little amplification compared to the treatment. Figure 23 shows the box-plot of Log10(NQR+1) expression of each primer designed and the difference in expression between the control and treatment. Each primer set was found to have a significantly different median in the treatment compared to the control (CASP *p-value* = < 0.001, CREB *p-value* = < 0.001,

Sacsin = 0.001, KCTD7 *p-value* = < 0.001, TRPM3 *p-value* = < 0.001, Mono *p-value* = < 0.001, IL411 *p-value* = < 0.001, Arach = < 0.001, TFF *p-value* = < 0.001, perl *p-value* = < 0.001, macro *p-value* = < 0.001, plex *p-value* = < 0.001). Figure 24 shows the mean expression between each mussel group within the treatment. In all primers sets verified, there were significant differences in expression between each mussel group (CASP *p-value* = < 0.04, CREB *p-value* = < 0.001, Sacsin = < 0.001, KCTD7 *p-value* = < 0.001, TRPM3 *p-value* = < 0.001, Mono *p-value* = < 0.001, IL411 *p-value* = < 0.001, Arach = < 0.001, TFF *p-value* = < 0.001, perl *p-value* = < 0.001, macro *p-value* = < 0.001, plex *p-value* = < 0.001), which indicates despite designing primers to be applicable for several mussel groups, variability still existed in terms of their expression in different mussel groups.

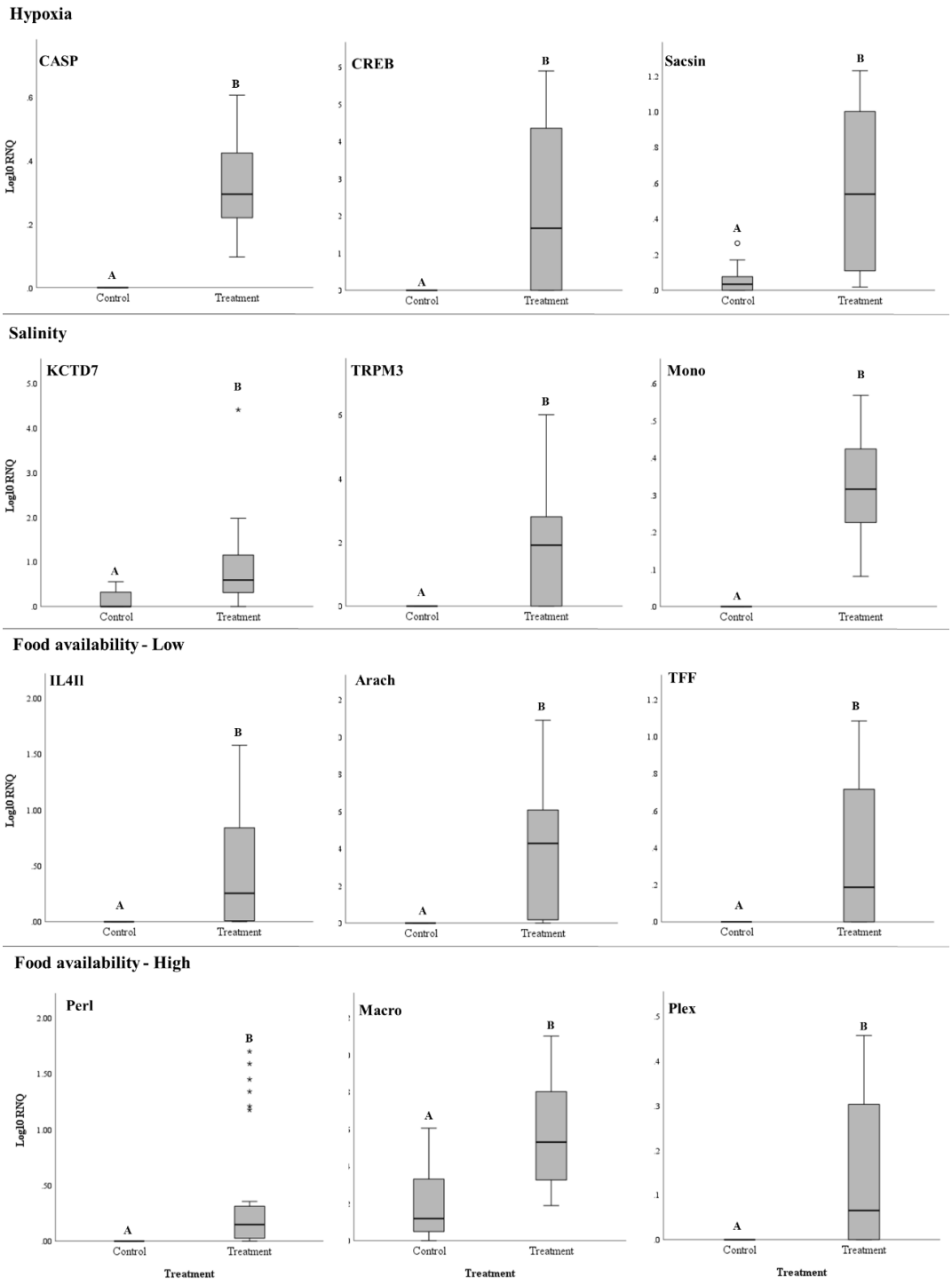

Figure 23. Boxplots showing the results of the test of medians. Graphs show the overall summary of differences in Log_{10}(NQR+1) between the treatment and control for each primer verified for a particular stressor (n = 16 mussels per group).

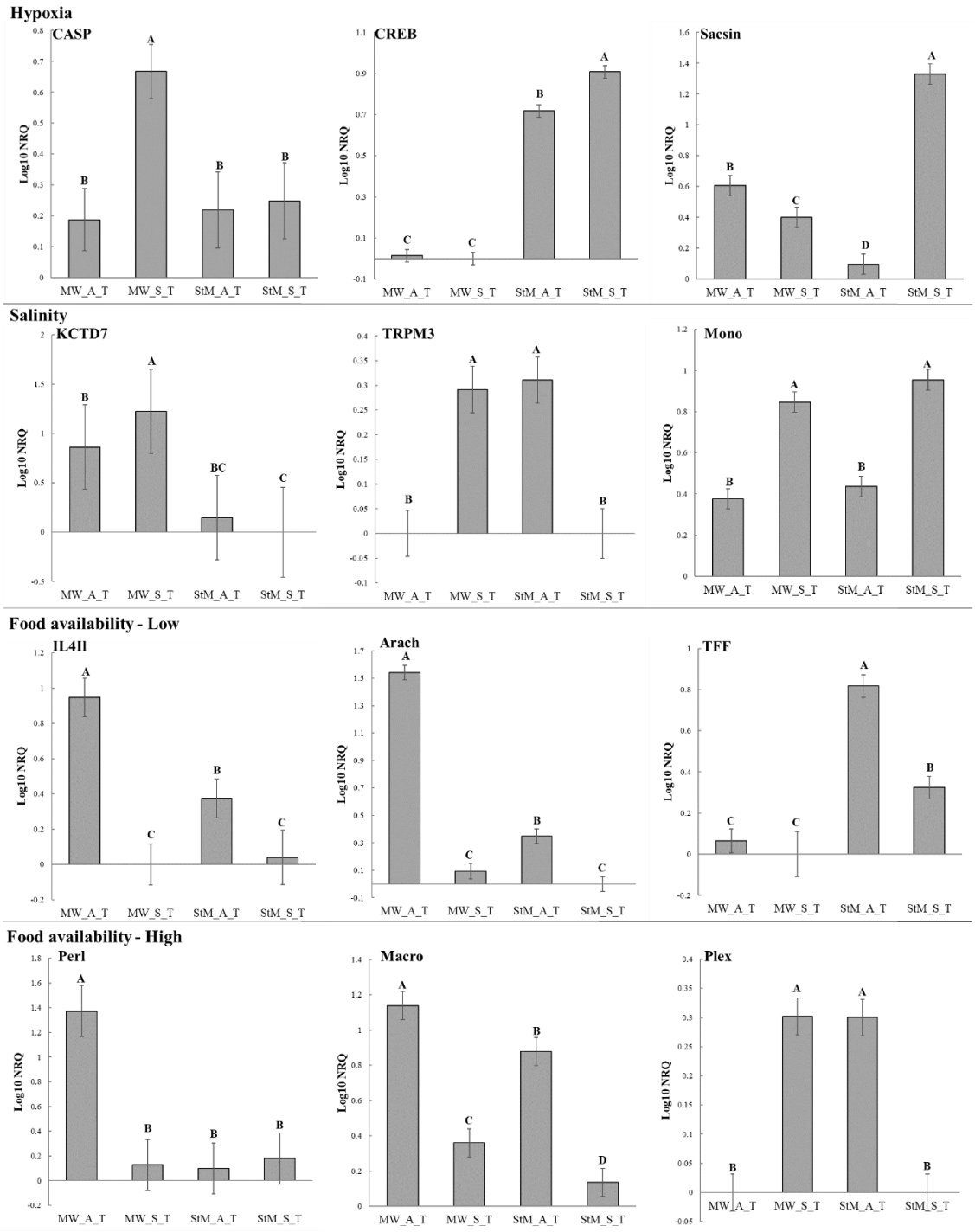

Figure 24. Estimates from the one-way ANOVA showing the mean Log_{10}(NQR+1) and confidence intervals of each primer set for each mussel group. Mussel groups without a common script were considered significantly different (*p-value* = < 0.05). (n = 4 mussel samples per bar)

5.4 Discussion

In the present study, three primers per stressor (hypoxia, hyposalinity, food availability (low, high) were successfully verified as candidate markers for detecting mussel stress. Many of the markers verified were considered novel to blue mussels but had links to the stressor of interest in other organisms. For example, CASP8 and FADD-like (CASP), verified for hypoxia, aids in prevention of apoptosis and autophagy pathways (Bedoui et al. 2020). In humans/mice, it has been found that under-expression of CASP protein during hypoxia/reoxygenation in cardiomyocytes resulted in increased lethal apoptosis and autophagy; however, when over-expressed, it resulted in protection and survival during hypoxic conditions (Liu et al. 2021). Therefore, the expression in mussels in the hypoxia trial might be associated with protection against apoptosis and autophagy in acute hypoxia. Another marker verified for hypoxia stress was CREB-binding protein (CREB) which is associated with transcription factors that have a role in cell growth, transformation, and development in mammals (Goodman and Smolik 2000). During hypoxia in mammals, it has been found to interact with hypoxia inducible factor as a coactivator that leads to transcription of genes that mediate the response against low oxygen (Ruas et al. 2010). Therefore, the detection of this transcript in hypoxia trials in this study demonstrate that CREB might have a similar role in mussels. In the hyposalinity trial, potassium channel tetramerization domain containing 14 (KCTD7) was verified as a good marker for hyposalinity stress and is known to be involved in K^+ transport by forming pores in membranes (Miller 2000). A study on *Crassostrea gigas* also found another potassium channel (KCTD1) over-expressed in response to hyposalinity stress (Zhao et al. 2012), therefore, the upregulation of KCTD7 may also play a role in response to hyposalinity and osmoconformation processes. Also, within the hyposalinity trial, transient receptor potential cation channel subfamily M member (TRPM3) was verified and may also have a role in osmoconformation. Transient receptor potential channels (TRP) are a family of ion channels that are involved with ion transport (Nilius and Owsianik 2011) and osmosensing during osmotic stress in mammalian epithelia cells (Harteneck and Reiter 2007); therefore, the over-expression in this study might be associated with sensing the change in salinity.

Other markers that were verified were known to be more generally associated with stress response and not definitively linked with a specific stressor. For example, Sacsin was verified as a marker in hypoxia stress and has been found to be both a chaperone and co-chaperone, that can assist both in folding and delivery of proteins to heatshock 70 protein (HSP) family (Anderson 2013). Sacsin's are not known to be over-expressed in hypoxia, however, chaperones including HSP's are known to be expressed during stressful environmental conditions to aid in folding of damaged proteins (Larade et al. 2002; Halpin et al. 2004; David et al. 2005; Gracey et al. 2008; Larade and Storey 2009; Anestis et al. 2010; Ivanina et al. 2016; Nie et al. 2018). Another marker that was verified in this study for hyposalinity stress was protein mono-ADP-ribosyltransferase PARP14 (mono), which is known to be involved with many biochemical processes including transcription regulation, stress responses, DNA repair, mitochondrial function, etc. (Schweiker et al. 2018). However, the link between this marker and hyposalinity stress is novel.

In the food availability trial, all markers verified were considered novel as relatively little is known about gene expression associated with feeding behaviour, digestion, etc. However, changes in food availability can result in changes in feeding physiology. In this study, Trefoil factor 2 (TFF) was verified as a marker. This gene encodes for peptides that have an important role in mucous in intestinal tracts of mammals (Aihara et al. 2017). Most of what is known about TFF implicates a role in defence against injury in intestinal tracts (Aihara et al. 2017). It may also have a role in particle capture during changes in food availability, as studies have found that the mucosal layer plays an important role in feeding physiology (Pales Espinosa and Allam 2013b, 2018; Pales Espinosa et al. 2016; Allam et al. 2021). In particular, c-type lectins, which are associated with the immune system, have been found to have an important role in feeding physiology during changes in food availability (Pales Espinosa and Allam 2013b, 2018; Pales Espinosa et al. 2016; Allam et al. 2021). In the present study, three immune genes were verified as markers for food availability, two for high food availability (Perlucin-like protein (Perl) and Macrophage expressed protein precursor (macro)), and one for low food availability (Interleukin 4 Induced 1 (IL4II). The marker Perl is part of the c-type lectin family and has been implicated as a potential pattern recognition protein in invertebrate's innate immune system

(Bi et al. 2020). However, its over-expression in this study might be associated with changes in food availability. The role of IL4II in low food availability and Macro in high food availability are less understood, but the link between the immune system and feeding physiology could mean a role in particle capture or response to changes in food availability is plausible. In the high food availability, there was also a marker identified as a plexin. Plexins are a diverse group of cell surface receptors that have a wide variety of functions including regulating signaling of the nervous system, vessel formation and immune response (Pascoe et al. 2015). Plexins link to high food availability is completely novel, but links to immune system suggest it could also be explored associated with particle capture. Finally, Arachidonate 5-Lipoxygenase was also verified as a marker in low food availability, but its role is unknown. Arachidonate 5-Lipoxygenase is known to play a role in eicosanoids metabolism such as leukotrienes, which in vertebrates are involved with inflammatory responses (Werz et al. 2002).

One of the challenges of this study was finding markers that were unique to each stressor. In human and mammalian models, biomarkers have been identified which aid in diagnosis or prognosis of many stress/disease states (Dhama et al. 2019). Biomarkers for humans/mammalian models have made use of markers associated with oxidative stress, immune markers, heat shock proteins and hormones/chemical metabolites (Dhama et al. 2019). Extensive research has been completed to understand the molecular signature or the interplay of different markers in particular stressors for successful diagnosis/prognosis (Dhama et al. 2019). While mechanisms associated with physiological responses to stress have been studied in mussels (*M. edulis*) (i.e. Bayne 1971, 1972; Bayne et al. 1973, 1981; Shumway 1977; Davenport 1979a, 1979b; Widdows et al. 1979, 1989 p. 1; Holwerda and De Zwaan 1980; De Zwaan et al. 1982; Hawkins et al. 1993; Clements et al. 2018, 2021), there are still a lot of unknowns about how molecular response to stress leads to observed physiological response. Recent studies have focused on making connections between genotypic and phenotypic responses to stress in mussels (Halpin et al. 2004; Gracey et al. 2008; Lockwood and Somero 2011; Woo et al. 2013; Gracey and Connor 2016; Falfushynska et al. 2020; Barrett et al. 2022). Unfortunately, research has focused more on general molecular stress responses rather than specific stress responses and this represents

a disconnect in the current understanding of the molecular mechanisms involved in responding to a particular stressor. In addition, biomarkers have been developed particularly in association with pollution and toxin monitoring programs (Fitzpatrick et al. 1997; Galloway et al. 2002; Rickwood and Galloway 2004; Bocquené et al. 2004; Leiniö and Lehtonen 2005; Gagné et al. 2008; Al-Subiai et al. 2011; Rola et al. 2012; Magara et al. 2019; Falfushynska et al. 2019). Other research in developing biomarkers in mussels associated with environmental stress have also used antioxidant, heat shock proteins, metallothioneins (Giannetto et al. 2017) or inflammatory responses (Falfushynska et al. 2020). While these markers are excellent indicators for stress, they could likely be expressed in response to several stressors and not one particular stressor. Other biomarkers have been designed with microRNA in mussels (Chen et al. 2017) and more specific genes such as Hypoxia-Inducible Factor α and Hif-prolyl Hydroxylase (Giannetto et al. 2015), which shows promise at being more specific to the stressors they were designed for. In this study, we identified markers by comparing gene expression in the control vs treatment of all sizes and sites and found hundreds to thousands of transcripts that were associated with stressors of interest. To determine transcripts that were specific to the stressor of interest, a comparison of the transcript among other stress trials within the transcriptome was completed. This ultimately led to a set of markers being discovered and validated. Future research should also follow up on ensuring that these markers are still specific in a real-world setting and in intermediate and chronic stress conditions as well, as it has been found that duration of stress can act on different sets of genes (Shi et al. 2019).

Another challenge in the present study, was that RT-qPCR found markers were expressed differently between individuals, sites (March Water, St. Mary's Bay) and sizes (adult, seed), and therefore, some markers would be better for some sites and sizes than others. While this is not ideal, it is also not unexpected and is consistent with findings in chapters 2–5. There are many reasons why this variation could have emerged including differences in developmental stage, energy reserves, metabolism, previous exposure to stressors, etc. (Thompson 1979; De Zwaan 1991; Sukhotin et al. 2003; Altieri 2006; Meng et al. 2018). However, the variability in expression between individuals, sites and sizes in markers can indicate that (1) the markers were not appropriate for all mussel sites and sizes, or (2) a

longer stress exposure time would be needed to see the expression of the marker in the groups. Future research should follow up on this point to understand why this difference in expression occurred.

Overall, the result of this study suggests that there needs to be more research done to validate that the markers can detect the specific stressor of interest in a real-world setting and in multiple sites and sizes. In addition, the differences in marker expression between sites and sizes indicate that more research is needed to understand why these differences are emerging. Marker panels that contain multiple markers for a particular stressor might be better suited for multiple sites and sizes. These marker panels would allow for early detection of stress in the blue mussel, before it leads to major physiological impacts including poor growth and death.

5.5 Conclusions

In each of the stress trials, markers were discovered, and primers were designed capable of detecting acute stress response. The results of this study represent the first steps in designing markers capable of detecting stress in blue mussel that can be used by the mussel aquaculture industry in PEI. The next steps must focus on validating the markers in real-world stress events, and on ensuring that the markers are useful for detecting the stress in intermediate, long-term, and chronic stress. In addition to the development of markers, this study highlights the variation of expression between individuals, sites, and sizes. Panels of markers that have multiple markers for a particular stressor will be useful in identifying acute stress in multiple sites and sizes before it impacts industry productivity.

Chapter 6 : Discussion

6.1 Conclusions

The goal of this research was to study the acute stress response of mussels experiencing hypoxia, hyposalinity, and low/high food availability from different sites and sizes of mussels from Prince Edward Island (PEI). It was hypothesized that by studying the acute stress response, markers could be discovered to detect early onset of stress before it leads to major impacts to mussel health. Differences and similarities in transcript expression in between sites and sizes of mussels from PEI were also explored, to understand if their responses were similar between different mussel groups. Overall, we found that acute hypoxia, hyposalinity, and food availability elicited significant and different transcriptomic responses.

The hypoxia trial found major shifts in transcriptomic response in association with metabolism, signalling, protein turnover, byssal thread production, stress response, immune, growth and development. The transcriptomic response showed signs of switching to anaerobic metabolism and signalling indicative to metabolic rate changes that would likely translate into phenotypic changes. In the seed mussels, there was under-expression of several growth, development, and byssal thread transcripts that may indicate that their first response is to shut down growth and attachment behaviour. Further, byssal thread production decline could result in increases in detachment from mussels socks and increases in predation.

Hyposalinity exposure resulted in major responses both in heart rate and transcript expression. Heart rate increased during the first six-hours to hyposalinity in adult mussels and could be associated with osmotic shock. Several over-expressed transcripts were associated with metabolism, osmoconformation, stress response, immune response, and antioxidants. Each size and site appeared to be having a unique response to the hyposalinity exposure, with St. Mary's Bay adults, expressing more transcripts compared to all other mussel groups.

Different food availability rations (1%, 5% and 10%) resulted in unique transcriptomic response to each food ration in all mussel groups; however, March Water adults appeared to be having a stronger response to the differences in food rations. Transcriptomic responses in the March Water mussels indicated, that mussels in 5% and 10% rations were expressing more transcripts associated with metabolism compared to the 1% ration, indicating that the higher rations were resulting in higher energy acquisition. Immune associated transcripts were over-expressed in higher food rations, implicating a potential decline in immune function at lower food availability. In all mussel groups, changes in transcripts were observed at different food rations associated with cilia, mucosal genes, lysosomes, digestive enzymes, and indicates that the acclimation process to different food rations can commence as early as 48 h after an acute change in food availability.

In each of the stress trials, markers were discovered, and primers were designed capable of detecting acute stress response. Marker discovery in this study represents significant steps forward in designing a test capable of detecting stress in blue mussels in the PEI aquaculture industry. The next steps must focus on validating the markers in real-world stress events and ensuring that the markers are useful for detecting the stress in intermediate and chronic stress. In addition to the development of markers, the variation of expression between individuals, sites, and sizes highlights the need for more research to be completed to understand genotypic and phenotypic variation between mussels of different sizes and sites in PEI. Differences in expression should be explored to understand if some sizes and site would be more susceptible to stress, or if there are multiple expression patterns that lead to the same phenotype.

6.2 Differences in transcriptomic responses between sites and sizes

One major finding in this research was that there were differences in transcriptomics between sizes and sites in all mussel stress trials. In addition, different pairwise comparisons resulted in different transcripts being found differentially expressed. Three types of comparisons were used in this research to discover differentially expressed transcripts (1) comparison between specific sites and sizes (2) comparisons between sizes (regardless of site) (3) control vs treatment (regardless of size or site). Each comparison

resulted in a subset of unique differentially expressed transcripts, with relatively little overlap between other pairwise comparisons. However, the comparisons that appeared to have the fewest transcripts in common were those comparing different sizes. This indicates that the size of mussel made a difference in terms of the transcriptomic response to environmental stress. There are many reasons why these differences could have emerged. It has been found that seed mussels allocate their energy to development and rapid growth, and little energy into reproduction (Thompson 1979). After ~ 35 mm in shell height, mussels will gradually shift to allocating more energy to reproduction (Guyondet et al. 2015). Differences in baseline physiological conditions have been found to result in differences in transcript expression patterns in other organisms (Boedigheimer et al. 2008). Epigenetics has also been found to have a role in regulating gene expression associated with growth and development at different life stages in bivalves and can result in variances in gene expression between sizes/ages (Riviere et al. 2013, 2017; Li et al. 2015c).

Differences in physiological responses to stress in between size/age bivalves has also been documented in several studies (Hole et al. 1992, 1993, 1995; Sukhotin et al. 2003; Zilberberg et al. 2011; Izagirre et al. 2014; Clark et al. 2016; Wu et al. 2017; Clements et al. 2021). Markers designed for osmotic and hypoxia stress in (*Perna perna*) (Zilberberg et al. 2011) and pollution in *M. galloprovincialis* (Izagirre et al. 2014) have been found to differ in expression depending on age/size of mussels. Several studies have also found that older mussels (*M. edulis*) have a lower capacity to recover after exposure to various stressors (hypoxia, high temperatures, pollution/toxins) compared to younger mussels (Freeman and Dickie 1979; Mallet et al. 1990; Hole et al. 1992, 1993, 1995). A recent study by Wu et al. (2017) found that mussels (*M. galloprovincialis*) at three life stages (D-stage, juvenile and adult) had differential responses to pollution exposure (cadmium), and that D-stage larvae were more susceptible, but that each size had a different set of pathways that they utilized in response to the stress. Therefore, adult and seed size mussels having different responses to stress in the present study is not a surprising result.

There were also apparent differences in transcript expression between sites in all trials. This is an interesting finding as it indicates that mussels may have different strategies it can utilize to respond to environmental stress. Environmental influences may play a role

in mussel responses to stress. Studies have found that mussels from different locations may exhibit differences in physiological traits (Altieri 2006; Nemova et al. 2013; Watson et al. 2018). For example, Nemova et al. (2013) found that the lipid membranes of the mussel (*M. edulis*) were different between the intertidal and subtidal mussels. Mussels in the intertidal zone contained higher levels of baseline cholesterol compared to the aquaculture mussels which contained more saturated fatty acids, n-6 polyunsaturated fatty acids and 22 non-methylene interrupted fatty acids (Nemova et al. 2013). The intertidal zone is also known to be a more stressful environment for mussels, as it experiences daily tidal cycles that can drastically impact oxygen, and temperature in this zone (Freire et al. 2011). It has been found that mussels that live in the intertidal zone have become more resilient to environmental fluctuations (Widdows and Shick 1985; Altieri 2006; Petes et al. 2008; Meng et al. 2018). Acclimation to differences in phytoplankton levels has been found between populations of mussels as well. For example, in locations with low food availability, mussels have acclimated to continue to filter at extremely low levels of phytoplankton while still maintaining growth (Strohmeier et al. 2009). Mussels have also been found to acclimate to environmental conditions by changing their feeding apparatus such as the gills and labial palps (Capelle et al. 2021). Differences in phenotypic responses between different locations may result through genetic differences, but also through epigenetic differences that impact transcript expression pathways (Watson et al. 2018).

It has also been found that there is inter-individual variation in performance between mussel sites in PEI, and this has been correlated with multilocus heterozygosity (Koehn and Gaffney 1984; Myrand et al. 2002), which can result in mussels having lower metabolic requirements, more efficient protein turnover and better ability to survive starvation (Koehn and Gaffney 1984; Diehl et al. 1985; Hawkins et al. 1986; Bayne and Hawkins 1997; LeBlanc et al. 2008). Mallet et al. (1990) found that site had an impact on summer mortality prevalence in PEI and speculated that it could be related to genetic factors. In addition, Tremblay et al. (2011) found that seed sites in Gulf of St. Lawrence can influence the survival of mussels, with mussel sites containing higher multilocus heterozygosity exhibiting an advantage. In this study, mussels from March Water and St.

Mary's Bay originated from wild seed. It is not known if there were differences in multilocus heterozygosity between these two sites.

Other research in mussels have also highlighted major variation in gene expression between sites, and indicates that gene expression response is highly complex, and that variation in environmental factors may be driving these differences (Place et al. 2008; Counihan et al. 2019). Poirier et al. (2021) examined different mussel aquaculture sites in PEI in terms of growth, and environmental differences. Two sites within the study, (March Water and Brudenell River) were highly relevant to this study, as the March Water site was used in this study, while Brudenell River is within the same watershed as the St. Mary's Bay site. Seed source from St. Mary's Bay also originated from Brudenell river. In addition, Poirier et al. (2021) monitored mussels between 2016–2018, which is a relevant timeframe for the mussels used in this study as they were collected in January 2017. At the March Water site in 2016, chlorophyll spring bloom began a month earlier than in Brudenell River, and March Water seemed to be higher throughout most months between the two sites (Poirier et al. 2021). It was also noted in the report March Water mussels seed in the year 2016 were smaller, but growth eventually caught up with other sites. Other environmental parameter trends including salinity, dissolved oxygen, pH, temperature, total dissolved solids, fluorescent dissolved organic matter were similar between the two sites, other then minor fluctuations (Poirier et al. 2021). Differences in spring bloom may have contributed to variances between the two site in the present study, as differences in food quality may impact the types of energy reserves and osmolytes that a bivalve stores (Yancey 2005; Narváez et al. 2008). For example, food supply can influence the amino acid composition of bivalves, particularly taurine (Hosoi et al. 2005; Bayne 2017). Freeman (1974) found that there were differences in growth in mussels (*M. edulis*) from two embayment's in Nova Scotia: St. Margaret's Bay and Bedford Basin and was attributed to differences in food supply.

6.3 Future directions

This study uncovered valuable information about transcriptomic responses of mussels from different sizes and sites in PEI. However, it also raised many questions about how stress

controls transcript expression and leads to observable phenotype. It will be valuable to investigate how differences in transcript expression in sizes and sites of mussels prepares different groups of mussels for environmental stress, particularly in the face of climate change. Future research should focus on understanding the origins of differences in expression, such as whether it originated from a genetic or epigenetic component. Understanding the origins of genotypic variability should be investigated to better understand if some sites are better equipped to handle stress or if mussel groups can become acclimatized in weeks to months or over generations. Some research has already started to be investigated on this subject in other bivalves (Parker et al. 2012, 2015, 2017; Zhao et al. 2017, 2018; Diaz et al. 2018; Kong et al. 2019) but having a local understanding of this in PEI and Atlantic Canada is valuable to mussel aquaculture stakeholders.

This research allowed for markers to be discovered for hypoxia, hyposalinity and food availability rations. However, it again, uncovered how variable markers can be to sizes and sites in PEI. Therefore, future research needs to be done to (1) validate markers are appropriate in real world setting (2) validate these markers in other time points such as at intermediate stress and chronic stress. In addition, this research highlights the need to do more research on understanding how baseline transcript expression pathways are linked with phenotype. Research has predominately been focused on understanding physiological and biochemical responses to stress (i.e. Bayne 1971, 1972; Bayne et al. 1973, 1981; Shumway 1977; Davenport 1979a, 1979b; Widdows et al. 1979, 1989; Holwerda and De Zwaan 1980; De Zwaan et al. 1982; Hawkins et al. 1993; Clements et al. 2018, 2021), however, the link between gene/transcript expression is only in the beginning stages of being understood. Human and mammalian models have been much more successful at identifying biomarkers, because of the extensive research that has been done to understand stress and disease states (Dhama et al. 2019). While biomarkers have been developed in mussels, most studies have predominately focused on general markers of stress and not specific (i.e. Fitzpatrick et al. 1997; Galloway et al. 2002; Rickwood and Galloway 2004; Bocquené et al. 2004; Leiniö and Lehtonen 2005; Gagné et al. 2008; Al-Subiai et al. 2011; Rola et al. 2012; Magara et al. 2019; Falfushynska et al. 2019). Finding specific markers to stress is exceptionally challenging, because often there are many reasons why a

gene/protein/metabolite can be expressed; however, it is even more challenging if little research has been investigated in understanding the gene/protein function (Dhama et al. 2019). In humans/mammalian models, panels of markers have been useful to investigate symptoms of physiological stress and disease states (Dhama et al. 2019), and this may be useful for future research in bivalves such as mussels.

Overall, the research in this study uncovered valuable information about the transcriptomic response of mussels to stress, but also uncovered several more questions that need to be addressed to move forward in marker validation. It also uncovered questions about how mussels from different sizes and sites cope with stress, which will particularly be important to answer in the face of climate change.

Appendix 1

Chapter 2: Supplemental excel file containing all differentially expressed transcripts in each pairwise comparisons in hypoxia trials.

Chapter 3: Supplemental excel file containing all differentially expressed transcripts in each pairwise comparisons in hyposalinity trials.

Chapter 4: Supplemental excel file containing all differentially expressed transcripts in each pairwise comparisons in food availability trials.

Appendix 2

Table 43. All KEGG pathways associated with differentially expressed transcripts in the hypoxia trial (Chapter 2) from different sizes and populations (A = adult; S = seed; MW = March Water; StM = St. Mary's Bay).

Category	Pathway	A		MW A		StM A		S		MW S		StM S	
		+	-	+	-	+	-	+	-	+	-	+	-
Amino acid metabolism	Tryptophan metabolism	0	0	0	0	0	0	2	-1	0	0	1	0
	Taurine and hypotaurine metabolism	0	0	0	0	0	0	1	0	0	-1	0	0
	Histidine metabolism	0	0	0	0	0	0	2	-1	0	0	1	0
	Amino sugar and nucleotide sugar metabolism	2	0	1	-1	1	0	0	-1	0	-1	1	0
	Cysteine and methionine metabolism	1	0	1	0	0	0	0	-1	0	-1	0	0
	Arginine and proline metabolism	0	0	0	0	0	0	2	-2	0	-1	1	0
	Glycine, serine and threonine metabolism	1	0	1	0	0	0	0	-3	0	0	1	0
	Arginine biosynthesis	0	0	0	0	0	-1	0	0	0	0	0	0
	Alanine, aspartate and glutamate metabolism	0	0	0	0	0	-1	0	0	0	-1	0	0
	Thiamine metabolism	0	0	0	0	0	0	0	0	0	-1	0	0
	beta-Alanine metabolism	0	0	0	0	0	0	2	-1	0	0	1	-1
	Lysine degradation	0	0	0	0	0	0	2	-2	0	0	1	-2
	Tyrosine metabolism	0	-1	0	0	0	-1	0	-1	1	0	1	-2
	Biosynthesis of amino acids	1	-2	0	-1	1	0	0	-3	0	-4	1	-2
Carbohydrate metabolism	Inositol phosphate metabolism	1	0	0	0	0	0	0	0	0	0	0	0
	Galactose metabolism	0	0	1	-1	0	0	1	0	0	0	0	0
	Butanoate metabolism	0	0	0	0	0	0	1	0	0	-1	1	0
	Ascorbate and aldarate metabolism	0	0	0	0	0	0	1	-1	0	0	1	0
	Fructose and mannose metabolism	0	0	1	0	1	-1	0	-1	0	0	1	-1
	Biosynthesis of nucleotide sugars	0	0	0	0	0	0	0	-1	0	0	0	0
	Pentose and glucuronate interconversions	0	-1	0	0	0	-1	0	0	0	0	0	0
	Pentose phosphate pathway	0	-1	0	0	1	0	0	0	0	0	0	0
	Pyruvate metabolism	0	-2	0	-1	0	-1	1	-1	0	0	2	-2
	Citrate cycle (TCA cycle)	0	-2	0	-2	0	0	0	0	0	-1	1	-2
	Starch and sucrose metabolism	0	0	0	0	0	0	0	0	1	0	0	0
	Glycolysis / Gluconeogenesis	1	-2	1	-1	1	-1	1	-3	0	-1	3	-3

Category	Pathway	A		MW A		StM A		S		MW S		StM S	
		+	-	+	-	+	-	+	-	+	-	+	-
Cofactors and vitamins	Pantothenate and CoA biosynthesis	0	0	0	0	0	0	1	0	0	0	1	0
	Terpenoid backbone biosynthesis	0	-1	0	0	0	0	1	0	0	-1	0	0
	Vitamin B6 metabolism	0	0	0	0	0	0	0	-1	1	0	0	0
	Retinol metabolism	0	0	0	0	0	-1	1	-2	0	0	2	-3
	Biosynthesis of cofactors	0	0	0	-1	1	0	1	-3	1	-3	3	0
Glycan metabolism	Various types of N-glycan biosynthesis	0	0	0	0	0	0	1	-1	0	-1	0	-1
	Valine, leucine and isoleucine degradation	0	0	0	0	0	0	2	-1	0	-2	2	0
	Other types of O-glycan biosynthesis	0	0	0	0	0	0	1	0	0	0	0	0
	N-Glycan biosynthesis	0	0	0	0	0	0	1	0	0	0	0	0
	Glycosphingolipid biosynthesis-globo and isoglobo series	0	0	0	0	0	0	1	0	0	-2	1	-1
	Glycosphingolipid biosynthesis	0	0	0	0	0	0	1	0	0	0	0	0
	Glycosaminoglycan biosynthesis-chondroitin sulfate / dermatan sulfate	0	0	0	0	0	0	1	0	1	0	1	0
	Glycosaminoglycan biosynthesis- keratan sulfate	0	0	0	0	0	0	1	0	0	0	0	0
	Glycerolipid metabolism	0	0	0	0	0	0	1	-1	0	0	2	0
	Mannose type O-glycan biosynthesis	0	0	0	0	0	0	1	-1	0	0	0	0
	Glycosphingolipid biosynthesis-lacto and neolacto series	0	0	0	0	0	0	0	-1	0	-1	1	0
	Glycosaminoglycan degradation	0	0	0	0	0	0	0	-1	0	-1	1	0
	Glycosaminoglycan biosynthesis-heparan sulfate / heparin	0	0	0	0	0	0	1	-1	1	-1	1	0
	Other glycan degradation	0	0	0	0	1	0	0	0	0	-1	0	0
	Glycosylphosphatidylinositol (GPI)-anchor biosynthesis	0	0	0	-1	0	0	0	0	0	0	0	0
	Glycosphingolipid biosynthesis-ganglio series	0	0	0	0	0	0	0	0	0	-2	0	0
	Glycosaminoglycan biosynthesis- chondroitin sulfate / dermatan sulfate	0	0	0	0	0	0	0	-1	0	0	0	0
Lipid metabolism	Sphingolipid metabolism	1	0	0	0	0	0	2	0	1	-1	0	0
	Glycerophospholipid metabolism	2	-1	0	0	0	0	0	-2	0	-2	1	0
	Fatty acid biosynthesis	0	0	0	0	0	0	0	-1	0	-1	0	0
	Fatty acid metabolism	0	0	0	0	0	0	0	-2	0	-2	0	0

Category	Pathway	A		MW A		StM A		S		MW S		StM S	
		+	-	+	-	+	-	+	-	+	-	+	-
	Fatty acid degradation	0	-1	1	0	0	-1	1	-2	0	-1	2	0
	Ether lipid metabolism	0	-1	0	0	0	0	0	-2	0	0	0	0
	alpha-Linolenic acid metabolism	0	-1	0	0	0	0	0	-2	0	0	0	0
	Linoleic acid metabolism	0	-1	0	0	0	0	0	-3	0	0	0	0
	Synthesis and degradation of ketone bodies	0	0	0	0	0	0	0	0	0	-1	1	0
	Biosynthesis of unsaturated fatty acids	0	0	0	0	0	0	0	0	0	-1	0	0
	Fatty acid elongation	0	0	0	0	0	0	0	0	0	-1	0	0
	Arachidonic acid metabolism	1	-1	1	0	0	0	0	-5	0	-1	0	0
Other	Oxidative phosphorylation	2	0	1	-1	1	0	0	0	1	0	2	0
	Selenocompound metabolism	1	0	0	0	0	0	0	0	0	0	0	0
	Drug metabolism-cytochrome P450	0	0	0	0	1	-1	1	0	0	-1	1	-1
	Pyrimidine metabolism	0	0	0	0	1	0	0	-1	0	-1	0	0
	Purine metabolism	0	0	2	-1	1	0	0	-1	0	-2	0	0
	Metabolism of xenobiotics by cytochrome P450	0	-2	0	0	1	-1	1	-1	0	-2	1	-1
	Drug metabolism-other enzymes	0	0	0	-1	0	0	1	-2	0	-3	2	0
	Glutathione metabolism	0	-1	0	0	1	0	2	-5	0	-3	1	0
	Ubiquinone and other terpenoid-quinone biosynthesis	0	0	0	-1	0	0	0	0	0	0	0	0
	Folate biosynthesis	0	0	0	0	0	0	0	0	0	-2	0	-2
	Drug metabolism	0	0	0	0	2	0	0	0	0	0	0	0
	Nitrogen metabolism	0	0	0	0	0	-1	0	0	1	0	0	-1
	D-Glutamine and D-glutamate metabolism	0	0	0	0	0	-1	0	0	0	0	0	-1
	2-Oxocarboxylic acid metabolism	0	-1	0	0	0	0	0	0	0	0	0	0
Cellular Process	Lysosome	2	-1	1	-1	3	0	5	-4	3	-6	2	-7
	Phagosome	2	-1	0	-3	2	-1	2	-1	4	-5	1	-1
	Autophagy-animal	1	0	1	-1	1	-1	4	-4	0	-4	0	-1
	Autophagy-other	0	0	0	0	0	0	0	0	0	-1	0	0
	Proteasome	1	0	1	-1	0	-1	0	0	1	0	0	-1
	Endocytosis	1	0	1	0	1	-2	1	-2	0	0	1	-2
	Mitophagy-animal	0	-1	0	0	0	0	0	0	0	0	0	0
	Peroxisome	1	-1	1	0	0	0	0	-2	0	-3	1	-3
	SNARE interactions in vesicular transport	0	0	0	0	0	0	0	0	1	0	1	0

Category	Pathway	A		MW A		StM A		S		MW S		StM S	
		+	-	+	-	+	-	+	-	+	-	+	-
	Spliceosome	0	-2	1	0	0	-1	0	-2	1	0	0	-1
Environmental Information Processing	Wnt signaling pathway	1	0	0	0	0	0	1	0	0	0	0	0
	FoxO signaling pathway	2	0	0	0	0	0	2	-3	1	-3	1	0
	mTOR signaling pathway	2	0	0	-1	0	-1	1	-2	0	-3	0	-1
	Notch signaling pathway	0	0	1	0	0	0	1	0	0	0	0	0
	ECM-receptor interaction	0	0	0	0	0	0	0	-1	1	-1	0	-2
	Fanconi anemia pathway	0	0	0	0	0	-2	0	-1	1	0	0	-2
	Neuroactive ligand-receptor interaction	1	0	0	0	0	0	0	-2	1	-1	0	0
	Phosphatidylinositol signaling system	0	0	0	0	0	0	0	-2	0	-2	1	0
	ABC transporters	0	0	0	0	0	0	0	0	0	-1	0	0
	TGF-beta signaling pathway	0	0	0	0	0	0	1	-2	0	0	0	0
Genetic Information Processing	Ribosome	5	-2	1	0	1	-1	2	-2	0	-1	1	-2
	mRNA surveillance pathway	0	0	1	0	0	0	2	0	0	0	1	0
	Base excision repair	0	0	0	0	0	0	1	0	0	0	0	0
	DNA replication	0	0	1	0	0	0	1	0	0	0	0	0
	Non-homologous end-joining	0	0	0	0	0	0	1	0	0	0	0	0
	Ribosome biogenesis in eukaryotes	0	-1	0	-1	0	0	1	0	1	-1	3	0
	Homologous recombination	0	0	0	0	0	-1	0	-1	1	0	0	-1
	Nucleocytoplasmic transport	0	0	0	0	0	0	0	-1	0	0	0	0
	Nucleotide metabolism	0	0	0	0	0	0	0	-1	0	0	0	0
	RNA degradation	0	0	0	0	0	0	0	-1	0	0	0	0
	Ubiquitin mediated proteolysis	1	-2	0	0	1	0	2	-3	3	-1	2	0
	Protein export	0	-1	0	0	0	0	0	-3	0	-2	0	0
	Protein processing in endoplasmic reticulum	0	0	0	0	0	-1	0	-5	0	-6	0	-1
	RNA polymerase	0	0	1	0	0	0	0	0	0	0	0	0
	RNA transport	0	0	1	0	0	0	0	0	1	-1	0	0
	Aminoacyl-tRNA biosynthesis	0	0	0	0	0	0	0	0	1	-1	0	0
	Basal transcription factors	0	0	0	0	1	0	0	0	0	0	1	0
	Nucleotide excision repair	0	0	0	0	0	0	0	0	0	0	1	0

Appendix 3

Table 44. All KEGG pathways associated with differentially expressed transcripts in the hyposalinity trial (Chapter 2) from different sizes and populations (A = adult; S = seed; MW = March Water; StM = St. Mary's Bay).

Category	Pathway	A		MW A		StM A		S		MW S		StM S	
		+	-	+	-	+	-	+	-	+	-	+	-
Amino acid metabolism	Cysteine and methionine metabolism	0	0	0	-1	0	0	0	-1	1	0	0	-1
	Arginine and proline metabolism	0	0	0	0	2	0	0	0	0	0	0	0
	Biosynthesis of amino acids	0	0	1	0	1	0	0	0	0	0	0	0
	Tyrosine metabolism	0	0	0	-1	1	0	0	0	0	0	0	0
	Glycine, serine and threonine metabolism	0	0	0	-1	0	0	0	0	0	0	0	0
	Valine, leucine and isoleucine degradation	0	0	0	0	1	0	0	0	0	0	0	0
Carbohydrate metabolism	Amino sugar and nucleotide sugar metabolism	0	0	0	0	0	0	1	0	0	0	0	0
	Pentose and glucuronate interconversions	1	0	0	0	0	0	0	0	0	0	0	0
	Citrate cycle (TCA cycle)	0	0	1	0	0	-1	0	0	1	0	0	0
	Pyruvate metabolism	0	0	0	0	0	-1	0	0	1	0	0	0
	Glycolysis / Gluconeogenesis	0	0	0	0	1	0	0	0	0	0	0	0
	Starch and sucrose metabolism	0	0	0	0	1	0	0	0	0	0	0	0
	Glyoxylate and dicarboxylate metabolism	0	0	0	0	0	0	0	0	1	0	0	0
	Inositol phosphate metabolism	0	0	0	0	1	0	0	0	0	0	0	0
Glycan metabolism	Other glycan degradation	1	0	0	-1	1	0	0	0	0	0	0	0
	Glycosphingolipid biosynthesis-lacto and neolacto series	0	-1	0	0	1	0	0	0	0	0	0	0
	Various types of N-glycan biosynthesis	0	-1	1	-1	0	0	0	0	0	0	0	0
	Glycosphingolipid biosynthesis-globo and isoglobo series	0	0	0	-1	1	0	0	0	0	0	0	0

Category	Pathway	A		MW A		StM A		S		MW S		StM S	
		+	-	+	-	+	-	+	-	+	-	+	-
	Glycosaminoglycan degradation	0	0	0	-1	0	0	0	0	0	0	0	0
	Glycosphingolipid biosynthesis-ganglio series	0	0	0	-1	0	0	0	0	0	0	0	0
	Mucin type O-glycan biosynthesis	0	0	0	0	1	0	0	0	0	0	0	0
	N-Glycan biosynthesis	0	0	1	0	0	0	0	0	0	0	0	0
	Other types of O-glycan biosynthesis	0	0	0	0	1	0	0	0	0	0	0	0
Lipid metabolism	Sphingolipid metabolism	1	0	0	0	0	0	1	0	0	0	0	0
	Linoleic acid metabolism	1	0	0	0	0	0	0	0	0	0	0	0
	Glycerophospholipid metabolism	0	-1	0	0	1	0	0	0	0	0	0	-1
	Arachidonic acid metabolism	0	0	0	0	1	0	0	0	0	-1	0	0
	alpha-Linolenic acid metabolism	0	0	0	0	2	0	0	0	0	0	0	0
	Ether lipid metabolism	0	0	0	0	1	0	0	0	0	0	0	-1
	Biosynthesis of unsaturated fatty acids	0	0	0	0	1	0	0	0	0	0	0	0
	Fatty acid degradation	0	0	0	0	1	0	0	0	0	0	0	0
	Fatty acid metabolism	0	0	0	0	1	0	0	0	0	0	0	0
	Glycerolipid metabolism	0	0	0	0	1	0	0	0	0	0	0	0
	Glycosphingolipid biosynthesis	0	0	0	0	0	0	0	0	1	0	0	0
	Steroid biosynthesis	0	0	0	0	0	0	0	0	0	0	0	-1
	Terpenoid backbone biosynthesis	0	0	0	0	0	-1	0	0	0	0	1	0
Other metabolism	Drug metabolism-other enzymes	2	0	0	0	2	0	1	0	0	0	0	0
	Metabolism of xenobiotics by cytochrome P450	1	0	0	0	0	0	1	0	1	0	0	0
	Drug metabolism-cytochrome P450	0	0	0	0	0	0	1	0	1	0	0	0
	Glutathione metabolism	0	0	0	0	0	0	1	0	2	0	0	0
	Oxidative phosphorylation	1	-1	0	0	9	-1	0	0	0	0	0	0
	Purine metabolism	0	-1	0	0	1	0	0	0	0	0	0	-1
	Sulfur metabolism	0	0	0	0	0	0	0	-1	0	0	0	0

Category	Pathway	A		MW A		StM A		S		MW S		StM S	
		+	-	+	-	+	-	+	-	+	-	+	-
	Retinol metabolism	1	0	0	0	0	0	0	0	0	0	0	0
Cellular Process	Lysosome	2	0	1	-1	6	0	2	0	1	0	0	0
	Endocytosis	0	0	0	0	3	-1	2	0	0	0	0	0
	Mitophagy-animal	0	0	0	0	1	0	1	0	0	0	0	0
	Phagosome	1	-1	0	0	5	0	1	0	0	0	0	0
	Peroxisome	0	-1	0	0	2	0	0	0	0	0	0	-1
	Autophagy-animal	0	0	0	0	1	0	0	0	1	0	0	0
	Proteasome	0	0	0	0	2	0	0	0	0	0	0	0
	Protein export	0	0	0	0	1	0	0	0	0	0	0	0
Environmental Information Processing	mTOR signaling pathway	0	-1	0	0	1	0	0	0	1	0	0	0
	Wnt signaling pathway	0	-1	0	0	0	0	0	0	1	0	0	0
	ABC transporters	0	0	0	0	1	0	0	0	0	0	0	0
	Fanconi anemia pathway	0	0	0	0	0	0	0	0	0	0	1	0
	Nucleotide excision repair	0	0	0	0	1	0	0	0	0	0	0	0
	Notch signaling pathway	0	0	0	-1	1	0	0	0	0	0	1	0
	Phosphatidylinositol signaling system	0	0	0	0	0	0	0	0	0	-1	1	0
	FoxO signaling pathway	0	0	0	0	1	0	0	0	0	0	0	0
	TGF-beta signaling pathway	0	0	0	0	1	0	0	0	0	0	0	0
Genetic Information Processing	Protein processing in endoplasmic reticulum	0	0	1	0	2	-2	2	0	0	0	0	0
	Ubiquitin mediated proteolysis	0	0	0	-1	5	-2	2	0	0	-1	0	0
	ECM-receptor interaction	0	0	0	0	1	0	1	0	0	0	0	-1
	Neuroactive ligand-receptor interaction	0	0	0	0	0	0	1	0	0	-1	0	0
	Base excision repair	0	0	0	0	1	0	1	0	0	0	0	0
	Ribosome biogenesis in eukaryotes	0	0	0	0	0	0	1	0	0	0	0	0
	mRNA surveillance pathway	0	0	0	0	0	0	1	-1	0	0	0	0
	Spliceosome	0	-1	0	0	1	-1	1	0	0	0	0	0
	DNA replication	0	-1	0	0	1	-1	0	0	0	0	0	0
	Nucleocytoplasmic transport	0	-2	0	0	0	0	1	0	0	0	0	0
	Ribosome	0	-4	0	0	3	-2	0	0	0	0	1	0

Appendix 4

Table 45. concentration of food being fed to adult and seed mussel every hour for each food ration (1%, 5%, 10%) in food availability trials (Chapter 4).

Ration	Adult feed concentration (cells/mL/h)	Seed feed concentration (cells/mL/h)
0–24 h (28 individual per tank)		
1% BW	~ 18,000	~ 3000
5% BW	~ 93,000	~ 15,000
10% BW	~ 180,000	~ 31,000
24–48 h (16 individuals per tank)		
1% BW	~ 10,000	~ 1,800
5% BW	~ 53,000	~ 9,000
10% BW	~ 106,000	~ 18,000

Appendix 5

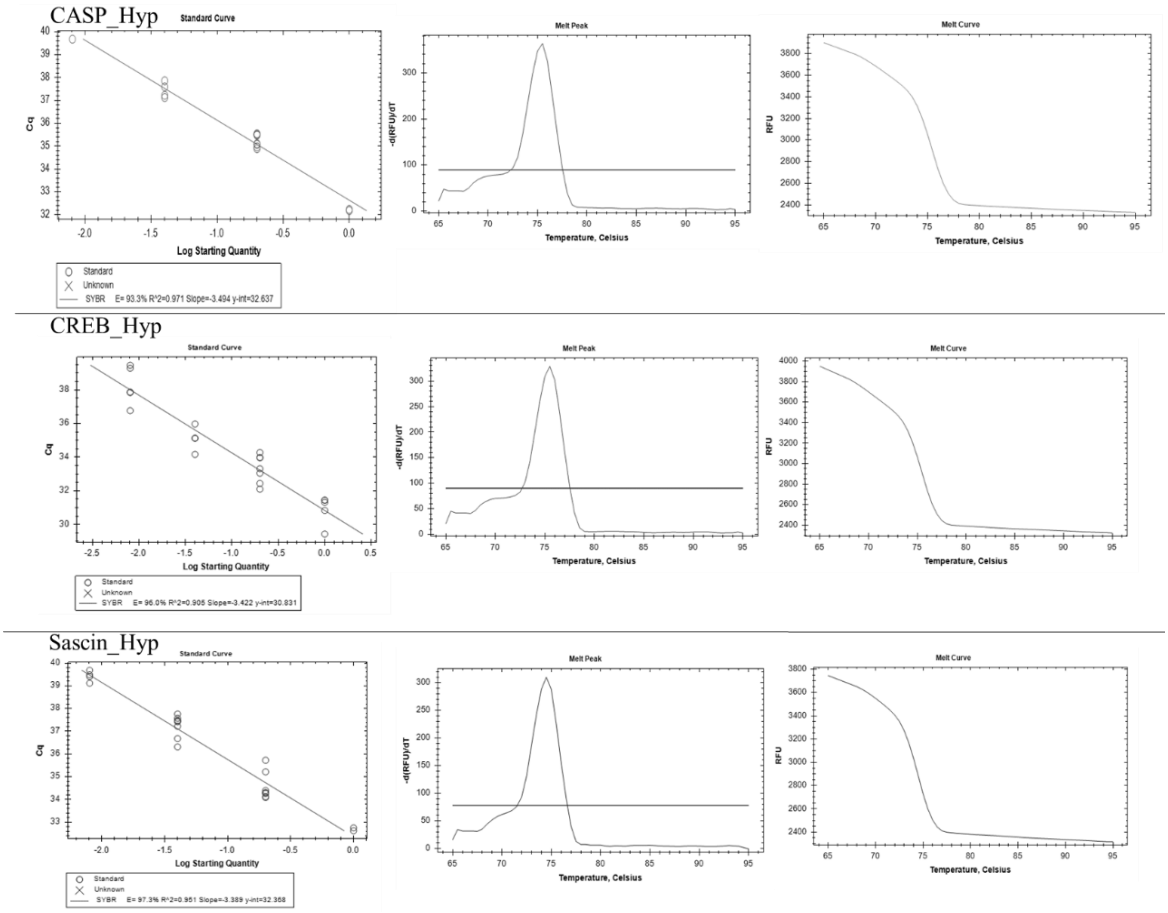

Figure 25. Standard curve of efficiency, melt peak and melt curve of each successfully verified primer associated with acute hypoxia (Chapter 5).

Appendix 6

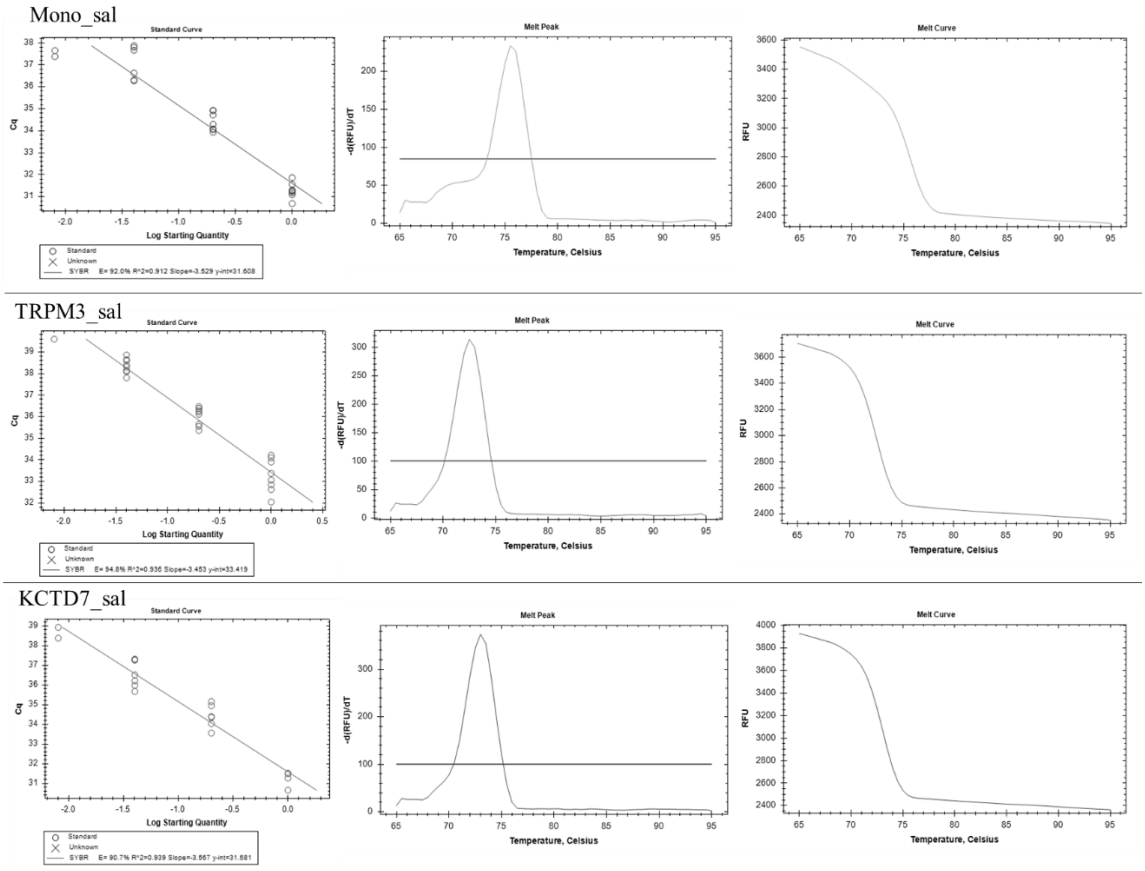

Figure 26. Standard curve of efficiency, melt peak and melt curve of each successfully verified primer associated with acute hyposalinity (Chapter 5).

Appendix 7

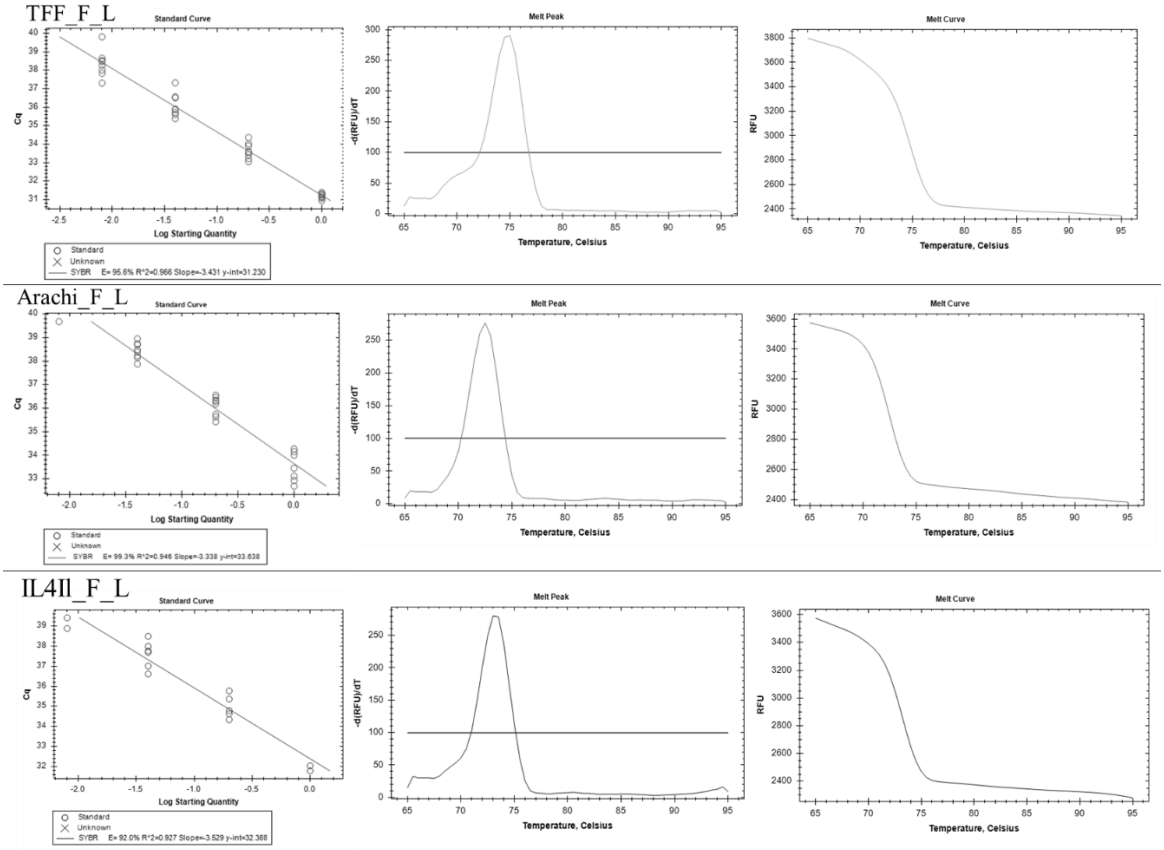

Figure 27. Standard curve of efficiency, melt peak and melt curve of each successfully verified primer associated with low food availability (Chapter 5).

Appendix 8

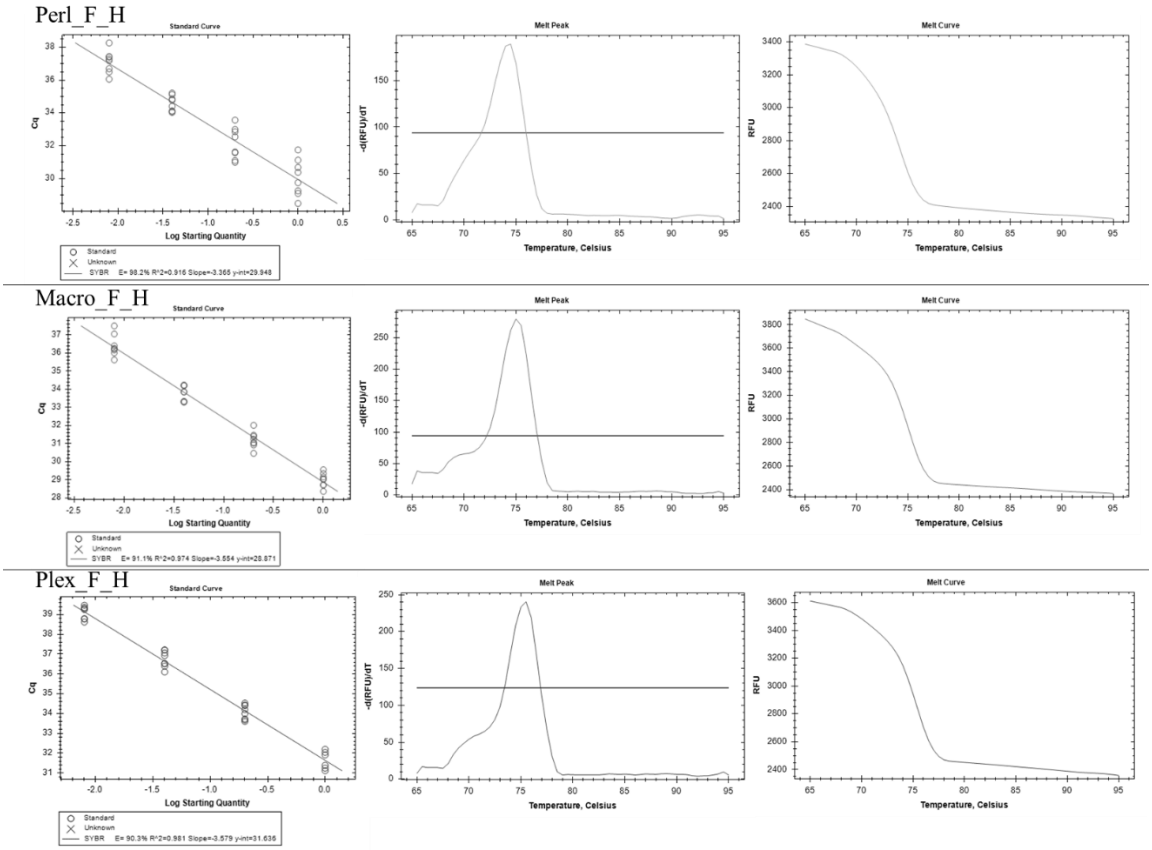

Figure 28. Standard curve of efficiency, melt peak and melt curve of each successfully verified primer associated with high food availability (Chapter 5).

Appendix 9

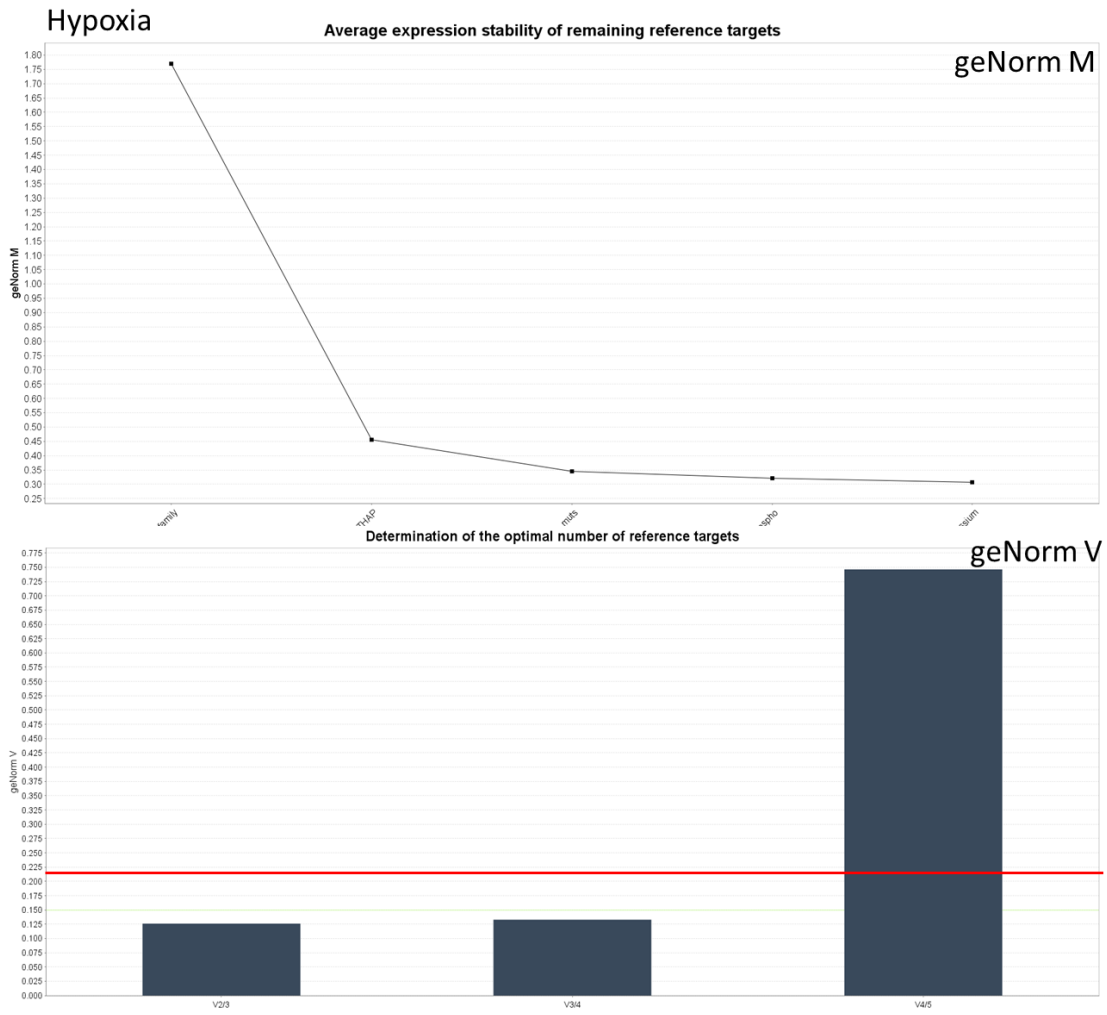

Figure 29. GeNorm algorithm indicating the ideal number of reference genes to utilize for normalization of RT-qPCR data for hypoxia primers (Chapter 5).

Appendix 10

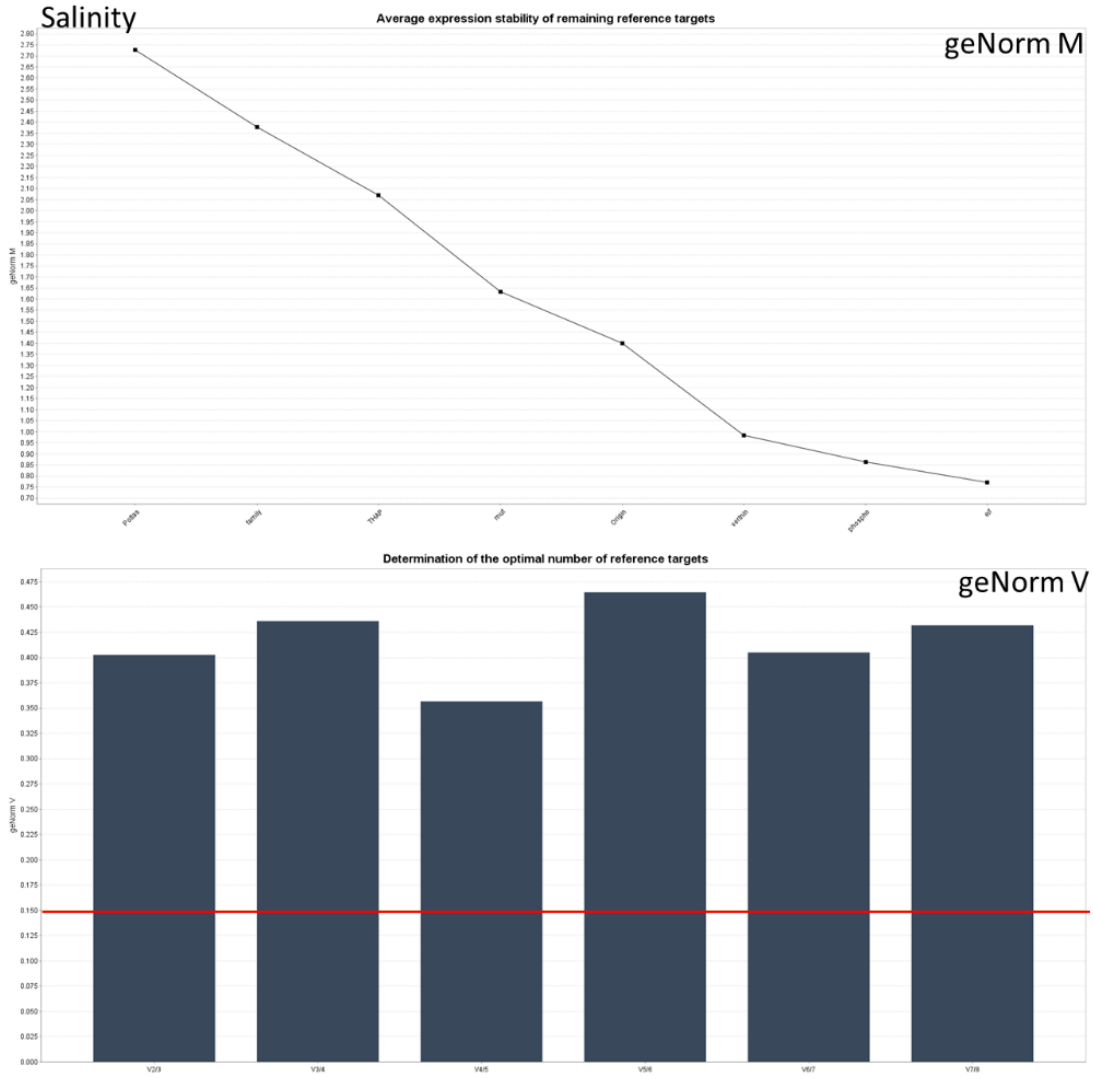

Figure 30. GeNorm algorithm indicating the ideal number of reference genes to utilize for normalization of RT-qPCR data in the hyposalinity primers (Chapter 5).

Appendix 11

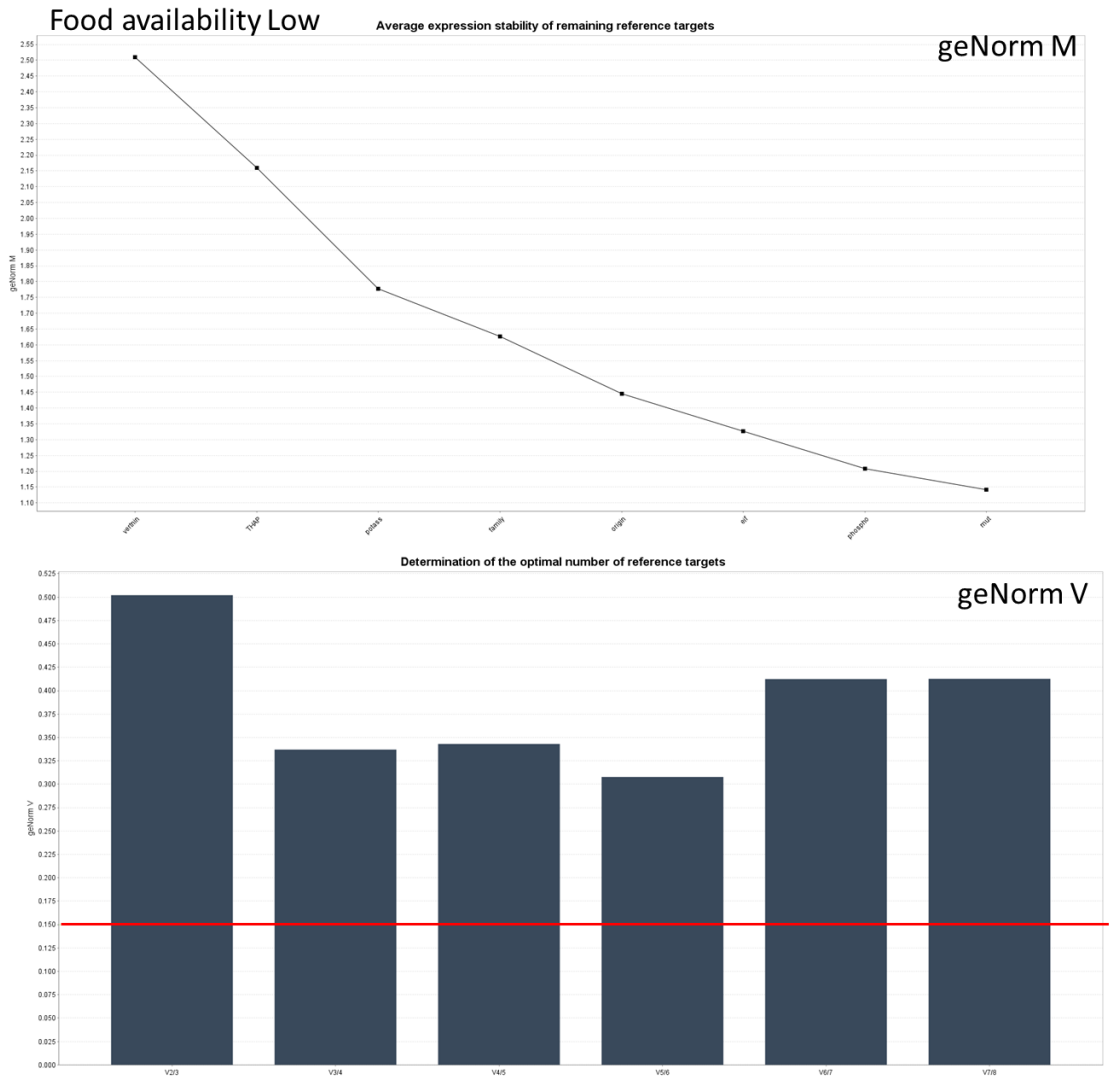

Figure 31. GeNorm algorithm indicating the ideal number of reference genes to utilize for normalization of RT-qPCR data for low food availability primers (Chapter 5).

Appendix 12

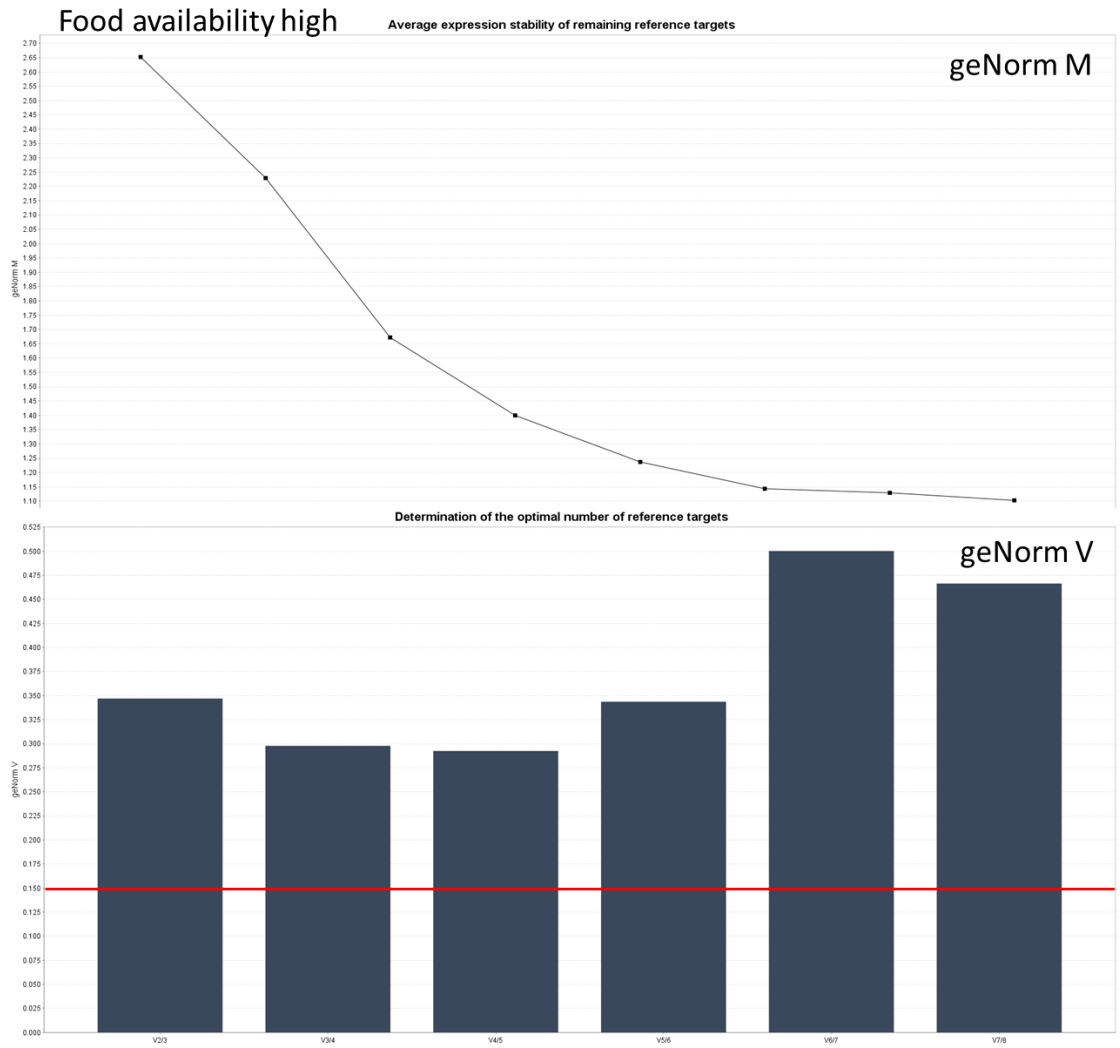

Figure 32. GeNorm algorithm indicating the ideal number of reference genes to utilize for normalization of RT-qPCR data for high food availability primers (Chapter 5).

Bibliography:

Abele, D., and Puntarulo, S. 2004. Formation of reactive species and induction of antioxidant defence systems in polar and temperate marine invertebrates and fish. Comparative Biochemistry and Physiology. Part A, Molecular & Integrative Physiology 138: 405–415. doi:10.1016/j.cbpb.2004.05.013.

Abuammar, H., Bhattacharjee, A., Simon-Vecsei, Z., Blastyák, A., Csordás, G., Páli, T., and Juhász, G. 2021. Ion channels and pumps in autophagy: a reciprocal relationship. Cells 10(12): 3537. doi:10.3390/cells10123537.

Afgan, E., Baker, D., Batut, B., van den Beek, M., Bouvier, D., Čech, M., Chilton, J., Clements, D., Coraor, N., Grüning, B.A., Guerler, A., Hillman-Jackson, J., Hiltemann, S., Jalili, V., Rasche, H., Soranzo, N., Goecks, J., Taylor, J., Nekrutenko, A., and Blankenberg, D. 2018. The Galaxy platform for accessible, reproducible and collaborative biomedical analyses: 2018 update. Nucleic Acids Research 46: W537–W544. doi:10.1093/nar/gky379.

Aihara, E., Engevik, K.A., and Montrose, M.H. 2017. Trefoil factor peptides and gastrointestinal function. Annual Review of Physiology 79: 357–380. doi:10.1146/annurev-physiol-021115-105447.

Akashige, S., and Fushimi, T. 1992. Growth, survival, and glycogen content of triploid pacific oyster *Crassostrea gigas* in the waters of Hiroshima, Japan. Nippon Suisan Gakkaishi 58: 1063–1071.

Allam, B., and Pales Espinosa, E. 2016. Bivalve immunity and response to infections: Are we looking at the right place? Fish & Shellfish Immunology 53: 4–12. doi:10.1016/j.fsi.2016.03.037.

Allam, S., Allam, B., and Pales Espinosa, E. 2021. Regulation of mucosal lectins in the oyster *Crassostrea virginica* in response to food availability and environmental factors. Journal of Molluscan Studies 87(1): eyaa037. doi:10.1093/mollus/eyaa037.

Almeida, E.A., Bainy, A.C.D., Dafre, A.L., Gomes, O.F., Medeiros, M.H.G., and Mascio, P. 2005. Oxidative stress in digestive gland and gill of the brown mussel (*Perna perna*) exposed to air and re-submersed. Journal of Experimental Marine Biology and Ecology 318: 21–30. doi:10.1016/j.jembe.2004.12.007.

Al-Subiai, S.N., Moody, A.J., Mustafa, S.A., and Jha, A.N. 2011. A multiple biomarker approach to investigate the effects of copper on the marine bivalve mollusc, *Mytilus edulis*. Ecotoxicology and Environmental Safety 74: 1913–1920. doi:10.1016/j.ecoenv.2011.07.012.

Altieri, A.H. 2006. Inducible variation in hypoxia tolerance across the intertidal–subtidal distribution of the blue mussel *Mytilus edulis*. Marine Ecology Progress Series 325: 295–300. doi:10.3354/meps325295.

Amanullah, A., Azam, N., Balliet, A., Hollander, C., Hoffman, B., Fornace, A., and Liebermann, D. 2003. Cell survival and a Gadd45-factor deficiency. Nature 424: 741–741. doi:10.1038/424741b.

Anderson, J.F. 2013. The role of sacsin as a molecular chaperone. Doctor of Philosophy, University of Texas Medical Branch, Texas, USA.

Anderson, P., and Kedersha, N. 2002. Stressful initiations. Journal of Cell Science 115: 3227–3234.

Andrade, M., De Marchi, L., Pretti, C., Chiellini, F., Morelli, A., Soares, A.M.V.M., Rocha, R.J.M., Figueira, E., and Freitas, R. 2018. Are the impacts of carbon nanotubes enhanced in *Mytilus galloprovincialis* submitted to air exposure? Aquatic Toxicology 202: 163–172. doi:10.1016/j.aquatox.2018.07.006.

Andrade, M., De Marchi, L., Soares, A.M.V.M., Rocha, R.J.M., Figueira, E., and Freitas, R. 2019. Are the effects induced by increased temperature enhanced in *Mytilus galloprovincialis* submitted to air exposure? Science of The Total Environment 647: 431–440. doi:10.1016/j.scitotenv.2018.07.293.

Andrews, S. 2018. FastQC A quality control tool for high throughput sequence data. Babraham Bioinformatics. [Online] https://www.bioinformatics.babraham.ac.uk/projects/fastqc/

Anestis, A., Lazou, A., Pörtner, H.O., and Michaelidis, B. 2007. Behavioral, metabolic, and molecular stress responses of marine bivalve *Mytilus galloprovincialis* during long-term acclimation at increasing ambient temperature. American Journal of Physiology. Regulatory, Integrative and Comparative Physiology 293: R911-921. doi:10.1152/ajpregu.00124.2007.

Anestis, A., Pörtner, H.O., and Michaelidis, B. 2010. Anaerobic metabolic patterns related to stress responses in hypoxia exposed mussels *Mytilus galloprovincialis*. Journal of Experimental Marine Biology and Ecology 394: 123–133. doi:10.1016/j.jembe.2010.08.008.

Arivalagan, J., Marie, B., Chiappetta, G., Vinh, J., Gallet, X., Lebon, M., M'Zoudi, S., Dubois, P., Berland, S., and Marie, A. 2020. Deciphering shell proteome within different Baltic populations of mytilid mussels illustrates important local variability and potential consequences in the context of changing marine conditions. Science of The Total Environment 745: 140878. doi:10.1016/j.scitotenv.2020.140878.

Arivalagan, J., Yarra, T., Marie, B., Sleight, V.A., Duvernois-Berthet, E., Clark, M.S., Marie, A., and Berland, S. 2017. Insights from the shell proteome: biomineralization to adaptation. Molecular Biology and Evolution 34: 66–77. doi:10.1093/molbev/msw219.

Artigaud, S., Lacroix, C., Richard, J., Flye-Sainte-Marie, J., Bargelloni, L., and Pichereau, V. 2015. Proteomic responses to hypoxia at different temperatures in the great scallop (*Pecten maximus*). PeerJ 3: e871. doi:10.7717/peerj.871.

Attig, H., Kamel, N., Sforzini, S., Dagnino, A., Jamel, J., Boussetta, H., Viarengo, A., and Banni, M. 2014. Effects of thermal stress and nickel exposure on biomarkers responses in *Mytilus galloprovincialis* (Lam). Marine Environmental Research 94: 65–71. doi:10.1016/j.marenvres.2013.12.006.

Babarro, J.M.F., and Carrington, E. 2013. Attachment strength of the mussel *Mytilus galloprovincialis*: effect of habitat and body size. Journal of Experimental Marine Biology and Ecology 443: 188–196. doi:10.1016/j.jembe.2013.02.035.

Babarro, J.M.F., Reiriz, M.J.F., and Labarta, U. 2008. Secretion of byssal threads and attachment strength of *Mytilus galloprovincialis*: the influence of size and food availability. Journal of the Marine Biological Association of the United Kingdom 88: 783–791. doi:10.1017/S0025315408001367.

Bahmet, I.N., Berger, V.J., and Halaman, V.V. 2005. Heart rate in the blue mussel *Mytilus edulis* (Bivalvia) under salinity change. Russian Journal of Marine Biology 31: 314–317.

Bakhmet, I., Nikolaev, K., Levakin, I., and Ekimov, D. 2019. Influence of *Himasthla elongata* (Trematoda: Echinostomatidae) metacercariae on heart rate in blue mussels (*Mytilus edulis*). Journal of Invertebrate Pathology 166: 107220. doi:10.1016/j.jip.2019.107220.

Bakhmet, I.N. 2017. Cardiac activity and oxygen consumption of blue mussels (*Mytilus edulis*) from the White Sea in relation to body mass, ambient temperature and food availability. Polar Biology 40: 1959–1964. doi:10.1007/s00300-017-2111-6.

Bakhmet, I.N., Berger, V.Ja., and Khalaman, V.V. 2005. The effect of salinity change on the heart rate of *Mytilus edulis* specimens from different ecological zones. Journal of Experimental Marine Biology and Ecology 318: 121–126. doi:10.1016/j.jembe.2004.11.023.

Barrett, A.J., and Kirschke, H. 1981. Cathepsin B, cathepsin H, and cathepsin L. Pages 535–561 in Methods in Enzymology. Academic Press. doi:10.1016/S0076-6879(81)80043-2.

Barrett, N.J., Thyrring, J., Harper, E.M., Sejr, M.K., Sørensen, J.G., Peck, L.S., and Clark, M.S. 2022. Molecular responses to thermal and osmotic stress in Arctic intertidal mussels (*Mytilus edulis*): the limits of resilience. Genes 13(1): 155. doi:10.3390/genes13010155.

Barton, A.D., Irwin, A.J., Finkel, Z.V., and Stock, C.A. 2016. Anthropogenic climate change drives shift and shuffle in North Atlantic phytoplankton communities. Proceedings of the National Academy of Sciences 113: 2964–2969.

Battle, H.I. 1932. Rhythmic sexual maturity and spawning of certain bivalve mollusks. Contributions to Canadian Biology and Fisheries 7: 255–276. doi:10.1139/f32-020.

Bayne, B.L. 1971. Ventilation, the heart beat and oxygen uptake by *Mytilus edulis L*. in declining oxygen tension. Comparative Biochemistry and Physiology Part A: Physiology 40: 1065–1085. doi:10.1016/0300-9629(71)90295-7.

Bayne, B.L. 1972. Some effects of stress in the adult on the larval development of *Mytilus edulis*. Nature 237: 459–459. doi:10.1038/237459a0.

Bayne, B.L. 1976. The biology of mussel larvae. Pages 81–115 in B.L. Bayne, ed. Marine mussels: their ecology and physiology. Cambridge University Press, Melbourne, Australia.

Bayne, B.L. 2004. Phenotypic flexibility and physiological tradeoffs in the feeding and growth of marine bivalve molluscs. Integrative and Comparative Biology 44: 425–432. doi:10.1093/icb/44.6.425.

Bayne, B.L. 2017. Biology of oysters. Academic Press.

Bayne, B.L., and Hawkins, A.J.S. 1997. Protein metabolism, the costs of growth, and genomic heterozygosity: Experiments with the mussel *Mytilus galloprovincialis* Lmk. Physiological Zoology 70: 391–402. doi:10.1086/515848.

Bayne, B.L., Klumpp, D.W., and Clarke, K.R. 1984. Aspects of feeding, including estimates of gut residence time, in three mytilid species (Bivalvia, Mollusca) at two contrasting sites in the Cape Peninsula, South Africa. Oecologia 64: 26–33. doi:10.1007/BF00377539.

Bayne, B.L., Moore, M.N., and Koehn, R.K. 1981. Lysosomes and the response by *Mytilus edulis* L. to an increase in salinity. Marine Biology Letters 4: 193–204.

Bayne, B.L., Salkeld, P.N., and Worrall, C.M. 1983. Reproductive effort and value in different populations of the marine mussel, *Mytilus edulis* L. Oecologia 59: 18–26. doi:10.1007/BF00388067.

Bayne, B.L., Thompson, R.J., and Widdows, J. 1973. Some effects of temperature and food on the rate of oxygen consumption by *Mytilus edulis*. Pages 181–193 in W. Wieser, ed. Effects of temperature on ectothermic organisms. Springer, Berlin, Heidelberg.

Beadman, H., Caldow, R., Kaiser, M., and Willows, R. 2003. How to toughen up your mussels: using mussel shell morphological plasticity to reduce predation losses. Marine Biology 142: 487–494. doi:10.1007/s00227-002-0977-4.

Bedoui, S., Herold, M.J., and Strasser, A. 2020. Emerging connectivity of programmed cell death pathways and its physiological implications. Nature Reviews Molecular Cell Biology 21: 678–695. doi:10.1038/s41580-020-0270-8.

Bolger, A.M., Lohse, M., and Usadel, B. 2014. Trimmomatic: a flexible trimmer for Illumina sequence data. Bioinformatics 30: 2114–2120. doi:10.1093/bioinformatics/btu170.

Belyi, V.A., Ak, P., Markert, E., Wang, H., Hu, W., Puzio-Kuter, A., and Levine, A.J. 2010. The origins and evolution of the p53 family of genes. Cold Spring Harbor Perspectives in Biology 2: a001198. doi:10.1101/cshperspect.a001198.

Benes, P., Vetvicka, V., and Fusek, M. 2008. Cathepsin D—Many functions of one aspartic protease. Critical Reviews in Oncology/Hematology 68: 12–28. doi:10.1016/j.critrevonc.2008.02.008.

Beninger, P.G., Veniot, A., and Poussart, Y. 1999. Principles of pseudofeces rejection on the bivalve mantle: integration in particle processing. Marine Ecology Progress Series 178: 259–269. doi:10.3354/meps178259.

Bernier, R., Jamieson, R., and Moore, A. 2018. State of the Atlantic Ocean synthesis report. Canadian Technical Report of Fisheries and Aquatic Sciences 3167: iii +: 149.

Bi, J., Ning, M., Xie, X., Fan, W., Huang, Y., Gu, W., Wang, W., Wang, L., and Meng, Q. 2020. A typical C-type lectin, perlucin-like protein, is involved in the innate immune defense of whiteleg shrimp *Litopenaeus vannamei*. Fish & Shellfish Immunology 103: 293–301. doi:10.1016/j.fsi.2020.05.046.

Bindoff, N.L., Cheung, W.W.L., Kairo, J.G., Arístegui, J., Guinder, V.A., Hallberg, R., Hilmi, N., Jiao, N., O'Donoghue, S., Suga, T., Acar, S., Alava, J.J., Allison, E., Arbic, B., Bambridge, T., Boyd, P.W., Bruggeman, J., Butenschön, M., Chávez, F.P., Cheng, L., Cinar, M., Costa, D., Defeo, O., Djoundourian, S., Domingues, C., Eddy, T., Endres, S., Fox, A., Free, C., Frölicher, T., Gattuso, J.-P., Gerber, G., Hallegraef, G., Harrison, M., Hennige, S., Hindell, M., Hogg, A., Ito, T., Kenny, T.-A., Kroeker, K., Kwiatkowski, L., Lam, V.W.Y., Laüfkotter, C., LeBillon, P., Bris, N.L., Lotze, H., MacKinnon, J., de Marffy-Mantuano, A., Martel, P., Molinos, J.G., Moseman-Valtierra, S., Motau, A., Mulsow, S., Mutombo, K., Oyinlola, M., Poloczanska, E.S., Pascal, N., Philip, M., Purkey, S., Rathore, S., Rebelo, X., Reygondeau, G., Rice, J., Richardson, A., Riebesell, U., Roach, C., Rocklöv, J., Roberts, M., Sloyan, B., Smith, M., Shurety, A., Wabnitz, C., and Whalen, C. 2019. Changing ocean, marine ecosystems, and dependent communities. IPCC special report on the ocean and cryosphere in a changing climate: 477–587.

Blagden, C.S., Currie, P.D., Ingham, P.W., and Hughes, S.M. 1997. Notochord induction of zebrafish slow muscle mediated by sonic hedgehog. Genes & Development 11: 2163–2175. doi:10.1101/gad.11.17.2163.

Bocquené, G., Chantereau, S., Clérendeau, C., Beausir, E., Ménard, D., Raffin, B., Minier, C., Burgeot, T., Leszkowicz, A.P., and Narbonne, J.-F. 2004. Biological effects of the "Erika" oil spill on the common mussel (*Mytilus edulis*). Aquatic Living Resources 17: 309–316. doi:10.1051/alr:2004033.

Boedigheimer, M.J., Wolfinger, R.D., Bass, M.B., Bushel, P.R., Chou, J.W., Cooper, M., Corton, J.C., Fostel, J., Hester, S., Lee, J.S., Liu, F., Liu, J., Qian, H.-R., Quackenbush, J., Pettit, S., and Thompson, K.L. 2008. Sources of variation in baseline gene expression levels from toxicogenomics study control animals across multiple laboratories. BMC Genomics 9: 285. doi:10.1186/1471-2164-9-285.

Booth, C.E., McDonald, D.G., and Walsh, P.J. 1984. Acid-base balance in the sea mussel, *Mytilus edulis*. I. Effects of hypoxia and air-exposure on hemolymph acid-base status. Marine Biology Letters 5: 347–358.

Bordin, S., and Tan, X. 2001. C1q arrests the cell cycle progression of fibroblasts in G1 phase: role of the cAMP/PKA-I pathway. Cellular Signalling 13: 119–123. doi:10.1016/S0898-6568(00)00139-X.

Borenfreund, E., and Puerner, J.A. 1985. Toxicity determined in vitro by morphological alterations and neutral red absorption. Toxicology letters 24: 119–124.

Bougrier, S., Hawkins, A.J.S., and Héral, M. 1997. Preingestive selection of different microalgal mixtures in *Crassostrea gigas* and *Mytilus edulis*, analysed by flow cytometry. Aquaculture 150: 123–134. doi:10.1016/S0044-8486(96)01457-3.

Bray, N.L., Pimentel, H., Melsted, P., and Pachter, L. 2016. Near-optimal probabilistic RNA-seq quantification. Nature Biotechnology 34: 525–527. doi:10.1038/nbt.3519.

Braby, C., and Somero, G. 2006. Following the heart: temperature and salinity effects on heart rate in native and invasive species of blue mussels (genus *Mytilus).* Journal of Experimental Biology 209: 2554–2566. doi:10.1242/jeb.02259.

Brenko, M.H., and Calabrese, A. 1969. The combined effects of salinity and temperature on larvae of the mussel *Mytilus edulis*. Marine Biology 4: 224–226.

Broderick, N.A. 2015. A common origin for immunity and digestion. Frontiers in Immunology 6: 1–3. doi:10.3389/fimmu.2015.00072.

Brown, A.D., and Simpson, J.R. 1972. Water relations of sugar-tolerant yeasts: the role of intracellular polyols. Journal of General Microbiology 72: 589–591. doi:10.1099/00221287-72-3-589.

Brun, N.T., Ross, N.W., and Boghen, A.D. 2000. Changes in the electrophoretic profiles of gill mucus proteases of the Eastern oyster *Crassostrea virginica* in response to infection by the Turbellarian *Urastoma cyprinae*. Journal of Invertebrate Pathology 75: 163–170. doi:10.1006/jipa.1999.4917.Bryant, D.M., Johnson, K., DiTommaso, T., Tickle, T., Couger, M.B., Payzin-Dogru, D., Lee, T.J., Leigh, N.D., Kuo, T.-H., Davis, F.G., Bateman, J., Bryant, S., Guzikowski, A.R., Tsai, S.L., Coyne, S., Ye, W.W., Freeman, R.M., Peshkin, L., Tabin, C.J., Regev, A., Haas, B.J., and Whited, J.L. 2017. A tissue-mapped Axolotl *de novo* transcriptome enables identification of limb regeneration factors. Cell Reports 18: 762–776. Elsevier. doi:10.1016/j.celrep.2016.12.063.

Bubel, A. 1976. An electron microscope study of the formation of the periostracum in the freshwater bivalve, *Anodonta cygnea*. Journal of Zoology 180: 211–232. doi:10.1111/j.1469-7998.1976.tb04674.x.

Burnett, N.P., Seabra, R., de Pirro, M., Wethey, D.S., Woodin, S.A., Helmuth, B., Zippay, M.L., Sara, G., Monaco, C., and Lima, F.P. 2013. An improved noninvasive method for measuring heartbeat of intertidal animals. Limnology and Oceanography: Methods 11: 91–100. doi:10.4319/lom.2013.11.91

Buzzelli, C.P., Jr, R.A.L., Powers, S.P., Peterson, C.H., McNinch, J.E., Pinckney, J.L., and Paerl, H.W. 2002. Estimating the spatial extent of bottom-water hypoxia and habitat degradation in a shallow estuary. Marine Ecology Progress Series 230: 103–112. doi:10.3354/meps230103.

Cabré, A., Marinov, I., and Leung, S. 2015. Consistent global responses of marine ecosystems to future climate change across the IPCC AR5 earth system models. Climate Dynamics 45: 1253–1280. doi:10.1007/s00382-014-2374-3.

Camacho, C., Coulouris, G., Avagyan, V., Ma, N., Papadopoulos, J., Bealer, K., and Madden, T.L. 2009. BLAST+: architecture and applications. BMC Bioinformatics 10: 421. doi:10.1186/1471-2105-10-421.

Canesi, L., Barmo, C., Fabbri, R., Ciacci, C., Vergani, L., Roch, P., and Gallo, G. 2010. Effects of vibrio challenge on digestive gland biomarkers and antioxidant gene expression in *Mytilus galloprovincialis*. Comparative Biochemistry and Physiology Part C: Toxicology & Pharmacology 152: 399–406. doi:10.1016/j.cbpc.2010.06.008.

Canesi, L., Betti, M., Ciacci, C., Lorusso, L., Pruzzo, C., and Gallo, G. 2006. Cell signalling in the immune response of mussel hemocytes. Invertebrate Survival Journal 3: 40–49.

Capelle, J.J., Hartog, E., van den Bogaart, L., Jansen, H.M., and Wijsman, J.W.M. 2021. Adaptation of gill-palp ratio by mussels after transplantation to culture plots with different seston conditions. Aquaculture 541: 736794. doi:10.1016/j.aquaculture.2021.736794.

Chapple, J.P., Smerdon, G.R., Berry, R.J., and Hawkins, A.J.S. 1998. Seasonal changes in stress-70 protein levels reflect thermal tolerance in the marine bivalve *Mytilus edulis* L. Journal of Experimental Marine Biology and Ecology 229: 53–68. doi:10.1016/S0022-0981(98)00040-9.

Châtel, A., Hamer, B., Jakšić, Ž., Vucelić, V., Talarmin, H., Dorange, G., Schröder, H.C., and Müller, W.E.G. 2011. Induction of apoptosis in mussel *Mytilus galloprovincialis* gills by model cytotoxic agents. Ecotoxicology 20: 2030–2041. doi:10.1007/s10646-011-0746-6.

Chen, H., Xin, L., Song, X., Wang, L., Wang, W., Liu, Z., Zhang, H., Wang, L., Zhou, Z., Qiu, L., and Song, L. 2017. A norepinephrine-responsive miRNA directly promotes CgHSP90AA1 expression in oyster haemocytes during desiccation. Fish & Shellfish Immunology 64: 297–307. doi:10.1016/j.fsi.2017.03.020.

Chen, J., Mai, K., Ma, H., Wang, X., Deng, D., Liu, X., Xu, W., Liufu, Z., Zhang, W., Tan, B., and Ai, Q. 2007a. Effects of dissolved oxygen on survival and immune responses of scallop (*Chlamys farreri*). Fish & Shellfish Immunology 22: 272–281. doi:10.1016/j.fsi.2006.06.003.

Chen, M., Yang, H., Delaporte, M., Zhao, S., and Xing, K. 2007b. Immune responses of the scallop *Chlamys farreri* after air exposure to different temperatures. Journal of Experimental Marine Biology and Ecology 345: 52–60. doi:10.1016/j.jembe.2007.01.007.

Chen, Y., Thai, P., Zhao, Y.-H., Ho, Y.-S., DeSouza, M.M., and Wu, R. 2003. Stimulation of airway mucin gene expression by interleukin (IL)-17 through IL-6 paracrine/autocrine loop. Journal of Biological Chemistry 278: 17036–17043. doi:10.1074/jbc.M210429200.

Cheung, W.W.L., Lam, V.W.Y., Sarmiento, J.L., Kearney, K., Watson, R., Zeller, D., and Pauly, D. 2010. Large-scale redistribution of maximum fisheries catch potential in the global ocean under climate change. Global Change Biology 16: 24–35. doi:10.1111/j.1365-2486.2009.01995.x.

Clark, M.S., Husmann, G., Thorne, M.A.S., Burns, G., Truebano, M., Peck, L.S., Abele, D., and Philipp, E.E.R. 2013. Hypoxia impacts large adults first: consequences in a warming world. Global Change Biology 19: 2251–2263. doi:10.1111/gcb.12197.

Clark, M.S., Peck, L.S., Arivalagan, J., Backeljau, T., Berland, S., Cardoso, J.C.R., Caurcel, C., Chapelle, G., De Noia, M., Dupont, S., Gharbi, K., Hoffman, J.I., Last, K.S., Marie, A., Melzner, F., Michalek, K., Morris, J., Power, D.M., Ramesh, K., Sanders, T., Sillanpää, K., Sleight, V.A., Stewart-Sinclair, P.J., Sundell, K., Telesca, L., Vendrami, D.L.J., Ventura, A., Wilding, T.A., Yarra, T., and Harper, E.M. 2020. Deciphering mollusc shell production: the roles of genetic mechanisms through to ecology, aquaculture and biomimetics. Biological Reviews 95: 1812–1837. doi:10.1111/brv.12640.

Clark, M.S., Peck, L.S., and Thyrring, J. 2021. Resilience in Greenland intertidal *Mytilus*: the hidden stress defense. Science of The Total Environment 767: 144366. doi:10.1016/j.scitotenv.2020.144366.

Clark, M.S., Thorne, M.A.S., Burns, G., and Peck, L.S. 2016. Age-related thermal response: the cellular resilience of juveniles. Cell Stress and Chaperones 21: 75–85. doi:10.1007/s12192-015-0640-x.

Clements, J.C., Hicks, C., Tremblay, R., and Comeau, L.A. 2018. Elevated seawater temperature, not pCO2, negatively affects post-spawning adult mussels (*Mytilus edulis*) under food limitation. Conservation Physiology 6: cox078. doi:10.1093/conphys/cox078.

Clements, J.C., Poirier, L.A., Pérez, F.F., Comeau, L.A., and Babarro, J.M.F. 2020. Behavioural responses to predators in Mediterranean mussels (*Mytilus galloprovincialis*) are unaffected by elevated pCO2. Marine Environmental Research 161: 105148. doi:10.1016/j.marenvres.2020.105148.

Clements, J.C., Ramesh, K., Nysveen, J., Dupont, S., and Jutfelt, F. 2021. Animal size and sea water temperature, but not pH, influence a repeatable startle response behaviour in a wide-ranging marine mollusc. Animal Behaviour 173: 191–205. doi:10.1016/j.anbehav.2020.12.008.

Cline, W.R. 1991. Scientific basis for the greenhouse effect. The Economic Journal 101: 904–919. doi:10.2307/2233863.

Cock, P.J.A., Chilton, J.M., Grüning, B., Johnson, J.E., and Soranzo, N. 2015. NCBI BLAST+ integrated into Galaxy. Gigascience 4. doi:10.1186/s13742-015-0080-7.

Coffin, M.R.S., Clements, J.C., Comeau, L.A., Guyondet, T., Maillet, M., Steeves, L., Winterburn, K., Babarro, J.M.F., Mallet, M.A., Haché, R., Poirier, L.A., Deb, S., and Filgueira, R. 2021. The killer within: endogenous bacteria accelerate oyster mortality during sustained anoxia. Limnology and Oceanography 9999: 1–16. doi:10.1002/lno.11798.

Coleman, N., and Trueman, E.R. 1971. The effect of aerial exposure on the activity of the mussels *Mytilus edulis L.* and *Modiolus modiolus* (L.). Journal of Experimental Marine Biology and Ecology 7: 295–304. doi:10.1016/0022-0981(71)90011-6.

Collicutt, J.M., and Hochachka, P.W. 1977. The anaerobic oyster heart: Coupling of glucose and aspartate fermentation. Journal of Comparative Physiology B 115: 147–157. doi:10.1007/BF00692526.

Collins, M., Peck, L.S., and Clark, M.S. 2021. Large within, and between, species differences in marine cellular responses: Unpredictability in a changing environment. Science of The Total Environment 794: 148594. doi:10.1016/j.scitotenv.2021.148594.

Collip, J. 1920. Studies on molluscan celomic fluid. Effect of change in environment on the carbon dioxide content of the celomic fluid. Anaerobic respiration in *Mya arenaria*. Journal of Biological Chemistry. 45: 23–49.

Collip, J.B. 1921. A further study of the respiratory processes in *Mya Arenaria* and other marine mollusca. Journal of Biological Chemistry 49: 297–310.

Comeau, L.A., Filgueira, Davidson, J., Nadeau, A., Guyondet, T., Sonier, R., Ramsay, A., and Davidson, J. 2017a. Population structure and grazing capacity of cultivated mussels in Prince Edward Island, Canada. Canadian Technical Report of Fisheries and Aquatic Sciences 3228: viii +: 23.

Comeau, L.A., Sonier, R., Guyondet, T., Landry, T., Ramsay, A., and Davidson, J. 2017b. Behavioural response of bivalve molluscs to calcium hydroxide. Aquaculture 466: 78–85. doi:10.1016/j.aquaculture.2016.09.045.

Conesa, A., and Götz, S. 2008. Blast2GO: A comprehensive suite for functional analysis in plant genomics. International Journal of Plant Genomics 2008: 619832. doi:10.1155/2008/619832.

Conesa, A., Götz, S., García-Gómez, J.M., Terol, J., Talón, M., and Robles, M. 2005. Blast2GO: a universal tool for annotation, visualization and analysis in functional genomics research. Bioinformatics 21: 3674–3676. doi:10.1093/bioinformatics/bti610.

Connor, K.M., Sung, A., Garcia, N.S., Gracey, A.Y., and German, D.P. 2016. Modulation of digestive physiology and biochemistry in *Mytilus californianus* in response to feeding level acclimation and microhabitat. Biology Open 5: 1200–1210. doi:10.1242/bio.019430.

Conus, S. 2010. Cathepsins and their involvement in immune responses. Swiss Medical Weekly 140: w13042. doi:10.4414/smw.2010.13042.

Conway, S.J., Izuhara, K., Kudo, Y., Litvin, J., Markwald, R., Ouyang, G., Arron, J.R., Holweg, C.T.J., and Kudo, A. 2014. The role of periostin in tissue remodeling across health and disease. Cellular and molecular life sciences: CMLS 71: 1279–1288. doi:10.1007/s00018-013-1494-y.

Coppola, F., Almeida, Â., Henriques, B., Soares, A.M.V.M., Figueira, E., Pereira, E., and Freitas, R. 2017. Biochemical impacts of Hg in *Mytilus galloprovincialis* under present and predicted warming scenarios. Science of The Total Environment 601–602: 1129–1138. doi:10.1016/j.scitotenv.2017.05.201.

Coppola, F., Almeida, Â., Henriques, B., Soares, A.M.V.M., Figueira, E., Pereira, E., and Freitas, R. 2018. Biochemical responses and accumulation patterns of *Mytilus galloprovincialis* exposed to thermal stress and Arsenic contamination. Ecotoxicology and Environmental Safety 147: 954–962. doi:10.1016/j.ecoenv.2017.09.051.

Counihan, K.L., Bowen, L., Ballachey, B., Coletti, H., Hollmen, T., Pister, B., and Wilson, T.L. 2019. Physiological and gene transcription assays to assess responses of mussels to environmental changes. PeerJ 7: e7800. doi:10.7717/peerj.7800.

Crane, R.L., Diaz Reyes, J.L., and Denny, M.W. 2021. Bivalves rapidly repair shells damaged by fatigue and bolster strength. Journal of Experimental Biology 224: jeb242681. doi:10.1242/jeb.242681.

Cranford, P.J., Ward, J.E., and Shumway, S.E. 2011. Bivalve filter feeding: variability and limits of the aquaculture biofilter. Pages 81–124 in S.E. Shumway, ed. Shellfish Aquaculture and the Environment. John Wiley & Sons, Ltd. doi:10.1002/9780470960967.ch4.

Crenshaw, M.A., and Neff, J.M. 1969. Decalcification at the mantle-shell Interface in molluscs. Integrative and Comparative Biology 9: 881–885. doi:10.1093/icb/9.3.881.

Cui, W., Ma, A., Huang, Z., Liu, Z., Yang, K., and Zhang, W. 2020. myo-inositol facilitates salinity tolerance by modulating multiple physiological functions in the turbot *Scophthalmus maximus*. Aquaculture 527: 735451. doi:10.1016/j.aquaculture.2020.735451.

Curtis, T.M., Williamson, R., and Depledge, M.H. 2000. Simultaneous, long-term monitoring of valve and cardiac activity in the blue mussel *Mytilus edulis* exposed to copper. Marine Biology 136: 837–846. doi:10.1007/s002270000297.

Davenport, J. 1979a. The isolation response of mussels exposed to falling sea-water concentrations. Journal of the Marine Biological Association of the United Kingdom 59: 123–132. doi:10.1017/S0025315400046221.

Davenport, J. 1979b. Is *Mytilus edulis* a short term osmoregulator? Comparative Biochemistry and Physiology Part A: Physiology 64: 91–95. doi:10.1016/0300-9629(79)90436-5.

Davenport, J., and Manley, A. 1978. The detection of heightened sea-water copper concentrations by the mussel *Mytilus edulis*. Journal of the Marine Biological Association of the United Kingdom 58: 843–850. doi:10.1017/S0025315400056800.

David, E., Tanguy, A., Pichavant, K., and Moraga, D. 2005. Response of the Pacific oyster *Crassostrea gigas* to hypoxia exposure under experimental conditions. The FEBS Journal 272: 5635–5652. doi:10.1111/j.1742-4658.2005.04960.x.

De Zwaan, A. 1983. Carbohydrate catabolism in bivalves. Pages 137–157 in P.V. Hochachka, ed. The Mollusca. Academic Press, New York.

De Zwaan, A. 1991. Molluscs. Pages 186–217 in C. Bryant, ed. Metazoan life without oxygen. Chapman and Hall, London, UK.

De Zwaan, A., Cortesi, P., van den Thillart, G., Brooks, S., Storey, K.B., Roos, J., van Lieshout, G., Cattani, O., and Vitali, G. 1992. Energy metabolism of bivalves at reduced oxygen tensions. Pages 1029–1039 in R.A. Vollenweider, R. Marchetti, and R. Viviani, eds. Marine Coastal Eutrophication. Elsevier, Amsterdam. doi:10.1016/B978-0-444-89990-3.50089-4.

De Zwaan, A., De Bont, A.M.T., and Hemelraard, J. 1983. The role of phosphoenolpyruvate carboxykinase in the anaerobic metabolism of the sea mussel *Mytilus edulis* L. Journal of comparative physiology 153: 267–274. doi:10.1007/BF00689630.

De Zwaan, A., De Bont, A.M.T., and Verhoeven, A. 1982. Anaerobic energy metabolism in isolated adductor muscle of the sea mussel *Mytilus edulis L*. Journal of comparative physiology 149: 137–143. doi:10.1007/BF00735724.

De Zwaan, A., Holwerda, D., and Veenhof, P. 1981. Anaerobic malate metabolism in mitochondria of the sea mussel *Mytilus edulis* L. Marine Biology Letters 2: 549–557.

De Zwaan, A., and Wijsman, T.C.M. 1976. Anaerobic metabolism in bivalvia (Mollusca) characteristics of anaerobic metabolism. Comparative Biochemistry and Physiology Part B: Comparative Biochemistry 54: 313–323. doi:10.1016/0305-0491(76)90247-9.

De Zwaan, A., and Zandee, D.I. 1972. Body distribution and seasonal changes in the glycogen content of the common sea mussel *Mytilus edulis*. Comparative Biochemistry and Physiology Part A: Physiology 43: 53–58. doi:10.1016/0300-9629(72)90468-9.

Delaporte, M., Soudant, P., Lambert, C., Moal, J., Pouvreau, S., and Samain, J.-F. 2006. Impact of food availability on energy storage and defense related hemocyte parameters of the Pacific oyster *Crassostrea gigas* during an experimental reproductive cycle. Aquaculture 254: 571–582. doi:10.1016/j.aquaculture.2005.10.006.

Deutsch, C., Brix, H., Ito, T., Frenzel, H., and Thompson, L. 2011. Climate-forced variability of ocean hypoxia. Science 333: 336–339. doi:10.1126/science.1202422.

Dhama, K., Latheef, S.K., Dadar, M., Samad, H.A., Munjal, A., Khandia, R., Karthik, K., Tiwari, R., Yatoo, Mohd.I., Bhatt, P., Chakraborty, S., Singh, K.P., Iqbal, H.M.N., Chaicumpa, W., and Joshi, S.K. 2019. Biomarkers in stress related diseases/disorders: diagnostic, prognostic, and therapeutic values. Frontiers in Molecular Biosciences 6: 91. doi:10.3389/fmolb.2019.00091.

Diaz, R., Lardies, M.A., Tapia, F.J., Tarifeño, E., and Vargas, C.A. 2018. Transgenerational effects of pCO2-driven ocean acidification on adult mussels *Mytilus chilensis* modulate physiological response to multiple stressors in larvae. Frontiers in Physiology 9: 1349. doi:10.3389/fphys.2018.01349.

Diaz, R.J., and Rosenberg, R. 2008. Spreading dead zones and consequences for marine ecosystems. Science 321: 926–929. doi:10.1126/science.1156401.

Diehl, W.J., Gaffney, P.M., McDonald, J.H., and Koehn, R.K. 1985. Relationship between weight-standardized oxygen consumption and multiple-locus heterozygosity in the mussel, *Mytilus edulis*. Pages 16–21 in P.E. Gibbs, ed. Proceedings of the 19th European Marine Biology Symposium.

Dionne, M. 2004. Relationship between diving ducks and mussel aquaculture in Prince Edward Island, Canada. University of New Brunswick, New Brunswick, Canada.154p.

Dionne, M., Lauzon-Guay, J.-S., Hamilton, D.J., and Barbeau, M.A. 2006. Protective socking material for cultivated mussels: a potential non-disruptive deterrent to reduce losses to diving ducks. Aquaculture International 14: 595–613. doi:10.1007/s10499-006-9058-x.

Dou, M., Jiao, Y., Zheng, J., Zhang, G., Li, H., Liu, J., and Yang, W. 2020. De novo transcriptome analysis of the mussel *Perna viridis* after exposure to the toxic dinoflagellate *Prorocentrum lima*. Ecotoxicology and Environmental Safety 192: 110265. doi:10.1016/j.ecoenv.2020.110265.

Dowd, W.W., Felton, C.A., Heymann, H.M., Kost, L.E., and Somero, G.N. 2013. Food availability, more than body temperature, drives correlated shifts in ATP-generating and antioxidant enzyme capacities in a population of intertidal mussels (*Mytilus californianus*). Journal of Experimental Marine Biology and Ecology 449: 171–185. doi:10.1016/j.jembe.2013.09.020.

Dowd, W.W., and Somero, G.N. 2013. Behavior and survival of *Mytilus* congeners following episodes of elevated body temperature in air and seawater. Journal of Experimental Biology 216: 502–514. doi:10.1242/jeb.076620.

Drury, C., Yang, J., and De Jong, T. 2016. Residual soil nitrogen. Pages 121–130 in R. Clearwater, T. Martin, and T. Hoppe, eds. Environmental sustainability of Canadian agriculture: Agri-environmental indicator report series, 4th edition. Agriculture and Agri-Food Canada, Ottawa, ON.

Duarte, C.M., Rodriguez-Navarro, A.B., Delgado-Huertas, A., and Krause-Jensen, D. 2020. Dense *Mytilus* beds along freshwater-influenced Greenland shores: resistance to corrosive waters under high food supply. Estuaries and Coasts 43: 387–395. doi:10.1007/s12237-019-00682-3.

Dutkiewicz, S., Scott, J.R., and Follows, M.J. 2013. Winners and losers: ecological and biogeochemical changes in a warming ocean. Global Biogeochemical Cycles 27: 463–477. doi:10.1002/gbc.20042.

Dyachuk, V., and Odintsova, N. 2009. Development of the larval muscle system in the mussel *Mytilus trossulus* (Mollusca, Bivalvia). Development, Growth & Differentiation 51: 69–79. doi:10.1111/j.1440-169X.2008.01081.x.

Dyachuk, V.A., Plotnikov, S.V., and Odintsova, N.A. 2005. Appearance of muscle proteins in ontogenesis of the mussel *Mytilus trossulus* (Bivalvia). Russian Journal of Marine Biology 31: 327–330. doi:10.1007/s11179-005-0097-3.

Efeyan, A., Zoncu, R., and Sabatini, D.M. 2012. Amino acids and mTORC1: from lysosomes to disease. Trends in Molecular Medicine 18: 524–533. doi:10.1016/j.molmed.2012.05.007.

Encomio, V., and Chu, F.-L.E. 2000. The effect of PCBs on glycogen reserves in the eastern oyster *Crassostrea virginica*. Marine Environmental Research 50: 45–49. doi:10.1016/S0141-1136(00)00044-1.

Ertl, N.G., O'Connor, W.A., and Elizur, A. 2019. Molecular effects of a variable environment on Sydney rock oysters, *Saccostrea glomerata*: Thermal and low salinity stress, and their synergistic effect. Marine Genomics 43: 19–32. doi:10.1016/j.margen.2018.10.003.

Estévez-Calvar, N., Romero, A., Figueras, A., and Novoa, B. 2013. Genes of the mitochondrial apoptotic pathway in *Mytilus galloprovincialis*. PLoS ONE 8: e61502. doi:10.1371/journal.pone.0061502.

Falfushynska, H., Piontkivska, H., and Sokolova, I.M. 2020. Effects of intermittent hypoxia on cell survival and inflammatory responses in the intertidal marine bivalves *Mytilus edulis* and *Crassostrea gigas*. The Journal of Experimental Biology 223: jeb217026. doi:10.1242/jeb.217026.

Falfushynska, H.I., Wu, F., Ye, F., Kasianchuk, N., Dutta, J., Dobretsov, S., and Sokolova, I.M. 2019. The effects of ZnO nanostructures of different morphology on bioenergetics and stress response biomarkers of the blue mussels *Mytilus edulis*. Science of The Total Environment 694: 133717. doi:10.1016/j.scitotenv.2019.133717.

Farías, L., and Cornejo, M. 2007. Effect of seasonal changes in bottom water oxygenation on sediment N oxides and N2O cycling in the coastal upwelling regime off central Chile (36.5°S). Progress in Oceanography 75: 561–575. doi:10.1016/j.pocean.2007.08.019.

Feder, J.H., Rossi, J.M., Solomon, J., Solomon, N., and Lindquist, S. 1992. The consequences of expressing hsp70 in *Drosophila* cells at normal temperatures. Genes & Development 6: 1402–1413. doi:10.1101/gad.6.8.1402.

Fegley, S.R., MacDonald, B.A., and Jacobsen, T.R. 1992. Short-term variation in the quantity and quality of seston available to benthic suspension feeders. Estuarine, Coastal and Shelf Science 34: 393–412. doi:10.1016/S0272-7714(05)80078-2.

Fennel, K., and Testa, J.M. 2019. Biogeochemical controls on coastal hypoxia. Annual Review of Marine Science 11: 105–130. doi:10.1146/annurev-marine-010318-095138.

Fernández, B., Campillo, J.A., Martínez-Gómez, C., and Benedicto, J. 2010. Antioxidant responses in gills of mussel (*Mytilus galloprovincialis*) as biomarkers of environmental stress along the Spanish Mediterranean coast. Aquatic Toxicology 99: 186–197. doi:10.1016/j.aquatox.2010.04.013.

Fernández-Reiriz, M., Labarta, U., Navarro, J., and Velasco, A. 2001. Enzymatic digestive activity in *Mytilus chilensis* (Hupé 1854) in response to food regimes and past feeding history. Journal of Comparative Physiology B 171: 449–456. doi:doi: 10.1007/s003600100194.

Filgueira, R., Guyondet, T., Comeau, L.A., and Grant, J. 2014. A fully-spatial ecosystem-DEB model of oyster (*Crassostrea virginica*) carrying capacity in the Richibucto Estuary, Eastern Canada. Journal of Marine Systems 136: 42–54. doi:10.1016/j.jmarsys.2014.03.015.

Filgueira, R., Guyondet, T., Comeau, L.A., and Tremblay, R. 2016. Bivalve aquaculture-environment interactions in the context of climate change. Global Change Biology 22: 3901–3913. doi:10.1111/gcb.13346.

Fisheries and Oceans Canada 2003. Profile of the blue mussel (*Mytilus edulis*). Department of Fisheries and Oceans, Moncton, New Brunswick.

Fisheries and Oceans Canada 2006. An economic analysis of the mussel industry in Prince Edward Island - Gulf Region (2006). Policy and Economics Branch, Gulf Region, Moncton, New Brunswick.

Fitzer, S.C., Chung, P., Maccherozzi, F., Dhesi, S.S., Kamenos, N.A., Phoenix, V.R., and Cusack, M. 2016. Biomineral shell formation under ocean acidification: a shift from order to chaos. Scientific Reports 6: 21076. doi:10.1038/srep21076.

Fitzer, S.C., Gabarda, S.T., Daly, L., Hughes, B., Dove, M., O'Connor, W., Potts, J., Scanes, P., and Byrne, M. 2018. Coastal acidification impacts on shell mineral structure of bivalve mollusks. Ecology and Evolution 8: 8973–8984. doi:10.1002/ece3.4416.

Fitzer, S.C., Phoenix, V.R., Cusack, M., and Kamenos, N.A. 2014. Ocean acidification impacts mussel control on biomineralization. Scientific Reports 4: 6218. doi:10.1038/srep06218.

Fitzpatrick, P.J., O'Halloran, J., Sheehan, D., and Walsh, A.R. 1997. Assessment of a glutathione S-transferase and related proteins in the gill and digestive gland of *Mytilus edulis* (L.), as potential organic pollution biomarkers. Biomarkers 2: 51–56. doi:10.1080/135475097231977.

Florkin, M. 1962. La régulation isosmotique intracellulaire chez les invertébrés marins euryhalins. Bulletin de la Classe des Sciences/Académie Royale de Belgique 48: 687–694.

Foreman, R.A., and Ellington, W.R. 1983. Effects of inhibitors and substrate supplementation on anaerobic energy metabolism in the ventricle of the oyster, *Crassostrea virginica*. Comparative Biochemistry and Physiology Part B: Comparative Biochemistry 74: 543–547. doi:10.1016/0305-0491(83)90226-2.

Foster-Smith, R. 1978. The function of the pallial organs of bivalves in controlling ingestion. Journal of Molluscan Studies 44: 83–99. doi:10.1093/oxfordjournals.mollus.a065419.

Fréchette, M. 2005. A comment on the methodology of stocking experiments. Aquaculture 250: 291–299. doi:10.1016/j.aquaculture.2005.05.004.

Freeman, K.R. 1974. Growth, mortality and seasonal cycle of *Mytilus edulis* in two Nova Scotian embayments. Fisheries and Marine Services: Technical Report 500: 112 pp.

Freeman, K.R., and Dickie, L.M. 1979. Growth and mortality of the blue mussel (*Mytilus edulis*) in relation to environmental indexing. Journal of the Fisheries Research Board of Canada 36: 1238–1249. doi:10.1139/f79-178.

Freire, C., and Sampaio, F. 2021. Stress and disease in aquaculture, and their effects on homeostasis and osmoregulation: the metabolic connection. Aquaculture Pharmacology: 273–295. doi:10.1016/B978-0-12-821339-1.00010-6.

Freire, C.A., Welker, A.F., Storey, J.M., Storey, K.B., and Hermes-Lima, M. 2011. Oxidative stress in estuarine and interidal environments (temperate and tropical). Pages 41–57 in D. Abele, J.P. Vazquez-Medina, and T. Zenteno-Savin, eds. Oxidative stress in aquatic ecosystems. John Wiley & Sons.

Freitas, R., Leite, C., Pinto, J., Costa, M., Monteiro, R., Henriques, B., Di Martino, F., Coppola, F., Soares, A.M.V.M., Solé, M., and Pereira, E. 2019. The influence of temperature and salinity on the impacts of lead in *Mytilus galloprovincialis*. Chemosphere 235: 403–412. doi:10.1016/j.chemosphere.2019.05.221.

Freites, L., Fernández-Reiriz, M.J., and Labarta, U. 2003. Biochemical composition and energy content of the mussel *Mytilus galloprovincialis* of subtidal and rocky shore origin: Influence of environmental variables and source of mussel seed. Ciencias marinas 29: 603–619.

Frey, N., Venturelli, S., Zender, L., and Bitzer, M. 2018. Cellular senescence in gastrointestinal diseases: from pathogenesis to therapeutics. Nature Reviews Gastroenterology & Hepatology 15: 81–95. doi:10.1038/nrgastro.2017.146.

Furuhashi, M. 2020. New insights into purine metabolism in metabolic diseases: role of xanthine oxidoreductase activity. American Journal of Physiology-Endocrinology and Metabolism 319: E827–E834. doi:10.1152/ajpendo.00378.2020.

Gagné, F., Burgeot, T., Hellou, J., St-Jean, S., Farcy, É., and Blaise, C. 2008. Spatial variations in biomarkers of *Mytilus edulis* mussels at four polluted regions spanning the Northern Hemisphere. Environmental Research 107: 201–217. doi:10.1016/j.envres.2007.09.013.

Galimany, E., Sunila, I., Hégaret, H., Ramón, M., and Wikfors, G.H. 2008. Experimental exposure of the blue mussel (*Mytilus edulis*, L.) to the toxic dinoflagellate *Alexandrium fundyense*: Histopathology, immune responses, and recovery. Harmful Algae 7: 702–711. doi:10.1016/j.hal.2008.02.006.

Galloway, T.S., Millward, N., Browne, M.A., and Depledge, M.H. 2002. Rapid assessment of organophosphorous/carbamate exposure in the bivalve mollusc *Mytilus edulis* using combined esterase activities as biomarkers. Aquatic Toxicology 61: 169–180. doi:10.1016/S0166-445X(02)00051-6.

Garcia-Garcia, E., Galindo-Villegas, J., and Mulero, V. 2013. Mucosal immunity in the gut: the non-vertebrate perspective. Development & Comparative Immunology 40: 278–288.

Garner, Y.L., and Litvaitis, M.K. 2013. Effects of wave exposure, temperature and epibiont fouling on byssal thread production and growth in the blue mussel, *Mytilus edulis*, in the Gulf of Maine. Journal of Experimental Marine Biology and Ecology 446: 52–56. doi:10.1016/j.jembe.2013.05.001.

Gartner-Kepkay, K.E., Dickie, L.M., Freeman, K.R., and Zouros, E. 1980. Genetic differences and environments of mussel populations in the Maritime provinces. Canadian Journal of Fisheries and Aquatic Sciences 37: 775–782. doi:10.1139/f80-104.

Geng, X., and Boufadel, M.C. 2017. The influence of evaporation and rainfall on supratidal groundwater dynamics and salinity structure in a sandy beach. Water Resources Research 53: 6218–6238. doi:10.1002/2016WR020344.

Geng, X., Boufadel, M.C., and Jackson, N.L. 2016. Evidence of salt accumulation in beach intertidal zone due to evaporation. Scientific Reports 6: 31486. doi:http://dx.doi.org.ezproxy.library.dal.ca/10.1038/srep31486.

Gerdol, M., and Venier, P. 2015. An updated molecular basis for mussel immunity. Fish & Shellfish Immunology 46: 17–38. doi:10.1016/j.fsi.2015.02.013.

Giannetto, A., Maisano, M., Cappello, T., Oliva, S., Parrino, V., Natalotto, A., De Marco, G., Barberi, C., Romeo, O., Mauceri, A., and Fasulo, S. 2015. Hypoxia-inducible factor α and Hif-prolyl hydroxylase characterization and gene expression in short-time air-exposed *Mytilus galloprovincialis*. Marine Biotechnology 17: 768–781. doi:10.1007/s10126-015-9655-7.

Giannetto, A., Maisano, M., Cappello, T., Oliva, S., Parrino, V., Natalotto, A., De Marco, G., and Fasulo, S. 2017. Effects of oxygen availability on oxidative stress biomarkers in the Mediterranean mussel *Mytilus galloprovincialis*. Marine Biotechnology 19: 614–626. doi:10.1007/s10126-017-9780-6.

Gilles, R. 1972. Osmoregulation in three molluscs: *Acanthochitona discrepans*(brown), *Glycymeris glycymeris* (l.) and *Mytilus edulis* (l.). The Biological Bulletin 142: 25–35. doi:10.2307/1540243.

Gobler, C.J., Doherty, O.M., Hattenrath-Lehmann, T.K., Griffith, A.W., Kang, Y., and Litaker, R.W. 2017. Ocean warming since 1982 has expanded the niche of toxic algal blooms in the North Atlantic and North Pacific oceans. Proceedings of the National Academy of Sciences 114: 4975–4980. doi:10.1073/pnas.1619575114.

Goodman, R.H., and Smolik, S. 2000. CBP/p300 in cell growth, transformation, and development. Genes Development 14: 1553–1577.

Goolish, E.M., and Burton, R.S. 1989. Energetics of osmoregulation in an intertidal copepod: effects of anoxia and lipid reserves on the pattern of free amino accumulation. Functional Ecology 3: 81–89. doi:10.2307/2389678.

Gorr, T.A., Gassmann, M., and Wappner, P. 2006. Sensing and responding to hypoxia via HIF in model invertebrates. Journal of Insect Physiology 52: 349–364. doi:10.1016/j.jinsphys.2006.01.002.

Gosling, E. 1992. Genetics of *Mytilus*. Pages 309–382 in E. Gosling, ed. The Mussel *Mytilus*: Ecology, Physiology, Genetics, and Culture.

Gosling, E. 2003. Bivalve Molluscs. Fishing New Books, Blackwell Publishing, Oxford, UK.

Götz, S., Arnold, R., Sebastián-León, P., Martín-Rodríguez, S., Tischler, P., Jehl, M.-A., Dopazo, J., Rattei, T., and Conesa, A. 2011. B2G-FAR, a species-centered GO annotation repository. Bioinformatics 27: 919–924. doi:10.1093/bioinformatics/btr059.

Götz, S., García-Gómez, J.M., Terol, J., Williams, T.D., Nagaraj, S.H., Nueda, M.J., Robles, M., Talón, M., Dopazo, J., and Conesa, A. 2008. High-throughput functional annotation and data mining with the Blast2GO suite. Nucleic Acids Research 36: 3420–3435. doi:10.1093/nar/gkn176.

Grabherr, M.G., Haas, B.J., Yassour, M., Levin, J.Z., Thompson, D.A., Amit, I., Adiconis, X., Fan, L., Raychowdhury, R., Zeng, Q., Chen, Z., Mauceli, E., Hacohen, N., Gnirke, A., Rhind, N., di Palma, F., Birren, B.W., Nusbaum, C., Lindblad-Toh, K., Friedman, N., and Regev, A. 2011. Full-length transcriptome assembly from RNA-Seq data without a reference genome. Nature Biotechnology 29: 644–652. doi:10.1038/nbt.1883.

Gracey, A.Y., Chaney, M.L., Boomhower, J.P., Tyburczy, W.R., Connor, K., and Somero, G.N. 2008. Rhythms of gene expression in a fluctuating intertidal environment. Current biology 18: 1501–1507. doi:10.1016/j.cub.2008.08.049.

Gracey, A.Y., and Connor, K. 2016. Transcriptional and metabolomic characterization of spontaneous metabolic cycles in *Mytilus californianus* under subtidal conditions. Marine Genomics 30: 35–41. doi:10.1016/j.margen.2016.07.004.

Graham, A. 1949. XXVII.—The molluscan stomach. Earth and Environmental Science Transactions of The Royal Society of Edinburgh 61: 737–761. doi:10.1017/S008045680001913X.

Granger Joly de Boissel, P., Fournier, M., Rodriguez-Lecompte, J.C., McKenna, P., Kibenge, F., and Siah, A. 2017. Functional and molecular responses of the blue mussel *Mytilus edulis'* hemocytes exposed to cadmium - An in vitro model and transcriptomic approach. Fish & Shellfish Immunology 67: 575–585. doi:10.1016/j.fsi.2017.06.001.

Grieshaber, M.K., Hardewig, I., Kreutzer, U., and Pörtner, H.-O. 1994. Physiological and metabolic responses to hypoxia in invertebrates. Pages 43–147 in Reviews of Physiology, Biochemistry and Pharmacology, Volume 125. Springer.

Griffith, A.W., Shumway, S.E., and Gobler, C.J. 2019. Differential mortality of North Atlantic bivalve molluscs during harmful algal blooms caused by the dinoflagellate, *Cochlodinium* (a.k.a. *Margalefidinium*) *polykrikoides*. Estuaries and Coasts 42: 190–203. doi:10.1007/s12237-018-0445-0.

Grimaldi, A., Tettamanti, G., Acquati, F., Bossi, E., Guidali, M.L., Banfi, S., Monti, L., Valvassori, R., and De Eguileor, M. 2008. A hedgehog homolog is involved in muscle formation and organization of *Sepia officinalis* (mollusca) mantle. Developmental Dynamics 237: 659–671. doi:10.1002/dvdy.21453.

Grimaldi, A., Tettamanti, G., Martin, B.L., Gaffield, W., Pownall, M.E., and Hughes, S.M. 2004. Hedgehog regulation of superficial slow muscle fibres in *Xenopus* and the evolution of tetrapod trunk myogenesis. Development 131: 3249–3262. doi:10.1242/dev.01194.

Guerreiro, A. da S., Rola, R.C., Almeida, D.V., and Sandrini, J.Z. 2018. Transcriptional levels of the cancer-related genes p53, TAp63/73, and ΔNp63/73 in the blue mussel (*Mytilus edulis*) after lead exposure. Invertebrate Biology 137: 60–65. doi:10.1111/ivb.12205.

Guyon, P., Chilton, M.-D., Petit, A., and Tempé, J. 1980. Agropine in "null-type" crown gall tumors: Evidence for generality of the opine concept. Proceedings of the National Academy of Sciences 77: 2693–2697. doi:10.1073/pnas.77.5.2693.

Guyondet, T., Comeau, L.A., Bacher, C., Grant, J., Rosland, R., Sonier, R., and Filgueira, R. 2015. Climate change influences carrying capacity in a coastal embayment dedicated to shellfish aquaculture. Estuaries and Coasts 38: 1593–1618. doi:10.1007/s12237-014-9899-x.

Haas, B.J., Papanicolaou, A., Yassour, M., Grabherr, M., Blood, P.D., Bowden, J., Couger, M.B., Eccles, D., Li, B., Lieber, M., MacManes, M.D., Ott, M., Orvis, J., Pochet, N., Strozzi, F., Weeks, N., Westerman, R., William, T., Dewey, C.N., Henschel, R., LeDuc, R.D., Friedman, N., and Regev, A. 2013. De novo transcript sequence reconstruction from RNA-seq using the Trinity platform for reference generation and analysis. Nature Protocols 8: 1494–1512. doi:10.1038/nprot.2013.084.

Haider, F., Falfushynska, H.I., Timm, S., and Sokolova, I.M. 2020a. Effects of hypoxia and reoxygenation on intermediary metabolite homeostasis of marine bivalves *Mytilus edulis* and *Crassostrea gigas.* Comparative Biochemistry and Physiology Part A: Molecular & Integrative Physiology 242:110657. doi:10.1016/j.cbpa.2020.110657.

Haider, F., Timm, S., Bruhns, T., Noor, M.N., and Sokolova, I.M. 2020b. Effects of prolonged food limitation on energy metabolism and burrowing activity of an infaunal marine bivalve, *Mya arenaria*. Comparative Biochemistry and Physiology Part A: Molecular & Integrative Physiology 250: 110780. doi:10.1016/j.cbpa.2020.110780.

Halliwell, B., and Gutteridge, J.M.C. 1999. Free radicals in biology and medicine. Oxford University Press, Oxford, New York.

Halpin, P.M., Menge, B.A., and Hofmann, G.E. 2004. Experimental demonstration of plasticity in the heat shock response of the intertidal mussel *Mytilus californianus*. Marine Ecology Progress Series 276: 137–145. doi:10.3354/meps276137.

Hamer, B., Hamer, D.P., Müller, W.E.G., and Batel, R. 2004. Stress-70 proteins in marine mussel *Mytilus galloprovincialis* as biomarkers of environmental pollution: a field study. Environment International 30: 873–882. doi:10.1016/j.envint.2004.02.008.

Hamer, B., Jakšić, Ž., Pavičić-Hamer, D., Perić, L., Medaković, D., Ivanković, D., Pavičić, J., Zilberberg, C., Schröder, H.C., Müller, W.E.G., Smodlaka, N., and Batel, R. 2008. Effect of hypoosmotic stress by low salinity acclimation of Mediterranean mussels *Mytilus galloprovincialis* on biological parameters used for pollution assessment. Aquatic Toxicology 89: 137–151. doi:10.1016/j.aquatox.2008.06.015.

Hand, S.C. 1998. Quiescence in *Artemia franciscana* embryos: reversible arrest of metabolism and gene expression at low oxygen levels. The Journal of Experimental Biology 201: 1233–1242.

Hardie, D.G., and Hawley, S.A. 2001. AMP-activated protein kinase: the energy charge hypothesis revisited. BioEssays 23: 1112–1119. doi:10.1002/bies.10009.

Harding, J.M. 2003. Evaluation of the neutral red assay as a stress response indicator in mussels (*Mytilus* spp.) in relation to seasonal, environmental, handling, harvesting, processing, and post-harvest storage conditions. Memorial University of Newfoundland.112p

Harding, J.M., Couturier, C., Parsons, G.J., and Ross, N.W. 2004. Evaluation of the neutral red assay as a stress response indicator in cultivated mussels (*Mytilus* spp.) in relation to post-harvest processing activities and storage conditions. Aquaculture 231: 315–326.

Harteneck, C., and Reiter, B. 2007. TRP channels activated by extracellular hypo-osmoticity in epithelia. Biochemical Society Transactions 35: 91–95. doi:10.1042/BST0350091.

Hatcher, A., Grant, J., and Schofield, B. 1997. Seasonal changes in the metabolism of cultured mussels (*Mytilus edulis* l.) from a Nova Scotian inlet: the effects of winter ice cover and nutritive stress. Journal of Experimental Marine Biology and Ecology 217: 63–78. doi:10.1016/S0022-0981(97)00042-7.

Hauton, C., Hawkins, L.E., and Hutchinson, S. 1998. The use of the neutral red retention assay to examine the effects of temperature and salinity on haemocytes of the European flat oyster *Ostrea edulis* (L). Comparative Biochemistry and Physiology Part B: Biochemistry and Molecular Biology 119: 619–623.

Hauton, C., Hawkins, L.E., and Hutchinson, S. 2001. Response of haemocyte lysosomes to bacterial inoculation in the oysters *Ostrea edulis* L. and *Crassostrea gigas* (Thunberg) and the scallop *Pecten maximus* (L.). Fish & Shellfish Immunology 11: 143–153. doi:10.1006/fsim.2000.0301.

Hawkins, A., and Bayne, B. 1992. Physiological interrelations, and the regulation of production [in *Mytilus*]. Pages 171–222 in E. Gosling, ed. The mussel *Mytilus*: Ecology, Physiology, Genetics, and Culture. Elsevier.

Hawkins, A., Bayne, B.L., and Day, A.J. 1986. Protein turnover, physiological energetics and heterozygosity in the blue mussel, *Mytilus edulis*: the basis of variable age-specific growth. Proceedings of the Royal Society of London. Series B. Biological Sciences 229: 161–176. doi:10.1098/rspb.1986.0080.

Hawkins, A., James, M., Hickman, R., Hatton, S., and Weatherhead, M. 1999. Modelling of suspension-feeding and growth in the green-lipped mussel *Perna canaliculus* exposed to natural and experimental variations of seston availability in the Marlborough Sounds, New Zealand. Marine Ecology Progress Series 191: 217–232. doi:10.3354/meps191217.

Hawkins, A.J.S., Navarro, E., and Iglesias, J.I.P. 1990. Comparative allometries of gut-passage time, gut content and metabolic faecal loss in *Mytilus edulis* and *Cerastoderma edule*. Marine Biology 105: 197–204. doi:10.1007/BF01344287.

Hawkins, L., Brooks, J., Brooks, S., and Hutchinson, S. 1993. The effect of tidal exposure on aspects of metabolic and immunological activity in the hard clam *Mercenaria mercenaria* (Linnaeus). Comparative biochemistry and physiology. A. 104: 225–228.

Hayes, J.M., Kim, S.K., Abitua, P.B., Park, T.J., Herrington, E.R., Kitayama, A., Grow, M.W., Ueno, N., and Wallingford, J.B. 2007. Identification of novel ciliogenesis factors using a new in vivo model for mucociliary epithelial development. Developmental Biology 312: 115–130. doi:10.1016/j.ydbio.2007.09.031.

He, L., Vasiliou, K., and Nebert, D.W. 2009. Analysis and update of the human solute carrier (SLC) gene superfamily. Human Genomics 3: 195. doi:10.1186/1479-7364-3-2-195.

Held, I.M., and Soden, B.J. 2006. Robust responses of the hydrological cycle to global warming. Journal of Climate 19: 5686–5699. doi:10.1175/JCLI3990.1.

Hellemans, J., and Vandesompele, J. 2011. PCR Troubleshooting and optimization: the essential guide. Page 236 in S. Kennedy and N. Oswald, eds. qPCR data analysis – unlocking the secret to successful results. Caister Academic Press.

Helly, J.J., and Levin, L.A. 2004. Global distribution of naturally occurring marine hypoxia on continental margins. Deep Sea Research Part I: Oceanographic Research Papers 51: 1159–1168. doi:10.1016/j.dsr.2004.03.009.

Henson, S.A., Cael, B.B., Allen, S.R., and Dutkiewicz, S. 2021. Future phytoplankton diversity in a changing climate. Nature Communications 12: 5372. doi:10.1038/s41467-021-25699-w.

Hicke, J., Lucatello, S., Mortsch, L., Dawson, J., Domínguez Aguilar, M., Enquist, C., Gilmore, E., Gutzler, D., Harper, S., Holsman, K., Jewett, E., Kohler, T., and Miller, K. 2022. North America. Page 95 in H.-O. Pörtner, D. Roberts, M. Tignor, E. Poloczanska, K. Mintenbeck, A. Alegría, M. Craig, S. Langsdorf, S. Löschke, V. Möller, A. Okem, and B. Rama, eds. Climate Change 2022: Impacts, Adaptation, and Vulnerability. Contribution of Working Group II to the Sixth Assessment Report of the Intergovernmental Panel on Climate Change. Cambridge University Press.

Hiebenthal, C., Philipp, E., Eisenhauer, A., and Wahl, M. 2013. Effects of seawater pCO2 and temperature on shell growth, shell stability, condition and cellular stress of Western Baltic Sea *Mytilus edulis* (L.) and *Arctica islandica* (L.). Marine Biology 160: 2073–2087. doi:10.1007/s00227-012-2080-9.

Hochachka, P.W., Buck, L.T., Doll, C.J., and Land, S.C. 1996. Unifying theory of hypoxia tolerance: molecular/metabolic defense and rescue mechanisms for surviving oxygen lack. Proceedings of the National Academy of Sciences of the United States of America 93: 9493–9498.

Hoegh-Guldberg, O., Cai, R., Poloczanska, E.S., Brewer, P.G., Sundby, S., Hilmi, K., Fabry, V.J., and Jung, S. 2014. The Ocean. Pages 1655–1731 in V.R. Barros, C.B. Field, D.J. Dokken, M.D. Mastrandrea, K.D. Mach, T.E. Bilir, M. Chatterjee, K.L. Ebi, Y.O. Estrada, R.C. Genova, B. Girma, E.S. Kissel, A.N. Levy, S. MacCracken, P.R. Mastrandrea, and L.L. White, eds. Climate Change 2014: Impacts, Adaptation, and Vulnerability. Part B: Regional Aspects. Contribution of Working Group II to the Fifth Assessment Report of the Intergovernmental Panel on Climate Change. Cambridge University Press, Cambridge, United Kingdom and New York, NY, USA.

Hoegh-Guldberg, O., Jacob, D., Taylor, M., Bindi, M., Brown, S., Camilloni, I., Diedhiou, A., Djalante, R., Ebi, K.L., Engelbrecht, F., Hijioka, Y., Mehrotra, S., Payne, A., Seneviratne, S.I., Thomas, A., Warren, R., Zhou, G., Halim, S.A., Achlatis, M., Allen, R., Berry, P., Boyer, C., Brilli, L., Byers, E., Cheung, W., Craig, M., Ellis, N., Evans, J., Fischer, H., Fraedrich, K., Fuss, S., Ganase, A., Gattuso, J.-P., Bolaños, T.G., Hanasaki, N., Hayes, K., Hirsch, A., Jones, C., Jung, T., Kanninen, M., Krinner, G., Lawrence, D., Ley, D., Liverman, D., Mahowald, N., Meissner, K.J., Millar, R., Mintenbeck, K., Mix, A.C., Notz, D., Nurse, L., Okem, A., Olsson, L., Oppenheimer, M., Paz, S., Petersen, J., Petzold, J., Preuschmann, S., Rahman, M.F., Scheuffele, H., Schleussner, C.-F., Séférian, R., Sillmann, J., Singh, C., Slade, R., Stephenson, K., Stephenson, T., Tebboth, M., Tschakert, P., Vautard, R., Wehner, M., Weyer, N.M., Whyte, F., Yohe, G., Zhang, X., Zougmoré, R.B., Marengo, J.A., Pereira, J., and Sherstyukov, B. 2018. Global Warming of 1.5°C. An IPCC Special Report on the impacts of global warming of 1.5°C above pre-industrial levels and related global greenhouse gas emission pathways, in the context of strengthening the global response to the threat of climate change, sustainable development, and efforts to eradicate poverty. Pages 175–311 in Impacts of 1.5°C of Global Warming on Natural and Human Systems.

Hohmann, S. 2015. An integrated view on a eukaryotic osmoregulation system. Current Genetics 61: 373–382. doi:10.1007/s00294-015-0475-0.

Hole, L., Moore, M., and Bellamy, D. 1993. Age-related cellular reactions to copper in the marine mussel *Mytilus edulis*. Marine Ecology Progress Series 94: 175–179. doi:10.3354/MEPS094175.

Hole, L., Moore, M., and Bellamy, D. 1995. Age-related cellular and physiological reactions to hypoxia and hyperthermia in marine mussels. Marine Ecology Progress Series 122: 173–178. doi:10.3354/meps122173.

Hole, L.M., Moore, M.N., and Bellamy, D. 1992. Age-related differences in the recovery of lysosomes from stress-induced pathological reactions in marine mussels. Marine environmental research 34: 75–80.

Holland, D., and Hannant, P. 1976. The glycogen content in winter and summer of oysters, *Ostrea edulis* L., of different ages. ICES Journal of Marine Science 36: 240–242.

Holland, D.L., and Spencer, B.E. 1973. Biochemical Changes in fed and starved oysters, *Ostrea Edulis* L. during larval development, metamorphosis and early spat growth. Journal of the Marine Biological Association of the United Kingdom 53: 287–298. doi:10.1017/S002531540002227X.

Holwerda, D.A., and De Zwaan, A. 1980. On the role of fumarate reductase in anaerobic carbohydrate catabolism of *Mytilus edulis* L. Comparative Biochemistry and Physiology Part B: Comparative Biochemistry 67: 447–453. doi:10.1016/0305-0491(80)90332-6.

Honkoop, P.J.C., Bayne, B.L., and Drent, J. 2003. Flexibility of size of gills and palps in the Sydney rock oyster *Saccostrea glomerata* (Gould, 1850) and the Pacific oyster *Crassostrea gigas* (Thunberg, 1793). Journal of Experimental Marine Biology and Ecology 282: 113–133. doi:10.1016/S0022-0981(02)00463-X.

Hosoi, M., Takeuchi, K., Sawada, H., and Toyohara, H. 2005. Expression and functional analysis of mussel taurine transporter, as a key molecule in cellular osmoconforming. Journal of Experimental Biology 208: 4203–4211. doi:10.1242/jeb.01868.

Hu, M., Li, L., Sui, Y., Li, J., Wang, Y., Lu, W., and Dupont, S. 2015. Effect of pH and temperature on antioxidant responses of the thick shell mussel *Mytilus coruscus*. Fish & Shellfish Immunology 46: 573–583. doi:10.1016/j.fsi.2015.07.025.

Huan, P., Wang, H., and Liu, B. 2012. Transcriptomic analysis of the clam *Meretrix meretrix* on different larval stages. Marine Biotechnology 14: 69–78. doi:10.1007/s10126-011-9389-0.

Hummel, H., de Wolf, L., Zurburg, W., Apon, L., Bogaards, R.H., and van Ruitenburg, M. 1989. The glycogen content in stressed marine bivalves: the initial absence of a decrease. Comparative Biochemistry and Physiology Part B: Comparative Biochemistry 94: 729–733. doi:10.1016/0305-0491(89)90157-0.

Hüning, A.K., Lange, S.M., Ramesh, K., Jacob, D.E., Jackson, D.J., Panknin, U., Gutowska, M.A., Philipp, E.E.R., Rosenstiel, P., Lucassen, M., and Melzner, F. 2016. A shell regeneration assay to identify biomineralization candidate genes in mytilid mussels. Marine Genomics 27: 57–67. doi:10.1016/j.margen.2016.03.011.

Hutchison, Z.L., Hendrick, V.J., Burrows, M.T., Wilson, B., and Last, K.S. 2016. Buried alive: the behavioural response of the mussels, *Modiolus modiolus* and *Mytilus edulis* to sudden burial by sediment. PLOS ONE 11: e0151471. doi:10.1371/journal.pone.0151471.

Ibarrola, I., Etxeberria, M., Iglesias, J.I.P., Urrutia, M.B., and Angulo, E. 2000. Acute and acclimated digestive responses of the cockle *Cerastoderma edule* (L.) to changes in the food quality and quantity: II. Enzymatic, cellular and tissular responses of the digestive gland. Journal of Experimental Marine Biology and Ecology 252: 199–219. doi:10.1016/S0022-0981(00)00235-5.

Ingham, P.W., and McMahon, A.P. 2001. Hedgehog signaling in animal development: paradigms and principles. Genes & Development 15: 3059–3087. doi:10.1101/gad.938601.

Ito, K., Morioka, M., Kimura, S., Tasaki, M., Inohaya, K., and Kudo, A. 2014. Differential reparative phenotypes between zebrafish and medaka after cardiac injury. Developmental Dynamics 243: 1106–1115. doi:10.1002/dvdy.24154.

Ivanina, A.V., Nesmelova, I., Leamy, L., Sokolov, E.P., and Sokolova, I.M. 2016. Intermittent hypoxia leads to functional reorganization of mitochondria and affects cellular bioenergetics in marine molluscs. Journal of Experimental Biology 219: 1659–1674. doi:10.1242/jeb.134700.

Izagirre, U., Garmendia, L., Soto, M., Etxebarria, N., and Marigómez, I. 2014. Health status assessment through an integrative biomarker approach in mussels of different ages with a different history of exposure to the Prestige oil spill. Science of The Total Environment 493: 65–78. doi:10.1016/j.scitotenv.2014.05.118.

Jindrich, K., and Degnan, B.M. 2016. The diversification of the basic leucine zipper family in eukaryotes correlates with the evolution of multicellularity. BMC Evolutionary Biology 16: 28. doi:10.1186/s12862-016-0598-z.

Johnson, E.H. 2020. Experimental tests of bivalve shell shape reveal potential tradeoffs between mechanical and behavioral defenses. Science Reports 10: 19425. doi:10.1038/s41598-020-76358-x.

Jones, S.S., Lima, F.P., and Wethey, D.S. 2010. Rising environmental temperatures and biogeography: poleward range contraction of the blue mussel, *Mytilus edulis* L., in the western Atlantic. Journal of Biogeography 37: 2243–2259.

Jørgensen, B., Møhlenberg, F., and Sten-Knudsen, O. 1986a. Nature of relation between ventilation and oxygen consumption in filter feeders. Marine Ecology Progress Series 29: 73–88. doi:10.3354/meps029073.

Jørgensen, C. 1981. Feeding and cleaning mechanisms in the suspension feeding bivalve *Mytilus edulis*. Marine Biology 65: 159–163. doi:10.1007/BF00397081.

Jørgensen, C. 1996. Bivalve filter feeding revisited. Marine Ecology Progress Series 142: 287–302. doi:10.3354/meps142287.

Jørgensen, C., Kørboe, T., Møhlenberg, F., and Riisgård, H. 1984. Ciliary and mucus-net filter feeding, with special reference to fluid mechanical Characteristics. Marine Ecology Progress Series 15: 283–292. doi:10.3354/meps015283.

Jørgensen, C.B. 1990. Bivalve filter feeding: hydrodynamics, bioenergetics, physiology and ecology. Olsen & Olsen, Fredensborg, Denmark.

Jørgensen, C.B., Famme, P., Kristensen, H.S., Larsen, P.S., Møhlenberg, F., and Riisgård, H.U. 1986b. The bivalve pump. Marine Ecology Progress Series 34: 69–77. Inter-Research Science Center.

Kage-Nakadai, E., Uehara, T., and Mitani, S. 2011. H+/myo-inositol transporter genes, hmit-1.1 and hmit-1.2, have roles in the osmoprotective response in *Caenorhabditis elegans*. Biochemical and Biophysical Research Communications 410: 471–477. doi:10.1016/j.bbrc.2011.06.001.

Kämpf, J., and Chapman, P. 2016. The functioning of coastal upwelling systems. Pages 31–65 in J. Kämpf and P. Chapman, eds. Upwelling Systems of the World: A Scientific Journey to the Most Productive Marine Ecosystems. Springer International Publishing, Cham. doi:10.1007/978-3-319-42524-5_2.

Kamykowski, D., and Zentara, S.-J. 1990. Hypoxia in the world ocean as recorded in the historical data set. Deep-Sea Research 37: 1861–1874.

Kanehisa, M., and Sato, Y. 2020. KEGG Mapper for inferring cellular functions from protein sequences. Protein Science: A Publication of the Protein Society 29: 28–35. doi:10.1002/pro.3711.

Käse, L., and Geuer, J. 2018. Phytoplankton Responses to Marine Climate Change – An Introduction. Pages 55–72 in S. Jungblut, V. Liebich, and M. Bode, eds. YOUMARES 8 – Oceans Across Boundaries: Learning from each other. Springer Nature Switzerland AG, Switzerland.

Kaspar, J.W., Niture, S.K., and Jaiswal, A.K. 2009. Nrf2:INrf2 (Keap1) signaling in oxidative stress. Free Radical Biology & Medicine 47: 1304–1309. doi:10.1016/j.freeradbiomed.2009.07.035.

Kassahn, K.S., Crozier, R.H., Pörtner, H.O., and Caley, M.J. 2009. Animal performance and stress: responses and tolerance limits at different levels of biological organisation. Biological Reviews of the Cambridge Philosophical Society 84: 277–292. doi:10.1111/j.1469-185X.2008.00073.x.

Kautsky, N., Johannesson, K., and Tedengren, M. 1990. Genotypic and phenotypic differences between Baltic and North Sea populations of *Mytilus edulis* evaluated through reciprocal transplantations. Marine Ecology Progress Series 59: 203–210. doi:10.3354/meps059203.

Kawamukai, M. 2016. Biosynthesis of coenzyme Q in eukaryotes. Bioscience, Biotechnology, and Biochemistry 80: 23–33. doi:10.1080/09168451.2015.1065172.

Keeling, R.F., Körtzinger, A., and Gruber, N. 2010. Ocean deoxygenation in a warming world. Annual Review of Marine Science 2: 199–229. doi:10.1146/annurev.marine.010908.163855.

Kefaloyianni, E., Gourgou, E., Ferle, V., Kotsakis, E., Gaitanaki, C., and Beis, I. 2005. Acute thermal stress and various heavy metals induce tissue-specific pro-or anti-apoptotic events via the p38-MAPK signal transduction pathway in *Mytilus galloprovincialis* (Lam.). Journal of Experimental Biology 208: 4427–4436. doi:10.1242/jeb.01924.

Khan, F.U., Chen, H., Gu, H., Wang, T., Dupont, S., Kong, H., Shang, Y., Wang, X., Lu, W., Hu, M., and Wang, Y. 2021. Antioxidant responses of the mussel *Mytilus coruscus* co-exposed to ocean acidification, hypoxia and warming. Marine Pollution Bulletin 162: 111869. doi:10.1016/j.marpolbul.2020.111869.

Kiang, J.G., and Tsokos, G.C. 1998. Heat Shock Protein 70 kDa: Molecular Biology, Biochemistry, and Physiology. Pharmacology & Therapeutics 80: 183–201. doi:10.1016/S0163-7258(98)00028-X.

Kishore, U., Gaboriaud, C., Waters, P., Shrive, A.K., Greenhough, T.J., Reid, K.B.M., Sim, R.B., and Arlaud, G.J. 2004. C1q and tumor necrosis factor superfamily: modularity and versatility. Trends in Immunology 25: 551–561. doi:10.1016/j.it.2004.08.006.

Kluytmans, J.H., de Bont, A.M.T., Janus, J., and Wusman, T.C.M. 1977. Time dependent changes and tissue specificities in the accumulation of anaerobic fermentation products in the sea mussel *Mytilus edulis* L. Comparative Biochemistry and Physiology Part B: Comparative Biochemistry 58: 81–87. doi:10.1016/0305-0491(77)90131-6.

Koehn, R.K., and Gaffney, P.M. 1984. Genetic heterozygosity and growth rate in *Mytilus edulis.* Marine Biology 82: 1–7. doi:10.1007/BF00392757.

Koehn, R.K., Hall, J.G., Innes, D.J., and Zera, A.J. 1984. Genetic differentiation of *Mytilus edulis* in eastern North America. Marine Biology 79: 117–126. doi:10.1007/BF00951820.

Kollmar, M. 2016. Fine-tuning motile cilia and flagella: Evolution of the dynein motor proteins from plants to humans at high resolution. Molecular Biology and Evolution 33: 3249–3267. doi:10.1093/molbev/msw213.

Kong, H., Jiang, X., Clements, J.C., Wang, T., Huang, X., Shang, Y., Chen, J., Hu, M., and Wang, Y. 2019. Transgenerational effects of short-term exposure to acidification and hypoxia on early developmental traits of the mussel *Mytilus edulis*. Marine Environmental Research 145: 73–80. doi:10.1016/j.marenvres.2019.02.011.

Kozuki, Y., Yamanaka, R., Matsushige, M., Saitoh, A., Otani, S., and Ishida, T. 2013. The after-effects of hypoxia exposure on the clam *Ruditapes philippinarum* in Omaehama beach, Japan. Estuarine, Coastal and Shelf Science 116: 50–56. doi:10.1016/j.ecss.2012.08.026.

Kotsyuba, E.P. 2017. Hypoxia-inducible factor 1α in the central nervous system of the scallop *Mizuhopecten yessoensis* Jay, 1857 (Bivalvia: Pectinidae) during anoxia and elevated temperatures. Russian Journal of Marine Biology 43: 293–301. doi:10.1134/S1063074017040071.

Kube, S., Sokolowski, A., Jansen, J.M., and Schiedek, D. 2007. Seasonal variability of free amino acids in two marine bivalves, *Macoma balthica* and *Mytilus* spp., in relation to environmental and physiological factors. Comparative Biochemistry and Physiology Part A: Molecular & Integrative Physiology 147: 1015–1027. doi:10.1016/j.cbpa.2007.03.012.

Kudo, Y., Siriwardena, B., Hatano, H., Ogawa, I., and Takata, T. 2007. Periostin: Novel diagnostic and therapeutic target for cancer. Histology and Histopathology 10: 1167–1174. doi:10.14670/HH-22.1167.

Kültz, D. 2020. Evolution of cellular stress response mechanisms. Journal of Experimental Zoology Part A: Ecological and Integrative Physiology 333: 359–378. doi:10.1002/jez.2347.

Kumar, S., Stecher, G., Li, M., Knyaz, C., and Tamura, K. 2018. MEGA X: Molecular Evolutionary Genetics Analysis across Computing Platforms. Molecular biology and evolution 35: 1547–1549. doi:10.1093/molbev/msy096.

Kumaresan, V., Bhatt, P., Palanisamy, R., Gnanam, A., Pasupuleti, M., and Arockiaraj, J. 2014. A murrel cysteine protease, cathepsin L: bioinformatics characterization, gene expression and proteolytic activity. Biologia 69: 395–406. doi:10.2478/s11756-013-0326-8.

Kwiatkowski, L., Torres, O., Bopp, L., Aumont, O., Chamberlain, M., Christian, J.R., Dunne, J.P., Gehlen, M., Ilyina, T., John, J.G., Lenton, A., Li, H., Lovenduski, N.S., Orr, J.C., Palmieri, J., Santana-Falcón, Y., Schwinger, J., Séférian, R., Stock, C.A., Tagliabue, A., Takano, Y., Tjiputra, J., Toyama, K., Tsujino, H., Watanabe, M., Yamamoto, A., Yool, A., and Ziehn, T. 2020. Twenty-first century ocean warming, acidification, deoxygenation, and upper-ocean nutrient and primary production decline from CMIP6 model projections. Biogeosciences 17: 3439–3470. doi:10.5194/bg-17-3439-2020.

La Porte, P.F. 2005. *Mytilus trossulus* hsp70 as a biomarker for arsenic exposure in the marine environment: Laboratory and real-world results. Biomarkers 10: 417–428. doi:10.1080/13547500500264371.

Labarta, U., Fernández-Reiriz, M.J., and Babarro, J.M.F. 1997. Differences in physiological energetics between intertidal and raft cultivated mussels *Mytilus galloprovincialis*. Marine Ecology Progress Series 152: 167–173. doi:10.3354/meps152167.

Labarta, U., Fernández-Reiriz, M.-J., Navarro, J., and Velasco, L. 2002. Enzymatic digestive activity in epifaunal *Mytilus chilensis* (Hupé,1854) and infaunal *Mulinia edulis* (King and Broderip,1832) bivalves in response to changes in food regimes in a natural environment. Marine Biology 140: 669–676. doi:10.1007/s00227-001-0742-0.

Lachance-Bernard, M., Daigle, G., Himmelman, J.H., and Fréchette, M. 2010. Biomass–density relationships and self-thinning of blue mussels (*Mytilus* spp.) reared on self-regulated longlines. Aquaculture 308: 34–43. doi:10.1016/j.aquaculture.2010.07.038.

Lacroix, C., Duvieilbourg, E., Guillou, N., Guyomarch, J., Bassoulet, C., Moraga, D., Chapalain, G., and Auffret, M. 2017. Seasonal monitoring of blue mussel (*Mytilus* spp.) populations in a harbor area: A focus on responses to environmental factors and chronic contamination. Marine Environmental Research 129: 24–35. doi:10.1016/j.marenvres.2017.04.008.

Lajus, D.L., and Sukhotin, A.A. 1998. A new approach for the assessment of stochastic variation: analysis of behavioural response in blue mussel (*Mytilus edulis* L.). Helgoländer Meeresunters. 52: 141–145. doi:10.1007/BF02908743.

Lambert, N., Chassé, J., Perrie, W., Long, Z., Guo, L., and Morrison, J.R. 2013. Projection of future river runoffs in Eastern Atlantic Canada from global and regional climate models. Canadian Technical Report of Hydrography and Ocean Sciences 288: viii +: 34.

Lang, F., Busch, G.L., and Völkl, H. 1998. The diversity of volume regulatory mechanisms. Cellular Physiology and Biochemistry 8: 1–45. doi:10.1159/000016269.

Langton, R.W. 1977. Digestive rhythms in the mussel *Mytilus edulis*. Marine Biology 41: 53–58. doi:10.1007/BF00390581.

Laplante, M., and Sabatini, D.M. 2009. mTOR signaling at a glance. Journal of Cell Science 122: 3589–3594. doi:10.1242/jcs.051011.

Larade, K., and Storey, K.B. 2002. Reversible suppression of protein synthesis in concert with polysome disaggregation during anoxia exposure in *Littorina littorea*. Molecular Cellular Biochemistry 232: 121–127. doi:10.1023/A:1014811017753.

Larade, K., and Storey, K.B. 2009. Living without oxygen: anoxia-responsive gene expression and regulation. Current Genomics 10: 76–85. doi:10.2174/138920209787847032.

Larade, K., Storey, K.B., and Storey, J.M. 2002. A profile of the metabolic responses to anoxia in marine invertebrates. Pages 27–46 in Cell and Molecular Response to Stress: Sensing, Signaling and Cell Adaptation. Elsevier. doi:10.1016/S1568-1254(02)80005-5.

Lassoued, J., Babarro, J.M.F., Padín, X.A., Comeau, L.A., Bejaoui, N., and Pérez, F.F. 2019. Behavioural and eco-physiological responses of the mussel *Mytilus galloprovincialis* to acidification and distinct feeding regimes. Marine Ecology Progress Series 626: 97–108. doi:10.3354/meps13075.

Le Chevalier, P., Sellos, D., and Van Wormhoudt, A. 1995. Purification and partial characterization of chymotrypsin-like proteases from the digestive gland of the scallop *Pecten maximus*. Comparative Biochemistry and Physiology Part B: Biochemistry and Molecular Biology 110: 777–784. doi:10.1016/0305-0491(94)00211-C.

Leblanc, N., Landry, T., Davidson, J., Tremblay, R., and McNiven, M. 2010. The effect of elevated water temperature stress on the mussel *Mytilus edulis* (L.), survival and genetic characteristics. Canadian technical report of fisheries and aquatic sciences 2900 vii +: 19.

LeBlanc, N., Tremblay, R., Davidson, J., Landry, T., and McNiven, M. 2008. The effect of selection treatments on Mytilus edulis, modifications of genetic and physiological characteristics. Marine Biology 153: 1141–1152. doi:10.1007/s00227-007-0885-8.

Leiniö, S., and Lehtonen, K.K. 2005. Seasonal variability in biomarkers in the bivalves *Mytilus edulis* and *Macoma balthica* from the northern Baltic Sea. Comparative Biochemistry and Physiology Part C: Toxicology & Pharmacology 140: 408–421. doi:10.1016/j.cca.2005.04.005.

Leite, C., Coppola, F., Monteiro, R., Russo, T., Polese, G., Silva, M.R.F., Lourenço, M.A.O., Ferreira, P., Soares, A.M.V.M., Pereira, E., and Freitas, R. 2020. Toxic impacts of rutile titanium dioxide in *Mytilus galloprovincialis* exposed to warming conditions. Chemosphere 252: 126563. doi:10.1016/j.chemosphere.2020.126563.

Lenihan, H.S., and Peterson, C.H. 1998. How habitat degradation through fishery disturbance enhances impacts of hypoxia on oyster reefs. Ecological Applications 8: 128–140. doi:https://doi.org/10.1890/1051-0761(1998)008[0128:HHDTFD]2.0.CO;2.

Lent, C.M. 1968. Air-gulping by the ribbed mussel *Modiolus demissus* (Dillwyn): effect and adaptive significance. The Biological Bulletin 134: 60–73. doi:10.2307/1539967.

Lesser, M.P., Bailey, M.A., Merselis, D.G., and Morrison, J.R. 2010. Physiological response of the blue mussel *Mytilus edulis* to differences in food and temperature in the Gulf of Maine. Comparative Biochemistry and Physiology Part A: Molecular & Integrative Physiology 156: 541–551. doi:10.1016/j.cbpa.2010.04.012.

Lewis, P. 1997. Climate trends in Atlantic Canada. Pages 180–183 in R. Shaw, ed. Climate Change and Climate Variability in Atlantic Canada.

Li, J., Ma, P., Liu, P., Chen, P., and Li, J. 2015a. The roles of Na+/K+-ATPase α-subunit gene from the ridgetail white prawn *Exopalaemon carinicauda* in response to salinity stresses. Fish & Shellfish Immunology 42: 264–271. doi:10.1016/j.fsi.2014.10.043.

Li, L., Lu, W., Sui, Y., Wang, Y., Gul, Y., and Dupont, S. 2015b. Conflicting effects of predator cue and ocean acidification on the mussel *Mytilus coruscus* byssus production. Journal of Shellfish Research 34: 393–400. doi:10.2983/035.034.0222.

Li, Y., Guan, Y., Li, Q., and He, M. 2015c. Analysis of DNA methylation in tissues and development stages of pearl oyster *Pinctada fucata*. Genes & Genomics 37: 263–270. doi:10.1007/s13258-014-0246-1.

Li, Y., Ren, L., Fu, H., Yang, B., Tian, J., Li, Q., Liu, Z., and Liu, S. 2021. Crosstalk between dopamine and insulin signaling in growth control of the oyster. General and Comparative Endocrinology 313: 113895. doi:10.1016/j.ygcen.2021.113895.

Li, Y.-F., Chen, Y.-W., Xu, J.-K., Ding, W.-Y., Shao, A.-Q., Zhu, Y.-T., Wang, C., Liang, X., and Yang, J.-L. 2019. Temperature elevation and *Vibrio cyclitrophicus* infection reduce the diversity of haemolymph microbiome of the mussel *Mytilus coruscus*. Scientific Reports 9:16391. doi:10.1038/s41598-019-52752-y.

Li, Y.-F., Yang, N., Liang, X., Yoshida, A., Osatomi, K., Power, D., Batista, F.M., and Yang, J.-L. 2018. Elevated seawater temperatures decrease microbial diversity in the gut of *Mytilus coruscus*. Frontiers in Physiology 9:839. doi:10.3389/fphys.2018.00839.

Liang, Y., Zhang, G., Wan, A., Zhao, Z., Wang, S., and Liu, Q. 2019. Nutrient-limitation induced diatom-dinoflagellate shift of spring phytoplankton community in an offshore shellfish farming area. Marine Pollution Bulletin 141: 1–8. doi:10.1016/j.marpolbul.2019.02.009.

Lim, H.-S., Diaz, R.J., Hong, J.-S., and Schaffner, L.C. 2006. Hypoxia and benthic community recovery in Korean coastal waters. Marine Pollution Bulletin 52: 1517–1526. doi:10.1016/j.marpolbul.2006.05.013.

Liu, D., Wu, H., Li, Y.Z., Yang, J., Yang, J., Ding, J.W., Zhou, G., Zhang, J., Wang, X., and Fan, Z.X. 2021. Cellular FADD-like IL-1β-converting enzyme-inhibitory protein attenuates myocardial ischemia/reperfusion injury via suppressing apoptosis and autophagy simultaneously. Nutrition, metabolism, and cardiovascular diseases: NMCD 31: 1916–1928. doi:10.1016/j.numecd.2021.02.026.

Liu, H., He, J., Chi, C., and Shao, J. 2014. Differential HSP70 expression in *Mytilus coruscus* under various stressors. Gene 543: 166–173. doi:10.1016/j.gene.2014.04.008.

Liu, H., Wu, J., Xu, M., and He, J. 2016. A novel biomarker for marine environmental pollution of HSP90 from *Mytilus coruscus*. Marine Pollution Bulletin 111: 428–434. doi:10.1016/j.marpolbul.2016.07.031.

Locke, A., Hanson, J.M., Ellis, K.M., Thompson, J., and Rochette, R. 2007. Invasion of the southern Gulf of St. Lawrence by the clubbed tunicate (*Styela clava* Herdman): Potential mechanisms for invasions of Prince Edward Island estuaries. Journal of Experimental Marine Biology and Ecology 342: 69–77. doi:10.1016/j.jembe.2006.10.016.

Lockwood, B.L., Sanders, J.G., and Somero, G.N. 2010. Transcriptomic responses to heat stress in invasive and native blue mussels (genus *Mytilus*): molecular correlates of invasive success. The Journal of Experimental Biology 213: 3548–3558. doi:10.1242/jeb.046094.

Lockwood, B.L., and Somero, G.N. 2011. Transcriptomic responses to salinity stress in invasive and native blue mussels (genus *Mytilus*). Molecular ecology 20: 517–529.

Lomelino, C.L., Andring, J.T., McKenna, R., and Kilberg, M.S. 2017. Asparagine synthetase: function, structure, and role in disease. The Journal of Biological Chemistry 292: 19952–19958. doi:10.1074/jbc.R117.819060.

Long, Z., Perrie, W., Chassé, J., Brickman, D., Guo, L., Drozdowski, A., and Hu, H. 2016. Impacts of climate change in the Gulf of St. Lawrence. Atmosphere-Ocean 54: 337–351. doi:10.1080/07055900.2015.1029869.

Louati, H., Zouari, N., Miled, N., and Gargouri, Y. 2011. A new chymotrypsin-like serine protease involved in dietary protein digestion in a primitive animal, *Scorpio maurus*: purification and biochemical characterization. Lipids in Health and Disease 10:121. doi:10.1186/1476-511X-10-121.

Love, M.I., Huber, W., and Anders, S. 2014. Moderated estimation of fold change and dispersion for RNA-seq data with DESeq2. Genome Biology 15: 550. doi:10.1186/s13059-014-0550-8.

Lowe, D.M., Moore, M.N., and Evans, B.M. 1992. Contaminant impact on interactions of molecular probes with lysosomes in living hepatocytes from dab *Limanda limanda*. Marine Ecology Progress Series 91: 135–140.

Lowe, D.M., and Pipe, R.K. 1994. Contaminant induced lysosomal membrane damage in marine mussel digestive cells: an in vitro study. Aquatic toxicology 30: 357–365. doi:10.1016/0166-445X(94)00045-X.

Lowe, D.M., Soverchia, C., and Moore, M.N. 1995. Lysosomal membrane responses in the blood and digestive cells of mussels experimentally exposed to fluoranthene. Aquatic Toxicology 33: 105–112. doi:10.1016/0166-445X(95)00015-V.

Lowe, R., Shirley, N., Bleackley, M., Dolan, S., and Shafee, T. 2017. Transcriptomics technologies. PLoS computational biology 13: e1005457.

MacCready, P., and Geyer, W.R. 2010. Advances in stuarine Physics. Annual Review of Marine Science 2: 35–58. Annual Reviews. doi:10.1146/annurev-marine-120308-081015.

MacNair, N. 2005. Invasive tunicates of concern for Prince Edward Island aquaculture. Aqua Info Aquaculture Note. Charlottetown: Department of Agriculture Fisheries and Aquaculture.

Magara, G., Khan, F.R., Pinti, M., Syberg, K., Inzirillo, A., and Elia, A.C. 2019. Effects of combined exposures of fluoranthene and polyethylene or polyhydroxybutyrate microplastics on oxidative stress biomarkers in the blue mussel (*Mytilus edulis*). Journal of Toxicology and Environmental Health, Part A 82: 616–625. doi:10.1080/15287394.2019.1633451.

Malachowicz, M., and Wenne, R. 2019. Mantle transcriptome sequencing of *Mytilus* spp. and identification of putative biomineralization genes. PeerJ 6: e6245. doi:10.7717/peerj.6245.

Mallet, A.L., Carve, C., and Freemam, K.R. 1990. Summer mortality of the blue mussel in eastern Canada: spatial, temporal, stock and age variation. Marine Ecology Progress Series 67: 35–41. doi:10.3354/meps067035.

Mann, R., and Gallager, S.M. 1985. Physiological and biochemical energetics of larvae of *Teredo navalis* L. and *Bankia gouldi* (Bartsch) (Bivalvia : Teredinidae). Journal of Experimental Marine Biology and Ecology 85: 211–228. doi:10.1016/0022-0981(85)90159-5.

Marsooli, R., Lin, N., Emanuel, K., and Feng, K. 2019. Climate change exacerbates hurricane flood hazards along US Atlantic and Gulf Coasts in spatially varying patterns. Nature Communications 10: 1–9. doi:10.1038/s41467-019-11755-z.

Matear, R.J., Hirst, A.C., and McNeil, B.I. 2000. Changes in dissolved oxygen in the Southern Ocean with climate change. Geochemistry, Geophysics, Geosystems 1(11). doi:10.1029/2000GC000086.

Matoo, O.B., Lannig, G., Bock, C., and Sokolova, I.M. 2021. Temperature but not ocean acidification affects energy metabolism and enzyme activities in the blue mussel, *Mytilus edulis.* Ecology and Evolution 11: 3366–3379. doi:10.1002/ece3.7289.

Matozzo, V., Chinellato, A., Munari, M., Bressan, M., and Marin, M.G. 2013. Can the combination of decreased pH and increased temperature values induce oxidative stress in the clam *Chamelea gallina* and the mussel *Mytilus galloprovincialis*? Marine Pollution Bulletin 72: 34–40. doi:10.1016/j.marpolbul.2013.05.004.

Matozzo, V., Chinellato, A., Munari, M., Finos, L., Bressan, M., and Marin, M.G. 2012. First evidence of immunomodulation in bivalves under seawater acidification and increased temperature. PLoS One 7: e33820.

Matozzo, V., Monari, M., Foschi, J., Papi, T., Cattani, O., and Marin, M.G. 2005. Exposure to anoxia of the clam *Chamelea gallina*. Journal of Experimental Marine Biology and Ecology 325: 163–174. doi:10.1016/j.jembe.2005.04.030.

May, M.A., Bishop, K.D., and Rawson, P.D. 2017. NMR Profiling of metabolites in larval and juvenile blue mussels (*Mytilus edulis*) under ambient and low salinity conditions. Metabolites 7: 33. doi:10.3390/metabo7030033.

Maynard, A., Bible, J.M., Pespeni, M.H., Sanford, E., and Evans, T.G. 2018. Transcriptomic responses to extreme low salinity among locally adapted populations of Olympia oyster (*Ostrea lurida*). Molecular Ecology 27: 4225–4240. doi:10.1111/mec.14863.

Mayrand, E., Sonier, T., and Comeau, L.A. 2015. Hot water immersion lowers survival, shell growth rate and lysosomal membrane stability of oysters *Crassostrea virginica* (Gmelin). Aquaculture Research 46: 1974–1987.

McAllen, R., and Taylor, A. 2001. The effect of salinity change on the oxygen consumption and swimming activity of the high-shore rockpool copepod *Tigriopus brevicornis*. Journal of Experimental Marine Biology and Ecology 263: 227–240. doi:10.1016/S0022-0981(01)00308-2.

McDade, J.E., and Tripp, M.R. 1967. Lysozyme in the hemolymph of the oyster, *Crassostrea virginica*. Journal of Invertebrate Pathology 9: 531–535. doi:10.1016/0022-2011(67)90134-6.

Mcmahon, R.F. 1988. Respiratory response to periodic emergence in intertidal molluscs. American Zoologist 28: 97–114. doi:10.1093/icb/28.1.97.

Melzner, F., Stange, P., Trübenbach, K., Thomsen, J., Casties, I., Panknin, U., Gorb, S.N., and Gutowska, M.A. 2011. Food supply and seawater pCO2 impact calcification and internal shell dissolution in the blue mussel *Mytilus edulis*. PLoS One 6: e24223. doi:10.1371/journal.pone.0024223.

Meng, J., Wang, T., Li, L., and Zhang, G. 2018. Inducible variation in anaerobic energy metabolism reflects hypoxia tolerance across the intertidal and subtidal distribution of the Pacific oyster (*Crassostrea gigas*). Marine Environmental Research 138: 135–143. doi:10.1016/j.marenvres.2018.04.002.

Meng, J., Zhu, Q., Zhang, L., Li, C., Li, L., She, Z., Huang, B., and Zhang, G. 2013. Genome and transcriptome analyses provide insight into the euryhaline adaptation mechanism of *Crassostrea gigas*. PLoS One 8: e58563. doi:10.1371/journal.pone.0058563.

Meng, X., Li, F., Wang, X., Liu, J., Ji, C., and Wu, H. 2020. Toxicological effects of graphene on mussel *Mytilus galloprovincialis* hemocytes after individual and combined exposure with triphenyl phosphate. Marine Pollution Bulletin 151: 110838. doi:10.1016/j.marpolbul.2019.110838.

Méthé, D., Comeau, L.A., Stryhn, H., Burka, J.F., Landry, T., and Davidson, J. 2017. Haemolymph fluid osmolality influences the neutral-red retention assay in the eastern oyster *Crassostrea virginica*. Journal of Molluscan Studies 83: 229–234. doi:10.1093/mollus/eyw050.

Méthé, D., Comeau, L.A., Stryhn, H., Landry, T., and Davidson, J. 2015. Stress response of *Crassostrea virginica* (Gmelin, 1791) oysters following a reciprocal transfer between upriver and downriver sites. Aquaculture Research 46: 2841–2850.

Michaelidis, B., Haas, D., and Grieshaber, M.K. 2005. Extracellular and intracellular acid-base status with regard to the energy metabolism in the oyster *Crassostrea gigas* during exposure to air. Physiological and Biochemical Zoology 78: 373–383. doi:10.1086/430223.

Miller, C. 2000. An overview of the potassium channel family. Genome Biology 1: 1–5. doi:10.1186/gb-2000-1-4-reviews0004.

Mitchell, J.F.B. 1989. The "Greenhouse" effect and climate change. Reviews of Geophysics 27: 115. doi:10.1029/RG027i001p00115.

Mitchell, J.P., and Carmody, R.J. 2018. Chapter two - NF-κB and the transcriptional control of inflammation. Pages 41–84 in F. Loos, ed. International Review of Cell and Molecular Biology. Academic Press. doi:10.1016/bs.ircmb.2017.07.007.

Møhlenberg, F., and Riisgård, H.U. 1978. Efficiency of particle retention in 13 species of suspension feeding bivalves. Ophelia 17: 239–246. doi:10.1080/00785326.1978.10425487.

Montagnani, M., Abrahamsson, A., Gälman, C., Eggertsen, G., Marschall, H.-U., Ravaioli, E., Einarsson, C., and Dawson, P.A. 2006. Analysis of ileal sodium/bile acid cotransporter and related nuclear receptor genes in a family with multiple cases of idiopathic bile acid malabsorption. World Journal of Gastroenterology 12(47):7710–7714. doi:10.3748/wjg.v12.i47.7710.

Moore, M.N. 1976. Cytochemical demonstration of latency of lysosomal hydrolases in digestive cells of the common mussel, *Mytilus edulis*, and changes induced by thermal stress. Cell and Tissue Research 175: 279–287. doi:10.1007/BF00218706.

Moore, M.N., Lowe, D.M., and Moore, S.L. 1979. Induction of lysosomal destabilization in marine bivalve mollusks exposed to air. Marine Biology Letters 1: 47–57.

Moriya, Y., Itoh, M., Okuda, S., Yoshizawa, A.C., and Kanehisa, M. 2007. KAAS: an automatic genome annotation and pathway reconstruction server. Nucleic Acids Research 35: W182-185. doi:10.1093/nar/gkm321.

Mort, J.S., and Buttle, D.J. 1997. Cathepsin B. The International Journal of Biochemistry & Cell Biology 29: 715–720. doi:10.1016/S1357-2725(96)00152-5.

Morton, B. 1992. The Evolution and Success of the Hereomyarian form in Mytiloida. Pages 21–48 in E. Gosling, ed. The mussel *Mytilus*: Ecology, Physiology, Genetics, and Culture. Elsevier.

Múgica, M., Sokolova, I.M., Izagirre, U., and Marigómez, I. 2015. Season-dependent effects of elevated temperature on stress biomarkers, energy metabolism and gamete development in mussels. Marine Environmental Research 103: 1–10. doi:10.1016/j.marenvres.2014.10.005.

Müller, M., Mentel, M., Hellemond, J.J. van, Henze, K., Woehle, C., Gould, S.B., Yu, R.-Y., Giezen, M. van der, Tielens, A.G.M., and Martin, W.F. 2012. Biochemistry and evolution of anaerobic energy metabolism in eukaryotes. Microbiology and Molecular Biology Reviews 76: 444–495. doi:10.1128/MMBR.05024-11.

Myrand, B., Guderley, H., and Himmelman, J.H. 2000. Reproduction and summer mortality of blue mussels *Mytilus edulis* in the Magdalen Islands, southern Gulf of St. Lawrence. Marine Ecology Progress Series 197: 193–207.

Myrand, B., Tremblay, R., and Sevigny, J.-M. 2002. Selection against blue mussels (*Mytilus edulis* L.) homozygotes under various stressful conditions. The Journal of Heredity 93: 238.

Myrand, B., Tremblay, R., and Sévigny, J.-M. 2009. Decreases in multi-locus heterozygosity in suspension-cultured mussels (*Mytilus edulis*) through loss of the more heterozygous individuals. Aquaculture 295: 188–194. doi:10.1016/j.aquaculture.2009.07.014.

Nachman Myrand, R.J., Giard, W., Favrel, P., Suresh, T., Sreekumar, S., and Holman, G.M. 1997. Insect myosuppressins and sulfakinins stimulate release of the digestive enzyme α-amylase in two invertebrates: the scallop *Pecten maximus* and insect *Rhynchophorus ferrugineus*. Annals of the New York Academy of Sciences 814: 335–338. doi:10.1111/j.1749-6632.1997.tb46178.x.

Nagarajan, R., Lea, S.E.G., and Goss-Custard, J.D. 2006. Seasonal variations in mussel, *Mytilus edulis* L. shell thickness and strength and their ecological implications. Journal of Experimental Marine Biology and Ecology 339: 241–250. doi:10.1016/j.jembe.2006.08.001.

Nappi, A.J., and Ottaviani, E. 2000. Cytotoxicity and cytotoxic molecules in invertebrates. BioEssays 22: 469–480. doi:10.1002/(SICI)1521-1878(200005)22:5<469::AID-BIES9>3.0.CO;2-4.

Narváez, M., Freites, L., Guevara, M., Mendoza, J., Guderley, H., Lodeiros, C.J., and Salazar, G. 2008. Food availability and reproduction affects lipid and fatty acid composition of the brown mussel*, Perna perna*, raised in suspension culture. Comparative Biochemistry and Physiology Part B: Biochemistry and Molecular Biology 149: 293–302. doi:10.1016/j.cbpb.2007.09.018.

Navarro, E., Iglesias, J.I.P., and Ortega, M.M. 1992. Natural sediment as a food source for the cockle *Cerastoderma edule* (L.): effect of variable particle concentration on feeding, digestion and the scope for growth. Journal of Experimental Marine Biology and Ecology 156: 69–87. doi:10.1016/0022-0981(92)90017-5.

Navarro, E., Méndez, S., Ibarrola, I., and Urrutia, M.B. 2009. Comparative utilization of phytoplankton and vascular plant detritus by the cockle *Cerastoderma edule*: digestive responses during diet acclimation. Aquatic Biology 6: 247–262. doi:10.3354/ab00127.

Navarro, J.M., Labarta, U., Fernández-Reiriz, M.J., and Velasco, A. 2003. Feeding behavior and differential absorption of biochemical components by the infaunal bivalve *Mulinia edulis* and the epibenthic *Mytilus chilensis* in response to changes in food regimes. Journal of Experimental Marine Biology and Ecology 287: 13–35. doi:10.1016/S0022-0981(02)00501-4.

Nederbragt, A.J., van Loon, A.E., and Dictus, W.J.A.G. 2002. Evolutionary biology: hedgehog crosses the snail's midline. Nature 417: 811–812. doi:10.1038/417811b.

Negri, A., Oliveri, C., Sforzini, S., Mignione, F., Viarengo, A., and Banni, M. 2013. Transcriptional response of the mussel *Mytilus galloprovincialis* (Lam.) following exposure to heat stress and copper. PLOS ONE 8: e66802. doi:10.1371/journal.pone.0066802.

Nell, J.A., Cox, E., Smith, I.R., and Maguire, G.B. 1994. Studies on triploid oysters in Australia. I. The farming potential of triploid Sydney rock oysters *Saccostrea commercialis* (Iredale and Roughley). Aquaculture 126: 243–255. doi:10.1016/0044-8486(94)90040-X.

Nemova, N.N., Fokina, N.N., Nefedova, Z.A., Ruokolainen, T.R., and Bakhmet, I.N. 2013. Modifications of gill lipid composition in littoral and cultured blue mussels *Mytilus edulis* L. under the influence of ambient salinity. Polar Record 49: 272–277. doi:10.1017/S0032247412000629.

Newell, C.R., Wildish, D.J., and MacDonald, B.A. 2001. The effects of velocity and seston concentration on the exhalant siphon area, valve gape and filtration rate of the mussel *Mytilus edulis*. Journal of Experimental Marine Biology and Ecology 262: 91–111. doi:10.1016/S0022-0981(01)00285-4.

Nguyen, T.V., and Alfaro, A.C. 2020. Applications of omics to investigate responses of bivalve haemocytes to pathogen infections and environmental stress. Aquaculture 518: 734488. doi:10.1016/j.aquaculture.2019.734488.

Nicholson, S. 2003. Cardiac and branchial physiology associated with copper accumulation and detoxication in the mytilid mussel *Perna viridis* (L.). Journal of Experimental Marine Biology and Ecology 295: 157–171. doi:10.1016/S0022-0981(03)00292-2.

Nie, H., Jiang, L., Chen, P., Huo, Z., Yang, F., and Yan, X. 2017. High throughput sequencing of RNA transcriptomes in *Ruditapes philippinarum* identifies genes involved in osmotic stress response. Scientific Reports 7: 4953. doi:10.1038/s41598-017-05397-8.

Nie, H., Liu, L., Wang, H., Huo, Z., and Yan, X. 2018. Stress levels over time in *Ruditapes philippinarum*: The effects of hypoxia and cold stress on hsp70 gene expression. Aquaculture Reports 12: 1–4. doi:10.1016/j.aqrep.2018.08.003.

Nie, H., Zheng, M., Wang, Z., Xu, Q., Yin, Z., Zhang, Y., and Yan, X. 2021. Transcriptomic analysis provides insights into candidate genes and molecular pathways involved in growth of Manila clam *Ruditapes philippinarum*. Functional & Integrative Genomics 21: 341–353. doi:10.1007/s10142-021-00780-1.

Nielsen, M.B., Vogensen, T.K., Thyrring, J., Sørensen, J.G., and Sejr, M.K. 2021. Freshening increases the susceptibility to heat stress in intertidal mussels (*Mytilus edulis*) from the Arctic. Journal of Animal Ecology 90: 1515–1524. doi:10.1111/1365-2656.13472.

Nielsen, N.F., Larsen, P.S., Riisgård, H.U., and Jørgensen, C.B. 1993. Fluid motion and particle retention in the gill of *Mytilus edulis*: Video recordings and numerical modelling. Marine Biology 116: 61–71. doi:10.1007/BF00350732.

Nilius, B., and Owsianik, G. 2011. The transient receptor potential family of ion channels. Genome Biology 12: 218. doi:10.1186/gb-2011-12-3-218.

Nonhoff, U., Ralser, M., Welzel, F., Piccini, I., Balzereit, D., Yaspo, M.-L., Lehrach, H., and Krobitsch, S. 2007. Ataxin-2 interacts with the DEAD/H-Box RNA Helicase DDX6 and interferes with P-Bodies and stress granules. Molecular Biology of the Cell 18: 1385–1396. doi:10.1091/mbc.e06-12-1120.

Norkko, J., Pilditch, C.A., Thrush, S.F., and Wells, R.M.G. 2005. Effects of food availability and hypoxia on bivalves: the value of using multiple parameters to measure bivalve condition in environmental studies. Marine Ecology Progress Series 298: 205–218 doi:10.3354/meps298205.

O'Donnell, M.J., George, M.N., and Carrington, E. 2013. Mussel byssus attachment weakened by ocean acidification. Nature Climate Change 3: 587–590. doi:10.1038/nclimate1846.

Okumuş, İ., and Stirling, H.P. 1994. Physiological energetics of cultivated mussel (*Mytilus edulis*) populations in two Scottish west coast sea lochs. Marine Biology 119: 125–131. doi:10.1007/BF00350114.

Olabarria, C., Gestoso, I., Lima, F.P., Vázquez, E., Comeau, L.A., Gomes, F., Seabra, R., and Babarro, J.M.F. 2016. Response of two mytilids to a heatwave: the complex interplay of physiology, behaviour and ecological Interactions. PLoS One 11: e0164330. doi:10.1371/journal.pone.0164330.

Ostrowski, L.A., Hall, A.C., and Mekhail, K. 2017. Ataxin-2: from RNA control to human health and disease. Genes 8: 157. doi:10.3390/genes8060157.

Owen, G. 1955. Observations on the stomach and digestive diverticula of the Lamellibranchia: I. The Anisomyaria and Eulamellibranchia. Journal of Cell Science 3: 517–537.

Owen, G. 1972. Lysosomes, peroxisomes and bivalves. Science Progress 60: 299–318.

Page, H.M., and Hubbard, D.M. 1987. Temporal and spatial patterns of growth in mussels *Mytilus edulis* on an offshore platform: relationships to water temperature and food availability. Journal of Experimental Marine Biology and Ecology 111: 159–179. doi:10.1016/0022-0981(87)90053-0.

Pales Espinosa, E., and Allam, B. 2013a. Food quality and season affect gene expression of the mucosal lectin MeML and particle sorting in the blue mussel *Mytilus edulis*. Marine Biology 160: 1441–1450. doi:10.1007/s00227-013-2196-6.

Pales Espinosa, E., and Allam, B. 2018. Reverse genetics demonstrate the role of mucosal C-type lectins in food particle selection in the oyster *Crassostrea virginica*. Journal of Experimental Biology 221: jeb174094. doi:10.1242/jeb.174094.

Pales Espinosa, E., Koller, A., and Allam, B. 2016. Proteomic characterization of mucosal secretions in the eastern oyster, *Crassostrea virginica*. Journal of proteomics 132: 63–76.

Pales Espinosa, E.P., and Allam, B. 2013b. Food quality and season affect gene expression of the mucosal lectin MeML and particle sorting in the blue mussel *Mytilus edulis*. Marine Biology 160: 1441–1450. doi:10.1007/s00227-013-2196-6.

Pampanin, D., Ballarin, L., Carotenuto, L., and Marin, M. 2002. Air exposure and functionality of *Chamelea gallina* haemocytes: effects on haematocrit, adhesion, phagocytosis and enzyme contents. Comparative Biochemistry and physiology. Part A, Molecular & Integrative Physiology 131: 605–614. doi:10.1016/s1095-6433(01)00512-8.

Papke, R.L., and Lindstrom, J.M. 2020. Nicotinic acetylcholine receptors: conventional and unconventional ligands and signaling. Neuropharmacology 168: 108021. doi:10.1016/j.neuropharm.2020.108021.

Parisi, M.G., Mauro, M., Sarà, G., and Cammarata, M. 2017. Temperature increases, hypoxia, and changes in food availability affect immunological biomarkers in the marine mussel *Mytilus galloprovincialis*. Journal of Comparative Physiology B 187: 1117–1126. doi:10.1007/s00360-017-1089-2.

Parker, L.M., O'Connor, W.A., Byrne, M., Coleman, R.A., Virtue, P., Dove, M., Gibbs, M., Spohr, L., Scanes, E., and Ross, P.M. 2017. Adult exposure to ocean acidification is maladaptive for larvae of the Sydney rock oyster *Saccostrea glomerata* in the presence of multiple stressors. Biology Letters 13: 20160798. doi:10.1098/rsbl.2016.0798.

Parker, L.M., O'Connor, W.A., Raftos, D.A., Pörtner, H.-O., and Ross, P.M. 2015. Persistence of positive carryover effects in the oyster, *Saccostrea glomerata*, following transgenerational exposure to ocean acidification. PLOS ONE 10: e0132276. doi:10.1371/journal.pone.0132276.

Parker, L.M., Ross, P.M., O'Connor, W.A., Borysko, L., Raftos, D.A., and Pörtner, H.-O. 2012. Adult exposure influences offspring response to ocean acidification in oysters. Global Change Biology 18: 82–92. doi:10.1111/j.1365-2486.2011.02520.x.

Pascoe, H.G., Wang, Y., and Zhang, X. 2015. Structural mechanisms of plexin signaling. Progress in Biophysics and Molecular Biology 118: 161–168. doi:10.1016/j.pbiomolbio.2015.03.006.

Pascoe, P., Parry, H., and Hawkins, A. 2009. Observations on the measurement and interpretation of clearance rate variations in suspension-feeding bivalve shellfish. Aquatic Biology 6: 181–190. doi:10.3354/ab00123.

Patterson, M.K., and Orr, G.R. 1968. Asparagine biosynthesis by the Novikoff Hepatoma isolation, purification, property, and mechanism studies of the enzyme system. The Journal of Biological Chemistry 243: 376–380.

Paulmier, A., and Ruiz-Pino, D. 2009. Oxygen minimum zones (OMZs) in the modern ocean. Progress in Oceanography 80: 113–128. doi:10.1016/j.pocean.2008.08.001.

Peck, L.S., Thorne, M.A.S., Hoffman, J.I., Morley, S.A., and Clark, M.S. 2015. Variability among individuals is generated at the gene expression level. Ecology 96: 2004–2014. doi:10.1890/14-0726.1.

Péden, R., Letendre, J., Rocher, B., Durand, F., Le Foll, F., Chan, P., Vaudry, D., and Bultelle, F. 2014. Impact of heat stress on *Mytilus edulis*: contaminants affect survival and HSP 70 proteoform expression. Journal of Xenobiotics 4(4892): 56–58. doi:10.4081/xeno.2014.4892.

Penney, R.W., Hart, M.J., and Templeman, N.D. 2007. Shell strength and appearance in cultured blue mussels *Mytilus edulis*, *M. trossulus* , and *M. edulis* × *M. trossulus* Hybrids. North American Journal of Aquaculture 69: 281–295. doi:10.1577/A06-044.1.

Pernet, F., Tremblay, R., Comeau, L., and Guderley, H. 2007. Temperature adaptation in two bivalve species from different thermal habitats: energetics and remodelling of membrane lipids. Journal of Experimental Biology 210: 2999–3014. doi:10.1242/jeb.006007.

Perry, R.J., Saunders, C.J., Nelson, J.M., Rizzo, M.J., Braco, J.T., and Johnson, E.C. 2020. Regulation of metabolism by an ensemble of different ion channel types: excitation-secretion coupling mechanisms of adipokinetic hormone producing cells in *Drosophila*. Frontiers in Physiology 11: 580618. doi:10.3389/fphys.2020.580618

Petes, L.E., Menge, B.A., and Harris, A.L. 2008. Intertidal mussels exhibit energetic trade-offs between reproduction and stress resistance. Ecological Monographs 78: 387–402. doi:10.1890/07-0605.1.

Philipp, E.E.R., Kraemer, L., Melzner, F., Poustka, A.J., Thieme, S., Findeisen, U., Schreiber, S., and Rosenstiel, P. 2012. Massively parallel RNA sequencing identifies a complex immune gene repertoire in the lophotrochozoan *Mytilus edulis*. PLOS ONE 7: e33091. doi:10.1371/journal.pone.0033091.

Pierce, S.K., and Greenberg, M.J. 1973. The initiation and control of free amino acid regulation of cell volume in salinity-stressed marine bivalves. Journal of Experimental Biology 59: 435–440.

Pierce, S.K., Rowland-Faux, L.M., and Crombie, B.N. 1995. The mechanism of glycine betaine regulation in response to hyperosmotic stress in oyster mitochondria: A comparative study of Atlantic and Chesapeake Bay oysters. Journal of Experimental Zoology 271: 161–170. doi:10.1002/jez.1402710302.

Place, S.P., O'Donnell, M.J., and Hofmann, G.E. 2008. Gene expression in the intertidal mussel *Mytilus californianus*: physiological response to environmental factors on a biogeographic scale. Marine Ecology Progress Series 356: 1–14. doi:10.3354/meps07354.

Poirier, L., Ramsay, A., Coffin, M., Davidson, J.D.P., and Comeau, L. 2021. Prince Edward Island's mussel monitoring program and associated environmental data. Canadian Manuscript Report of Fisheries and Aquatic Sciences 3226: vi +: 17.

Potts, W.T.W. 1958. The inorganic and amino acid composition of some lamellibranch mussels. Journal of Experimental Biology 35: 749–764. doi:10.1242/jeb.35.4.749.

Poulain, C., Lorrain, A., Flye-Sainte-Marie, J., Amice, E., Morize, E., and Paulet, Y.-M. 2011. An environmentally induced tidal periodicity of microgrowth increment formation in subtidal populations of the clam *Ruditapes philippinarum*. Journal of Experimental Marine Biology and Ecology 397: 58–64. doi:10.1016/j.jembe.2010.11.001.

Pourmozaffar, S., Jahromi, S.T., Rameshi, H., Sadeghi, A., Bagheri, T., Behzadi, S., Gozari, M., Zahedi, M.R., and Lazarjani, S.A. 2020. The role of salinity in physiological responses of bivalves. Reviews in Aquaculture 12: 1548–1566. doi:10.1111/raq.12397.

Prieto, D., Markaide, P., Urrutxurtu, I., Navarro, E., Artigaud, S., Fleury, E., Ibarrola, I., and Urrutia, M.B. 2019. Gill transcriptomic analysis in fast- and slow-growing individuals of *Mytilus galloprovincialis*. Aquaculture 511: UNSP 734242. doi:10.1016/j.aquaculture.2019.734242.

Pruski, A.M., and Dixon, D.R. 2002. Effects of cadmium on nuclear integrity and DNA repair efficiency in the gill cells of *Mytilus edulis* L. Aquatic Toxicology 57: 127–137. doi:10.1016/S0166-445X(01)00192-8.

Qi, P., and Tang, Z. 2020. The Nrf2 molecule trigger antioxidant defense against acute benzo(a)pyrene exposure in the thick shell mussel *Mytilus coruscus*. Aquatic Toxicology 226: 105554. doi:10.1016/j.aquatox.2020.105554.

Qiu, J., Tremblay, R., and Bourget, E. 2002. Ontogenetic changes in hyposaline tolerance in the mussels *Mytilus edulis* and *M. trossulus*: implications for distribution. Marine Ecology Progress Series 228: 143–152. doi:10.3354/meps228143.

Rabalais, N.N., Díaz, R.J., Levin, L.A., Turner, R.E., Gilbert, D., and Zhang, J. 2010. Dynamics and distribution of natural and human-caused hypoxia. Biogeosciences 7: 585–619. doi:https://doi.org/10.5194/bg-7-585-2010.

Rafrafi, S., and Uglow, R.F. 2009. Nitrogenous compounds changes in emersed oysters: *Crassostrea gigas*. Estuarine, Coastal and Shelf Science 81: 210–214. doi:10.1016/j.ecss.2008.10.011.

Rahman, M.A., Henderson, S., Miller-Ezzy, P., Li, X.X., and Qin, J.G. 2019. Immune response to temperature stress in three bivalve species: Pacific oyster *Crassostrea gigas*, Mediterranean mussel *Mytilus galloprovincialis* and mud cockle *Katelysia rhytiphora*. Fish & Shellfish Immunology 86: 868–874. doi:10.1016/j.fsi.2018.12.017.

Ramsay, A., Davidson, J., Bourque, D., and Stryhn, H. 2009. Recruitment patterns and population development of the invasive ascidian *Ciona intestinalis* in Prince Edward Island, Canada. Aquatic Invasions 4: 169–176. doi:10.3391/ai.2009.4.1.17.

Ramsay, A., Davidson, J., Landry, T., and Arsenault, G. 2008. Process of invasiveness among exotic tunicates in Prince Edward Island, Canada. Biological Invasions 10: 1311–1316. doi:10.1007/s10530-007-9205-y.

Raven, P., Johnson, G., Mason, K., Losos, J., and Singer, S. 2008. How Cells Harvest Energy. Page in Biology, 8th edition. McGraw Hill, New York, New York.

Redmond, K.J., Berry, M., Pampanin, D.M., and Andersen, O.K. 2017. Valve gape behaviour of mussels (Mytilus edulis) exposed to dispersed crude oil as an environmental monitoring endpoint. Marine Pollution Bulletin 117: 330–339. doi:10.1016/j.marpolbul.2017.02.005.

Redpath, K.J., and Davenport, J. 1988. The effect of copper, zinc and cadmium on the pumping rate of *Mytilus edulis* L. Aquatic Toxicology 13: 217–225. doi:10.1016/0166-445X(88)90054-9.

Reid, D., Western, W., Rounce, T., Bogdan, D., Churchill, J., van Bochove, E., Thériault, G., and Denault, J. 2016. Phosphorus. Pages 131–142 in Environmental Sustainability of Canadian Agriculture. Agriculture and Agri-Food Canada, Ottawa, ON.

Reimer, O., and Tedengren, M. 1997. Predator-induced changes in byssal attachment, aggregation and migration in the blue mussel, Mytilus edulis. Marine and Freshwater Behaviour and Physiology 30: 251–266. Taylor & Francis. doi:10.1080/10236249709379029.

Rein, T. 2020. Post-translational modifications and stress adaptation: the paradigm of FKBP51. Biochemical Society Transactions 48: 441–449. doi:10.1042/BST20190332.

Reinke, A.W., Baek, J., Ashenberg, O., and Keating, A.E. 2013. Networks of bZIP protein-protein interactions diversified over a billion years of evolution. Science 340: 730–734. doi:10.1126/science.1233465.

Rhein, M., Rintoul, S.R., Aoki, S., Compos, E., Chambers, D., Feely, R.A., Gulev, S., Johnson, G.C., Josey, S.A., Kostianoy, A., Mauritzen, C., Roemmich, D., Talley, L.D., and Wang, F. 2013. Observations: Ocean. Pages 291–300 in T.F. Stocker, D. Qin, G.-K. Plattner, M. Tigmor, S.K. Allen, J. Boschung, A. Nauels, Y. Xia, V. Bex, and P.M. Midgley, eds. Climate Change 2013: The Physical Science Basis. Contribution of Working Group I to the Fifth Assessment Report of the Intergovernmental Panel on Climate Change. Cambridge University Press, Cambridge, United Kingdom and New York, NY, USA.

Rickwood, C.J., and Galloway, T.S. 2004. Acetylcholinesterase inhibition as a biomarker of adverse effect: A study of *Mytilus edulis* exposed to the priority pollutant chlorfenvinphos. Aquatic Toxicology 67: 45–56. doi:10.1016/j.aquatox.2003.11.004.

Rigato, D., Branco, P., Silva, C., Machado-Neto, J., Costa-Lotufo, L., and Jimenez, P. 2020. BIRC7 (baculoviral IAP repeat containing 7). Atlas of Genetics and Cytogenetics in Oncology and Haematology 24: 234–247.

Riisgård, H. 1988. Efficiency of particle retention and filtration rate in 6 species of Northeast American bivalves. Marine Ecology Progress Series 45: 217–223. doi:10.3354/meps045217.

Riisgård, H. 1991. Filtration rate and growth in the blue mussel *Mytilus edulis* Linneaus 1758: Dependence on algal concentration. Journal of Shellfish Research 10: 29–36.

Riisgård, H.U., Egede, P.P., and Barreiro Saavedra, I. 2011. Feeding behaviour of the mussel, *Mytilus edulis*: new observations, with a minireview of current knowledge. Journal of Marine Biology 2011: e312459. Hindawi. doi:10.1155/2011/312459.

Riisgård, H.U., Kittner, C., and Seerup, D. 2003. Regulation of opening state and filtration rate in filter-feeding bivalves (*Cardium edule, Mytilus edulis, Mya arenaria*) in response to low algal concentration. Journal of Experimental Marine Biology and Ecology 284: 105–127. doi:10.1016/S0022-0981(02)00496-3.

Riisgård, H.U., and Larsen, P.S. 2001. Minireview: Ciliary filter feeding and bio-fluid mechanics—present understanding and unsolved problems. Limnology and Oceanography 46(4): 882–891.

Riisgård, H.U., and Larsen, P.S. 2015. Physiologically regulated valve-closure makes mussels long-term starvation survivors: test of hypothesis. Journal of Molluscan Studies 81: 303–307. doi:10.1093/mollus/eyu087.

Riisgård, H.U., Larsen, P.S., and Nielsen, N.F. 1996. Particle capture in the mussel *Mytilus edulis*: The role of latero-frontal cirri. Marine Biology 127: 259–266. doi:10.1007/BF00942111.

Riisgård, H.U., Pleissner, D., Lundgreen, K., and Larsen, P.S. 2013. Growth of mussels *Mytilus edulis* at algal (*Rhodomonas salina*) concentrations below and above saturation levels for reduced filtration rate. Marine Biology Research 9: 1005–1017. doi:10.1080/17451000.2012.742549.

Ringwood, A.H., Conners, D.E., and Hoguet, J. 1998. Effects of natural and anthropogenic stressors on lysosomal destabilization in oysters *Crassostrea virginica*. Marine Ecology Progress Series 166: 163–171. doi:10.3354/meps166163.

Rivera-Ingraham, G.A., and Lignot, J.-H. 2017. Osmoregulation, bioenergetics and oxidative stress in coastal marine invertebrates: raising the questions for future research. Journal of Experimental Biology 220: 1749–1760. doi:10.1242/jeb.135624.

Rivera-Ingraham, G.A., Rocchetta, I., Meyer, S., and Abele, D. 2013. Oxygen radical formation in anoxic transgression and anoxia-reoxygenation: Foe or phantom? Experiments with a hypoxia tolerant bivalve. Marine Environmental Research 92: 110–119. doi:10.1016/j.marenvres.2013.09.007.

Riviere, G., He, Y., Tecchio, S., Crowell, E., Gras, M., Sourdaine, P., Guo, X., and Favrel, P. 2017. Dynamics of DNA methylomes underlie oyster development. PLOS Genetics 13: e1006807. doi:10.1371/journal.pgen.1006807.

Riviere, G., Wu, G.-C., Fellous, A., Goux, D., Sourdaine, P., and Favrel, P. 2013. DNA Methylation is crucial for the early development in the oyster *Crassostrea gigas.* Marine Biotechnology 15: 739–753. doi:10.1007/s10126-013-9523-2.

Roberts, E.A., Newcomb, L.A., McCartha, M.M., Harrington, K.J., LaFramboise, S.A., Carrington, E., and Sebens, K.P. 2021. Resource allocation to a structural biomaterial: Induced production of byssal threads decreases growth of a marine mussel. Functional Ecology 35: 1222–1239. doi:10.1111/1365-2435.13788.

Robertson, R.F., El-Haj, A.J., Clarke, A., and Taylor, E.W. 2001. Effects of temperature on specific dynamic action and protein synthesis rates in the Baltic isopod crustacean, *Saduria entomon*. Journal of Experimental Marine Biology and Ecology 1: 113–129.

Robinson, C. 2019. Microbial respiration, the engine of ocean deoxygenation. Frontiers in Marine Science 5:533. doi:10.3389/fmars.2018.00533.

Robinson, M.D., McCarthy, D.J., and Smyth, G.K. 2010. edgeR: a Bioconductor package for differential expression analysis of digital gene expression data. Bioinformatics 26: 139–140. doi:10.1093/bioinformatics/btp616.

Rola, R.C., Monteiro, M. da C., Reis, S.R. da S., and Sandrini, J.Z. 2012. Molecular and biochemical biomarkers responses in the mussel *Mytilus edulis* collected from Southern Brazil coast. Marine Pollution Bulletin 64: 766–771. doi:10.1016/j.marpolbul.2012.01.004.

Romero, A., Estévez-Calvar, N., Dios, S., Figueras, A., and Novoa, B. 2011. New Insights into the Apoptotic Process in Mollusks: Characterization of Caspase Genes in *Mytilus galloprovincialis*. PLOS ONE 6: e17003. doi:10.1371/journal.pone.0017003.

Romero, A., Novoa, B., and Figueras, A. 2015. The complexity of apoptotic cell death in mollusks: An update. Fish & Shellfish Immunology 46: 79–87. doi:10.1016/j.fsi.2015.03.038.

Rovero, F., Hughes, R.N., and Chelazzi, G. 1999. Cardiac and behavioural responses of mussels to risk of predation by dogwhelks. Animal Behaviour 58: 707–714. doi:10.1006/anbe.1999.1176.

Roznere, A., Watters, T., Wolfe, B., and Marymegan, D. 2014. Nontargeted metabolomics reveals biochemical pathways altered in response to captivity and food limitation in the freshwater mussel *Amblema plicata*. Comparative Biochemistry and Physiology Part D: Genomics and Proteomics 12: 53–60.

Ruas, J.L., Berchner-Pfannschmidt, U., Malik, S., Gradin, K., Fandrey, J., Roeder, R.G., Pereira, T., and Poellinger, L. 2010. Complex regulation of the transactivation function of hypoxia-inducible factor-1α by direct interaction with two distinct domains of the CREB-binding protein/p300. Journal of Biological Chemistry 285: 2601–2609. doi:10.1074/jbc.M109.021824.

Rush, W.D., Kiehl, J.T., Shields, C.A., and Zachos, J.C. 2021. Increased frequency of extreme precipitation events in the North Atlantic during the PETM: Observations and theory. Palaeogeography, Palaeoclimatology, Palaeoecology 568: 110289. doi:10.1016/j.palaeo.2021.110289.

Russell, M.W., Mestecky, J., Strober, W., Lambrecht, B.N., Kelsall, B.L., and Cheroutre, H. 2015. Chapter 1: The Mucosal Immune System. Pages 3–8 in J. Mestecky, W. Strober, M.W. Russell, B.L. Kelsall, H. Cheroutre, and B.N. Lambrecht, eds. Mucosal Immunology (Fourth Edition). Academic Press, Boston. doi:10.1016/B978-0-12-415847-4.00001-X.

Rzymski, T., and Harris, A.L. 2007. The Unfolded Protein Response and Integrated Stress Response to Anoxia. Clinical Cancer Research 13: 2537–2540. doi:10.1158/1078-0432.CCR-06-2126.

Sabatini, D.M. 2017. Twenty-five years of mTOR: Uncovering the link from nutrients to growth. Proceedings of the National Academy of Sciences 114: 11818–11825.

Saco, A., Panebianco, A., Blanco, S., Novoa, B., Diz, A.P., and Figueras, A. 2021. Integration of transcriptomics and proteomics improves the characterization of the role of mussel gills in a bacterial waterborne infection. Frontiers in Marine Science 8: 735309. doi:10.3389/fmars.2021.735309.

Sadler, D.E., Lemasson, A.J., and Knights, A.M. 2018. The effects of elevated CO2 on shell properties and susceptibility to predation in mussels *Mytilus edulis*. Marine Environmental Research 139: 162–168. doi:10.1016/j.marenvres.2018.05.017.

Saliba, A.-E., Westermann, A.J., Gorski, S.A., and Vogel, J. 2014. Single-cell RNA-seq: advances and future challenges. Nucleic acids research 42: 8845–8860.

Salih, D.A., and Brunet, A. 2008. FoxO transcription factors in the maintenance of cellular homeostasis during aging. Current Opinion in Cell Biology 20: 126–136. doi:10.1016/j.ceb.2008.02.005.

Salminen, A., and Kaarniranta, K. 2010. ER stress and hormetic regulation of the aging process. Ageing Research Reviews 9: 211–217. doi:10.1016/j.arr.2010.04.003.

Sanders, T., Schmittmann, L., Nascimento-Schulze, J.C., and Melzner, F. 2018. High calcification costs limit mussel growth at low salinity. Frontiers in Marine Science 5: 9. Frontiers. doi:10.3389/fmars.2018.00352.

Santos, S., and Simon, J. 1980. Response of soft-bottom benthos to annual catastrophic disturbance in a South Florida estuary. Marine Ecology Progress Series 3: 347–355. doi:10.3354/meps003347.

Schmitt, R. 2008. Salinity and the global water cycle. Oceanography 21: 12–19.

Schulz, T.K.F., and Kluytmans, J.H. 1983. Pathway of propionate synthesis in the sea mussel *Mytilus edulis* L. Comparative Biochemistry and Physiology Part B: Comparative Biochemistry 75: 365–372. doi:10.1016/0305-0491(83)90341-3.

Schwartz, J., Dubos, M.-P., Pasquier, J., Zatylny-Gaudin, C., and Favrel, P. 2018. Emergence of a cholecystokinin/sulfakinin signalling system in Lophotrochozoa. Scientific Reports 8: 16424. doi:10.1038/s41598-018-34700-4.

Schweiker, S.S., Tauber, A.L., Sherry, M.E., and Levonis, S.M. 2018. Structure, function and inhibition of Poly(ADP-ribose)polymerase, member 14 (PARP14). Mini-Reviews in Medicinal Chemistry 18: 1659–1669. doi:10.2174/1389557518666180816111749.

Scott, R.C., Schuldiner, O., and Neufeld, T.P. 2004. Role and regulation of starvation-induced autophagy in the *Drosophila* fat body. Developmental Cell 7: 167–178. doi:10.1016/j.devcel.2004.07.009.

Seed, R. 1969. The ecology of *Mytilus edulis* L. (Lamellibranchiata) on exposed rocky shores. Oecologia 3: 277–316.

Seed, R. 1976. Chapter 2: Ecology. Pages 13–67 in B.L. Bayne, ed. Marine mussels: their ecology and physiology. Cambridge University Press, Melbourne, Australia.

Seo, E., Sazi, T., Togawa, M., Nagata, O., Murakami, M., Kojima, S., and Seo, Y. 2016. A portable infrared photoplethysmograph: heartbeat of *Mytilus galloprovincialis* analyzed by MRI and application to Bathymodiolus septemdierum. Biology open 5: 1752–1757. doi:10.1242/bio.020909

Seuront, L., Nicastro, K.R., Zardi, G.I., and Goberville, E. 2019. Decreased thermal tolerance under recurrent heat stress conditions explains summer mass mortality of the blue mussel *Mytilus edulis*. Scientific Reports 9: 17498. doi:10.1038/s41598-019-53580-w.

Sevrioukova, I.F. 2011. Apoptosis-Inducing Factor: Structure, function, and redox regulation. Antioxidants & Redox Signaling 14: 2545–2579. doi:10.1089/ars.2010.3445.

Shen, H., and Nugegoda, D. 2022. Real-time automated behavioural monitoring of mussels during contaminant exposures using an improved microcontroller-based device. Science of The Total Environment 806: 150567. doi:10.1016/j.scitotenv.2021.150567.

Shen, M., Di, G., Li, M., Fu, J., Dai, Q., Miao, X., Huang, M., You, W., and Ke, C. 2018. Proteomics studies on the three larval stages of development and metamorphosis of *Babylonia areolata*. Scientific Reports 8: 6269. doi:10.1038/s41598-018-24645-z.

Shi, K.-P., Dong, S.-L., Zhou, Y.-G., Li, Y., Gao, Q.-F., and Sun, D.-J. 2019. RNA-seq reveals temporal differences in the transcriptome response to acute heat stress in the Atlantic salmon (Salmo salar). Comparative Biochemistry and Physiology Part D: Genomics and Proteomics 30: 169–178. doi:10.1016/j.cbd.2018.12.011.

Shimeld, S.M. 1999. The evolution of the hedgehog gene family in chordates: insights from amphioxus hedgehog. Development Genes and Evolution 209: 40–47. doi:10.1007/s004270050225.

Shin, P.K.S., Yang, F.Y., Chiu, M.Y., and Cheung, S.G. 2009. Cues from the predator crab Thalamita danae fed different prey can affect scope for growth in the prey mussel *Perna viridis*. Marine and Freshwater Behaviour and Physiology 42: 343–355. doi:10.1080/10236240903454202.

Shumway, S.E. 1977. Effect of salinity fluctuation on the osmotic pressure and Na+, Ca2+and Mg2+ion concentrations in the heamolymph of bivalve molluscs. Marine Biology 41: 153–177. doi:10.1007/BF00394023.

Shumway, S.E., Gabbott, P.A., and Youngson, A. 1977. The effect of fluctuating salinity on the concentrations of free amino acids and ninhydrin-positive substances in the adductor muscles of eight species of bivalve molluscs. Journal of Experimental Marine Biology and Ecology 29: 131–150. doi:10.1016/0022-0981(77)90044-2.

Silverman, H., and Roberto, F. 2010. Chapter 18: Byssus formation in *Mytilus*. Pages 273–282 in J. Von Byern and I. Grunwald, eds. Biological adhesion systems: from nature to technical and medical application. Springer.

Slobodskova, V.V., Zhukovskaya, A.F., and Chelomin, V.P. 2012. DNA damage in the gill cells of the marine scallop *Mizuhopecten yessoensis* during anoxic stress and aerobic recovery. Ocean Science Journal 47: 95–100. doi:10.1007/s12601-012-0010-x.

Smith, G., and Ramsay, A. 2014. PEI Mussel Monitoring Program. Prince Edward Island Department of Fisheries, Aquaculture and Rural Development, Montague, PEI.

Smith, G., and Ramsay, A. 2021. PEI Mussel Monitoring Program. Technical Report #268, Prince Edward Island Department of Fisheries & Communities Aquaculture Division, Charlottetown, PEI.

Smith, L.D., and Jennings, J.A. 2000. Induced defensive responses by the bivalve *Mytilus edulis* to predators with different attack modes. Marine Biology 136: 461–469. doi:10.1007/s002270050705.

Sokolova, I.M. 2013. Energy-limited tolerance to stress as a conceptual framework to integrate the effects of multiple stressors. Integrative and Comparative Biology 53: 597–608. doi:10.1093/icb/ict028.

Sokolova, I.M., Sukhotin, A.A., and Lannig, G. 2012. Stress effects on metabolism and energy budgets in mollusks. Pages 263–280 in J. Vazquez-Medina and T. Zenteno-Savin, eds. Oxidative Stress in Aquatic Ecosystems. Wiley-Blackwell.

Soldatov, A.A., Andreenko, T.I., Sysoeva, I.V., and Sysoev, A.A. 2009. Tissue specificity of metabolism in bivalve mollusc *Anadara inaequivalvis* Br. under conditions of experimental anoxia. Zhurnal Evoliutsionnoi Biokhimii I Fiziologii 45: 284–289.

Solé, M., Porte, C., and Albaigés, J. 1995. Seasonal variation in the mixed-function oxygenase system and antioxidant enzymes of the mussel *Mytilus galloprovincialis*. Environmental Toxicology and Chemistry 14: 157–164. doi:10.1002/etc.5620140118.

Song, H., Wignall, P.B., Chu, D., Tong, J., Sun, Y., Song, H., He, W., and Tian, L. 2014. Anoxia/high temperature double whammy during the Permian-Triassic marine crisis and its aftermath. Scientific Reports 4: 4132. doi:10.1038/srep04132.

Song, L., Wang, L., Qiu, L., and Zhang, H. 2010. Chapter 3: Bivalve Immunity. Pages 44–65 in K. Soderhall, ed. Advances in Experimental Medicine and Biology: Invertebrate Immunity. Springer Science + Business Media, LLC, New York, New York.

Sonier, R., Filgueira, R., Guyondet, T., Tremblay, R., Olivier, F., Meziane, T., Starr, M., LeBlanc, A.R., and Comeau, L.A. 2016. Picophytoplankton contribution to *Mytilus edulis* growth in an intensive culture environment. Marine Biology 163: 73. doi:10.1007/s00227-016-2845-7.

Soot-Ryen, T. 1955. A report on the family Mytilidae (Pelecypoda). Allan Hancock Pacific Expedition 20: 174 p.

Sørensen, J.G., Kristensen, T.N., and Loeschcke, V. 2003. The evolutionary and ecological role of heat shock proteins. Ecology Letters 6: 1025–1037. doi:10.1046/j.1461-0248.2003.00528.x@10.1111.

South, P.M., Delorme, N.J., Skelton, B.M., Floerl, O., and Jeffs, A.G. 2022. The loss of seed mussels in longline aquaculture. Reviews in Aquaculture 14: 440–455. doi:10.1111/raq.12608.

Statistics Canada 2021. Aquaculture, production and value. https://www150.statcan.gc.ca/t1/tbl1/en/tv.action?pid=3210010701.

Steeves, L., Strohmeier, T., Filgueira, R., and Strand, Ø. 2020. Exploring feeding physiology of *Mytilus edulis* across geographic and fjord gradients in low-seston environments. Marine Ecology Progress Series 651: 71–84. doi:10.3354/meps13455.

Steeves, L.E., Filgueira, R., Guyondet, T., Chassé, J., and Comeau, L. 2018. Past, present, and future: performance of two bivalve species under changing environmental conditions. Frontiers in Marine Science 5: 184. doi:10.3389/fmars.2018.00184.

Steimle, F., and Sindermann, C. 1978. Review of oxygen depletion and associated mass mortalities of shellfish in the Middle Atlantic Bight in 1976. Marine Fisheries Review 1356: 17–26.

Storey, K.B. 1985. Fructose 2,6-bisphosphate and anaerobic metabolism in marine molluscs. FEBS Letters 181: 245–248. doi:10.1016/0014-5793(85)80268-4.

Storey, K.B. 1996. Oxidative stress: animal adaptations in nature. Brazilian journal of medical and biological research 20: 1715–1733.

Storey, K.B., and Storey, J.M. 1990. Metabolic rate depression and biochemical adaptation in anaerobiosis, hibernation and estivation. The Quarterly Review of Biology 65: 145–174. doi:10.1086/416717.

Storey, K.B., and Storey, J.M. 2004. Metabolic rate depression in animals: transcriptional and translational controls. Biological Reviews 79: 207–233. doi:10.1017/S1464793103006195.

Storey, K.B., and Storey, J.M. 2007. Tribute to P. L. Lutz: putting life on `pause' – molecular regulation of hypometabolism. Journal of Experimental Biology 210: 1700–1714. doi:10.1242/jeb.02716.

Stowe, K. 1983. Ocean Science. 2nd edition. John Wiley & Sons, Inc.

Stramma, L., Johnson, G.C., Sprintall, J., and Mohrholz, V. 2008. Expanding oxygen-minimum zones in the tropical oceans. Science 320: 655–658. doi:10.1126/science.1153847.

Strohmeier, T., Strand, Ø., and Cranford, P. 2009. Clearance rates of the great scallop (Pecten maximus) and blue mussel (*Mytilus edulis*) at low natural seston concentrations. Marine Biology 156: 1781–1795. doi:10.1007/s00227-009-1212-3.

Sugi, H., Ohno, T., and Moriya, M. 2020. Mechanism and function of the catch state in molluscan smooth muscle: a historical perspective. International Journal of Molecular Sciences 21: 7576. doi:10.3390/ijms21207576.

Sui, Y., Hu, M., Huang, X., Wang, Y., and Lu, W. 2015. Anti-predatory responses of the thick shell mussel *Mytilus coruscus* exposed to seawater acidification and hypoxia. Marine Environmental Research 109: 159–167. doi:10.1016/j.marenvres.2015.07.008.

Sukhotin, A.A., Lajus, D.L., and Lesin, P.A. 2003. Influence of age and size on pumping activity and stress resistance in the marine bivalve *Mytilus edulis* L. Journal of Experimental Marine Biology and Ecology 284: 129–144. doi:10.1016/S0022-0981(02)00497-5.

Tagliarolo, M., and McQuaid, C. 2015. Field measurements indicate unexpected, serious underestimation of mussel heart rates and thermal tolerance by laboratory studies. PLoS ONE 11: e0146341. doi:10.1371/journal.pone.0146341.

Takahashi, K.H. 2019. Multiple modes of canalization: Links between genetic, environmental canalizations and developmental stability, and their trait-specificity. Seminars in Cell & Developmental Biology 88: 14–20. doi:10.1016/j.semcdb.2018.05.018.

Tang, F., Kemp, J.S., and Aldridge, D. 2020. Life on the edge: Compensatory growth and feeding rates at environmental extremes mediates potential ecosystem engineering by an invasive bivalve. Science of The Total Environment 706: 10 p. doi:10.17863/CAM.47627.

Tarailo-Graovac, M., Drögemöller, B.I., Wasserman, W.W., Ross, C.J.D., van den Ouweland, A.M.W., Darin, N., Kollberg, G., van Karnebeek, C.D.M., and Blomqvist, M. 2017. Identification of a large intronic transposal insertion in SLC17A5 causing sialic acid storage disease. Orphanet Journal of Rare Diseases 12: 28. doi:10.1186/s13023-017-0584-6.

Tian, Y., Shang, Y., Guo, R., Chang, Y., and Jiang, Y. 2019. Salinity stress-induced differentially expressed miRNAs and target genes in sea cucumbers *Apostichopus japonicus*. Cell Stress Chaperones 24: 719–733. doi:10.1007/s12192-019-00996-y.

Thompson, R., and Bayne, B. 1974. Some relationships between growth, metabolism and food in the mussel *Mytilus edulis*. Marine Biology 27: 317–326.

Thompson, R., Ratcliffe, N., and Bayne, B. 1974. Effects of starvation on structure and function in the digestive gland of the mussel (*Mytilus edulis* L.). Journal of Marine Biological Association of the United Kingdom 54: 699–712.

Thompson, R.J. 1979. Fecundity and Reproductive Effort in the blue mussel (*Mytilus edulis*), the sea urchin (*Strongylocentrotus droebachiensis*), and the snow crab (*Chionoecetes opilio*) from populations in Nova Scotia and Newfoundland. Journal of Fisheries Research Board of Canada 36: 955–964. doi:10.1139/f79-133.

Thompson, R.J., and Bayne, B.L. 1972. Active metabolism associated with feeding in the mussel *Mytilus edulis* L. Journal of Experimental Marine Biology and Ecology 9: 111–124. doi:10.1016/0022-0981(72)90011-1.

Thompson, R.J., Bayne, C.J., Moore, M.N., and Carefoot, T.H. 1978. Haemolymph volume, changes in the biochemical composition of the blood, and cytological responses of the digestive cells in *Mytilus californianus* Conrad, induced by nutritional, thermal and exposure stress. Journal of comparative physiology 127: 287–298. doi:10.1007/BF00738412.

Thomsen, J., and Melzner, F. 2010. Moderate seawater acidification does not elicit long-term metabolic depression in the blue mussel *Mytilus edulis*. Marine Biology 157: 2667–2676.

Tielens, A.G.M. 2000. The carbohydrate metabolism of *Fasciola hepatica*, an example of biochemical adaptations in parasitic helminths. Acta Parasitologica 45: 59–66.

Tomanek, L., and Zuzow, M.J. 2010. The proteomic response of the mussel congeners *Mytilus galloprovincialis* and *M. trossulus* to acute heat stress: implications for thermal tolerance limits and metabolic costs of thermal stress. Journal of Experimental Biology 213: 3559–3574. doi:10.1242/jeb.041228.

Tomanek, L., Zuzow, M.J., Hitt, L., Serafini, L., and Valenzuela, J.J. 2012. Proteomics of hyposaline stress in blue mussel congeners (genus *Mytilus*): implications for biogeographic range limits in response to climate change. Journal of Experimental Biology 215: 3905–3916. doi:10.1242/jeb.076448.

Torossian, J.L., Hosek, K.E., Donelan, S.C., Trussell, G.C., Helmuth, B.S., and Zippay, M.L. 2020. Physiological and biochemical responses to acute environmental stress and predation risk in the blue mussel, *Mytilus edulis*. Journal of Sea Research 159: 101891. doi:10.1016/j.seares.2020.101891.

Towle, D.W., Henry, R.P., and Terwilliger, N.B. 2011. Microarray-detected changes in gene expression in gills of green crabs (*Carcinus maenas*) upon dilution of environmental salinity. Comparative Biochemistry and Physiology Part D: Genomics and Proteomics 6: 115–125. doi:10.1016/j.cbd.2010.11.001.

Tremblay, R., Landry, T., Leblanc, N., Pernet, F., Barkhouse, C., and Sévigny, J.-M. 2011. Physiological and biochemical indicators of mussel seed quality in relation to temperatures. Aquatic Living Resources 24: 273–282. doi:10.1051/alr/2011113.

Tremblay, R., Myrand, B., and Guderley, H. 1998. Temporal variation of lysosomal capacities in relation to susceptibility of mussels, *Mytilus edulis*, to summer mortality. Marine Biology 132: 641–649. doi:10.1007/s002270050429.

Tunkijjanukij, S., Giæver, H., Chin, C.C.Q., and Olafsen, J.A. 1998. Sialic acid in hemolymph and affinity purified lectins from two marine bivalves. Comparative Biochemistry and Physiology Part B: Biochemistry and Molecular Biology 119: 705–713. doi:10.1016/S0305-0491(98)00046-7.

Tweedley, J.R., Hallett, C.S., Warwick, R.M., Clarke, K.R., and Potter, I.C. 2015. The hypoxia that developed in a microtidal estuary following an extreme storm produced dramatic changes in the benthos. Marine Freshwater Research. 67: 327–341. doi:10.1071/MF14216.

Uzaki, N., Kai, M., Aoyama, H., and Suzuki, T. 2003. Changes in mortality rate and glycogen content of the Manila clam *Ruditapes philippinarum* during the development of oxygen-deficient waters. Fisheries science 69: 936–943. doi:10.1046/j.1444-2906.2003.00710.x.

Vabulas, R.M., Raychaudhuri, S., Hayer-Hartl, M., and Hartl, F.U. 2010. Protein folding in the cytoplasm and the heat shock response. Cold Spring Harbor Perspectives in Biology 2: a004390. doi:10.1101/cshperspect.a004390.

Vahl, O. 1972. Efficiency of particle retention in *Mytilus edulis* L. Ophelia 10: 17–25. doi:10.1080/00785326.1972.10430098.

Valenzuela-Miranda, D., Del Río-Portilla, M.A., and Gallardo-Escárate, C. 2015. Characterization of the growth-related transcriptome in California red abalone (*Haliotis rufescens*) through RNA-Seq analysis. Marine Genomics 24: 199–202. doi:10.1016/j.margen.2015.05.009.

Van Colen, C., Montserrat, F., Vincx, M., Herman, P.M.J., Ysebaert, T., and Degraer, S. 2010. Long-term divergent tidal flat benthic community recovery following hypoxia-induced mortality. Marine Pollution Bulletin 60: 178–186. doi:10.1016/j.marpolbul.2009.09.028.

Van den Berg, R.H., Faber-Krol, M.C., Sim, R.B., and Daha, M.R. 1998. The First Subcomponent of complement, C1q, triggers the production of IL-8, IL-6, and monocyte chemoattractant peptide-1 by human umbilical vein endothelial Cells. The Journal of Immunology 161: 6924–6930.

Van Hellemond, J.J., Klockiewicz, M., Gaasenbeek, C.P., Roos, M.H., and Tielens, A.G. 1995. Rhodoquinone and complex II of the electron transport chain in anaerobically functioning eukaryotes. The Journal of Biological Chemistry 270: 31065–31070. doi:10.1074/jbc.270.52.31065.

Van Weel, P. 1961. The comparative physiology of digestion in molluscs. American Zoologist 1: 245–252.

Van Winkle, W. 1970. Effect of environmental factors on byssal thread formation. Marine Biology 7: 143–148. doi:10.1007/BF00354918.

Van Zon, A., Mossink, M.H., Scheper, R.J., Sonneveld, P., and Wiemer, E.A.C. 2003. The vault complex. Cellular and Molecular Life Sciences 60: 1828–1837. doi:10.1007/s00018-003-3030-y.

Vandesompele, J., De Preter, K., Pattyn, F., Poppe, B., Van Roy, N., De Paepe, A., and Speleman, F. 2002. Accurate normalization of real-time quantitative RT-PCR data by geometric averaging of multiple internal control genes. Genome Biology 3: research0034.1 doi:10.1186/gb-2002-3-7-research0034.

Verity, P.G., Alber, M., and Bricker, S.B. 2006. Development of hypoxia in well-mixed subtropical estuaries in the Southeastern USA. Estuaries and Coasts 29: 665–673. doi:10.1007/BF02784291.

Vezzulli, L., Colwell, R.R., and Pruzzo, C. 2013. Ocean warming and spread of pathogenic *Vibrios* in the aquatic environment. Microbial Ecology 65: 817–825. doi:10.1007/s00248-012-0163-2.

Viarengo, A., Lowe, D., Bolognesi, C., Fabbri, E., and Koehler, A. 2007. The use of biomarkers in biomonitoring: a 2-tier approach assessing the level of pollutant-induced stress syndrome in sentinel organisms. Comparative biochemistry and physiology. Toxicology & pharmacology 146: 281–300. doi:10.1016/j.cbpc.2007.04.011.

Vogeler, S., Carboni, S., Li, X., and Joyce, A. 2021. Phylogenetic analysis of the caspase family in bivalves: implications for programmed cell death, immune response and development. BMC Genomics 22: 80. doi:10.1186/s12864-021-07380-0.

Voges, D., Zwickl, P., and Baumeister, W. 1999. The 26S proteasome: a molecular machine designed for controlled proteolysis. Annual Review of Biochemistry 68: 1015–1068. doi:10.1146/annurev.biochem.68.1.1015.

Vuorinen, I., Antsulevich, A.E., and Maximovich, N.V. 2002. Spatial distribution and growth of the common mussel *Mytilus edulis* L. in the archipelago of SW-Finland, northern Baltic Sea. Boreal Environment Research 7: 41–52.

Waddington, C. 1942. Canalization of development and the inheritance of acquired characters. Nature 150: 563–565.

Wang, J., Fang, L., Wu, Q., Li, D., Huo, Z., and Yan, X. 2020. Genome-wide identification and characterization of the AMPK genes and their distinct expression patterns in response to air exposure in the Manila clam (*Ruditapes philippinarum*). Genes & Genomics 42: 1–12. doi:10.1007/s13258-019-00872-0.

Wang, W., and Widdows, J. 1993. Metabolic responses of the common mussel *Mytilus edulis* to hypoxia and anoxia. Marine Ecology Progress Series 95: 205–214. doi:10.3354/meps095205.

Wang, Y., Hu, M., Cheung, S.G., Shin, P.K.S., Lu, W., and Li, J. 2012a. Chronic hypoxia and low salinity impair anti-predatory responses of the green-lipped mussel *Perna viridis*. Marine Environmental Research 77: 84–89. doi:10.1016/j.marenvres.2012.02.006.

Wang, Y., Hu, M., Cheung, S.G., Shin, P.K.S., Lu, W., and Li, J. 2012b. Immune parameter changes of hemocytes in green-lipped mussel *Perna viridis* exposure to hypoxia and hyposalinity. Aquaculture 356–357: 22–29. doi:10.1016/j.aquaculture.2012.06.001.

Wang, Y., Hu, M., Cheung, S.G., Shin, P.K.S., Lu, W., and Li, J. 2013. Antipredatory responses of *Perna viridis* (Linnaeus, 1758) under acute hypoxia and low salinity. Journal of Molluscan Studies 79: 42–50. doi:10.1093/mollus/eys035.

Wang, Y., Hu, M., Shin, P.K.S., and Cheung, S.G. 2011a. Immune responses to combined effect of hypoxia and high temperature in the green-lipped mussel *Perna viridis*. Marine Pollution Bulletin 63: 201–208. doi:10.1016/j.marpolbul.2011.05.035.

Wang, Y., Hu, M., Wong, W.H., Shin, P.K.S., and Cheung, S.G. 2011b. The combined effects of oxygen availability and salinity on physiological responses and scope for growth in the green-lipped mussel *Perna viridis*. Marine Pollution Bulletin 63: 255–261. doi:10.1016/j.marpolbul.2011.02.004.

Watson, R., Baldanzi, S., Pérez-Figueroa, A., Gouws, G., and Porri, F. 2018. Morphological and epigenetic variation in mussels from contrasting environments. Marine Biology 165(50). doi:10.1007/s00227-018-3310-6.

Welch, W.J. 1993. How cells respond to stress. Scientific American 268: 56–64.

Wenne, R., Zbawicka, M., Bach, L., Strelkov, P., Gantsevich, M., Kukliński, P., Kijewski, T., McDonald, J.H., Sundsaasen, K.K., Árnyasi, M., and others 2020. Trans-

Atlantic distribution and introgression as inferred from single nucleotide polymorphism: Mussels *Mytilus* and environmental factors. Genes 11: 530. doi:10.3390/genes11050530.

Werner, I. 2004. The influence of salinity on the heat-shock protein response of *Potamocorbula amurensis* (Bivalvia). Marine Environmental Research 58: 803–807. doi:10.1016/j.marenvres.2004.03.097.

Werz, O., Bürkert, E., Samuelsson, B., Rådmark, O., and Steinhilber, D. 2002. Activation of 5-lipoxygenase by cell stress is calcium independent in human polymorphonuclear leukocytes. Blood 99: 1044–1052. doi:10.1182/blood.V99.3.1044.

Widdows, J. 1973a. The effects of temperature on the metabolism and activity of *Mytilus edulis*. Netherlands Journal of Sea Research 7: 387–398. doi:10.1016/0077-7579(73)90060-4.

Widdows, J. 1973b. Effect of temperature and food on the heart beat, ventilation rate and oxygen uptake of *Mytilus edulis*. Marine Biology 20: 269–276. doi:10.1007/BF00354270.

Widdows, J. 1978. Physiological indices of stress in *Mytilus edulis*. Journal of the Marine Biological Association of the United Kingdom 58: 125–142.

Widdows, J., Bayne, B.L., Livingstone, D.R., Newell, R.I.E., and Donkin, P. 1979a. Physiological and biochemical responses of bivalve mollusks to exposure to air. Comparative Biochemistry and Physiology A-Physiology 62: 301–308.

Widdows, J., Fieth, P., and Worrall, C.M. 1979b. Relationships between seston, available food and feeding activity in the common mussel *Mytilus edulis*. Marine Biology 50: 195–207. doi:10.1007/BF00394201.

Widdows, J., Newell, R.I.E., and Mann, R. 1989. Effects of hypoxia and anoxia on survival, energy metabolism, and feeding of oyster larvae (*Crassostrea virginica*, Gmelin). The Biological Bulletin 177: 154–166. doi:10.2307/1541843.

Widdows, J., and Shick, J.M. 1985. Physiological responses of *Mytilus edulis* and *Cardium edule* to aerial exposure. Marine Biology 85: 217–232. doi:10.1007/BF00393242.

Wiedmer, T., Zhao, J., Li, L., Zhou, Q., Hevener, A., Olefsky, J.M., Curtiss, L.K., and Sims, P.J. 2004. Adiposity, dyslipidemia, and insulin resistance in mice with targeted deletion of phospholipid scramblase 3 (PLSCR3). Proceedings of the National Academy of Sciences 101: 13296–13301. doi:10.1073/pnas.0405354101.

Williamson, P. 2016. Phospholipid scramblases. Lipid Insights 8: 41–44. doi:10.4137/LPI.S31785.

Willmer, P. 2006. Osmoregulation in Invertebrates. John Wiley & Sons, Ltd. doi:10.1038/npg.els.0003646.

Wilson, T.J.B., Cooley, S.R., Tai, T.C., Cheung, W.W.L., and Tyedmers, P.H. 2020. Potential socioeconomic impacts from ocean acidification and climate change effects on Atlantic Canadian fisheries. PLOS ONE 15: e0226544. doi:10.1371/journal.pone.0226544.

Winter, J., and Langton, R. 1975. Feeding experiments with *Mytilus edulis* L. at small laboratory scale. I. The influence of the total amount of food ingested and food concentration on growth. Pages 565–581 in 10th European Symposium on Marine Biology. Ostend, Belgium.

Winter, J.E. 1973. The filtration rate of *Mytilus edulis* and its dependence on algal concentration, measured by a continuous automatic recording apparatus. Marine Biology 22: 317–328. doi:10.1007/BF00391388.

Wollam, J., Magomedova, L., Magner, D.B., Shen, Y., Rottiers, V., Motola, D.L., Mangelsdorf, D.J., Cummins, C.L., and Antebi, A. 2011. The Rieske oxygenase DAF-36 functions as a cholesterol 7-desaturase in steroidogenic pathways governing longevity. Aging Cell 10: 879–884. doi:10.1111/j.1474-9726.2011.00733.x.

Wong, W., and Cheung, S.G. 2003. Site-related differences in the feeding physiology of the green mussel *Perna viridis*: A reciprocal transplantation experiment. Marine Ecology Progress Series 258: 147–159. doi:10.3354/meps258147.

Wong, W.H., and Levinton, J.S. 2004. Culture of the blue mussel *Mytilus edulis* (Linnaeus, 1758) fed both phytoplankton and zooplankton: a microcosm experiment. Aquaculture Research 35: 965–969. doi:10.1111/j.1365-2109.2004.01107.x.

Woo, S., Denis, V., Won, H., Shin, K., Lee, G., Lee, T.-K., and Yum, S. 2013. Expressions of oxidative stress-related genes and antioxidant enzyme activities in *Mytilus galloprovincialis* (Bivalvia, Mollusca) exposed to hypoxia. Zoological Studies 52: 15. doi:10.1186/1810-522X-52-15.

Wouters, B.G., and Koritzinsky, M. 2008. Hypoxia signalling through mTOR and the unfolded protein response in cancer. Nature Reviews Cancer 8: 851–864. doi:10.1038/nrc2501.

Wu, F., Sokolov, E.P., Khomich, A., Fettkenhauer, C., Schnell, G., Seitz, H., and Sokolova, I.M. 2021. Interactive effects of ZnO nanoparticles and temperature on molecular and cellular stress responses of the blue mussel *Mytilus edulis.* Science of The Total Environment 818: 151785. doi:10.1016/j.scitotenv.2021.151785.

Wu, F., Xie, Z., Lan, Y., Dupont, S., Sun, M., Cui, S., Huang, X., Huang, W., Liu, L., Hu, M., Lu, W., and Wang, Y. 2018. Short-term exposure of *Mytilus coruscus* to decreased pH and salinity change impacts immune parameters of their haemocytes. Frontiers in Physiology 9: 166. doi:10.3389/fphys.2018.00166.

Wu, H., Ji, C., Wei, L., Zhao, J., and Lu, H. 2013. Proteomic and metabolomic responses in hepatopancreas of *Mytilus galloprovincialis* challenged by *Micrococcus luteus and Vibrio anguillarum*. Journal of Proteomics 94: 54–67. doi:10.1016/j.jprot.2013.09.001.

Wu, H., Xu, L., Yu, D., and Ji, C. 2017. Differential metabolic responses in three life stages of mussels *Mytilus galloprovincialis* exposed to cadmium. Ecotoxicology 26: 74–80. doi:10.1007/s10646-016-1741-8.

Xiao, S., Wong, N.-K., Li, J., Lin, Y., Zhang, Y., Ma, H., Mo, R., Zhang, Y., and Yu, Z. 2018. Analysis of in situ transcriptomes reveals divergent adaptive response to hyper- and hypo-salinity in the Hong Kong oyster, *Crassostrea hongkongensis*. Frontiers in Physiology 9:1491. doi:10.3389/fphys.2018.01491.

Xu, B., Chen, M., Yang, H., and Zhao, S. 2008. Starvation-induced changes of hemocyte parameters in the Zhikong scallop *Chlamys farreri*. Journal of Shellfish Research 27: 1195–1200. doi:10.2983/0730-8000-27.5.1195.

Xu, Y., Cao, J., Huang, S., Feng, D., Zhang, W., Zhu, X., and Yan, X. 2015. Characterization of tetratricopeptide repeat-containing proteins critical for cilia formation and function. PLOS ONE 10: e0124378. doi:10.1371/journal.pone.0124378.

Yamada, M., Oritani, K., Kaisho, T., Ishikawa, J., Yoshida, H., Takahashi, I., Kawamoto, S., Ishida, N., Ujiie, H., Mosaie, H., Botto, M., Tomiyama Yoshiaki, and Matsuzawa, Y. 2004. Complement C1q regulates LPS-induced cytokine production in bone marrow-derived dendritic cells. European Journal of Immunology 34: 221–230.

Yancey, P.H. 2001. Water stress, osmolytes and proteins. American Zoologist 41: 699–709.

Yancey, P.H. 2005. Organic osmolytes as compatible, metabolic and counteracting cytoprotectants in high osmolarity and other stresses. Journal of Experimental Biology 208: 2819–2830. doi:10.1242/jeb.01730.

Yancey, P.H., Clark, M.E., Hand, S.C., Bowlus, R.D., and Somero, G.N. 1982. Living with water stress: evolution of osmolyte systems. Science 217: 1214–1222. doi:10.1126/science.7112124.

Yang, J., He, J., Liu, L., He, M., Zhang, X., Buttino, I., Guo, B., Yan, X., and Liao, Z. 2022. Expression profiles of antimicrobial peptides in *Mytilus coruscus*. Aquaculture 548: 737709. doi:10.1016/j.aquaculture.2021.737709.

Yao, C.-L., and Somero, G.N. 2012. The impact of acute temperature stress on hemocytes of invasive and native mussels (*Mytilus galloprovincialis* and *Mytilus californianus*): DNA damage, membrane integrity, apoptosis and signaling pathways. Journal of Experimental Biology 215: 4267–4277. doi:10.1242/jeb.073577.

Yarra, T., Blaxter, M., and Clark, M.S. 2021a. A bivalve biomineralization toolbox. Molecular Biology and Evolution 38: 4043–4055. doi:10.1093/molbev/msab153.

Yarra, T., Ramesh, K., Blaxter, M., Hüning, A., Melzner, F., and Clark, M.S. 2021b. Transcriptomic analysis of shell repair and biomineralization in the blue mussel, *Mytilus edulis*. BMC Genomics 22: 437. doi:10.1186/s12864-021-07751-7.

Yu, H., Li, H., and Li, Q. 2017. Molecular characterization and expression profiles of myosin essential light chain gene in the Pacific oyster *Crassostrea gigas*. Comparative Biochemistry and Physiology Part B: Biochemistry and Molecular Biology 213: 1–7. doi:10.1016/j.cbpb.2017.07.007.

Zhang, G., Li, L., Meng, J., Qi, H., Qu, T., Xu, F., and Zhang, L. 2016. Molecular Basis for Adaptation of Oysters to Stressful Marine Intertidal Environments. Annual Review of Animal Biosciences 4: 357–381. doi:10.1146/annurev-animal-022114-110903.

Zhang, W., Siraj, S., Zhang, R., and Chen, Q. 2017. Mitophagy receptor FUNDC1 regulates mitochondrial homeostasis and protects the heart from I/R injury. Autophagy 13: 1080–1081. doi:10.1080/15548627.2017.1300224.

Zhang, X., Flato, G., Kirchmeier-Young, M., Vincent, L., Wan, H., Wang, X., Rong, R., Fyfe, J., Li, G., and Kharin, V. 2019. Changes in temperature and precipitation across Canada; Chapter 4. Pages 112–193 in Canada's changing climate report. Government of Canada, Ottawa, Ontario. doi:10.4095/314614.

Zhao, L., Schöne, B.R., Mertz-Kraus, R., and Yang, F. 2017. Sodium provides unique insights into transgenerational effects of ocean acidification on bivalve shell formation. Science of The Total Environment 577: 360–366. doi:10.1016/j.scitotenv.2016.10.200.

Zhao, L., Yang, F., Milano, S., Han, T., Walliser, E.O., and Schöne, B.R. 2018. Transgenerational acclimation to seawater acidification in the Manila clam *Ruditapes philippinarum:* Preferential uptake of metabolic carbon. Science of The Total Environment 627: 95–103. doi:10.1016/j.scitotenv.2018.01.225.

Zhao, X., Yu, H., Kong, L., and Li, Q. 2012. Transcriptomic responses to salinity stress in the Pacific Oyster *Crassostrea gigas*. PloS one 7: e46244. doi:10.1371/journal.pone.0046244.

Zhao, X., Yu, H., Kong, L., Liu, S., and Li, Q. 2014. Comparative Transcriptome analysis of two oysters, *Crassostrea gigas* and *Crassostrea hongkongensis* provides insights into adaptation to hypo-osmotic conditions. PLOS ONE 9: e111915. Public Library of Science. doi:10.1371/journal.pone.0111915.

Zilberberg, C., Sereno, D., Lima, G., Custódio, M.R., and Lôbo-Hajdu, G. 2011. Effect of mussel's gender and size on a stress response biomarker. Water, Air, & Soil Pollution 217: 317–320. doi:10.1007/s11270-010-0589-4.

Zittier, Z.M.C., Bock, C., Lannig, G., and Pörtner, H.O. 2015. Impact of ocean acidification on thermal tolerance and acid–base regulation of *Mytilus edulis* (L.) from the North Sea. Journal of Experimental Marine Biology and Ecology 473: 16–25. doi:10.1016/j.jembe.2015.08.001.

Zurburg, W., and De Zwaan, A. 1981. The role of amino acids in anaerobiosis and osmoregulation in bivalves. Journal of Experimental Zoology 215: 315–325. doi:10.1002/jez.1402150309.